STUDY ON THE ADAPTIVE GROWTH OF ESCHERICHIA COLI SUPPORTED BY TWO-COMPONENT SIGNAL TRANSDUCTION SYSTEMS

三宅, 裕可里 / MIYAKE, Yukari

(開始ページ / Start Page)
1
(終了ページ / End Page)
144
(発行年 / Year)
2020-03-24
(学位授与番号 / Degree Number)
32675甲第489号
(学位授与年月日 / Date of Granted)
2020-03-24
(学位名 / Degree Name)
博士(生命科学)
(学位授与機関 / Degree Grantor)
法政大学 (Hosei University)
(URL)
https://doi.org/10.15002/00022979

Doctoral Dissertation Reviewed by

Hosei University

STUDY ON THE ADAPTIVE GROWTH OF *ESCHERICHIA COLI* SUPPORTED BY TWO-COMPONENT SIGNAL TRANSDUCTION SYSTEMS

YUKARI MIYAKE

Department of Frontier Bioscience

Graduate School of Science and Engineering

Hosei University

March, 2020

Table of contents

ABBREVIATIONS

A	Adenine
AcP	Acetyl-phosphate
Ap	Ampicillin
ATP	Adenosine triphosphate
bp	Base pair
C	Cytidine
cAMP	Cyclic adenosine monophosphate
Cas9	CRISPR associated protein 9
COGs	The clusters of orthologous groups of proteins
CRISPR	Clustered regularly interspaced short palindromic repeats
crRNA	CRISPR-RNA
CTP	Cytidine triphosphate
DBD	C-terminal DNA-binding domain
DDW	Deionized distilled water
FITC	Fluorescein isothiocyanate
G	Guanine
G6P	Glucose-6-phosphate
gSELEX	Genomic Systematic evolution of ligands with exponential enrichment
HK	Histidine kinase
HoSeI	Homologous sequence integration
IPTG	Isopropyl β- d-1-thiogalactopyranoside
Km	Kanamycin
LB	Luria-Bertani
Mw	Molecular weight
Ni-NTA	Ni-nitrilotriacetic acid
NMR	Nuclear magnetic resonance
nt	Nucleotide
OD	Optical density
ORF	Open reading frame
PAGE	Polyacrylamide gel electrophoresis
PAM	Proto-spacer adjacent motif
PC	Principal component
PCA	Principal component analysis
PCR	Polymerase chain reaction

PM	Phenotype Microarray
PTS	The phosphotransferase system
R	Purine
RD, REC	N-terminal receiver domain
RR	Response regulator
SDS	Sodium dodecyl sulfate
sgRNA	single-guide RNA
SK	Sensor kinase
T	Thymine
TCA	Tricarboxylic acid
TCS	Two-component system
TF	Transcription factor
TMAO	Trimethylamine oxide
tracrRNA	Trans-activating crRNA
tRNA	Transfer RNA
UDP	Uridine diphosphate
Y	Pyrimidine

SUMMARY

Bacteria survive in the environment with three systems: a system for sensing environmental conditions, a system for responding to sensed signals, and an adaptation system for proper survival in the environment. An adapting bacterial cell performs cell division to increase the number of sister cells, termed adaptive growth. Two-component systems (TCSs), representing the signal transduction systems widely conserved in bacteria, consist of a pair of one sensor kinase (SK) and one response regulator (RR). One SK autophosphorylates with stimuli (stage-1), and the cognate RR is activated by the SK (stage-2), and the resulting activated RR regulates a set of gene expressions (stage-3). Most cognate pairs of one SK and one RR genes are expressed in the single transcription unit. The signal transduction of TCS mostly represents a high specificity, but a certain cross-regulation has been identified at three stages of the signal transduction pathways.

In this study, I have focused on revealing the contribution of TCSs for fast growth as an adaptive growth strategy of *Escherichia coli*. I first identified novel regulatory targets of a TCS YpdAB (PyrSR), predicted to participate in the regulation of utilization of exometabolites. For induction of PyrSR function, the major exometabolite pyruvate in growing *E. coli* K-12 was identified as the inducer. One unique feature of PyrSR is its cross-talk with another pyruvate-sensing BtsSR at the TCS stage 1 for fine-tuning of pyruvate reutilization. Next, I analyzed all of 36 TCS gene promoter activities in various environmental conditions to get the insight into the comprehensive TCSs expression profile in the *E. coli* K-12 genome. Systematic promoter assay and principal component analysis showed the functional classification of TCS gene promoters of *E. coli* growing under three different carbon source conditions. These results might be available to understand bacterial responses and adaptations via the TCS network.

In order to clarify the role of TCSs on an adaptive growth, multi-gene knockout strains are required in addition to single-gene knockout strains. Therefore, I developed the novel genome editing technology, the HoSeI (Homologous Sequence Integration) method, based on CRISPR-Cas9. The HoSeI method bred a set of gene-knockout strains, including single TCS gene knockout strains and all 34 RR gene- or 30 SK gene-deprived strains. The statistics of single-cell observation showed novel epistasis in which an arbitrary pair of *phoP*, *phoB*, and *ompR* genes, stably expressed by positive feedback regulation, support the optimum adaptive growth of *E. coli* in a manner independent of the cognate SK. According to the characterization of TCS-deprived strain, TCSs enable the cell to adapt to the environmental changes and to increase the cell population. TCSs also contribute to maintaining the cell fitness for environments to acquire a fast response speed, a fast-initial growth rate, and a larger cell mass.

CHAPTER 1. INTRODUCTION

1-1. Adaptive growth of bacteria

Bacteria survive and then increase their population by binary cell division in a timely manner. Individual bacterial cells sense changing environmental signals, transduce those environmental signals into biological responses, and adapt to the environmental change by biological responses. Successful integration of these biological stress responses must induce adaptive growth to obtain a continuous chance for the production of offspring (Fig. 1-1). Bacteria are able to survive in various environments by changing the expression pattern of their genome, which takes place by controlling the promoter recognition properties of RNA polymerase by transcription factors (Ishihama 2010 and 2012). Transcription factors (TFs) are classified as those that facilitate direct sensing and indirect sensing of environmental signals. The Lac repressor and Crp activator are good examples of direct sensing TFs and sense lactose and cAMP, respectively. A response regulator (RR) is a typical example of an indirect sensing TF and is activated by phosphorylation by the cognate sensor kinase (SK), detecting environmental signals at the membrane (Egger *et al.* 1997; Hoch 2000). Direct sensing TFs temporally support bacterial growth because extracellular nutrients stimulate intracellular metabolism and produce signal metabolites that activate those TFs. Indirect sensing TFs, such as RR, are known to be important for temporal survival but are not known for aiding continuous growth.

Recent massive amounts of genomic information show the core genome, a set of species-specific genes, and pan genome, representing non-conserved genes (Touchon *et al.* 2009). Within the core genome, there is a set of genes involved in central and secondary metabolism, cell cycle, and gene expression, many of which are essential for growth (Touchon *et al.* 2009). In addition to genes coding for essential biological functions, regulatory genes are conserved in the core genome but are not essential for growth (Touchon *et al.* 2009) (Fig. 1-1). One of the core-genome regulatory genes is the RR gene, which is a unique signal transduction component that is only conserved among prokaryotes.

1-2. Two-component system (TCS)

The two-component system (TCS) is mostly conserved among bacteria and typically consists of a cognate pair of one sensor kinase (SK) and one response regulator (RR) (Stock *et al.* 1990). In general, SKs, which are localized on the bacterial membrane, sense physical or chemical signals at N terminus and then phosphorylate at the conserved histidine residue in the cytoplasmic transmitter domain of C terminus (Yamamoto *et al.* 2005) (Fig. 1-2). SKs stably form a homodimer,

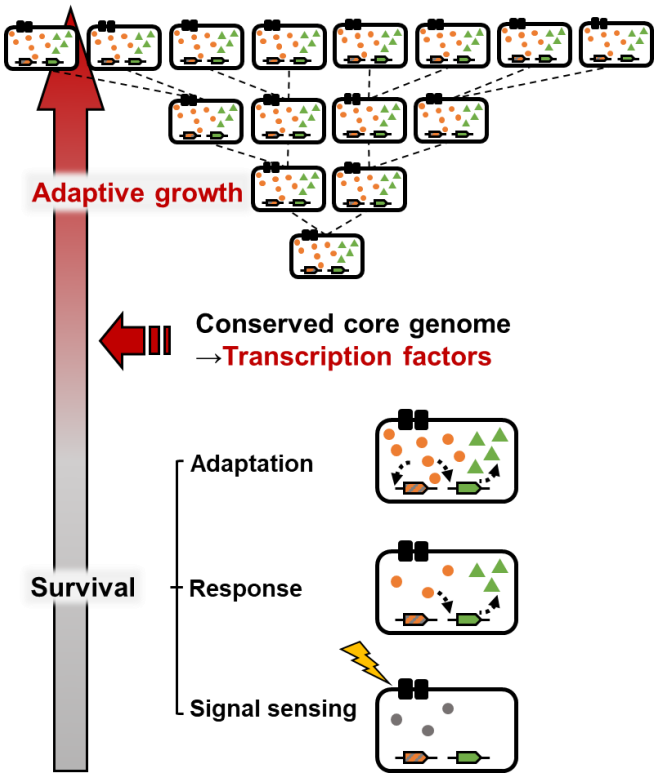

Fig. 1-1. The adaptive growth of bacteria. Bacteria cells sense environmental signals, respond to environmental changes by regulation of the gene expression, and adapt to the environment by maintaining the gene expression profile for individual survival. Successful integration of these biological stress responses must induce adaptive growth to obtain a continuous chance for the production of offspring. It is, however, little known how such stress response contributes to bacterial growth for descendants. In addition to genes coding for essential biological functions, regulatory genes are conserved in the core genome but are not essential for growth (Touchon *et al.* 2009).

and each monomer in the dimer phosphorylate the other (Zschiedrich *et al.* 2016; Jacob-Dubuisson *et al.* 2018). The phosphate is transferred to the conserved aspartate residue of a receiver domain of the cognate RR (Yamamoto *et al.* 2005). Recent studies of the molecular structure of RRs believe that the monomeric unphosphorylated RR forms a closed conformation with an interaction between the REC and DBD effector domains. In contrast, the phosphorylated RR stimulates dimerization by the interaction between receiver domains and forms an extended conformation that altered the surface of DNA-binding domains in a dimer for recognition of the target promoters (Gao *et al.* 2019) (Fig. 1-2). The phosphorylated RR, which binds to the promoter, recruits, or inhibits RNA polymerase for the regulation of transcription reaction.

Although the general mechanisms and functions of TCSs are common in bacteria, the essentiality of them are different between gram-positive and gram-negative bacteria. In gram-positive bacteria, most of TCSs have been estimated as nonessential whereas the WalRK system is known as the highly conserved essential TCS for growth. The essentiality of WalRK has been revealed in *Bucillus* (e.g. *Bacillus suctilis*), *Streptococcus pneumoniae*, and *Staphylococcus aureus* (Fabret and Hoch 1998; Lange *et al.* 1999; Martin *et al.* 1999; Throup *et al.* 2000; Wagner *et al.*

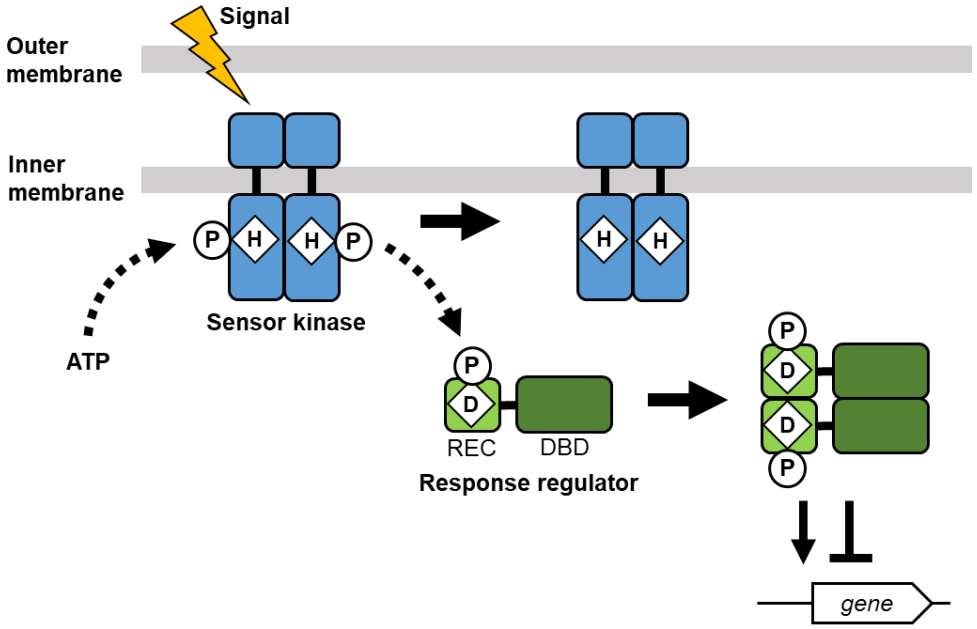

Fig. 1-2. The overview of the two-component signal transduction system. The two-component system (TCS) is mostly conserved among bacteria. A TCS consists of a cognate pair of one sensor kinase (SK, shown by blue boxes) and one response regulator (RR, shown by green boxes) (Stock *et al.* 1990). In general, SKs, which are localized on the bacterial membrane, sense physical or chemical signals and then phosphorylate at the conserved histidine residue (shown as H) (Yamamoto *et al.* 2005). SKs transfer the phosphate (shown as P) to the conserved aspartate residue (shown as D) of a receiver (REC) domain of the cognate RR (Yamamoto *et al.* 2005). Recent studies of the molecular structure of RRs believe that the monomeric unphosphorylated RR forms a closed conformation with an interaction between the REC domain and DNA-binding domain (DBD). In contrast, the phosphorylated RR stimulates dimerization by the interaction between REC domains and forms an extended conformation that altered the surface of DBDs in a dimer for recognition of the target promoters (Gao *et al.* 2019) (shown with a white arrow). The phosphorylated RR, which binds to the promoter, recruits, or inhibits RNA polymerase for the regulation of transcription reaction.

2002). The WalRK system regulates the expression of major virulence genes, cell wall metabolism, and biofilm formation (Delaune *et al.* 2012; Dubrac *et al.* 2004 and 2007). Also, recent analysis of TCS-deprived *S. aureus* concluded the WalRK system is needed for growing cells but not for growth arrested cells (Villanueva *et al.* 2018). On the other hand, an essential TCS for growth is unknown in gram-negative bacteria. Since single knockouts of each TCS do not show a lethal effect when bacteria grow under the condition with no specific environmental changes, TCSs in gram-negative bacteria are thought as nonessential systems for growth (Baba *et al.* 2006).

1-3. TCSs in *Escherichia coli* K-12

In most of the bacterial genome, conserved RR genes are designed in core-genome, which are a set of genes involved in central and secondary metabolisms, cell cycle, and gene expression, many of which are essential for growth (Touchon *et al.* 2009). The genome sequence of *Escherichia coli* K-12 predicts 30 TCS systems (Fig. 1-3A) (Mizuno 1997; Yamamoto *et al.* 2005). The function

of responses by TCSs of *E. coli* K-12 divides into four response groups, the stress response, the metal response, the metabolic response, and the respirational response (Yamamoto 2014) (Table 1-1). The stress response group includes osmo-sensing EnvZ-OmpR, envelope stress-sensing BaeSR, CpxAR, and RcsCB, and pH-sensing EvgSA and RstAB, which control a set of genes involved in the homeostasis of the cellular osmolyte and proton and repair damage on the cell surface. The metal response group includes Fe-sensing BasSR, Cu-sensing CusSR, Mg-sensing PhoQP, and K-sensing KdpDE, which control a set of genes involved in the homeostasis of cellular metals. The metabolic response group includes acetoacetate-sensing AtoSC, nitrogen-sensing NtrBC, and phosphate-sensing PhoRB, which control the related genes for nutrient responses. The respiration response group includes reduction-sensing ArcBA, nitrate/nitrite-sensing NarQP and NarXL, TMAO-sensing TorSR, which control a set of genes involved in aerobic and anaerobic respiration. The signal transduction of TCS mostly represents a high specificity (Laub and Goulian 2007), but a certain cross-regulation has been identified at three stages of the signal transduction pathways: in the recognition of signals by SKs (stage-1); in the phosphorylation of RRs by SKs (stage-2); and in the recognition of target promoters by RRs (stage-3) (Yamamoto 2014; Yamamoto *et al.* 2005; Yoshida *et al.* 2015) (Fig. 1-3B). The cross-regulation among TCSs is thought to increase the flexibility of responses to complex environmental factors.

Phenotype microarray assays of TCS mutants show that 22 TCS mutants have altered growth phenotypes, including defective growth of the *uhpAB* mutant, which uses glucose-6-phosphate and fructose-6-phosphate as carbon sources, and defective growth of the *dcuSR* mutant, which uses dicarboxylates as carbon sources (Zhou *et al*. 2003). In addition to such expected metabolic phenotypes in relation to carbon sources, at least 6 species of TCS single knockouts, *arcA*, *atoSC*, *barA*, *ompR-envZ*, *phoPQ*, and *uvrY* mutants, show increased growth or respiration in the presence of unused carbon sources based on the parent strain (Zhou *et al*. 2003). Growth phenotypes are thought to result from a sophisticated signal transduction network by cross-talk among TCSs in *E. coli*. Glucose is one of the favorite carbon sources in *E. coli* because glucose has a high affinity for the phosphotransferase system (Postma *et al*. 1993; Deutscher *et al*. 2006). Glucose is directly catabolized into glycolysis and then is consumed through the tricarboxylic acid cycle (Deutscher *et al*. 2006). Catabolism of glucose occurs prior to metabolism of other carbon sources, resulting in catabolite repression by the regulatory networks that are induced by glucose (Stülke and Hillen 1999; Bettenbrock *et al*. 2006). *E. coli* also catabolizes glycerol by enzymatic reactions, which are mainly involved in a glycerol kinase and two glycerol-3-phosphate dehydrogenases (Lin 1976; Booth 2005). Metabolic flux analysis of *E. coli* chemostat culture in the presence of both glucose and glycerol shows that a high dilution rate of culture increases the glucose consumption rate, in which the level of the *arcA* transcript increases (Yao 2016), implying that TCSs largely contribute to adaptive growth in the presence of different carbon sources.

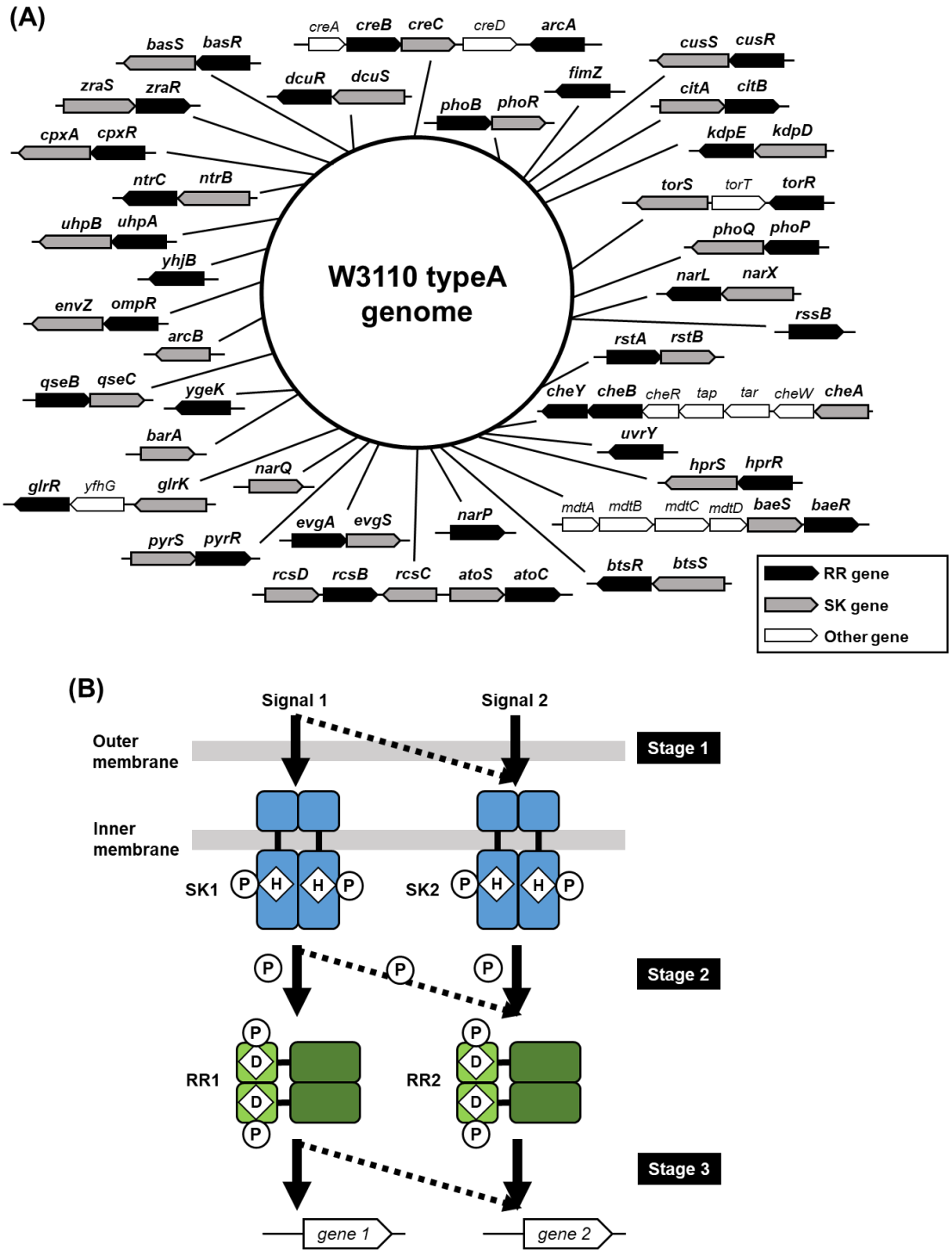

Fig. 1-3. Two-component system genes in the *E. coli* K-12 W3110 genome. [A] All two-component system genes in the *E. coli* K-12 W3110 genome (4.6 Mb) are shown with arrows. Each arrow shows sensor kinase genes (gray), response regulator genes (black), and other genes in the operon (white), respectively. The direction of arrows shows the direction of genes in the *E. coli* genome. **[B]** A cross-regulation among TCSs. A certain cross-regulation has been identified at three stages of the signal transduction pathways: in the recognition of signals by SKs (stage-1); in the phosphorylation of RRs by SKs (stage-2); and in the recognition of target promoters by RRs (stage-3) (Yamamoto, 2014; Yamamoto *et al.* 2005; Yoshida *et al.* 2015). Each of SKs, RRs, and target genes are shown with a blue box, a green box, and a white arrow, respectively. Each residue is shown as H (histidine) and D (aspartate), and the phosphate is shown as P.

Table 1-1. Two-component systems in *E. coli*.

Signal		SK		RR	Target
Respiration					
Redox condition	→	ArcB	→	ArcA	*icdA* p and other 70 gene promoters
Citrate	→	CitA	→	CitB	*appY* p, *citC* p, *dpiB* p, *exuT* p, *mdh* p
C4 dicarboxylates	→	DcuS	→	DcuR	*dctA* p, *dcuB* p, *dcuS* p, *dpiB* p, *frdA* p
Nitrate, Nitrite	→	NarQ	→	NarP	*nrfA* p and othter 13 gene promoters
Nitrate, Nitrite	→	NarX	→	NarL	*nirB* p and other 33 gene promoters
TMAO	→	TorS	→	TorR	*torC* p and other 9 gene promoters
Metabolism					
Acetoacetate	→	AtoS	→	AtoC	*atoD* p, *atoS* p
Short chain aliphatic carboxylic acids	→	BarA	→	UvrY	*csrB* p, *csrC* p, *luxS* p, *uhpT* p, *ydeP* p
Glycolytic carbon products	→	CreC	→	CreB	*creD* p and other 7 gene promoters
Nitrogen limitation	→	NtrB	→	NtrC	*glnA* p and other 19 gene promoters
External Pi Limitation	→	PhoR	→	PhoB	*phoA* p and other 30 gene promoters
Glucose-6-phosphate	→	UhpB	→	UhpA	*uhpT* p
Carbon starvation, Extracellular pyruvate	→	BtsS	→	BtsR	*yjiY* p
Extracellular Pyruvate	→	YpdA	→	YpdB	*mglA* p?, *srlD* p?, *yjhT* p?, *yhjX* p
Metal response					
High Fe(III)	→	BasS	→	BasR	*ais* p and othter 11 gene promoters
High Cu(II)	→	CusS	→	CusR	*cusC* p, *cusR* p, *cyoA* p, *yedX* p
Low K(I)	→	KdpD	→	KdpE	*kdpF* p
Low Mg(II)	→	PhoQ	→	PhoP	*mgtA* p and other 33 gene promoters
High Zn(II) and Pb(II)	→	ZraS	→	ZraR	*zraP* p, *zraS* p
Stress response					
Envelope stress	→	BaeS	→	BaeR	*acrD* p, *mdtA* p, *spy* p, *ycaC* p
Envelope stress	→	CpxA	→	CpxR	*cpxP* p and other 40 gene promoters
Extracellular osmorality	→	EnvZ	→	OmpR	*ompC* p and other 13 gene promoters
Low pH, high alkali metal (Na+, K+)	→	EvgS	→	EvgA	*ydeO* p and other 9 gene promoters
Bacterial hormone?	→	GlrK	→	GlrR	*glmY* p, *yfhK* p, *rpoE* p
Bacterial hormone	→	QseC	→	QseB	*basR* p, *flhD* p, *qseB* p, *ygiW* p
Membrane perturbation	→	RcsC			
		RcsD	→	RcsB	*wza* p and other 23 gene promoters
Low pH	→	RstB	→	RstA	*asr* p, *csgD* p, *narG* p, *ompF* p
H_2O_2	→	HprS	→	HprR	*cusC* p, *cusR* p, *cyoA* p, *yedVW* p, *yedX* p
Increased level of σ^s?	→	?	→	RssB	Degration of σ^s
Chemotaxis					
Attractant & repellent	→	CheA	→	CheB	Demethylation of chemotaxis receptor
			→	CheY	Changing flagellar rotation
Unknown					
?	→	?	→	FimZ	Fimbrial expression ?
?	→	?	→	YgeK	?
?	→	?	→	YhjB	?

Among genes coding TCS factors, 22 pairs of SK and RR genes are polycistronic transcribed and 6 transcription units, *phoB-phoR*, *phoP-phoQ*, *qseB-qseC*, *ompR-envZ*, *cpxR-cpxA*, and *basR-basS*, show positive feedback regulation. However, it is not clear which of TCS genes is dominantly expressed in complex environmental factors.

1-4. Autoregulation of TCS genes

Several TFs are autoregulated during the response to environmental signals. In *E. coli*, more than 50% of identified TFs in the genome are positively or negatively autoregulated (Ishihama, 2012; Hermsen *et al.* 2010). Positive autoregulation leads to a fast response and impacts the response dynamics (Gao *et al.* 2018; Maeda *et al.* 2006). Among ~30 positively autoregulated TFs in the *E. coli* genome (Hermsen *et al.* 2010), 10 of those are RRs of TCSs (PhoB, CusR, CitB, PhoP, EvgA, GlrR, QseB, OmpR, CpxR, and BasR), and 34 RRs have been characterized in the *E. coli* genome. On the other hand, negatively autoregulated RRs are less common than positively autoregulated RRs in TCSs (Goulian 2010). A recent report showed that coupled positive and negative feedback allowed both a fast response and optimal RR protein levels in the PhoB/PhoR system in *E. coli* (Gao *et al.* 2018). However, the contribution of coupled autoregulation for continuous bacterial growth is poorly understood.

1-5. Objective of this study

According to the previous reports, bacterial cells drive the adaptive growth effectively using the high conserved bacterial signal transduction systems. However, the contribution of comprehensive TCS network to the adaptive growth is still unclear. In this study, I firstly focused on searching the new regulatory target genes and the specific inducer of an unknown response regulator, YpdB, to confirm its regulatory role. Based on the results and previous reports about the functions of TCS proteins, I analyzed all of 36 TCS gene (operon) promoter activities in various environmental conditions to get the insight into the comprehensive TCSs expression profile in the *E. coli* K-12 genome. Then, to clarify the role of TCSs on the adaptive growth, I developed the novel genome editing technology, the HoSeI (Homologous Sequence Integration) method based on CRISPR-Cas9, and isolated a set of TCS gene knockout strains. Using obtained mutants, I investigated the effects of TCSs on the single-cell growth and phenotypic characterization of the all RR- or SK-deprived mutant.

CHAPTER 2. REGULATORY ROLES OF PYRUVAYTE-SENSING TWO-COMPONENT SYSTEM PYRSR (YPDAB)

2-1. Introduction

When the rate of production of metabolites exceeds the level needed for cell growth, excess metabolites are secreted into the extracellular environment (Holms 1996). Upon entry into poor nutrient conditions, exometabolites are taken up again and reused for continued growth and survival. This pathway appears essential for growth-coupled maintenance of the homeostasis of intracellular metabolites (Shimada and Tanaka 2016; Yasid *et al.*2016). The genetic system(s) involved in the metabolite efflux and reutilization of exometabolites, however, remains poorly understood even for the best-characterized model prokaryote *Escherichia coli*. Up to the present time, two LytTR-family two-component systems (TCSs) of *E. coli* K-12, BtsSR (renamed from YehUT) and PyrSR (herein renamed from YpdAB), have been proposed to be involved in the uptake of overflowed exometabolites (Fried *et al*. 2013; Behr *et al.*2017a; Behr *et al.*2017b). The PyrSR and BtsSR TCSs were identified to regulate the expression of only a single target *yhjX* and *btsT* (renamed from *yjiY*), respectively (Kraxemberger *et al.* 2012; Fried *et al*. 2013).

In this study, I newly identified a total of eight regulatory targets of PyrR (YpdB), including the hitherto identified *yhjX*. After analysis of the influence of exometabolites on the regulatory function of PyrR, I found the involvement of PyrSR (YpdAB) in sensing external pyruvate and its uptake. As to sensing the exometabolite pyruvate, the involvement of BtsSR and PyrSR has been proposed (Fried *et al*. 2013; Behr *et al.* 2017b). Here I confirmed that both PyrSR and BtsSR monitor a single and the same exometabolite pyruvate, but interestingly each sensing different concentrations of pyruvate. To note this unique cross-talk between PyrSR and BtsSR at the signal-sensing step (stage 1) and the phosphotransfer step (stage 2) of TCS signal transduction pathway, I propose to rename YpdAB to PyrSR (regulator of pyruvate reutilization).

2-2. Materials and Methods

2-2-1. Bacterial strains, plasmids and chemicals

Escherichia coli K-12 stains and plasmids used in this study are listed in Table 2-1. Primers used for construction of TF expression vectors and the plasmids for reporter assays are described in Table 2-2.

Table 2-1. Bacterial strains and plasmids used in this study.

Name	Purpose	Reference
Strains		
W3110 type A	Templete of TF expression; Substrate in SELEX screening	Jishage and Ishihama 1997
BL21(DE3)	Expression of TF	Studier *et al.* 1986
BW25113	Reporter assay	Dstsenko and Wanner 1997
JW5388	BW25113 *pyrS (ypdA)* mutant; Reporter assay	Baba *et al*. 2006
JW2378	BW25113 *pyrR (ypdB)* mutant; Reporter assay	Baba *et al*. 2006
JW3516	BW25113 *yhjX* mutant; Reporter assay	Baba *et al*. 2006
JW5353	BW25113 *btsS* (*yehU*) mutant; Reporter assay	Baba *et al*. 2006
JW5352	BW25113 *btsR (yehT)* mutant; Reporter assay	Baba *et al*. 2006
JW5791	BW25113 *btsT (yjiY)* mutant; Reporter assay	Baba *et al*. 2006
Plasmids		
pYpdB	YpdB expression	This report
pBtsR	BtsR expression	This report
pLUXyhjX	Reporter assay of *yhjX* promoter	This report
pLUXxthA	Reporter assay of *xthA* promoter	This report
pLUXastC	Reporter assay of *astC* promoter	This report
pLUXyghW	Reporter assay of *yghW* promoter	This report
pLUXbtsT	Reporter assay of *btsT* promoter	This report
pLUXyfjD	Reporter assay of *yfjD* promoter	This report
pLUXpbpC	Reporter assay of *pbpC* promoter	This report
pLUXyhcC	Reporter assay of *yhcC* promoter	This report
pLUXgltB	Reporter assay of *gltB* promoter	This report

2-2-2. Purification of PyrR and BtsR proteins

Transcription factors (TFs), PyrR and BtsR, were overexpressed and affinity purified following the standard procedure (Yamamoto *et al.* 2005).

2-2-3. Genomic SELEX screening

Genomic SELEX (Systematic evolution of ligands with exponential enrichment) screening was carried out according to the standard procedure (Shimada *et al.*2005; 2018). The sequence of TF-bound DNA fragments obtained by gSELEX screening was identified by using both SELEX-clos (cloning-sequencing) and SELEX-chip (tilling-array) methods.

2-2-4. Gel shift assay

The gel shift assay was performed according to the standard procedure (Ogasawara *et al.* 2007). Probes of the PyrR-binding target sequences were generated by PCR amplification using a pair of primers, one FITC-labeled and another unlabeled, and Ex Taq DNA polymerase. FITC-labeled DNA in gels was detected using LAS-4000 IR multicolor (GE).

2-2-5. DNase footprinting assay

DNase-I footprinting assay of TF-bound DNA sequences was carried out according to the standard procedure (Shimada *et al.* 2011) using FITC-labeled DNA probes.

Table 2-2. Primers used in this study.

Primer	Sequence (5' → 3')	Purpose
EcoRV-F	CTTGGTTATGCCGGTACTGC	a
EcoRV-R	GCGATGCTGTCGGAATGGAC	a
yhjX-S	CTATGTGACCTTCTACGTGA	b
yfjD-S	CATTCTTGAGGCACTGGAAG	b
pbpC-S	AATGGCGAACCGTTAACTGA	b
gltB-S	ATCTGCGTGGTCTTATCACC	b
ypdB-S	CAATCTGAACAAAATACGCG	c
ypdB-T	TTTCACTTTGCTGCGGCTGA	c
yhjX-S	TCGTCTTCACCTCGACTTTACTACTCCACTTCGCG	b, d
yhjX-T	ACTAACTAGAGGATCGCCTAATACAAAACCGCGTT	d
xthA-S	TCGTCTTCACCTCGAAGGCTAACTGGAAATCAAGG	b, d
xthA-T	ACTAACTAGAGGATCTATCGTCATGAACTTTTGTC	d
astC-S	TCGTCTTCACCTCGAATCGATGGTTGTTAATGATG	b, d
astC-T	ACTAACTAGAGGATCCTTCGCCACGTACCGGTATA	d
yghW-S	TCGTCTTCACCTCGAATGTTGCTCAATCAAAATAT	b, d
yghW-T	ACTAACTAGAGGATCGGAAAGCGCGCCATTAAACA	d
btsT-S	TCGTCTTCACCTCGATTTGTCATTCTTTAAGGCATTAAAG	b, d
btsT-T	ACTAACTAGAGGATCAGTAAAACCTGGCATGTATTGATTA	d
yfjD-S	TCGTCTTCACCTCGAATCACTATGCCCGTTTTTGCTCTGC	d
yfjD-T	ACTAACTAGAGGATCGGGAAACTCCTTTTCTGGGTTTAGC	d
pbpC-S	TCGTCTTCACCTCGACACTTTCGCAGCAGGCGTTTGGTGA	d
pbpC-T	ACTAACTAGAGGATCTTACGGTCTGACAATCAGCAGATCT	d
yhcC-S	TCGTCTTCACCTCGAATCGTGAACCTCCCCCAGGCTCTGC	d
yhcC-T	ACTAACTAGAGGATCAGTTGCTCGGCAATGGAACGATGCT	d
gltB-S	TCGTCTTCACCTCGAAGTTGCTCGGCAATGGAACGATGCT	d
gltB-T	ACTAACTAGAGGATCATCGTGAACCTCCCCCAGGCTCTGC	d
LUX-R-FITC*	CCGTCCATTTGTGATAATAGTGG	b

* FITC is conjugated at 5' end; [a]Construction of gSELEX probe; [b]Construction of gel shift assay probe; [c]Construction of expression plasmid; [d]Consturction of reporter assay vector

2-2-6. Lux reporter assay

The single-copy lux (luciferase) reporter system was employed for detection of the promoter activity (Blouin *et al.*1996). For construction of Lux reporter plasmids, about 500 bp long segment of the test promoter was PCR amplified using the genome of *E. coli* W3110 as the template and a pair of primers (listed in Table 2-2), and inserted into pLUX vector using an In-Fusion HD cloning kit (Clontech, Mountain View, CA, USA) (Yamanaka *et al.* 2014). Transformants carrying

reporter plasmids grown in M9 glycerol medium were transferred into fresh M9 medium containing a single carbon source. The cell suspension was transferred to a microtiter plate (96-well microplate), and the Lux activity was monitored with an automated plate reader MTP-880 (Corona).

2-3. Results

2-3-1. Search for PyrR-binding locations by gSELEX screening: SELEX-clos analysis

For identification of the regulatory targets of PyrR, gSELEX (Shimada *et al.*2005; 2018) was employed using purified PyrR and a mixture of 200–300 bp long genome fragments from *E. coli* K-12 W3110 as the DNA substrate. After gSELEX screening in the presence and absence of AcP, PyrR-bound DNA fragments were affinity isolated using Ni-NTA. The mixture of original genomic DNA fragments formed smeared bands on PAGE, but after repetition of gSELEX screening, PyrR-bound DNA formed sharper bands on PAGE (Fig. 2-1), indicating the enrichment of specific DNA fragments with PyrR-binding activity. The difference of PAGE pattern in the presence and absence of AcP indicated enrichment of the different species of DNA fragment between non-phosphorylated and phosphorylated PyrR.

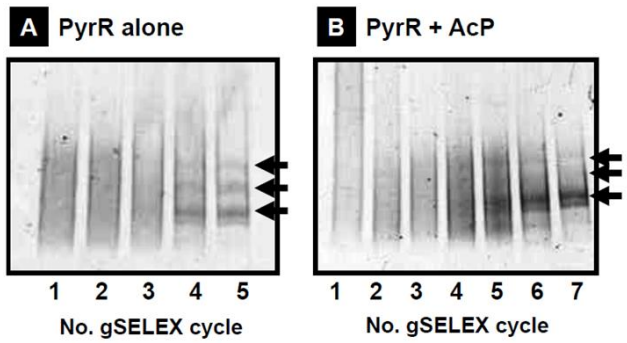

Figure 2-1. gSELEX screening of PyrR-binding DNA fragments. gSELEX screening was carried out in the absence **(A)** or presence **(B)** of AcP for identification of regulatory targets of PyrR. At each cycle, PyrR-bound DNA segments were analyzed by PAGE. After repetition of gSELEX, specific DNA segments were enriched, which formed specific gel bands.

To identify the binding sites of PyrR, DNA segments isolated after four cycles of SELEX were subjected to SELEX-clos analysis. After sequencing more than 200 independent clones, identical sequences were detected more than three times for three regions in the absence of AcP (PyrR alone) and for five regions in the presence of AcP (Table 2-3, indicated as S-clos). For both samples, the most abundant sequences were located in the spacer upstream of the *yhjX* gene and downstream of the *yhjY* gene (Fig. 2-2A1). This finding indicates that the major target of PyrR is

the *yhjX* gene encoding the MFS-family transporter with unknown function. Besides the *yhjX* gene, the binding of PyrR was found, both in the absence and presence of AcP, inside spacer between *astC* and *xthA*, and upstream of *pbpC* (Table 2-3 and Fig. 2-2A2). In the absence of AcP, its binding was also identified prior to *yghW*, while in the presence of AcP, inside spacer between *yhcC* and *gltB*, and prior to *yfjD* (Table 2-3 and Fig. 2-2A2).

Table 2-3. Regulatory targets of PyrR identified by gSELEX screening

Function	Left gene			Right gene	Function	gSELEX system[a]
[A] PyrR alone						
Succinylornithine transaminase	*astC*	<	>	*xthA*	Exonuclease III	S-clos S-chip
PBP1c murein transglycosylse	*pbpC*	<	<	*yfhM*	Hypothetical protein	S-clos S-chip
Membrane fatty acid composition	*yghW*	<	<	*yghX*	Psedogene	S-chip
Oxalate-formate antiporter	*yhjX*	<	<	*yhjY*	Putative lipase	S-clos S-chip
[B] PyrR + AcP						
Succinylornithine transaminase	*astC*	<	>	*xthA*	Exonuclease III	S-clos S-chip
Inner membrane protein	*ypjD*	>	>	*yfjD*	Inner membrane proein	S-clos S-chip
PBP1c murein transglycosylse	*pbpC*	<	<	*yfhM*	Hypothetical protein	S-clos S-chip
Putative Fe-S oxidoreductase	*yhcC*	<	>	*gltB*	Glutamate synthase	S-clos S-chip
Oxalate-formate antiporter	*yhjX*	<	<	*yhjY*	Putative lipase	S-clos S-chip

PyrR-binding sequences were isolated by gSELEX screening and analyzed by SELEX-clos and SELEX-chip for identification of their locations on the *E. coli* K-12 genome.
[a]S-clos = SELEX-clos method; S-chip = SELEX-chip method (Shimada *et al.* 2018).

2-3-2. Search for PyrR-binding locations by gSELEX screening: SELEX-chip analysis

For detailed mapping of the PyrR-binding sites, a mixture of DNA fragments obtained after six cycles of gSELEX was subjected to SELEX-chip analysis (Shimada *et al*. 2018). Apparently, a single high-level peak of PyrR-binding was identified within spacer between the *yhjX* and *yhjY* genes (Fig. 2-2B1) in good agreement with the SELEX-clos analysis. In addition, several minor peaks were identified in the absence of AcP, including two low-level but significant peaks, one inside the spacer between *astC* and *xthA* and another prior to *yghW* (Fig. 2-2B1 and Table 2-3). The *yghW* promoter overlaps with the promoter for the *morA* gene that is located on the opposite strand of the *yghX* gene (Kurata *et al.*2013), implying possible influence of this PyrR binding on the expression of ModE-regulated *morA* gene. In addition to these three targets, PyrR binding was identified inside open reading frames (ORFs) of the *abgA*, *ydaG* and *yhfS* genes. TF binding inside ORF has been identified only for a specific set of TFs (Ishihama *et al*. 2016), implying as yet unidentified regulatory role(s) for these ORF-binding TFs. In the presence of AcP, five sites of PyrR binding were identified by SELEX-chip: one major target in front of the *yhjX* gene and four

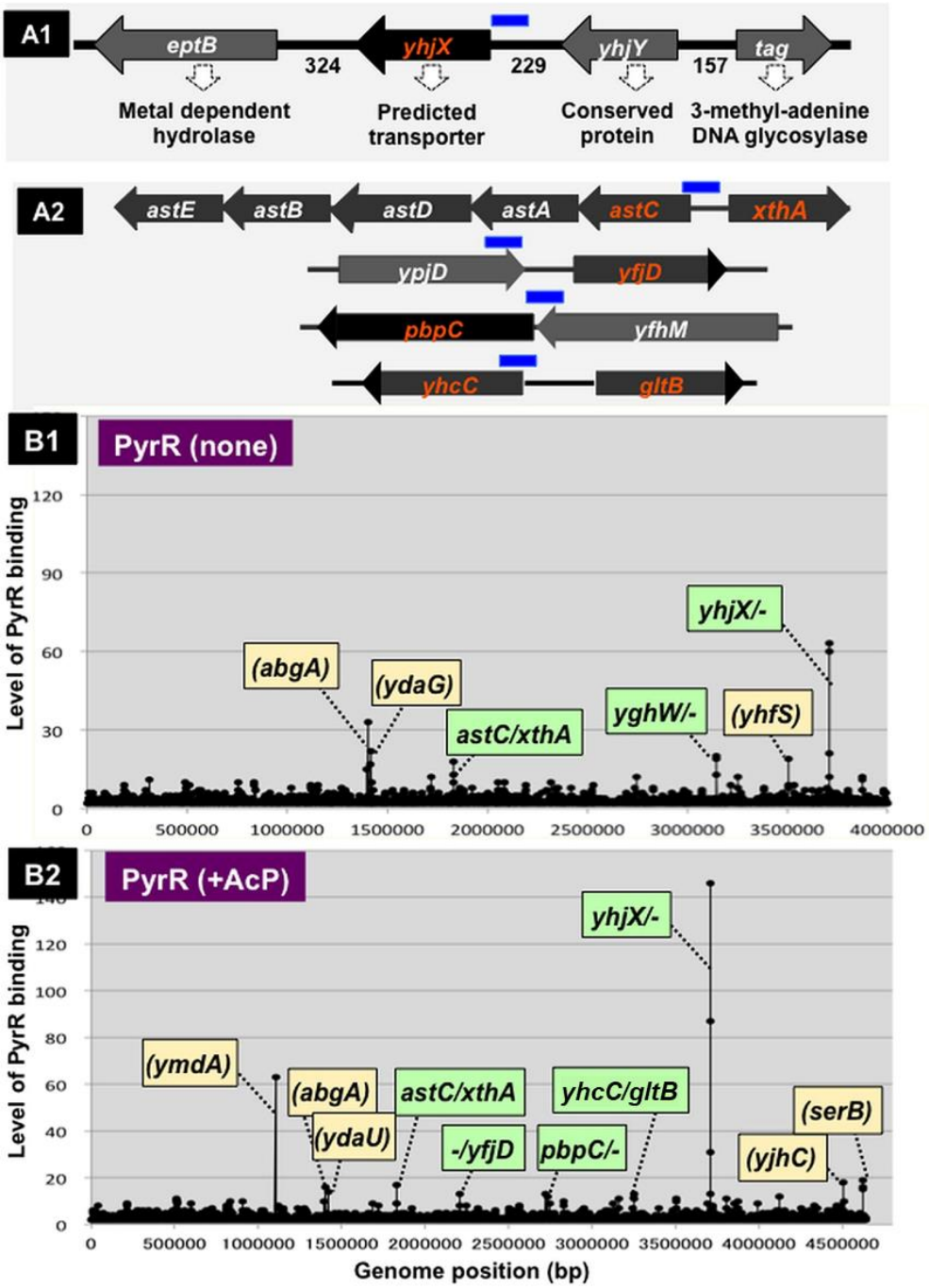

Figure 2-2. Mapping of PyrR-binding sites along the *E. coli* K-12 genome. [A] SELEX-clos analysis. gSELEX screening was carried out by mixing 5 pmol of *E. coli* K-12 genome DNA segments and 10 pmol of purified PyrR. PyrR-binding DNA fragments were affinity isolated and subjected to SELEX-clos method for mapping the location of PyrR-binding sites. The most abundant clones contained the *yhjX* promoter sequence **(A1)** while **(A2)** shows the PyrR-binding sites identified in more than three independent clones (for the whole set of SELEX-clos clones, see Table 2-3). Blue bars above the map indicate the location of PyrR-binding segments, while the genes shown in red indicate possible regulatory targets of PyrR. The number of clones correlates with the affinity of PyrR binding. **[B]** SELEX-chip analysis. PyrR-binding DNA fragments were isolated in the absence **(B1)** and presence **(B2)** of 10 mM AcP and mapped along the *E. coli* K-12 genome by SELEX-chip method using an *E. coli* tilling array. The locations of PyrR-binding site inside spacers are shown under green background, while those inside ORF are shown under pale orange background. Peak height correlates with the level of fluorescent probe (and thus PyrR binding).

minor peaks, inside the *astC-xthA* and *yhcC-gltB* spacers and in front of *yfjD* and *pbpC* (Fig. 2-2B2). All these targets were identified by SELEX-clos (Table 2-3).

Taken SELEX-clos and SELEX-chip together, a total of six binding sites for PyrR were identified (Table 2-3), from which a maximum of eight targets (*yhjX*, *pbpC*, *yfjD*, *yhcC*, *gltBD*, *yghW*, *astCADBE* and *xthA*) were predicted to be under the direct control of PyrR. Among these possible regulatory targets of PyrR, the *yhjX* gene was the most abundant clone in SELEX-clos (Fig. 2-2A1) and the highest peak in SELEX-chip (Fig. 2-2B). The regulatory roles of PyrR binding on these newly identified sites were analyzed in detail.

2-3-3. Confirmation of PyrR binding to its targets: gel shift assay

For experimental confirmation of PyrR binding to these targets, I carried out the gel shift assays *in vitro* for detection of PyrR-DNA complex formation. For this purpose, a set of DNA probes was constructed, each carrying the sequence of the predicted PyrR-binding sites (Table 2-2). The gel shift assay indicated that the slowly migrating PyrR-DNA complexes were detected for all eight probes (Fig. 2-3A). The formation of probe-PyrR complex was detected for the *yhjX* probe at the lowest concentration of PyrR, confirming the highest affinity of PyrR to the *yhjX* target. Four probes (*yhjX*, *yfjD*, *pbpC* and *gltB*) formed PyrR-DNA complexes that slowly migrated on PAGE (Fig. 2-3A, a1 to a4). As to four probes, *astC*, *xthA*, *yghW* and *yhcC*, clear bands of PyrR-probe complexes were not detected (Fig. 2-3A, a6 to a9), and then the binding of PyrR for these probes was judged based on the decrease or disappearance of free unbound probes. In the presence of AcP, the binding affinity significantly increased for the *yhjX* and *yhcC* probes, but the level of probe-PyrR complexes rather decreased for other six probes. Thus, the phosphorylation of PyrR increased its binding to *yhjX* and *yhcC*, but decreased its binding to *yfjD*, *pbpC*, *gltB*, *astC*, *xthA* and *yghW* (Fig. 2-3A).

2-3-4. Identification of the PyrR-binding sequence: DNase footprinting analysis

To identify the recognition and binding sequence of PyrR, I next performed DNase footprinting analysis using the *yhjX-yhjY* spacer with the highest affinity to PyrR. A total of about 60 bp long sequence was protected by PyrR between –73 to –133 bp upstream the initiation codon of the *yhjX* gene. Within this rather long sequence, two 10 bp long direct repeats of ATGAAATGCC sequence were found, which were separated by an intervening spacer of 11 bp (Fig. 2-3B). The size of PyrR is only 244 residues (Mw, 28,721), and thus the sequence of 60 bp long DNA could be covered by two PyrR protomers, each recognizing one unit of this direct repeat sequences. Within each consensus sequence, two DNase-hypersensitive sites were identified, implying that the

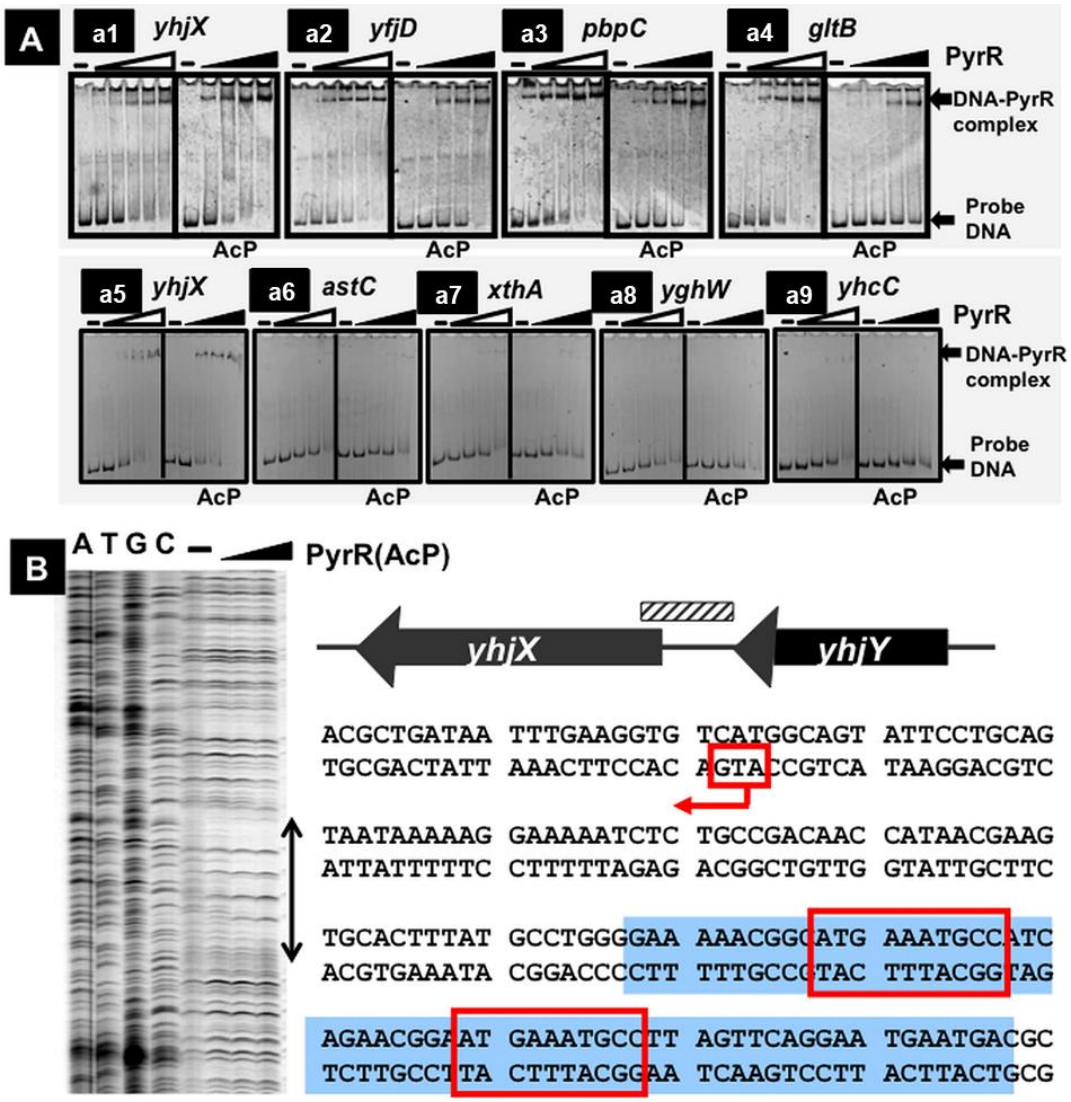

Figure 2-3. Analysis of PyrR-binding sequences on the *E. coli* K-12 genome. [A] Gel shift assay. Fluorescent-labeled DNA segments with PyrR-binding activity were prepared by PCR amplification using a pair of primers, one FITC-labeled and another unlabeled, and Ex Taq DNA polymerase. Mixtures of each probe and increasing amounts of purified PyrR were incubated for 30 min at 37°C in the presence (closed bars) and absence (open bars) of AcP and then directly subjected to PAGE analysis. FITC-labeled DNA in gels was detected using LAS-4000 IR multicolor (GE). **[B]** DNase-I footprinting assay. PyrR-binding sequence between the *yhjX* and *yhjY* genes was mapped by DNase footprinting assay. The fluorescent DNA probe containing the *yhjX* and *yhjY* region was mixed with purified PyrR in the presence of AcP and incubated for 30 min at 25°C. After DNase treatment for 30 s at 25°C, the region protected by PyrR was identified after PAGE analysis in the presence of 7 M urea. The protected sequence is indicated on the gel pattern, and this sequence is shown under blue background in the sequence map. The conserved palindromic sequences are indicated by red.

activated PyrR induces the formation of an as yet unidentified higher order structure inside the PyrR-bound DNA. The recognition sequence of PyrR in the *yhjX* promoter agrees well with the published findings (Kraxenberger *et al.*2012; Fried *et al.* 2013; Behr *et al.* 2016).

2-3-5. Effect of PyrR on expression *in vivo* of the target genes: reporter assay

As an attempt to examine regulation *in vivo* of the promoters of predicted target genes by PyrR, I employed the single-copy LUX reporter system (Blouin *et al.*1996). About 500 bp long promoter segments of all eight PyrR target genes were PCR amplified and inserted into pLUX vector (for details, see Tables 2-1 and 2-2). Each plasmid was transformed into both wild-type *E. coli* BW25113 and mutant JW2378 lacking the *pyrR* gene. Secretion of exometabolites has been suggested to be high in rich media and to increase in stationary phase, but the exometabolite composition differs depending on culture media (Paczia *et al.* 2012; Yasid *et al.* 2016). The transformants were then grown in both LB and M9-glycerol media, and the LUX activity was measured at both exponential growth and stationary phases. In wild-type cells grown in LB medium, the *yhjX* promoter-directed LUX activity was high in exponential growth phase and then decreased markedly in the stationary phase (Fig. 2-4A). I then predicted that PyrSR monitors an exometabolite(s) present in LB culture and induces the expression of YhjX transporter for uptake as yet unidentified exometabolite(s). In contrast, the *yhjX* promoter stayed low in cells grown in M9-glycerol culture (Fig. 2-4B). The expression level of other three targets, *xthA*, *astC* and *yghW*, increased in the stationary phase. I then predicted a hypothesis that the expression of these genes is repressed in exponentially phase in M9-glycerol culture, but derepressed in response to an exometabolite(s) secreted in the stationary phase. In both LB and M9-glycerol cultures, however, the composition of exometabolites remains unidentified.

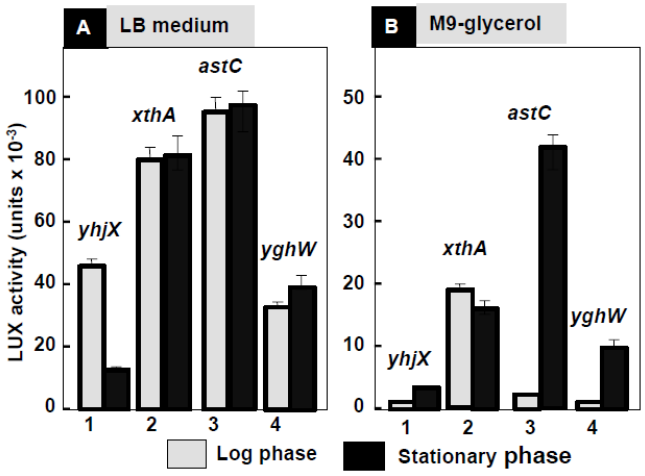

Figure 2-4. Regulatory role of PyrR on target promoters. Reporter assay was performed for the target promoters identified by gSELEX. Transformants carrying each pLUX reporter plasmid were grown in either LB **(A)** or M9-glycerol medium **(B)**. LUX assay was performed at both exponential phase (open bar) and stationary phase (filled bar).

2-3-6. Search for an inducer(s) affecting the expression of PyrR targets

As an attempt to find an exometabolite(s) affecting the function of PyrSR, I performed the reporter assay of *yhjX* promoter in the presence and absence of some known exometabolites, including acetate, pyruvate, alanine, serine and valine. Preculture grown in M9-glycerol was transferred into M9 medium containing 10 mM each of the exometabolites. The rate of cell growth in M9-pyruvate was as high as that in M9-glycerol, but after prolonged culture more than 12 h, the growth was much higher for that in M9-pyruvate (data not shown), implying that pyruvate is a good nutrient for wild-type *E. coli* K-12. The growth in M9-acetate, M9-alanine, M9-serine and M9-valine was detected only after 12 h. This finding indicates that *E. coli* K-12 is able to grow in the presence of pyruvate as a sole carbon source.

Since both PyrSR and BtsSR recognize the same exometabolite pyruvate (Vilhena *et al.* 2018; Behr *et al.* 2017b), the influence of pyruvate concentration on two TCSs was analyzed by measuring the activity of PyrSR-regulated *yhjX* promoter and BtsSR-regulated *btsT* promoter. The *btsT* gene (renamed from *yjiY*) is the only regulatory target of BtsSR so far identified (Behr *et al.* 2017b). The PyrSR-dependent *yhjX* promoter activity increased with an increase in pyruvate concentration (Fig. 2-5A), finally reaching maximum around 10–50 mM (data not shown). In contrast, the *btsT* promoter activity was maximum at 0.1 mM pyruvate, but thereafter decreased (Fig. 2-5B).

Using the same reporter assay system, I next measured growth-dependent variation of the activity of two promoters in the presence of 1- and 10-mM pyruvate. At 10 mM pyruvate, the *yhjX* promoter activity was high in the exponential growth phase, but concomitant with the consumption of pyruvate, its activity marked decreased finally to undetecTable level (Fig. 2-5C). On the other hand, the *btsT* promoter activity was high at 1 mM pyruvate, but at 10 mM pyruvate, it was low in the beginning but exhibited growth-dependent increase up to the early stationary phase (12 h culture) (Fig. 2-5D), implying the expression of the *btsT* promoter only after reduction of pyruvate concentration. This finding indicates that both PyrSR and BtsSR monitor the same exometabolite pyruvate, but of different concentrations.

2-3-7. Involvement of PyrSR in pyruvate-dependent regulation

To confirm the involvement of PyrSR in pyruvate-dependent regulation of the *yhjX* gene, I analyzed the *yhjX* promoter activity in a set of mutants, each lacking *pyrS* (sensor kinase), *pyrR* (response regulator) or *yhjX* (the major target of PyrSR). The PyrSR-dependent *yhjX* promoter was not activated in the absence of PyrS or PyrR (Fig. 2-6A), supporting the prediction of PyrSR involvement in *yhjX* expression. This promoter activity was not affected in the absence of its own

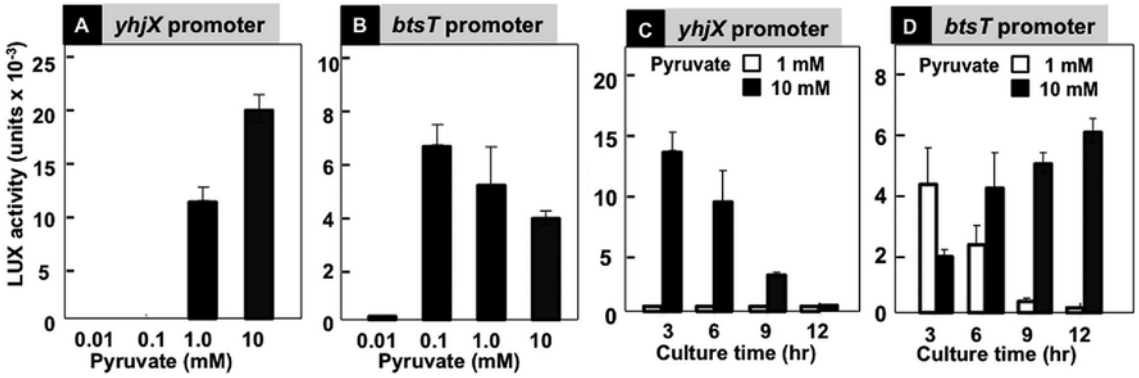

Figure 2-5. Influence of the pyruvate concentration on the *yhjX* and *btsT* promoters. [A] Reporter assay of the PyrR-regulated *yhjX* promoter. Preculture of *E. coli* K-12 transformant carrying pLUXyhjX plasmid in M9-glycerol medium was transferred into fresh M9 medium containing the indicated concentrations of pyruvate. After shaking culture at 37°C for 3 h, LUX activity was measured with an automated plate reader MTP-880 (Corona). **[B]** Reporter assay of the BtsR-regulated *btsT* promoter. Preculture of *E. coli* K-12 transformant carrying pLUXbtsT plasmid in M9-glycerol transferred into fresh M9 medium containing the indicated concentrations of pyruvate. After shaking culture at 37°C for 3 h, LUX activity was measured as above. **[C]** Growth-dependent variation of the *yhjX* promoter activity. Preculture of *E. coli* K-12 transformant carrying pLUXyhjX plasmid in M9-glycerol medium was transferred into fresh M9 medium containing either 1 mM (open bars) or 10 mM pyruvate (filled bars). After shaking culture at 37°C, LUX activity was measured at the indicated times. **[D]** Growth-dependent variation of the *btsT* promoter activity. Preculture of *E. coli* K-12 transformant carrying pLUXbtsT plasmid in M9-glycerol medium was transferred into fresh M9 medium containing either 1 mM (open bars) or 10 mM pyruvate (filled bars). After shaking culture at 37°C, LUX activity was measured at the indicated times.

regulatory target YhjX, suggesting that pyruvate uptake is possible in the absence of YhjX transporter. Likewise, the promoter of BtsSR-dependent *btsT* gene was completely inactivated in the absence of BtsS or BtsR (Fig. 2-6B). The activity of *btsT* promoter decreased, to certain extents, even in the absence of PyrS and PyrR, possibly through protein–protein interaction between YhjX and BtsR (Behr *et al.* 2017a), or otherwise through indirect influence of the altered expression of an as yet unidentified direct target of PyrSR.

2-3-8. Identification of the novel regulatory targets of PyrSR

Using gSELEX screening, I identified six binding sites for PyrR and eight possible regulatory targets. To examine regulation *in vivo* of all eight predicted targets by PyrR, I constructed the LUX reporter assay system for detection of promoter activity of all eight targets, and transformed into both wild-type and the *pyrR* mutant. Transformants were grown in M9-pyruvate medium, and the activity of promoters was measured at both log phase and stationary phase. In log phase, the promoter activity in the *pyrR* mutant decreased for *yhjX* and *ychC* (Fig. 2-7A), supporting the hypothesis that two targets are activated by PyrR. In contrast, the activity of *astC*, *xthA*, *yfjD*, *gltB*, *yghW* and *pbpC* increased in the absence of PyrR (Fig. 2-7A). Upon entry into stationary phase, the pyruvate level decreased after consumption this single carbon source, leading to inactivation of

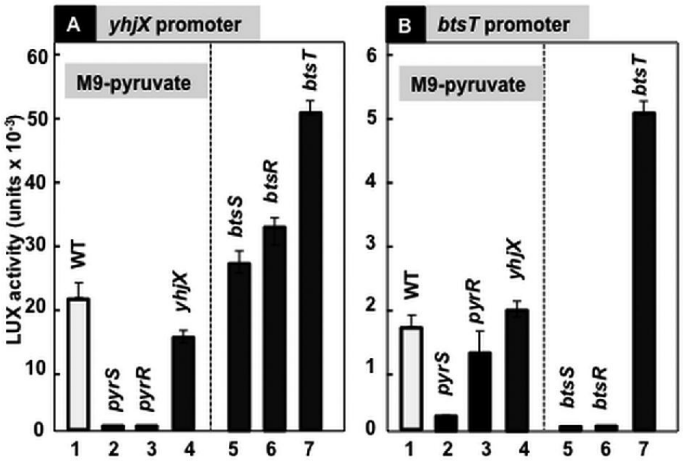

Figure 2-6. Regulatory roles of PyrSR on the *yhjX* and *btsT* promoter. [A] Regulatory roles of PyrSR on the *yhjX* promoter. Reporter plasmid pLUXyhjX was transformed into wild-type BW25113, *pyrS* mutant JW5388, *pyrR* mutant JW2378, *yhjX* mutant JW3516, *btsS* mutant JW5353, *btsR* mutant JW5352 and *btsT* mutant JW5791. Transformants were grown in M9–10 mM pyruvate medium, and LUX activity was measured after 3 h culture. **[B]** Regulatory roles of BtsSR on the *btsT* promoter. Reporter plasmid pLUXbtsT was transformed into the same set of *E. coli* as noted in A. LUX activity was measured under the same conditions as in **A**.

PyrR. As a result, the promoter level in the *pyrR* mutant is essentially the same with wild-type (Fig. 2-7B). PyrR is activated *in vivo* through phosphorylation by PyrS. I then examined possible influence of knockout on the newly identified PyrR targets. In the absence of PyrS, the level of both *yhjX* and *yhcC* promoters decreased (Fig. 2-7C), indicating the involvement of PyrS in the activation of these two promoters. On the other hand, the activity of *gltB* promoter increased in the absence of PyrS (Fig. 2-7C), supporting the repressor function of PyrS over the *gltB* promoter. The *astC* promoter was, however, not so much affected in the *pyrS* mutant (Fig. 2-7C), supposedly low affinity of this promoter to PyrR.

The reporter assays altogether indicate that PyrR is a dual regulator, working as an activator for *yhjX* and *yhcC*, and as a repressor for other six targets. Noteworthy is that two TCSs, PyrSR and BtsSR, recognize the same pyruvate as an inducer, but each recognizing different concentrations of pyruvate. I then propose a unique cross-talk between low-affinity PyrSR and high-affinity BtsSR at the stage 1 of TCS signal transduction (Fig. 2-8).

2-4. Discussion

2-4-1. Metabolic roles of pyruvate as an exometabolite

Pyruvate plays a key role for connection a variety of metabolic pathways. Reflecting its key regulatory role, multiple transport systems are involved in the dynamic control of homeostasis between intracellular and extracellular pyruvate levels (Lang *et al*. 1987; Fried *et al*. 2013). CstA

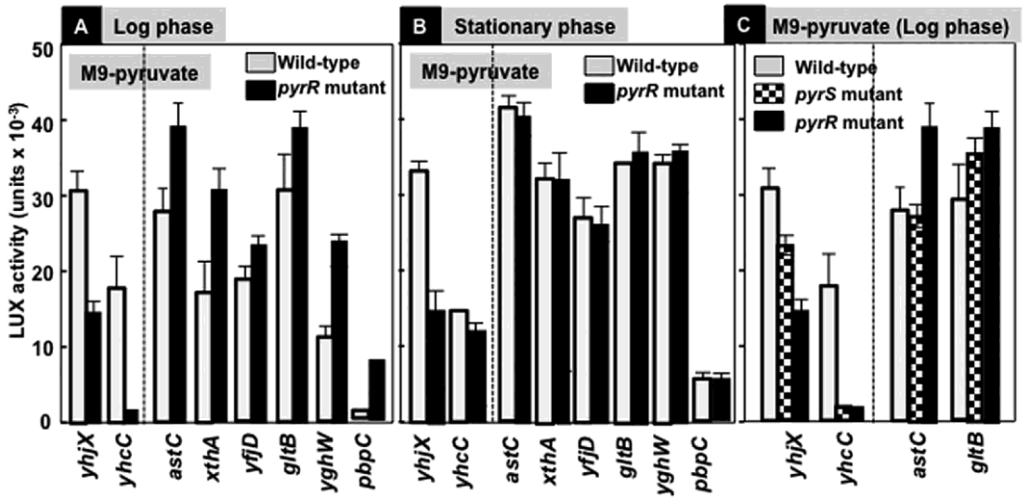

Figure 2-7. Influence of PyrSR on the promoter activity of newly identified regulatory targets. Reporter assay plasmids of all eight regulatory targets of PyrR (see Table 2-1) were transformed into wild-type BW25113 and *pyrR* mutant JW2378. Transformants were grown in M9–10 mM pyruvate, and LUX activity was measured in the middle of log phase (3 h culture) **(A)** or stationary phase (24 h culture) **(B)**. **[C]** Reporter assay was also performed for the set of three strains, wild-type, *pyrS* mutant and *pyrR* mutant. LUX activity was measured in the middle of exponential phase (3 h culture).

and YbdD, both functionally related to carbon starvation proteins, have been proposed to comprise the constitutive pyruvate transporter system in *E. coli* (Hwang *et al.* 2018). BtsT was proposed to be involved in uptake of amino acids/peptides or pyruvate (Kraxenberger *et al.*2012). Recently, however, BtsT was identified as an inducible pyruvate/H^+ symporter (Kristoficova *et al.* 2018). On the other hand, the membrane protein YhjX, the major target of PyrSR TCS, has also been implied to be involved in pyruvate uptake (Fried *et al*. 2013), but this hypothesis has not yet been proven. Here I confirmed the induction of *yhjX* expression by PyrSR in response to high concentrations of pyruvate. The protein–protein interaction assays *in vivo* suggested that the two systems, BtsT and YhjX, form a single and large signaling unit (Behr *et al*. 2014). The reporter assay indicated considerable interplay between the *yhjX* and *btsT* genes.

2-4-2. Regulatory targets of PyrR

By using gSELEX screening, I identified six binding sites for PyrR and predicted eight regulatory targets, which are involved in the modulation of structure and function of the membrane, including the major target YhjX transporter, PbpC (murein transglycosylase) and YghW (regulator of membrane fatty acid composition), and in the stress response to environmental conditions, including YhcC (putative membrane-associated Fe-S oxidoreductase) and XthA (exonuclease for repair). Two targets, GltBDF (glutamate biosynthesis) and AstCADBE (arginine degradation), are involved in the synthesis of glutamate. Pyruvate is integrated into TCA cycle via acetyl-CoA or

oxaloacetate. Glutamate is then formed by amination of α-ketoglutarate, an intermediate of TCA cycle, and thereafter most amino acids are synthesized through transamination using glutamate. Arginine is synthesized from glutamate via ornithine, and further degraded by AstABCDE enzymes for regeneration of glutamate. Taken together, I propose that the exometabolite pyruvate exerts a major influence on expression of a set of key operons for membrane modulation, stress response and synthesis of amino acids via glutamate.

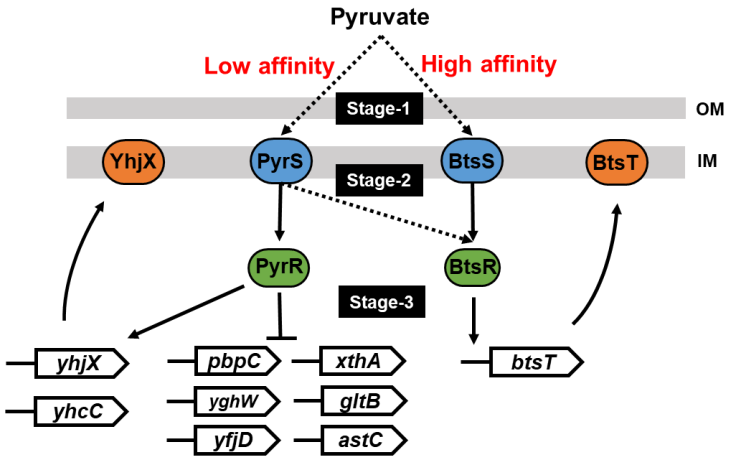

Figure 2-8. Overview of the proposed model. Both PyrSR and BtsSR sense the same pyruvate as an external inducer, indicating cross-talk at stage-1 of TCS signal transduction between PyrSR and BtsSR. However, PyrSR responds to high concentrations of pyruvate, while BtsSR responds to low concentrations of pyruvate. These results agree well with the previous report (Behr *et al*. 2017). Also, PyrSR possibly regulates the expression of the *btsT* gene through protein-protein interaction between PyrS and BtsR, suggesting a cross-talk at stage-2. I want to emphasize that two TFs regulate different sets of target genes.

2-4-3. Cross-talk between PyrSR and BtsSR

Although the majority of TCSs operate through strict cognate HK-RR interactions, certain levels of cross-talk have been proposed since the discovery of TCSs (Stock *et al*. 1989). Cross-talk of the TCS signal transduction takes place at all three stages: signal recognition by HK (stage 1), RR phosphorylation by HK (stage 2) and target recognition by RR (stage 3). Previously, the cross-talk at this stage 2 was analyzed by measuring TCS histidine kinase (HK)-dependent phosphorylation *in vitro* of TCS response regulator (RR) (Yamamoto *et al.* 2005). Among a total of 692 possible cross-talk pairs of RR phosphorylation *in vitro* between 25 HKs and 34 RRs, cross-talk was observed only for 3% pairs. In some TCSs, a single HK phosphorylates multiple RR targets while one RR can be phosphorylated by more than one HK (Laub and Goulian 2007). Also, the cross-talk at stage 3 between six NarL-family RRs, EvgA, NarL, NarP, RcsB, UhpA and UvrY (Yoshida *et al*. 2015) was analyzed. Through the cross-talk at stage 3, different TCSs, each sensing a different environment, converge in controlling the expression of the same target genes. In

agreement with the previous proposal by Steiner *et al.* (2018), I confirmed the TCS cross-talk at stage 1 for recognition of a single and the same exometabolite, pyruvate, between two HKs, PyrS and BtsS (Fig. 2-8). Noteworthy is that different sets of the genes are induced depending on the level of exometabolite pyruvate by two pyruvate-sensing TCSs, high-affinity BtsSR and low-affinity PyrSR. I then propose these two TCSs collaborate in sensing a single and the same exometabolite but controlling different sets of targets for its uptake and reutilization. Functional similarity between PyrR and BtsR is in good agreement with their structural similarity. BtsR shares essentially the same domain structure with PyrR with more than 30% sequence identity (Kraxenberget *et al.* 2012).

CHAPTER 3. FUNCTIONAL CLASSIFICATION OF THE TCS PROMOTERS

3-1. Introduction

In Chapter 2, I analyzed PyrSR (renamed from YpdAB) and identified the novel regulatory targets of PyrR, which are involved in uptake and reutilization of the exometabolite pyruvate. The analysis of PyrSR also suggested the TCS cross-talk at stage 1 between two TCS systems, PyrSR and BtsSR. According to these results, functional characterizations of whole TCS systems are deeply understood in *E. coli*.

Phenotype microarray assays of TCS mutants show that 22 TCS mutants have altered growth phenotypes (Zhou *et al*. 2003). Growth phenotypes are thought to result from a sophisticated signal transduction network by cross-talk among TCSs in *E. coli*. Glucose is one of the favorite carbon sources in *E. coli* because glucose has a high affinity for the phosphotransferase system (Postma *et al*. 1993; Deutscher *et al*. 2006). Glucose is directly catabolized into glycolysis and then is consumed through the tricarboxylic acid cycle (Deutscher *et al*. 2006). Catabolism of glucose occurs prior to metabolism of other carbon sources, resulting in catabolite repression by the regulatory networks that are induced by glucose (Stülke and Hillen 1999; Bettenbrock *et al*. 2006). *E. coli* also catabolizes glycerol by enzymatic reactions, which are mainly involved in a glycerol kinase and two glycerol-3-phosphate dehydrogenases (Lin 1976; Booth 2005). Metabolic flux analysis of *E. coli* chemostat culture in the presence of both glucose and glycerol shows that a high dilution rate of culture increases the glucose consumption rate, in which the level of the *arcA* transcript increases (Yao 2016), implying that TCSs largely contribute to adaptive growth in the presence of different carbon sources. Among the genes coding TCS factors of *E. coli*, 22 pairs of SK and RR genes are transcribed in a polycistronic fashion (Fig. 3-1). However, it is not clear which TCS genes are dominantly expressed in complex environments. To obtain comprehensive insight into the TCS promoter activity profile of *E. coli* growing under minimum nutrient conditions, I constructed a set of luciferase reporter plasmids that have TCS gene promoters. Systematic TCS promoter assays and principal component analysis was used to functionally classify TCS gene promoters of *E. coli* growing under different carbon source and temperature conditions.

3-2. Materials and Methods

3-2-1. *E. coli* strains, plasmids, oligonucleotides, and culture conditions

The used *Escherichia coli* strains, plasmids, and oligonucleotides were listed in Tables 3-1 and Appendix Table 1. *E. coli* cells harboring LUX reporter plasmids were grown in M9 medium.

Table 3-1. Bacterial strains and plasmids used in this study.

Name	Characterization	Reference
Strains		
W3110 type A	Wild type, complete σ set	Jishage and Ishihama, 1997
DH5α	F^- λ^- Φ80*lacZΔ*M15 Δ(*lacZYA-argF*)*U169 deoR recA1 endA1 hsdR17*(r_K-, m_K+) *phoA supE44 thi-1 gyrA96 relA1*	Takara Bio
Plasmids		
pLUX	*kan*, *luxCDABE*	Burton *et al.* 2010
pLUX-arcAp_1	pLUX, *arcA promoter-luxCDABE*	This study
pLUX-arcBp_10	pLUX, *arcB promoter-luxCDABE*	This study
pLUX-atoSp_12	pLUX, *atoS promoter-luxCDABE*	This study
pLUX-mdtAp_3	pLUX, *mdtA promoter-luxCDABE*	This study
pLUX-barAp_1	pLUX, *barA promoter-luxCDABE*	This study
pLUX-uvrYp_10	pLUX, *uvrY promoter-luxCDABE*	This study
pLUX-basRp_1	pLUX, *basR promoter-luxCDABE*	This study
pLUX-citAp_3	pLUX, *citA promoter-luxCDABE*	This study
pLUX-cpxRp_2	pLUX, *cpxR promoter-luxCDABE*	This study
pLUX-creAp_2	pLUX, *creA promoter-luxCDABE*	This study
pLUX-cusRp	pLUX, *cusR promoter-luxCDABE*	This study
pLUX-dcuSp_4	pLUX, *dcuS promoter-luxCDABE*	This study
pLUX-ompRp	pLUX, *ompR promoter-luxCDABE*	This study
pLUX-evgAp_1	pLUX, *evgA promoter-luxCDABE*	This study
pLUX-fimZp_1	pLUX, *fimZ promoter-luxCDABE*	This study
pLUX-zraSp_1	pLUX, *zraS promoter-luxCDABE*	This study
pLUX-kdpDp_1	pLUX, *kdpD promoter-luxCDABE*	This study
pLUX-narQp_1	pLUX, *narQ promoter-luxCDABE*	This study
pLUX-narPp_10	pLUX, *narP promoter-luxCDABE*	This study
pLUX-narXp_6	pLUX, *narX promoter-luxCDABE*	This study
pLUX-glnAp_5	pLUX, *glnA promoter-luxCDABE*	This study
pLUX-phoPp	pLUX, *phoP promoter-luxCDABE*	This study
pLUX-phoBp_3	pLUX, *phoB promoter-luxCDABE*	This study
pLUX-qseBp	pLUX, *qseB promoter-luxCDABE*	This study
pLUX-rcsDp_5	pLUX, *rcsD promoter-luxCDABE*	This study
pLUX-rcsBp_2	pLUX, *rcsB promoter-luxCDABE*	This study
pLUX-rcsCp_1	pLUX, *rcsC promoter-luxCDABE*	This study
pLUX-rstAp_1	pLUX, *rstA promoter-luxCDABE*	This study
pLUX-torSp_6	pLUX, *torS promoter-luxCDABE*	This study
pLUX-torRp_2	pLUX, *torR promoter-luxCDABE*	This study
pLUX-ivbLp_8	pLUX, *ivbL promoter-luxCDABE*	This study
pLUX-hprRp	pLUX, *hprR promoter-luxCDABE*	This study
pLUX-btsSp_1	pLUX, *btsS promoter-luxCDABE*	This study
pLUX-glrKp_2	pLUX, *glrK promoter-luxCDABE*	This study
pLUX-glrRp_4	pLUX, *glrR promoter-luxCDABE*	This study
pLUX-pyrSp_5	pLUX, *pyrS promoter-luxCDABE*	This study

3-2-2. Construction of Luciferase reporter plasmid

Luciferase reporter plasmids were constructed as previously described (Yamanaka *et al.* 2018; 2020). The promoter regions of each TCS genes (operons) were PCR amplified using the *E. coli* K-12 W3110 type A genome as the template and a pair of specific primers (listed in Appendix Table 1, see also Fig. 3-1). The amplified fragments were inserted into pLUX vectors (Burton *et al.* 2010) using the In-Fusion HD cloning kit (Takara Bio). The DNA sequence of insertion on the resulting plasmids was confirmed by DNA sequencing (Appendix Table 1). More information on the cloned TCS promoters is provided in Appendix Figure 1 and Appendix Table 2 in detail.

3-2-3. Lux reporter assay

Lux reporter assays were also performed as previously described (Yamanaka *et al*. 2018; 2020). Each lux reporter plasmid was used to transform *E. coli* K-12 W3110 type A. Transformants were inoculated in M9-glucose, M9-glycerol, or M9-glycolic acid medium containing 50 μg/mL kanamycin and then were shaken overnight at 30°C, 37°C, or 42°C. The cells were inoculated into fresh M9 medium containing glucose, glycerol, or glycolic acid as a single carbon source. The culture was incubated at 30°C, 37°C, or 42°C with shaking. Then, the cultures were collected at 2, 4, 6, and 8 hours, and were transferred into a 96-well microplate; turbidity ($OD_{600\ nm}$) and bioluminescence were measured with a plate reader MTP-880 (Corona). The promoter activity was evaluated as the ratio of luciferase activity to turbidity (LUX/OD). The assays were run in duplicate.

3-2-4. Principal component analysis

Principal component analysis (PCA) was performed with R software (https://www.R-project.org/). The dataset of 72 samples was prepared by 42 variable values, which were experiment number, culture time, culture temperature, three carbon sources, and 36 promoter activities except for PuvrY promoter. The loadings of the variable were calculated with the principal component scores, and then the scatter plot of PCA illustrated the correlation between PC1 and PC2 as the PCA biplot for two values of PC score of samples and loadings of variables. To examine the correlation coefficients for PCA and the original variable, factor analysis was also performed with R software (https://www.R-project.org/), calculating the loading factor.

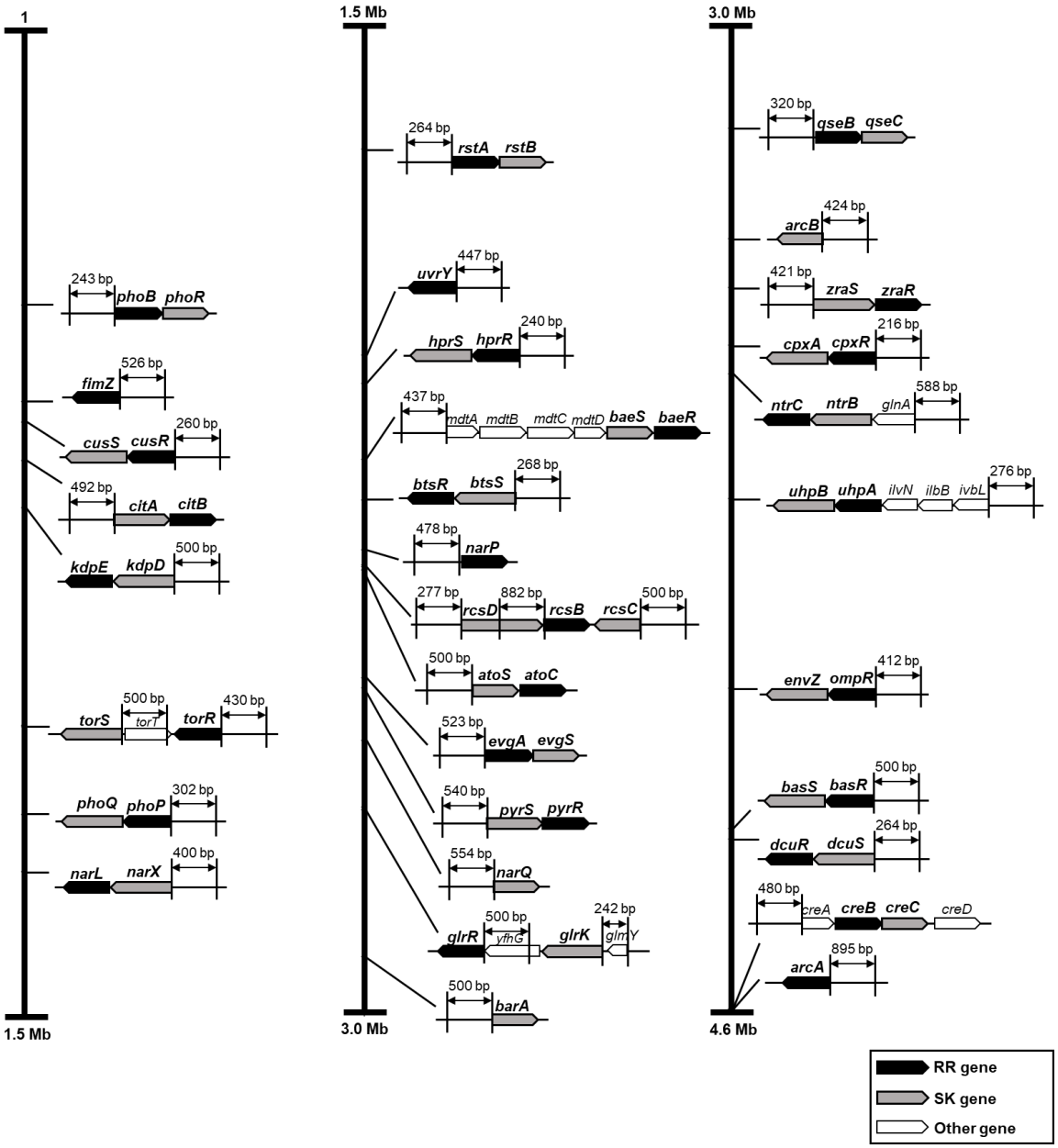

Figure 3-1. Two-component genes in the *E. coli* K-12 W3110 genome. All two-component system genes and their promoter regions in the *E. coli* K-12 W3110 genome (4.6 Mb) are shown with arrows and length (bp). Each arrow shows sensor kinase genes (gray), response regulator genes (black), and other genes in the operon (white). The direction of the arrows shows the direction of genes in the *E. coli* genome.

3-3. Results

3-3-1. Comprehensive lux reporter analysis of all TCS genes (operons) in *E. coli* K-12

The *Escherichia coli* K-12 genome predicates 34 RR genes and 30 SK genes for TCS. Among the total of 34 TCS genes, 22 pairs of cognate SK and RR are transcribed polycistronic fashion (Fig. 3-1). The remaining 14 genes are transcribed in a monocistronic fashion and are called

orphan genes (Fig. 3-1). To investigate the comprehensive expression profile of TCS genes in several environmental conditions, I used luciferase (lux) reporter system that is useful for high-throughput analysis without disrupting cells. The promoter-less reporter vector pLUX is a derivative of the pSC101 low copy replicon (Burton *et al.* 2010). I constructed a set of 36 lux reporter plasmids for all TCS gene-expressing promoters. The cloned promoters were upstream of the orphan gene and the first gene of the polycistronic transcription units, as described in Methods (Fig. 3-1). The parent strain, *E. coli* W3110 type A, was transformed by a set of 36 TCS lux reporter plasmids. Transformants were inoculated in M9 medium overnight, and each overnight culture was transferred into M9 medium containing glucose, glycerol, or glycolic acid as a single carbon source and grown at 30°C, 37°C, or 42°C with shaking. The cultures at 2, 4, 6, and 8 hours were then used in a lux assay. As a result, most TCS promoters were more or less activated *in vivo* at 37°C and 42°C, whereas the activities of half of 36 TCS promoters were not detected *in vivo* at 30°C (see below). Under all conditions tested in this study, only PuvrY, the *uvrY* promoter showed no activity (see below).

3-3-2. Functional grouping of TCS promoters by principal component analysis

To evaluate the functional features of the TCS promoters of *E. coli*, principal component analysis (PCA) was used with two sets of experimental data. The dataset was prepared with 72 components consisting of the activities of 36 promoters and the conditions of the number of experiments, the growth time, growth temperature, and three carbon sources. The PuvrY activity was removed from the dataset to avoid bias in the PCA calculation because some columns of the dataset had no values. The PCA analysis indicated 42 principal components (PCs), but no PCs could completely describe the characterization of TCS promoter activities (data not shown). PC1 showed the highest proportion of variance (23.4%), and PC2 explained 11.9% of the proportion of variance (Table 3-2). Twelve PCs (PC1~PC12) explained about 80% of all 72 data points. Next, the eigenvectors were calculated from PC1 and PC2 (Table 3-2), and then they were used to generate a scatter plot (Fig. 3-2). The biplot of the eigenvectors divided 35 promoters into 4 groups: Group I contained 12 promoters (PbtsS, PcpxR, PdcuS, PkdpD, PmdtA, PnarX, PompR, PphoP, PpyrS, PrstA, PtorR, and PzraS), Group II contained 7 promoters (ParcA, PglrK, PhprR, PivbL, PrcsB, PrcsC, and PtorS), Group III contained 7 promoters (ParcB, PatoS, PcreA, PcusR, PevgA, PglnA, and PrcsD), and Group IV contained 9 promoters (PbarA, PbasR, PcitA, PfimZ, PglrR, PnarP, PnarQ, PphoB, and PqseB); there was also a negative control (vector). To identify which factors determined this classification, a biplot of the principal component scores from PC1 and PC2 was created. The biplot showed two functional classifications featuring a carbon source and a growth temperature (Fig. 3-3). In the case of the carbon source, the spots of glucose varied on PC2, but the

Table 3-2. The results of PCA for TCS promoters.

Pricinpal component	PC1	PC2	PC3	PC4	PC5	PC6	PC7	PC8	PC9	PC10	PC11	PC12
Standard deviation	3.134	2.2346	1.80581	1.6615	1.53811	1.3733	1.30369	1.26189	1.14504	1.12883	1.07455	1.03872
Proportion of variance	0.2339	0.1189	0.07764	0.06573	0.05633	0.0449	0.04047	0.03791	0.03122	0.03034	0.02749	0.02569
Cumulative proportion	0.2339	0.3528	0.4304	0.49612	0.55245	0.5974	0.63782	0.67574	0.70695	0.73729	0.76479	0.79048
Eigenvector												
Time	0.005	-0.05	0.122	-0.045	0.219	-0.137	0.05	-0.122	0.105	-0.576	0.229	-0.11
Temp	-0.069	0.199	0.13	0.024	-0.279	-0.097	0.096	-0.207	0.272	-0.009	0.087	-0.111
glucose	-0.054	-0.205	-0.062	0.401	-0.11	-0.03	-0.137	-0.112	0.199	-0.016	0.124	0.114
glycerol	-0.156	0.113	-0.067	-0.357	0.236	0.03	-0.14	-0.142	-0.096	0.071	0.059	0.008
glycolic acid	0.21	0.092	0.129	-0.043	-0.126	0	0.277	0.254	-0.103	-0.055	-0.183	-0.122
Hours	-0.118	0.036	-0.025	0.169	0.119	-0.015	0.417	0.267	-0.026	0.036	0.131	-0.194
vector	-0.049	0.017	-0.159	-0.084	-0.126	-0.029	0.177	0.095	-0.328	0.09	0.434	0.333
ParcA	-0.231	-0.055	-0.202	-0.142	0.061	0.022	-0.071	-0.047	0.19	-0.068	0.094	-0.1
ParcB	-0.107	-0.287	0.335	-0.116	-0.076	-0.079	0.047	0.033	-0.087	0.09	0.054	-0.017
PatoS	-0.053	-0.35	0.267	-0.128	-0.101	-0.082	0.036	-0.001	-0.108	0.096	0.034	-0.032
PmdtA	-0.169	0.164	0.269	0.055	0.097	0.03	0.007	0.09	-0.09	0.006	-0.009	0.023
PbarA	0.011	-0.028	0.058	-0.102	0.098	-0.055	-0.183	-0.084	-0.132	-0.146	0.109	0.574
PbasR	-0.036	0.039	0.196	0.015	0.042	-0.075	0.158	0.207	0.07	-0.248	0.112	-0.212
PcitA	0.055	0.027	0.087	-0.096	-0.209	0.625	-0.008	-0.076	0.022	-0.103	0.103	-0.015
PcpxR	-0.267	0.127	0.053	0.031	-0.08	-0.044	-0.063	-0.089	0.058	-0.029	-0.002	0.032
PcreA	-0.057	-0.337	0.292	-0.124	-0.125	-0.009	0.043	-0.004	-0.102	0.07	0.047	-0.02
PcusR	-0.161	-0.309	-0.091	-0.038	-0.1	0.016	-0.131	0.127	0.081	-0.046	-0.042	-0.075
PdcuS	-0.188	0.171	0.242	0.077	0.028	0.047	-0.056	0.116	0.084	0.008	-0.103	0.172
PompR	-0.19	0.067	-0.147	-0.216	-0.148	-0.062	0.117	-0.08	-0.023	-0.034	-0.237	-0.07
PevgA	-0.135	-0.351	0.117	-0.04	-0.141	-0.072	-0.007	-0.111	0.016	0.042	-0.107	-0.027
PfimZ	0.047	0.022	0.077	-0.076	-0.244	0.613	0.02	-0.105	0.024	-0.062	0.108	-0.055
PzraS	-0.078	0.11	0.251	-0.052	0.102	0.06	-0.017	0.134	0.103	-0.359	0.006	0.229
PkdpD	-0.249	0.173	0.136	0.149	-0.068	-0.045	0.004	-0.119	0.044	0.076	0.091	0.001
PnarQ	-0.02	0.023	0.023	0.144	-0.084	-0.077	0.093	-0.102	0.345	0.308	0.455	-0.011
PnarP	-0.01	-0.048	-0.044	-0.04	0.37	0.159	0.401	-0.26	0.09	0.135	-0.074	0.081
PnarX	-0.209	0.134	0.173	-0.034	0.018	-0.051	-0.091	-0.139	0.073	0.033	0.063	-0.051
PglnA	-0.066	-0.267	-0.096	0.259	0.084	0.153	-0.123	0.258	0.051	-0.09	-0.073	0.048
PphoP	-0.13	0.059	0.023	0.33	-0.081	0.022	0.003	-0.207	-0.419	0.033	-0.102	-0.074
PphoB	0.021	0	-0.01	-0.059	0.186	0.018	-0.243	-0.041	-0.211	0.046	0.327	-0.464
PqseB	-0.03	-0.005	-0.014	0.224	-0.057	-0.032	0.033	-0.313	-0.377	-0.332	-0.014	-0.121
PrcsD	-0.038	-0.198	0.015	0.043	0.349	0.168	0.38	-0.14	0.054	0.038	-0.036	0.083
PrcsB	-0.251	-0.054	-0.085	-0.048	0.057	0.043	0.083	-0.222	0.07	0.034	-0.22	0.008
PrcsC	-0.246	-0.136	0.018	-0.101	0.042	0.026	0.135	0.029	-0.016	-0.02	0.064	0.074
PrstA	-0.248	0.08	0.013	0.075	0.009	0.091	-0.008	0.243	0.023	0.053	-0.068	0.012
PtorS	-0.227	-0.094	-0.178	-0.029	-0.087	0.021	0.011	0.081	0.045	-0.226	-0.078	-0.106
PtorR	-0.236	0.127	0.109	0.03	-0.007	0.028	-0.029	0.092	0.059	-0.021	-0.053	0.042
PivbL	-0.149	-0.058	0.027	0.061	0.384	0.187	-0.287	0.05	-0.08	0.121	0.088	-0.162
PhprR	-0.185	-0.031	-0.23	0.025	-0.014	0.112	-0.075	0.304	0.03	0.028	0.001	0.023
PbtsS	-0.216	0.175	0.139	0.028	0.014	0.044	0.016	0.076	-0.262	0.214	-0.063	-0.015
PglrK	-0.226	-0.002	-0.256	-0.093	-0.165	-0.054	0.091	-0.147	-0.021	-0.1	-0.091	-0.026
PglrR	-0.078	-0.081	-0.1	0.401	-0.012	0.077	0.113	-0.024	-0.101	-0.106	0.114	0.116
PpyrS	-0.159	0.038	-0.229	-0.216	-0.146	-0.048	0.166	0.159	-0.145	-0.102	0.304	0.021

spots of glycerol were more scattered on PC1 even though some of the spots overlapped each other (Fig. 3-3A). The spots of glycolic acid mostly plotted together. On the other hand, in the case of growth temperature, the spots of three classifications (30°C, 37°C, and 42°C) varied on PC2 at 30°C and on PC1 at 42°C despite them being partially overlapping (Fig. 3-3B). In good agreement with the biplots of the principal component score, the grouping of TCS promoters by eigenvectors

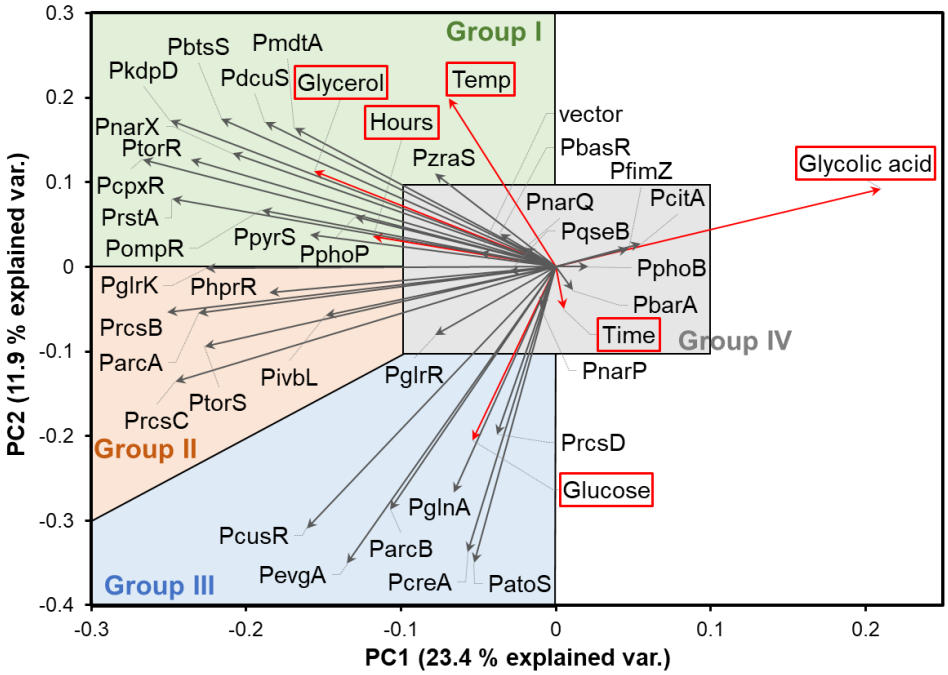

Figure 3-2. The biplot of eigenvectors produced by principal component analysis. Based on the lux reporter assay data (see Fig. 3-4), a principal component analysis was performed with R software to characterize TCS promoters. The PuvrY activity was removed from the dataset to avoid bias in the PCA calculation because the dataset had columns with no values. The analysis indicated 42 principal components (PCs), and no PCs could completely describe the characterization of TCS promoter activities (see Table 3-2). PC1 showed the highest proportion of variance (23.4%), and PC2 was responsible for 11.9% of the proportion of variance. Computed eigenvectors of both environmental conditions and promoters were plotted and compared in a graph using PC1 (shown on the x-axis) and PC2 (shown on the y-axis). The plotted eigenvectors (gray arrows, see Table 3-2) showed four promoter groups (Group I-IV, colored with green, orange, blue, and gray, respectively). The eigenvector of each growth condition (Glucose, Glycerol, Glycolic acid, Temp., Hours, and Time) is shown in a red square.

consisted of the functional classifications for carbon source and growth temperature (Figs. 3-2 and 3-3). Thus, Group I is related to growth temperatures or glycerol, and Group III is related to glucose.

3-3-3. Expression pattern of functional TCS promoter groups *in vivo*

PCA predicted four functional groups: Group I showed induction of the promoter by both higher temperature and glycerol; Group II showed induction of the promoter by 37°C; Group III was related to both lower temperature and glucose; and Group IV showed no significantly induced promoter activity based on either temperature or carbon source, except for PglrR. To confirm the functional grouping of TCS promoter activity, the time course pattern of expression from promoters in each group was examined by lux reporter assays (Fig. 3-4). Most of the 12 Group I promoters were highly induced in the presence of glycerol at 42°C (Fig. 3-4A). However, the strength of the PpyrS and PompR promoters was maximal at 37°C, and the PphoP promoter strength was maximal in the presence of glucose (Fig. 3-4A). Among 12 Group I promoters, the activities of PcpxR and

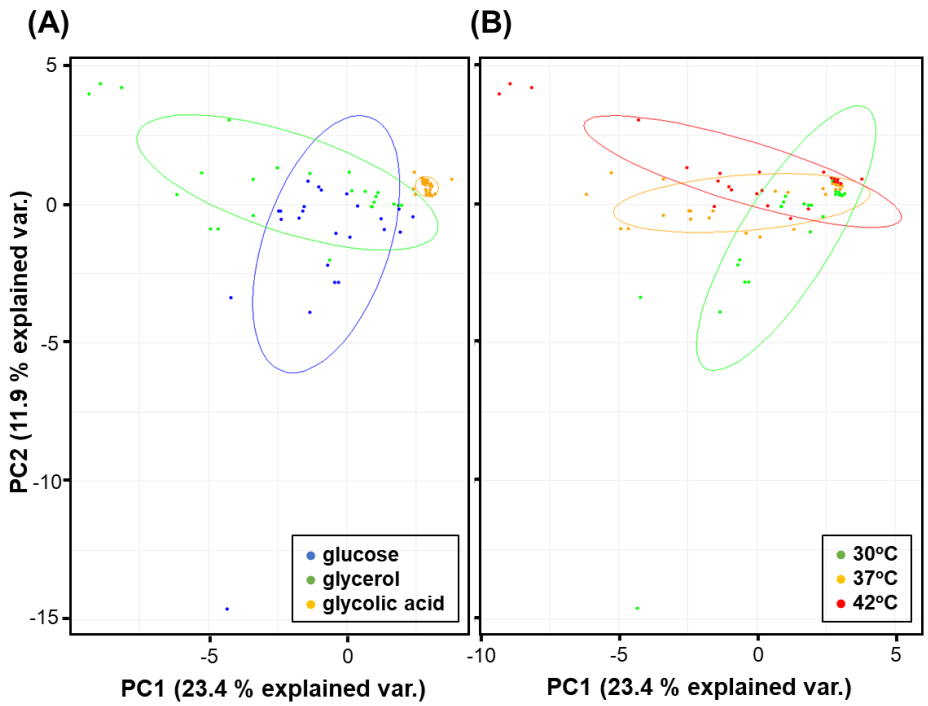

Figure 3-3. Two biplots of principal component scores from principal component analysis. PCA was performed as described in Fig. 3-2. Computed principal component scores (shown in **A** and **B**) of both environmental conditions and promoters were plotted and compared in a graph using PC1 (shown on the x-axis) and PC2 (shown on the y-axis). **[A]** The plotted principal component scores were divided into three groups depending on three carbon sources: glucose (blue), glycerol (green), and glycolic acid (orange). **[B]** The plotted principal component scores were divided into three groups depending on temperature: 30°C (green), 37°C (orange), and 42°C (red).

PnarX increased throughout growth time, whereas 3 promoters, PrstA, PtorR, and PkdpD, were induced 4 hours after incubation; 7 promoters, PpyrS, PbtsS, PdcuS, PompR, PmdtA, PphoP, and PzraS were induced 6 hours later (Fig. 3-4A). Group II promoters were activated in the presence of glucose or glycerol in the temperature-independent manner (Fig. 3-4B). Overall, 3 of 7 Group III promoters, PglnA, PcusR, and PevgA, were relatively more increased at 30°C and 37°C than they were at 42°C (Fig. 3-4C). The rest of the Group III promoters, ParcB, PcreA, PrcsD, and PatoS, were activated 4 hours after incubation at 30°C. The activity of PglnA was only induced in the presence of glucose. Group IV promoters had low or no activities in each condition, except for PglrR (Fig. 3-4D). PglrR showed higher activity in the presence of glucose. These experimental results were in good agreement with the predictions made by PCA.

3-3-4. Further classification from factor loadings

PC1 and PC2 contribute 23.4% or 11.9% of the promoter activity data. To clarify the correlation between principal component score and eigenvector value of PCs, I calculated the coefficient of correlation as factor loading in each PC (Table 3-3). In the case of PC1, twenty-one

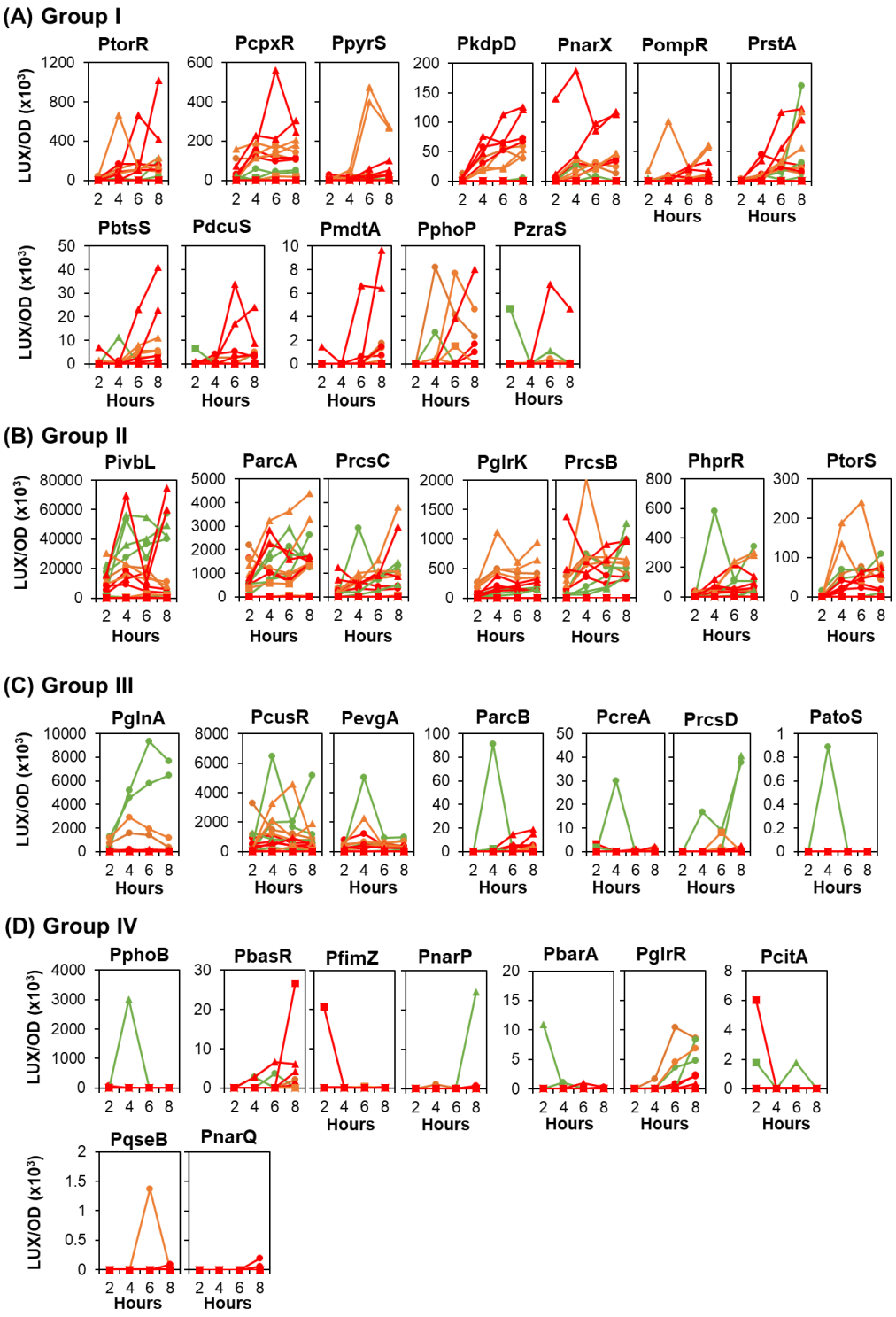

Figure 3-4. *E. coli* TCS promoter activities of *in vivo*. The promoter regions of TCS genes (operons) are shown in Fig. 3-1 and Appendix Figure 1. The PCR-amplified promoter regions of each TCS gene (operon) were inserted into pLUX vectors (Burton *et al*. 2010) to construct a set of lux reporter plasmids. Lux reporter assays were performed as previously described (Yamanaka *et al*. 2020). *E. coli* K-12 W3110 type A was transformed with each lux reporter plasmid. Transformants were inoculated in M9 medium and then were inoculated into fresh M9 medium containing glucose (circles), glycerol (triangles), or glycolic acid (squares) as a single carbon source. The cultures were then incubated at 30°C (green), 37°C (orange), or 42°C (red) with shaking. Then, the cultures were collected at 2, 4, 6, and 8 hours and were transferred into a 96-well microplate. The turbidity ($OD_{600\ nm}$) and bioluminescence were measured with a plate reader MTP-880 (Corona). The promoter activity was evaluated as the ratio of LUX/OD.

of the components showed valid correlations, having coefficients of correlation of less than -0.4 (Table 3-3). Glycerol showed a negative correlation and Glycolic acid showed a positive correlation. In addition to the correlation of growth conditions, a negative correlation was found in 20 TCS promoters (ParcA, PmdtA, PcpxR, PcusR, PdcuS, PompR, PevgA, PkdpD, PnarX, PphoP, PrcsB, PrcsC, PrstA, PtorS, PtorR, PivbL, PhprR, PbtsS, PglrK, and PpyrS). These results indicate that PC1 could group the TCS promoters for activation in the presence of glycerol (Table 3-3). On the other hand, a temperature and glucose showed positive or negative correlations with PC2, indicating that 7 TCS promoters (ParcB, PatoS, PcreA, PcusR, PevgA, PglnA, and PrcsD) with negative correlations could be activated in the presence of glucose at lower temperature. PglnA, PphoP, and PglrR positively correlated with PC4, indicating that these promoters are induced in the presence of glucose (Table 3-3). Additionally, PC5 explained the contribution by growth temperature and 3 of the TCS promoter activities (PnarP, PrcsD, and PivbL).

3-4. Discussion

I first determined the profile of all TCS promoters in *E. coli* growing under minimum nutrient conditions *in vivo* by employing a luciferase reporter system and PCA analysis. The profile shows two functional groups of TCS promoters featuring temperature and carbon source conditions. The results summarizing the expression features of *E. coli* TCS promoters *in vivo* are shown in Table 3-4. As unexpected, TCS promoter classification showed a correlation between growth temperature and the availability of carbon sources. Group I promoters were activated by a high temperature and the presence of glycerol that is poorly catabolized in *E. coli* (Table 3-4). On the other hand, Group II promoters were activated by both glucose and glycerol availability, which is accessible for *E. coli* (Table 3-4). The 7 promoters in Group III were induced in the presence of glucose at lower temperature. This implies that glycerol-inducing promoters could be activated by higher thermal energy with and without catabolite repression, whereas glucose-inducing promoters could not require much thermal energy.

Twelve TCS promoters belonged to Group I (Fig. 3-2 and Table 3-4). PbtsS, one of the Group I promoters, was activated by high temperature and glycerol (Fig. 3-4A and Table 3-4). BtsSR, expressed from PbtsS, is similar to PysSR, thereby cross-talking between BtsSR and PysSR for pyruvate reutilization (Behr *et al.* 2017; Miyake *et al.* 2019). The activity of the PpyrS promoter was only significantly changed by the presence of glycerol at 37°C (Table 3-4). This difference between the PbtsS and PpyrS promoters could indicate that BtsSR senses extracellular pyruvate more sensitively than PysSR (Behr *et al.* 2017; Miyake *et al.* 2019). The activity of ParcA in the presence of glycerol was higher at a high temperature than it was in the presence of glucose (Fig. 3-4B). This result agrees that the level of *arcA* mRNA increases when *E. coli* favors glycerol as a

Table 3-3. Factor loading of specific principal components

Principal component	PC1	PC2	PC4	PC5
Temperature	-0.21682472	**0.44427142**	0.03986384	**-0.42888704**
Glucose	-0.16983160	**-0.45825497**	**0.66577691**	-0.16929370
Glycerol	**-0.48782337**	0.25298397	**-0.59386148**	0.36304836
Glycolic acid	**0.65765498**	0.20527100	-0.07191543	-0.19375466
vector	-0.15224173	0.03729441	-0.13971391	-0.19446134
ParcA	**-0.72524872**	-0.12259723	-0.23633934	0.09418658
ParcB	-0.33489621	**-0.64057691**	-0.19308489	-0.11728429
PatoS	-0.16537781	**-0.78175930**	-0.21197194	-0.15500712
PmdtA	**-0.52824881**	0.36543623	0.09116987	0.14932349
PbarA	0.03380565	-0.06270781	-0.16957044	0.15093316
PbasR	-0.11347753	0.08781539	0.02560787	0.06487884
PcitA	0.17307228	0.05942230	-0.15919346	-0.32173626
PcpxR	**-0.83782393**	0.28345525	0.05147703	-0.12322616
PcreA	-0.17724067	**-0.75259792**	-0.20657494	-0.19162280
PcusR	**-0.50594822**	**-0.69108525**	-0.06330238	-0.15420133
PdcuS	**-0.58785176**	0.38143737	0.12834624	0.04371870
PompR	**-0.59568728**	0.14954498	-0.35820574	-0.22731693
PevgA	**-0.42299651**	**-0.78485256**	-0.06673456	-0.21673122
PfimZ	0.14665881	0.04959664	-0.12647768	-0.37482406
PzraS	-0.24568951	0.24689120	-0.08698115	0.15752979
PkdpD	**-0.78009920**	0.38643648	0.24833633	-0.10501359
PnarQ	-0.06195891	0.05214700	0.23941801	-0.12947539
PnarP	-0.02979450	-0.10722257	-0.06661888	**0.56885772**
PnarX	**-0.65628308**	0.29985979	-0.05637997	0.02754385
PglnA	-0.20768242	**-0.59722891**	**0.42983936**	0.12968686
PphoP	**-0.40693119**	0.13166264	**0.54884419**	-0.12442542
PphoB	0.06617775	-0.00045573	-0.09786426	0.28604017
PqseB	-0.09391094	-0.01032019	0.37194516	-0.08727420
PrcsD	-0.11869908	**-0.44200406**	0.07188664	**0.53751540**
PrcsB	**-0.78598553**	-0.12063795	-0.07895795	0.08750806
PrcsC	**-0.77185969**	-0.30435668	-0.16807518	0.06476447
PrstA	**-0.77783688**	0.17939564	0.12417837	0.01379246
PtorS	**-0.71254280**	-0.21069616	-0.04806227	-0.13329863
PtorR	**-0.73889466**	0.28489481	0.05007823	-0.01012738
PivbL	**-0.46774791**	-0.12957261	0.10128944	**0.59097901**
PhprR	**-0.57988093**	-0.06872313	0.04083956	-0.02165839
PbtsS	**-0.67657290**	0.39136564	0.04703742	0.02100707
PglrK	**-0.70848266**	-0.00376705	-0.15393446	-0.25397489
PglrR	-0.24526494	-0.18190787	**0.66560389**	-0.01920670
PpyrS	**-0.49872607**	0.08538516	-0.35897598	-0.22415198

The positive or negative corelated factors are shown in red (factor loading >0.4) or blue (factor loading <-0.4), respectively.

Table 3-4. Summary of the feature of all *E. coli* TCS promoter.

Promoter	Group	Temperature	Carbon sources		
			Glucose	Glycerol	Glycolic acid
PbtsS	**I**	↑ (higher temp.)		↑	
PcpxR	**I**	↑ (higher temp.)	↑	↑	
PdcuS	**I**	↑ (higher temp.)		↑	
PkdpD	**I**	↑ (higher temp.)	↑	↑	
PmdtA	**I**	↑ (higher temp.)		↑	
PnarX	**I**	↑ (higher temp.)		↑	
PompR	**I**	↑ (mid temp.)		↑	
PphoP	**I**	↑ (higher temp.)	↑	↑	
PpyrS	**I**	↑ (mid temp.)		↑	
PrstA	**I**	↑ (higher temp.)		↑	
PtorR	**I**	↑ (higher temp.)		↑	
PzraS	**I**			↑	
ParcA	**II**		↑	↑	
PglrK	**II**		↑	↑	
PhprR	**II**		↑	↑	
PivbL	**II**		↑	↑	
PrcsB	**II**		↑	↑	
PrcsC	**II**		↑ (lower temp.)	↑	
PtorS	**II**		↑	↑	
ParcB	**III**	↑ (low temp.)	↑		
PatoS	**III**	↑ (low temp.)	↑		
PcreA	**III**	↑ (low temp.)	↑		
PcusR	**III**	↑ (lower temp.)	↑	↑ (mid temp.)	
PevgA	**III**	↑ (lower temp.)	↑	↑ (mid temp.)	
PglnA	**III**	↑ (lower temp.)	↑		
PrcsD	**III**	↑ (low temp.)	↑		
PbarA	**IV**				
PbasR	**IV**				↑ (late phase)
PcitA	**IV**				↑ (early phase)
PfimZ	**IV**				↑ (early phase)
PglrR	**IV**		↑		
PnarP	**IV**				
PnarQ	**IV**				
PphoB	**IV**	↑ (lower temp.)		↑	
PqseB	**IV**				

carbon source (Yao *et al*. 2016). However, the *arcB* promoter, which drives the expression of the cognate SK ArcB of ArcA, was sorted into Group III but not Group II. Previous work with phenotype microarrays showed that the growth phenotypes of the *arcA* and *arcB* mutants did not completely overlap (Zhou *et al*. 2003). Transcriptome analysis also showed a difference in the genome expression profile when comparing the *arcA* and *arcB* mutants (Oshima *et al*. 2002). This

evidence suggests that ArcA is activated not only by ArcB but also by other SKs. Group III included all 7 promoters, PglnA, PcusR, PevgA, ParcB, PcreA, PrcsD, and PatoS, that were activated in the presence of glucose at low or middle temperature (Fig. 3-4C and Table 3-4), suggesting that *E. coli* could induce the biosynthesis of such TCS factors from Group III promoters throughout growth by catabolism of glucose. Group III promoters regulated the expression of ArcB, AtoSC, CreBC, CusSR, EvgSA, NtrBC, and RcsDB (Fig. 3-1), and they are controlled by different sigma factor(s). PcusR and PrcsD are regulated by sigma 70 (Franke *et al*. 2001; Krin *et al*. 2010). The PglnA promoter is known to be dually controlled by both sigma 54 and sigma 70 (Tian *et al*. 2001; Reichenbach *et al*. 2009). Two of three sigma factors (sigma 70, sigma 32, or sigma 38) contribute to regulating the gene expression levels of PcreA and PevgA (Amemura *et al*. 1986; Nonaka *et al*. 2006; Tanabe *et al*. 1998). The specific sigma factors for ParcB and PatoS are unknown. Among Group III promoters, correlation analysis by factor loadings indicated that two promoters (PcusR and PevgA) were more highly activated in the presence of glycerol (Table 3-3). These promoters are positively regulated by sigma 70.

No activity of PuvrY was found under any growth conditions in this study (Fig. 3-4D). UvrY is a response regulator that regulates a set of genes involved in DNA repair or carbon metabolism under any nutrient conditions (Suzuki *et al*. 2002; Zere *et al*. 2015). One possibility is that a small level of *uvrY* mRNA is significantly translated into UvrY protein *in vivo*. A recent report showed that the *uvrY* transcript is activated by the RNA-binding protein CsrA (Camacho *et al*. 2015). In addition to the *uvrY* promoter, the strength of several TCS promoters is known to be not directly reflected by the translational level of TCS factors in *E. coli*. Quantitative western blotting for transcription factors of *E. coli* K-12 showed the following decreasing order for the intracellular response regulators: PhoP -> PhoB -> CitB -> OmpR -> NarL -> CpxR -> UhpA -> RstA -> EvgA -> KdpE -> TorR -> UvrY -> QseB -> ArcA (Ishihama *et al*. 2014); these expression results were not correlated with the order of promoter strength measured in this study. All of the TCS promoter strengths measured here might not necessarily reflect the level of mRNAs and/or proteins of TCS because the promoter strength might depend on positive feedback regulation. To date, several TCS genes have been found to be post-transcriptionally regulated by small RNAs, most of which access mRNA of TCS genes to control translation by ribosomes. For example, *phoP* mRNA binds to two species of small RNAs, MicA and GcvB (Coornaert *et al*. 2010; 2013). Additionally, *ompR* mRNA binds to two species of small RNAs, OmrA and OmrB, which are activated by EnvZ-OmpR, creating a negative feedback loop regulation (Guillier and Gottesman 2008). The small RNA GcvB is also suggested to repress the *fimZ* gene in *E. coli* and *Salmonella typhimurium* (Pulvermacher *et al*. 2009). FimZ is the regulator of fimbriae in *S. typhimurium* and biofilm formation in *E. coli* (Saini *et al*. 2009; Domka *et al*. 2007). FimZ also increases the resistance to kanamycin and β-lactam antibiotics in *E. coli* by overexpressing the FimZ protein

(Hirakawa *et al*. 2003; 2003a). Since the *E. coli* strain used in this study carried the kanamycin-resistant plasmid pLUX, PfimZ was probably not transcribed for kanamycin resistance and was also repressed by GcvB at the posttranscriptional level under all conditions examined in this study.

Taken together, PCA of the comprehensive lux reporter assay is useful for classifying promoters by functional activity *in vivo*, which is believed to provide us with genetic information to enable analysis of unknown TCS functions in *E. coli*.

CHAPTER 4. THE HOMOLOGOUS SEQUENCE INTEGRATION (HOSEI) METHOD FOR MULTI-GENE KNOCKOUT IN THE *E. COLI* GENOME

4-1. Introduction

Bacteria survive in the environment with three systems: a system for sensing environmental conditions, a system for responding to sensed signals, and an adaptation system for proper survival in the environment. An adapting bacterial cell performs cell division to increase the number of sister cells, termed adaptive growth. Two-component systems (TCSs), representing the main bacterial signal transduction systems, consist of a pair of one sensor kinase (SK) and one response regulator (RR), and RR genes are highly conserved in most bacterial genomes as part of the core genome. The *Escherichia coli* genome has an estimated 34 RR genes and 30 SK genes in total. To reveal the contribution of TCSs for the fast growth as an adaptive growth strategy of *E. coli*, multi-gene knockout strains are required in addition to single-gene knockout strains.

Here, the novel genome editing technology, the HoSeI (Homologous Sequence Integration) method, was developed based on CRISPR-Cas9. This newly developed system isolated a set of gene knockout strains including the all 34 RR genes knockout strain and the all 30 SK gene knockout strain.

4-2. Materials and Methods

4-2-1. *E. coli* strains, plasmids, oligonucleotides, culture conditions

The used *E. coli* strains, plasmids, and oligonucleotides are listed in Table 4-1, Table 4-2, Appendix Table 3, and Appendix Table 4, respectively. *E. coli* K-12 W3110 type A strain was used as a parent type (Jishage and Ishihama. 1997). *E. coli* strains were grown in M9-glucose or LB medium.

Table 4-1. Bacterial strains used in this study.

Name	Characterization	Number of deprived RR/SK genes	Reference
W3110 typeA	Parent strain, complete σ set	0	Jishage *et al.* 1997
YMA00201	W3110 typeA, *phoB* (P29X)	1	This study
YMA02201	YMA00201, *phoP* (G53X)	2	This study
YMA02302	YMA02201, *ompR* (L16X)	3	This study
YMA02601	YMA02302, *citB* (L16X)	4	This study

Table 4-1. Bacterial strains used in this study. (Continued.)

Name	Characterization	Number of deprived RR/SK genes	Reference
YMA04701	YMA02601, *narL* (P16X)	5	This study
YMA04814	YMA04701, *cpxR* (R11X)	6	This study
YMA04901	YMA04814, *uhpA* (G16X)	7	This study
YMA05001	YMA04901, *rstA* (L21X)	8	This study
YMA05103	YMA05001, *evgA* (R40X)	9	This study
YMA05201	YMA05103, *kdpE* (T19X)	10	This study
YMA05401	YMA05201, *torR* (P12X)	11	This study
YMA05601	YMA05401, *uvrY* (G31X)	12	This study
YMA05701	YMA05601, *qseB* (G33X)	13	This study
YMA07601	YMA05701, *arcA* (A25X)	14	This study
YMA07701	YMA07601, *atoC* (P49X)	15	This study
YMA07806	YMA07701, *baeR* (P11X)	16	This study
YMA07901	YMA07806, *ntrC* (G25X)	17	This study
YMA08001	YMA07901, *rcsB* (P13X)	18	This study
YMA08108	YMA08001, *pyrR* (Q25X)	19	This study
YMA08201	YMA08108, *btsR* (P11X)	20	This study
YMA08302	YMA08201, *creB* (L19X)	21	This study
YMA08401	YMA08302, *basR* (T22X)	22	This study
YMA08601	YMA08401, *cusR* (G19X)	23	This study
YMA08701	YMA08601, *narP* (A38X)	24	This study
YMA08801	YMA08701, *zraR* (H17X)	25	This study
YMA09703	YMA08801, *rssB* (W26X)	26	This study
YMA09801	YMA09703, *glrR* (P15X)	27	This study
YMA09901	YMA09801, *fimZ* (P13X)	28	This study
YMA10005	YMA09901, *ygeK* (P13X)	29	This study
YMA10101	YMA10005, *dcuR* (P25X)	30	This study
YMA10801	YMA10101, *yhjB* (G26X)	31	This study
YMA11402	YMA10801, *cheB* (S12X)	32	This study
YMA11501	YMA11402, *cheY* (T16X)	33	This study
YMA11623	YMA11501, *hprR* (Q13X)	34	This study
SSA00515	W3110 typeA, *cusS* (R15X)	1	This study
SSA00701	SSA00515, *zraS* (V21X)	2	This study
SSA00904	SSA00701, *kdpD* (L14X)	3	This study
SSA01102	SSA00904, *phoQ* (T50X)	4	This study
SSA01202	SSA01102, *basS* (W32X)	5	This study
SSA02601	SSA01202, *baeS* (L14X)	6	This study
SSA02702	SSA02601, *cpxA* (W14X)	7	This study
SSA02801	SSA02702, *envZ* (A13X)	8	This study
SSA03001	SSA02801, *evgS* (T17X)	9	This study
SSA03102	SSA03001, *glrK* (L17X)	10	This study
SSA03201	SSA03102, *qseC* (A32X)	11	This study
SSA03302	SSA03201, *rcsC* (T10X)	12	This study
SSA03401	SSA03302, *rcsD* (L31X)	13	This study
SSA03502	SSA03401, *rstB* (L22X)	14	This study

Table 4-1. Bacterial strains used in this study. (Continued.)

Name	Characterization	Number of deprived RR/SK genes	Reference
SSA03601	SSA03502, *hprS* (G22X)	15	This study
SSA03701	SSA03601, *atoS* (M19X)	16	This study
SSA03801	SSA03701, *barA* (L15X)	17	This study
SSA03901	SSA03801, *creC* (A24X)	18	This study
SSA04001	SSA03901, *ntrB* (L27X)	19	This study
SSA04102	SSA04001, *phoR* (L19X)	20	This study
SSA04205	SSA04102, *uhpB* (A20X)	21	This study
SSA04301	SSA04205, *btsS* (Q35X)	22	This study
SSA04401	SSA04301, *pyrS* (L22X)	23	This study
SSA04504	SSA04401, *arcB* (L20X)	24	This study
SSA04601	SSA04504, *citA* (L37X)	25	This study
SSA04701	SSA04601, *dcuS* (P14X)	26	This study
SSA04801	SSA04701, *narQ* (R13X)	27	This study
SSA04902	SSA04801, *narX* (Q14X)	28	This study
SSA05001	SSA04902, *torS* (L15X)	29	This study
SSA05102	SSA05001, *cheA* (L20X)	30	This study

4-2-2. Construction of sgRNA expression plasmid

To construct the sgRNA expression vector plasmid, 227 bp of the DNA sequence of the promoter and sgRNA was referred to as the pTarget series harboring sgRNAs constructed by previous work (Jiang *et al.* 2015). The designed 227 bp DNA sequence introducing the *Not* I recognition site immediately upstream of tracrRNA (trans-activating CRISPR RNA) was synthesized and cloned into the pEX-A2 vector by Eurofin genomics (Tokyo, Japan), resulting in the construction of psgRNA (Table 4-2). Insertion DNA for the target sequence, which was designed using Cas-Designer (http://www.rgenome.net/cas-designer/), was prepared by hybridization of a pair of complementary synthetic oligonucleotides in length of 50-nt each (see DNA sequence shown in Appendix Table 3). The DNA was inserted into the *Not* I site of psgRNA vector by the In-Fusion system (Takara Bio, Japan). The inserted DNA sequence on the resulting plasmids was confirmed by DNA sequencing (Appendix Table 3).

Table 4-2. Plasmids used in this study.

Name	Characterization	Reference
pCas	*repA*^{ts} *kan* P_{cas}-*cas9* P_{araB}-*red lacI*^{q} P_{trc}-sgRNA-pMB1	Jiang *et al.* 2015
psgRNA	pMB1 *bla* P-sgRNA (sgRNA cloning vector)	This study
psgRNA-phoP	pMB1 *bla* P-sgRNA-*phoP*	This study
psgRNA-phoB	pMB1 *bla* P-sgRNA-*phoB*	This study
psgRNA-citB	pMB1 *bla* P-sgRNA-*citB*	This study

Table 4-2. Plasmids used in this study. (Continued.)

Name	Characterization	Reference
psgRNA-ompR	pMB1 *bla* P-sgRNA-*ompR*	This study
psgRNA-narL	pMB1 *bla* P-sgRNA-*narL*	This study
psgRNA-cpxR	pMB1 *bla* P-sgRNA-*cpxR*	This study
psgRNA-uhpA	pMB1 *bla* P-sgRNA-*uhpA*	This study
psgRNA-rstA	pMB1 *bla* P-sgRNA-*rstA*	This study
psgRNA-evgA	pMB1 *bla* P-sgRNA-*evgA*	This study
psgRNA-kdpE	pMB1 *bla* P-sgRNA-*kdpE*	This study
psgRNA-torR	pMB1 *bla* P-sgRNA-*torR*	This study
psgRNA-uvrY	pMB1 *bla* P-sgRNA-*uvrY*	This study
psgRNA-qseB	pMB1 *bla* P-sgRNA-*qseB*	This study
psgRNA-arcA	pMB1 *bla* P-sgRNA-*arcA*	This study
psgRNA-atoC	pMB1 *bla* P-sgRNA-*atoC*	This study
psgRNA-baeR	pMB1 *bla* P-sgRNA-*baeR*	This study
psgRNA-ntrC	pMB1 *bla* P-sgRNA-*ntrC*	This study
psgRNA-rcsB	pMB1 *bla* P-sgRNA-*rcsB*	This study
psgRNA-pyrR	pMB1 *bla* P-sgRNA-*pyrR*	This study
psgRNA-btsR	pMB1 *bla* P-sgRNA-*btsR*	This study
psgRNA-creB	pMB1 *bla* P-sgRNA-*creB*	This study
psgRNA-basR	pMB1 *bla* P-sgRNA-*basR*	This study
psgRNA-cusR	pMB1 *bla* P-sgRNA-*cusR*	This study
psgRNA-narP	pMB1 *bla* P-sgRNA-*narP*	This study
psgRNA-zraR	pMB1 *bla* P-sgRNA-*zraR*	This study
psgRNA-rssB	pMB1 *bla* P-sgRNA-*rssB*	This study
psgRNA-glrR	pMB1 *bla* P-sgRNA-*glrR*	This study
psgRNA-fimZ	pMB1 *bla* P-sgRNA-*fimZ*	This study
psgRNA-ygeK	pMB1 *bla* P-sgRNA-*ygeK*	This study
psgRNA-dcuR	pMB1 *bla* P-sgRNA-*dcuR*	This study
psgRNA-yhjB	pMB1 *bla* P-sgRNA-*yhjB*	This study
psgRNA-cheB	pMB1 *bla* P-sgRNA-*cheB*	This study
psgRNA-cheY	pMB1 *bla* P-sgRNA-*cheY*	This study
psgRNA-hprR	pMB1 *bla* P-sgRNA-*hprR*	This study
psgRNA-cusS	pMB1 *bla* P-sgRNA-*cusS*	This study
psgRNA-zraS	pMB1 *bla* P-sgRNA-*zraS*	This study
psgRNA-kdpD	pMB1 *bla* P-sgRNA-*kdpD*	This study
psgRNA-phoQ	pMB1 *bla* P-sgRNA-*phoQ*	This study
psgRNA-basS	pMB1 *bla* P-sgRNA-*basS*	This study
psgRNA-baeS	pMB1 *bla* P-sgRNA-*baeS*	This study
psgRNA-cpxA	pMB1 *bla* P-sgRNA-*cpxA*	This study
psgRNA-envZ	pMB1 *bla* P-sgRNA-*envZ*	This study
psgRNA-evgS	pMB1 *bla* P-sgRNA-*evgS*	This study
psgRNA-glrK	pMB1 *bla* P-sgRNA-*glrK*	This study
psgRNA-qseC	pMB1 *bla* P-sgRNA-*qseC*	This study
psgRNA-rcsC	pMB1 *bla* P-sgRNA-*rcsC*	This study
psgRNA-rcsD	pMB1 *bla* P-sgRNA-*rcsD*	This study
psgRNA-rstB	pMB1 *bla* P-sgRNA-*rstB*	This study

Table 4-2. Plasmids used in this study. (Continued.)

Name	Characterization	Reference
psgRNA-hprS	pMB1 *bla* P-sgRNA-*hprS*	This study
psgRNA-atoS	pMB1 *bla* P-sgRNA-*atoS*	This study
psgRNA-barA	pMB1 *bla* P-sgRNA-*barA*	This study
psgRNA-creC	pMB1 *bla* P-sgRNA-*creC*	This study
psgRNA-ntrB	pMB1 *bla* P-sgRNA-*ntrB*	This study
psgRNA-phoR	pMB1 *bla* P-sgRNA-*phoR*	This study
psgRNA-uhpB	pMB1 *bla* P-sgRNA-*uhpB*	This study
psgRNA-btsS	pMB1 *bla* P-sgRNA-*btsS*	This study
psgRNA-pyrS	pMB1 *bla* P-sgRNA-*pyrS*	This study
psgRNA-arcB	pMB1 *bla* P-sgRNA-*arcB*	This study
psgRNA-citA	pMB1 *bla* P-sgRNA-*citA*	This study
psgRNA-dcuS	pMB1 *bla* P-sgRNA-*dcuS*	This study
psgRNA-narQ	pMB1 *bla* P-sgRNA-*narQ*	This study
psgRNA-narX	pMB1 *bla* P-sgRNA-*narX*	This study
psgRNA-torS	pMB1 *bla* P-sgRNA-*torS*	This study
psgRNA-cheA	pMB1 *bla* P-sgRNA-*cheA*	This study

4-2-3. Multi-gene knockout in the *E. coli* genome by the HoSeI method based on CRISPR-Cas

The W3110 type A strain harboring pCas was grown in LB medium containing 1% arabinose and 50 μg/mL kanamycin to logarithmic phase and then was collected and suspended in a solution of 0.1 M $CaCl_2$. This suspension of *E. coli* was subjected to transformation by the psgRNA-target (shown in Table 4-2) and DNA fragment to recover the digested site by CRISPR-Cas9. The 83-bp DNA fragments were prepared by hybridization of a pair of complementary synthetic oligonucleotides (see the DNA sequences shown in Appendix Table 4). In comparison with no colonies observed on LB agar containing 100 μg/mL ampicillin by transformation with only psgRNA-target, the addition of the DNA fragment produced transformants that grew on LB agar containing ampicillin. To verify the introduction of a stop codon on the target gene of the genome, genomic DNA was prepared from the transformant and used as a template for amplification of the target sequence by PCR using a pair of oligonucleotides, as shown in Appendix Table 3. The introduction of a stop codon on the target gene was confirmed by DNA sequencing of the amplified DNA.

4-2-4. Identification of the whole genome sequence of *E. coli* strains

Identification of the whole genome sequence of W3110 type A and RR- and SK-deprived mutants was performed by high-throughput sequencing (Bioengineering Lab). Briefly, genomic DNA was extracted from the LB culture of each strain by using the Wizard® Genomic DNA Purification Kit (Promega). Prepared genomic DNA was fragmented into about 400 bp, created a

DNA library, and sequenced by DNBSEQ-G400 (Bioengineering Lab). Reads (7-8 M 2×150 bp) were mapped and compared with two reference genomes, W3110 (GenBank: AP009048.1) and MG1655 (GenBank: U00096.3), using CLC Genomics Workbench 8.5.1 (Qiagen).

4-2-5. Growth kinetics

The parent strain W3110 type A and isolated mutants were grown in LB or M9-glucose medium to stationary phase and diluted in LB or M9-glucose to an $OD_{600\ nm}$= 0.01. The diluted suspension in L-shaped test tubes was inoculated to the stationary phase at various temperature (27℃, 32℃, 37℃, or 42℃) and the growth was monitored measuring the $OD_{600\ nm}$ every 15 mins using the TVS062CA Compact rocking incubator (Advantec). Triplicates were inoculated for each strain tested.

4-2-6. Phenotype Microarray

To compare the growth characterization under the various environmental conditions of the isolated multi-gene knockout strains with the parent strain, phenotype microarray (PM) testing was performed using the OmniLog® Phenotype MicroArray™ system (BioLog). Each strain was inoculated in the M9-glucose medium at 37℃ up to a stationary phase. The precultured cells were collected (c.f. 5,000 rpm for 5 min at 4℃) and resuspended with 2 ml of IF-0 [5 g/L NaCl (Nacalai), 0.3 g/L of Pluronic F-68 (Sigma), 0.1 g/L of Phytagel (Sigma), and 10 ml/L of triethanolamine (Sigma), pH 7.1]. After centrifugation (c.f. 5,000 rpm for 5min at 4℃), resuspension of cells in 2 ml of IF-0 was added to 6 ml of IF-0 to adjust transmittance to 42%T. Then, the diluted cell suspension (42%T) was added to 20 ml of IF-0 to prepare the cell suspension. For a PM1 or 2 plates, the following reagents; 9.16 ml of 1.2x IF-0 [6 g/L NaCl (Nacalai), 0.36 g/L of Pluronic F-68 (Sigma), 0.12 g/L of Phytagel (Sigma), and 12 ml/L of triethanolamine (Sigma), pH 7.1], 1.73 ml of autoclaved DDW, 110 µl of 100x Redox dye Mix A (BioLog), and 2.2 ml of the prepared cell suspension, were mixed to prepare the culture suspension. For PM3-8 plates, the mixture; 9.16 ml of 1.2x IF-0, 1.73 ml of autoclaved DDW, 110 µl of 100x Redox dye Mix A (BioLog), 2.2 ml of the prepared cell suspension, and 110 µl of 2 M sodium succinate/ 200 µM ferric citrate, were prepared as the culture suspension. For PM9-20 plates, the mixture; 9.16 ml of IF-10a GN BASE (1.2x) (BioLog), 1.73 ml of autoclaved DDW, 110 µl of 100x Redox dye Mix A (BioLog), and 55 µl of the prepared cell suspension to prepare the culture suspension. Then, 100 µl of the culture suspension was applied to each well of a PM plate, and PM plates were incubated for 96 hours at 37℃ in the Omnilog® Phenotype MicroArray incubator (Biolog). The growth of cells in each well was measured as the level of reduced tetrazolium redox dye, every 15 mins up to 96 hours.

4-2-7. Computational analysis of designed sgRNAs

The multiple alignments of the 20-nt target sequences designed for sgRNA in this study were estimated using ClustalW and WebLogo3 (http://weblogo.threeplusone.com/, Crooks *et al.* 2004). To get the secondary and tertiary structure prediction of sgRNAs, the full length of 100-nt each sgRNA was analyzed using CentroidFold (http://rtools.cbrc.jp/centroidfold/, Sato *et al.* 2009) and Rascal (Yamasaki *et al.* 2014).

4-3. Results

4-3-1. Construction of multi-gene knockout strains in *E. coli* using HoSeI method

The CRISPR-Cas system is available to knock out genes in the *E. coli* genome by insertion of an antibiotic resistance marker gene (Jiang *et al.* 2015). A novel gene knockout system by introducing a nonsense codon, a homologous sequence integration (HoSeI) method, was developed to overcome the limitations of antibiotic resistance marker genes. It is readily feasible for us to design and isolate multi-gene knockout strains of *E coli*. The designed sgRNA (single-guide RNA)

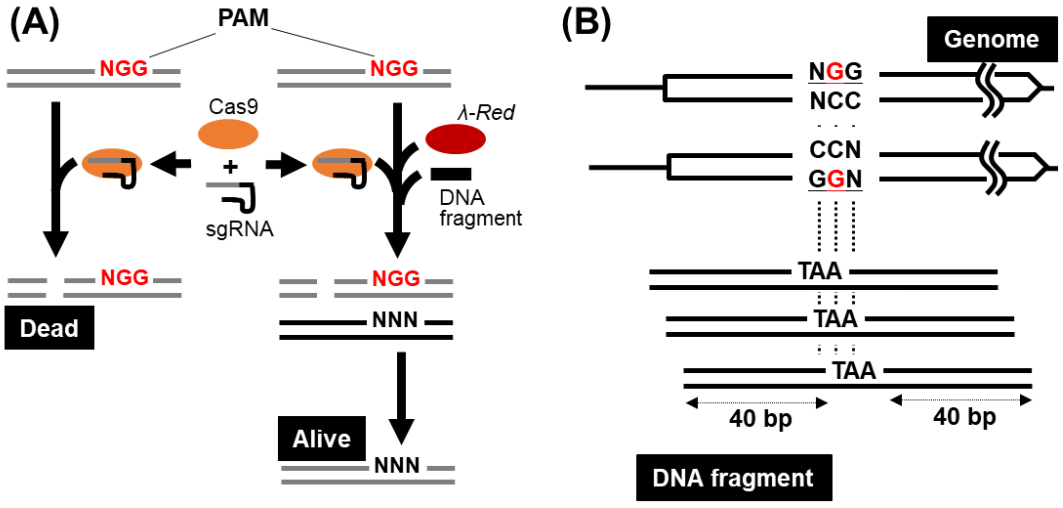

Figure 4-1. The homologous sequence integration (HoSeI) method for multi-gene knockout in the *E. coli* genome. **[A]** The overview of the HoSeI method. The HoSeI method is based on previously reported genome editing method using CRISPR-Cas (Jiang *et al.* 2014). The sgRNA expressed from psgRNA and *Streptococcus pyogenes* Cas9 endonuclease expressed from pCas cause a site-specific double-strand break at the recognized site by the protospacer adjacent motif (PAM) for sgRNA, resulting in cell death of *E. coli* (left). In the HoSeI method, the recombination of DNA fragment by lambda-Red recombinase recovers the digestion of the *E. coli* genome and enables *E. coli* cell to avoid cell death (right). **[B]** The design of DNA fragment for replacing PAM with nonsense codon. To knockout protein-coding gene, I designed the DNA fragment containing TAA, introducing both nonsense codon and mutated PAM, with 40 bp-long homology arms on both sides.

(A)

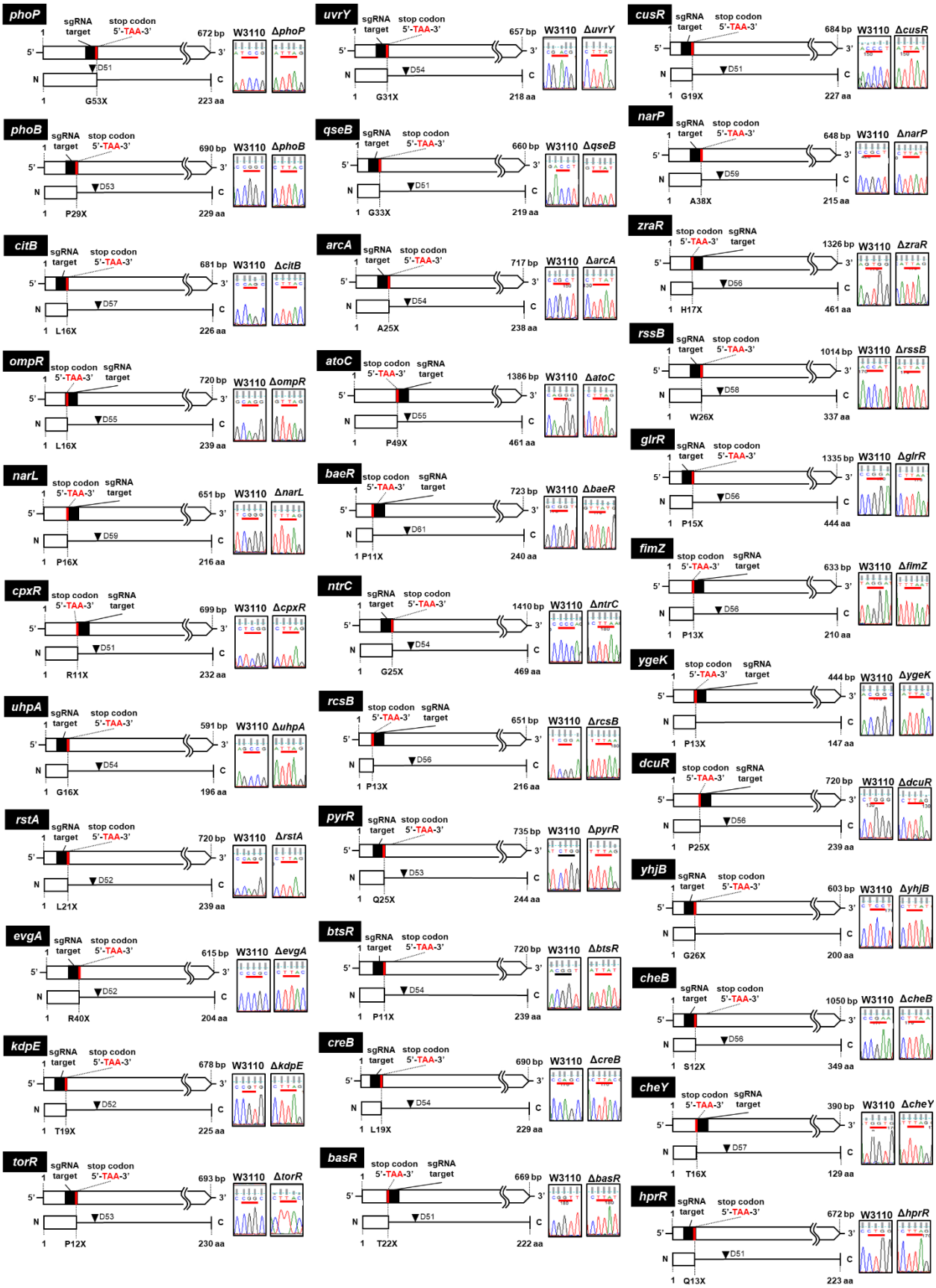
phoP
sgRNA target
stop codon 5'-TAA-3'
672 bp
W3110
ΔphoP
D51
G53X
223 aa
phoB
690 bp
D53
P29X
229 aa
citB
681 bp
D57
L16X
226 aa
ompR
720 bp
D55
L16X
239 aa
narL
651 bp
D59
P16X
216 aa
cpxR
699 bp
D51
R11X
232 aa
uhpA
591 bp
D54
G16X
196 aa
rstA
720 bp
D52
L21X
239 aa
evgA
615 bp
D52
R40X
204 aa
kdpE
678 bp
D52
T19X
225 aa
torR
693 bp
D53
P12X
230 aa
uvrY
657 bp
D54
G31X
218 aa
qseB
660 bp
D51
G33X
219 aa
arcA
717 bp
D54
A25X
238 aa
atoC
1386 bp
D55
P49X
461 aa
baeR
723 bp
D61
P11X
240 aa
ntrC
1410 bp
D54
G25X
469 aa
rcsB
651 bp
D56
P13X
216 aa
pyrR
735 bp
D53
Q25X
244 aa
btsR
720 bp
D54
P11X
239 aa
creB
690 bp
D54
L19X
229 aa
basR
669 bp
D51
T22X
222 aa
cusR
684 bp
D51
G19X
227 aa
narP
648 bp
D59
A38X
215 aa
zraR
1326 bp
D56
H17X
461 aa
rssB
1014 bp
D58
W26X
337 aa
glrR
1335 bp
D56
P15X
444 aa
fimZ
633 bp
D56
P13X
210 aa
ygeK
444 bp
P13X
147 aa
dcuR
720 bp
D56
P25X
239 aa
yhjB
603 bp
G26X
200 aa
cheB
1050 bp
D56
S12X
349 aa
cheY
390 bp
D57
T16X
129 aa
hprR
672 bp
D51
Q13X
223 aa

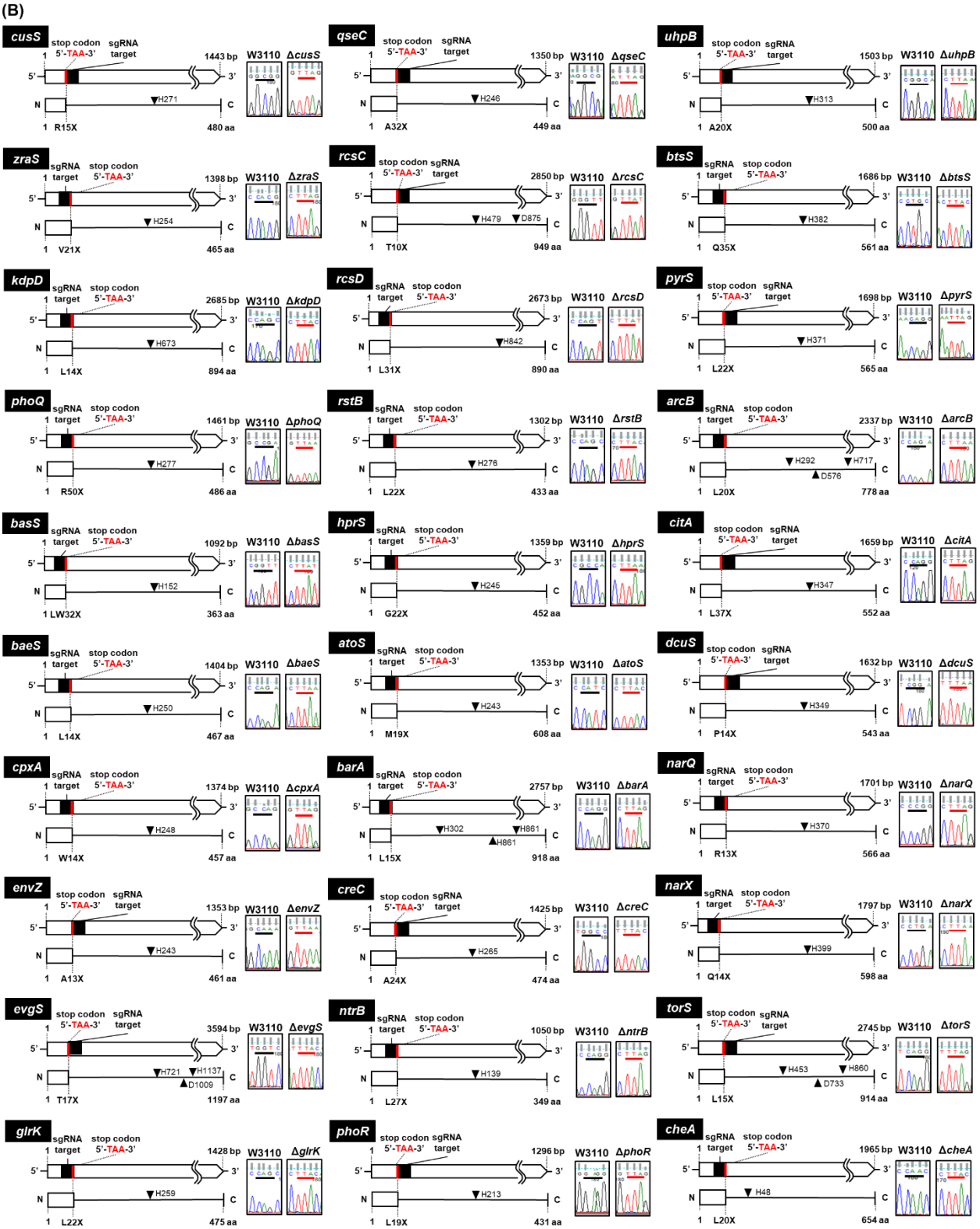

Figure 4-2. Construction of TCS gene knockout in the *E. coli* genome. TCS gene knockout strains were isolated using the HoSeI method (Fig. 4-1). The ORFs of each gene and their length are shown as an arrow. RR genes are shown in **A** and SK genes are shown in **B**. The positions of the integrated stop codon and the sgRNA target region are marked in red or black, respectively. The box with bar under the gene arrow shows the truncated protein. The filled triangle represents the conserved aspartic acid (D) residue or histidine (H) residue. The introduction of stop codon on target gene was confirmed by DNA sequencing on the amplified DNA.

containing the recognition sequence for the *E. coli* genome specifically digests the genome, resulting in a dead phenotype (Fig. 4-1A). The designed DNA fragment containing the following sequence, however, recombines with the genome at the injury site by lambda-Red recombinase, resulting in a living phenotype (Fig. 4-1A). To knock out gene function, the DNA fragment is designed to introduce the stop codon, TAA, instead of the PAM sequence (Fig. 4-1B). For knockout of each gene, I constructed sgRNA-expressing plasmids (Table 4-2). None of the constructed psgRNA plasmids caused *E. coli* harboring pCas to gain ampicillin resistance (data not shown). The addition of the designed DNA fragment, including the nonsense codon for the target gene, recovered the transformation of *E. coli* harboring pCas by psgRNA. The proper introduction of the nonsense codon, TAA, was confirmed by Sanger sequencing in all cases (Fig. 4-2). A psgRNA-free transformant was isolated by IPTG-inducible sgRNA for the psgRNA plasmid from pCas as previously described (Jiang *et al.* 2015). The isolated psgRNA-free transformant was subjected to further gene knockout by repeating the HoSeI system. In addition to all single knockouts of TCS genes, these experiments bred the strains of all of 34 RR gene or 30 SK gene knockout (Table 4-1).

4-3-2. Comparison of the genome sequence of the isolated strains

The complete genome sequences of the parent strain W3110 type A and generated RR- and SK-deprived mutants were carried out by high-throughput sequencing (Bioengineering Lab). Then, I first compared the parent strain genome with two reference *E. coli* K-12 genomes, W3110 (GenBank: AP009048.1) and MG1655 (GenBank: U00096.3). As a result, W3110 type A genome showed a mosaic structure of W3110 and MG1655. For example, W3110 type A has a CPZ-55 prophage region, which was only found in MG1655, and showed insertion or deletion of some IS elements, which W3110 only has (Table 4-3). W3110 type A genome was also mosaic in sequence differences between W3110 and MG1655. In addition, the Rac prophage region and seven genes (*ynaJ*, *uspE*, *fnr*, *ogt*, *abgT*, *abgB*, and *abgA*) were lost in the W3110 type A genome (Table 4-3). Some gene sequences of W3110 type A were uniquely different from both W3110 and MG1655, including the *rpoS* gene. The codon of *rpoS* coding 33rd amino acid residue was TAG (stop codon) in W3110 and CAG (Glutamine) in MG1655, but TAT (Tyrosine) in W3110 type A.

Based on the characteristics of the genome structure of W3110 type A, a comparison of the RR- or SK-knockout strain with the parent strain identified mutations in each genome (Table 4-4 and 4-5). The SK-mutant showed mutations in the 30 of target SK genes, and no other unexpected mutation was detected (Table 4-4). On the other hand, four spontaneous mutations were found in the RR-mutant genome in addition to the introduction of nonsense codon into 34 RR genes (Table 4-5). They were a silent mutation in the *lolE* gene (Leu328, CTG to TTG), a missense mutation in the *yihQ* gene (Ser528Cys, AGC to TGC), a 1-nt substitution in the intergenic region of *hydN* and

ascG genes, and 315 bp deletion in the intergenic region of *insAB* and *yfbQ* genes. The result of further sequencing analysis of all thirty-three RR mutants (Δ1RR to Δ33RR) identified these spontaneous mutations were generated at a different time of breeding (Table 4-6).

Table 4-3. Characterization of W3110 typeA genome.

Location[a]	Function	Changes			W3110 type A
		W3110[b]	MG1655[c]	W3110 type A	
crl	sigma factor-binding protein, stimulates RNA polymerase holoenzyme formation		*insA*, *insB*		W3110
ylbE	putative protein	Glu38 (GAA)	Glu38 (GAG), Lys86fs	Glu38 (GAG), Lys86fs	MG1655
folD	5,10-methylene-tetrahydrofolate dehydrogenase 5,10-methylene-tetrahydrofolate cyclohydrolase	Leu36 (CTG)	Leu36 (CTG)	Gln36 (CAG)	
yccE	hypothetical protein	Arg415 (CGT)	Arg415 (CGT)	Cys415 (TGT)	
ycdT	diguanylate cyclase, membrane-anchored	Val130 (GTA)	Ala130 (GCA)	Ala130 (GCA)	MG1655
ycdU / serX		different number of repeat			MG1655
csgC / ymdA		*insC*, *insD*		*insC*, *insD*	W3110
ychE / oppA		*insC*	*insH*		
oppA	oligopeptide transporter subunit	Ser273 (AGC)	Ser273 (AGC)	Gly273 (GGC)	
acnA	aconitate hydratase 1	Gly522 (GGC)	Ser522 (AGC)	Gly522 (GGC)	W3110
ynaJ, uspE, fnr, ogt, abgT, abgB, abgA				deletion	
ydaO (*ttcA*)	tRNA 2-thiocytidine biosynthesis protein	Gln6 (CAA), Thr8 (ACA)	Gln6 (CAA), Thr8 (ACA)	Glu6 (GAA), Ser8 (AGT)	
intR, ydaQ, ydaC, lar, recT, recE, racC, ydaE, kil, sieB, ydaF, ydaG, racR, ydaS, ydaT, ydaU, ydaV, ydaW, rzpR, rzoR, trkG, ynaK, ydaY, ynaA, lomR (insH is inserted), sfR, tfaR, pinR, ynaE	Rac prophage region			deletion	
intQ	pseudogene, Qin prophage	Leu274 (CTC)	Phe274 (TTC)	Leu274 (CTC)	W3110
ynhF / purR				1-nt substitution	
flhD / uspC		*insH*	*insA*, *insB*	*insH*	W3110
yedJ	putative hydrolase	V219 (GTT)	V219 (GTC)	V219 (GTT)	W3110
gatC	galactitol-specific enzyme IIC component of PTS	Gly306fs		Gly306fs	W3110
gatA	galactitol-specific enzyme IIA component of PTS	*insH*			MG1655
rcsC	hybrid sensory kinase in two-component regulatory system with RcsB and RcsD	*insD*, *insC*			MG1655
lrhA / ulaA(yfbQ)		*insA*, *insB*		*insA*, *insB*	W3110
intZ, yffL, yffM, yffN, yffO, yffP, yffQ, yffR, yffS	CPZ-55 prophage	deletion			MG1655
rpoS	RNA polymerase, sigma S (sigma 38) factor	Stop33 (TAG)	Gln33 (CAG)	Tyr33 (TAT)	
pyrG	CTP synthetase	Asp450 (GAC)	Asp450 (GAC)	His450 (CAC)	
tdcE / tdcD		*insH*			MG1655
crp	DNA-binding transcriptional dual regulator	Lys29 (AAG)	Thr29 (ACG)	Lys29 (AAG)	W3110
glpR	DNA-binding transcriptional repressor	Ala51fs		Ala51fs	W3110
yieE / yieZ		*insD*, *insC*			MG1655
tnaA / tnaC		*insH*			MG1655
tnaB	tryptophan transporter of low affinity	*insH*		insertion? (not *insH*)	MG1655
rffM	UDP-N-acetyl-D-mannosaminuronic acid transferase	Val91 (GTT)	Val91 (GTT)	Ile91 (ATT)	
yjcS / alsK		*insH*			MG1655
dcuA	C4-dicarboxylate antiporter			insertion?	
dcuA / aspA	Repeat region: REP321j	different number of repeat		12_13insCG	MG1655

[a]Intergenic regions are shown as gene / gene. [b]GenBank: AP009048.1 [c]GenBank: U00096.3

Table 4-4. Mutations in the SK-deprived strain genome.

Location	Function	Changes	
		Parent	Δ30SK
phoR	SK in TCS with PhoB	Leu19 (CTC)	Stop19 (TAA)
cusS	SK in TCS with CusR, senses copper ions	Arg15 (CGC)	Stop15 (TAA)
citA	SK in TCS with citB	Leu37 (CTG)	Stop37 (TAA)
kdpD	fused SK in TCS with KdpE	Leu14 (CTG)	Stop14 (TAA)
torS	hybrid SK in TCS with TorR	Leu15 (CTG)	Stop15 (TAA)
phoQ	SK in TCS with PhoP	Arg50 (CGG)	Stop50 (TAA)
narX	SK in TCS with NarL	Gln14 (CAG)	Stop14 (TAA)
rstB	SK in TCS with RstA	Leu22 (CTG)	Stop22 (TAA)
cheA	fused chemotactic SK (soluble) in TCS with CheB and CheY	Leu20 (TTG)	Stop20 (TAA)
hprS	predicted SK in TCS with HprR	Gly22 (GGC)	Stop22 (TAA)
baeS	SK in TCS with BaeR	Leu14 (CTG)	Stop14 (TAA)
btsS	predicted SK in TCS with BtsR	Gln35 (CAG)	Stop35 (TAA)
rcsD	phosphotransfer intermediate protein in TCS with RcsBC	Leu31 (CTG)	Stop31 (TAA)
rcsC	hybrid SK in TCS with RcsBD	Thr31 (ACC)	Stop31 (TAA)
atoS	SK in TCS with AtoC	Met19 (ATG)	Stop19 (TAA)
evgS	hybrid SK in TCS with EvgA	Thr17 (ACC)	Stop17 (TAA)
pyrS	predicted SK in TCS with PyrR	Leu22 (CTG)	Stop22 (TAA)
narQ	SK in TCS with NarP (NarL)	Arg13 (CGG)	Stop13 (TAA)
glrK	predicted SK in TCS	Leu17 (CTG)	Stop17 (TAA)
barA	hybrid SK in TCS with UvrY	Leu15 (CTG)	Stop15 (TAA)
qseC	SK in TCS with QseB	Ala32 (GCC)	Stop32 (TAA)
arcB	hybrid SK in TCS with ArcA	Leu20 (CTG)	Stop20 (TAA)
zraS	SK in TCS with ZraR	Val21 (GTG)	Stop21 (TAA)
cpxA	SK in TCS with CpxR	Trp14 (TGG)	Stop14 (TAA)
ntrB	SK in TCS with NtrC	Leu27 (CTG)	Stop27 (TAA)
uhpB	SK in TCS with UhpA	Ala20 (GCC)	Stop20 (TAA)
envZ	SK in TCS with OmpR	Ala13 (GCC)	Stop13 (TAA)
basS	SK in TCS with BasR	Trp32 (TGG)	Stop32 (TAA)
dcuS	SK in TCS with DcuR	Pro14 (CCG)	Stop14 (TAA)
creC	SK in TCS with CreB or PhoB	Ala24 (GCC)	Stop24 (TAA)

Table 4-5. Mutations in the RR-deprived strain genome.

Location	Function	Changes	
		Parent	Δ34RR
phoB	RR in TCS with PhoR (or CreC)	Pro29 (CCG)	Stop29 (TAA)
fimZ	predicted DNA-binding transcriptional regulator	Pro13 (CCT)	Stop13 (TAA)
cusR	RR in TCS with CusS	Gly19 (GGG)	Stop19 (TAA)
citB	RR in TCS with CitA	Leu16 (CTG)	Stop16 (TAA)
kdpE	RR in TCS with KdpD	Thr19 (ACG)	Stop19 (TAA)
torR	RR in TCS with TorS	Pro12 (CCG)	Stop12 (TAA)
lolE	outer membrane-specific lipoprotein transporter subunit	Leu328 (CTG)	Leu328 (TTG)
phoP	RR in TCS with PhoQ	Gly53 (GGA)	Stop53 (TAA)
narL	RR in TCS with NarX (or NarQ)	Pro16 (CCG)	Stop16 (TAA)
rssB	response regulator of RpoS	Trp26 (TGG)	Stop26 (TAA)
rstA	RR in TCS with RstB	Leu24 (CTG)	Stop24 (TAA)
cheY	chemotaxis regulator transmitting signal to flagellar motor component	Thr16 (ACC)	Stop16 (TAA)
cheB	fused chemotaxis regulator and protein-glutamate methylesterase in TCS with CheA	Ser12 (TCG)	Stop12 (TAA)
uvrY	RR in TCS with BarA	Gly31 (GGT)	Stop31 (TAA)
hprR	predicted RR in TCS with HprS	Gln13 (CAG)	Stop13 (TAA)
baeR	RR in TCS with BaeS	Pro11 (CCG)	Stop11 (TAA)
btsR	predicted RR in TCS with BtsS	Pro11 (CCG)	Stop11 (TAA)
narP	RR in TCS with NarQ or NarX	Ala38 (GCG)	Stop38 (TAA)
rcsB	RR in TCS with RcsCD	Pro13 (CCG)	Stop13 (TAA)
atoC	fused RR of *ato* opeon, in TCS with AtoS	Pro49 (CCT)	Stop49 (TAA)
insAB / *yfbQ*			315 bp deletion
evgA	RR in TCS with EvgS	Arg40 (CGG)	Stop40 (TAA)
pyrR	predicted RR in TCS with PyrS	Gln25 (CAG)	Stop25 (TAA)
glrR	predicted RR in TCS	Pro15 (CCG)	Stop15 (TAA)
hydN / *ascG*			1-nt substitution
ygeK	predicted DNA-binding transcriptional regulator	Pro13 (CCG)	Stop13 (TAA)
qseB	RR in TCS with QseC	Gly33 (GGT)	Stop33 (TAA)
zraR	fused RR in TCS with ZraS	His17 (CAC)	Stop17 (TAA)
cpxR	RR in TCS with CpxA	Arg11 (CGA)	Stop11 (TAA)
yihQ	alpha-glucosidase	Ser528 (AGC)	Cys528 (TGC)
ntrC	fused RR in TCS with GlnL, nitrogen regulator I (NRI)	Gly25 (GGG)	Stop25 (TAA)
uhpA	RR in TCS wtih UhpB	Gly16 (GGC)	Stop16 (TAA)
yhjB	predicted RR in TCS	Gly26 (GGA)	Stop26 (TAA)
ompR	RR in TCS with EnvZ	Leu16 (CTG)	Stop16 (TAA)
basR	RR in TCS with BasS	Thr22 (ACC)	Stop22 (TAA)
dcuR	RR in TCS with DcuS	Pro25 (CCA)	Stop25 (TAA)
creB	RR in TCS with CreC	Leu19 (CTG)	Stop19 (TAA)
arcA	RR in TCS with ArcB or CpxA	Ala25 (GCG)	Stop25 (TAA)

Intergenic regions are shown as gene / gene.

Strain	Unexpected changes			
	***lolE* Leu328 (CTG→TTG)**	***insAB/yfbQ* (315 bp deletion)**	***hydN/ascG* (1-nt substitution)**	***yihQ* Ser528Cys (AGC→TGC)**
Δ1RR	-	-	-	-
Δ2RR	-	-	-	-
Δ3RR	-	-	-	-
Δ4RR	-	-	-	-
Δ5RR	-	-	-	-
Δ6RR	-	-	-	-
Δ7RR	-	-	-	-
Δ8RR	-	-	-	-
Δ9RR	-	-	-	-
Δ10RR	-	+	-	-
Δ11RR	-	+	-	-
Δ12RR	-	+	-	-
Δ13RR	-	+	-	-
Δ14RR	-	+	-	-
Δ15RR	-	+	-	-
Δ16RR	-	+	-	-
Δ17RR	-	+	-	-
Δ18RR	-	+	-	-
Δ19RR	-	+	-	-
Δ20RR	-	+	-	-
Δ21RR	-	+	-	-
Δ22RR	-	+	-	-
Δ23RR	-	+	-	-
Δ24RR	-	+	-	-
Δ25RR	+	+	-	-
Δ26RR	+	+	-	-
Δ27RR	+	+	-	+
Δ28RR	+	+	-	+
Δ29RR	+	+	-	+
Δ30RR	+	+	-	+
Δ31RR	+	+	-	+
Δ32RR	+	+	+	+
Δ33RR	+	+	+	+
Δ34RR	+	+	+	+

4-3-3. The phenotypic analysis of the TCS gene-deprived strain

The RR gene- and SK gene-deprived strains isolated by the HoSeI method and the parent strain were grown in LB or M9-glucose medium to stationary phase at various temperatures (27℃, 32℃, 37℃, or 42℃) and the growth was monitored measuring the $OD_{600\ nm}$ every 15 mins. Surprisingly, there were no significant differences in both the growth rate and the $OD_{600\ nm}$ value of stationary phase between the parent strain and the mutants in LB medium (Fig. 4-3A-D). All three strains proliferated slightly slower in 27℃ and 32℃ than in 37℃ and 42℃, but the $OD_{600\ nm}$ value reached a plateau in 24 hours in each temperature condition.

In contrast, all strains showed a larger growth variability in M9-glucose medium than in LB medium (Fig. 4-3E-H). The growth rate of the parent increased with the rise in temperature.

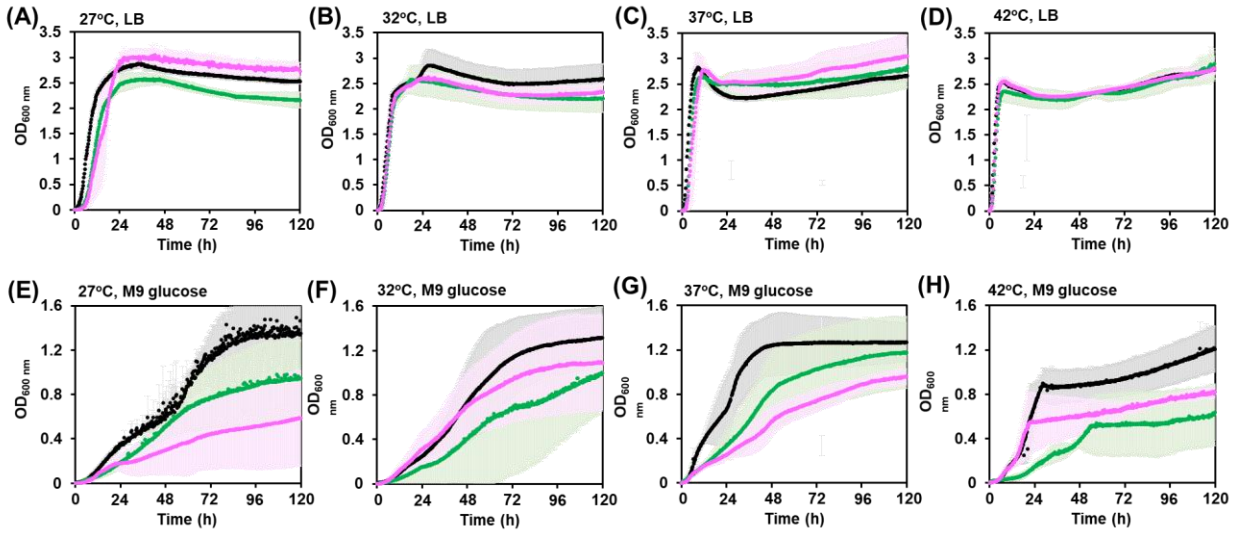

Figure 4-3. The growth kinetics of the isolated RR- and SK-deprived strains. The parent strain W3110 type A (black), the SK-deprived strain (green), and the RR-deprived strain (magenta) were grown in LB or M9-glucose medium to stationary phase and diluted in LB (**A-D**) or M9-glucose (**E-H**) to an $OD_{600\ nm}$= 0.01. The diluted suspension in L-shaped test tubes was inoculated to the stationary phase at various temperature (27°C in **A** and **E**; 32°C in **B** and **F**; 37°C in **C** and **G**; and 42°C in **D** and **H**), and the growth was monitored measuring the $OD_{600\ nm}$ every 15 mins up to 120 hours using the TVS062CA Compact rocking incubator (Advantec). Triplicates were inoculated for each strain, and the average of them is shown as a dot plot. The error bars show standard deviation.

In comparison to this, the growth of the RR mutant clearly delayed at 27°C and 37°C (Fig. 4-3E and G). Although the RR mutant grew slightly faster at 42°C, the mutant did not show the rapid growth in the log phase at 27°C, 32°C, and 37°C, and it took much longer time to reach the stationary phase than the parent strain. Additionally, the mutant indicated the lower $OD_{600\ nm}$ value of the stationary phase at each temperature (Fig. 4-3E-H). The SK mutant showed growth delays under all temperature conditions in M9-glucose, and the growth rate at the log phase was a bit faster with the rise in temperature up to 37°C. The cell mass of the SK mutant at 120 hours after incubation was also larger with temperature increase and similar to the parent strain at 37°C, even though it still took a long time to reach the maximum level (Fig. 4-3E-G). Interestingly, the comparison between RR- and SK-defective mutants represented that the RR deprivation caused slower growth at 27°C, whereas SK deprivation brought about slower growth at 42°C (Fig. 4-3EH). Taken together, the TCS-deprived strains drive cell division as fast as the parent strain does under the nutrient-rich conditions such as the LB medium. Under the poor nutrient conditions like the M9-glucose medium, however, the mutants show the slower cell growth in the log phase and the smaller cell population in the stationary phase.

Next, to compare the growth characterization under the various environmental conditions of the isolated multi-gene knockout strains with the parent strain, I performed phenotype microarray (PM) testing using the OmniLog® Phenotype MicroArray™ system (BioLog). Each strain was

grown at 37°C for 96 hours under the diverse culture conditions, including various nutrients, osmolytes, pH, and inhibitory compounds. After 96 hours, the growth of the parent strain was assigned to four types by the growth rate and the size of cell mass, (i) cells rapidly grew and reached the stationary phase in 24 hours; (ii) the growth was delayed, but the maximum size of cell mass was similar to the cells in (i); (iii) cells showed growth delay and smaller cell population at 96 hours; (iv) cells did not grow (Appendix Tables 5 to 8). The growth of two mutant strains was evaluated by comparing with the parent strain, (i) cells grew under the condition which the parent did not grow; (ii) both the growth rate and the maximum cell mass were similar to the parent; (iii) the growth was slower than the parent, but the maximum cell population was the same as the parent; (iv) the growth was delayed and cell population was smaller than that of the parent; (v) cells did not grow (Appendix Tables 5 to 8). As a result of PM testing, among the 1920 environmental conditions, 581 or 443 conditions showed the growth differences between the parent strain and RR- or SK-deprived mutant, respectively.

The nutrient availability test showed the parent strain could proliferate using 53 of 768 tested nutrients (Appendix Figure 2A-E and Appendix Table 5). All 53 conditions are related to carbon source utilization, so that the growth of the parent strain was not detected in the presence of any other nutrients (Appendix Figure 2B-E). The SK mutant grew 42 of 53 conditions (Table 4-7). The growth of the SK mutant was delayed under 30 of 42 conditions, and 10 of them caused a smaller cell population. Growth defect was found under 11 conditions (Succinic Acid, D,D-Malic Acid, L-Glutamine, Bromo-Succinic Acid, L-Arabinose, Uridine, Pyruvic acid, D-Alanine, Fumaric Acid, 3-0-b-D-Galactopyranosyl-D-Arabinose, and b-Methyl-D-Galactoside) (Table 4-7, Appendix Figure 2A and Appendix Table 5). In contrast, the RR mutant only grew under 7 of 53 conditions (D-Serine, D-Mannitol, D-Glucose-1-Phosphate, Maltotriose, L-Serine, Methyl Pyruvate, and D-Glucosamine) (Table 4-7, Appendix Figure 2A, and Appendix Table 5). Under the 4 of 7 conditions (D-Serine, D-Mannitol, L-Serine, and D-Glucosamine), the growth of the mutant was considerably slower than the parent strain (Fig. 4-4A). The rest of them (D-Glucose-1-Phosphate, Maltotriose, and Methyl Pyruvate) indicated the decrease in the maximum cell population at 96 hours. The SK mutant grew more quickly than the RR mutant under all 7 conditions in which the RR mutant was available, suggesting that deprivation of RR affects more severe on the utilization of carbon sources.

The result of the interrogation of osmotic effects exhibited the mutants has a lower tolerance for osmotic pressure than the parent strain (Table 4-7, Appendix Figure 2F, and Appendix Table 6). Both mutants grew under low osmolyte concentration, but the growth under high concentration was quite different between the RR- and the SK-deprivation. The growth of RR mutant completely depleted in the presence of more than 3% of NaCl (Appendix Table 6). Although some osmolytes were available for the RR mutant to grow, the maximum cell population was

smaller than the parent strain. In contrast, most osmolytes were not lethal for the SK mutant even in high concentrations. The elapsed time until the log phase was longer in some conditions, nevertheless the mutant could reach the same level of cell mass as the parent at 96 hours after incubation (Appendix Figure 2F). The RR mutant showed a slight growth delay at pH 4.5, but its growth rate was similar to the parent strain in other pH conditions (Table 4-7, Appendix Figure 2G, and Appendix Table 7). At pH 9.5, however, the mutant did not grow in 19 of 28 states in which the parent strain rapidly proliferated. Also, in most cases, the RR mutant formed smaller cell mass. The SK mutant did not show remarkable changes under pH 4.5, but the SK mutant differed with the parent in the availability of compounds under pH 9.5. These findings revealed that the defect of SK mostly affects the initial growth rate but not the cell population; however, the RR-deprivation extremely reduces the growth capacity.

Table 4-7. Summary of Phenotype Microarray

Categories	Parent	Δ34 RR				Δ30 SK			
		◎	○	△	×	◎	○	△	×
Carbon sources	53	0	4	3	46	12	20	10	11
Osmolytes	76	1	2	28	35	26	25	11	14
pH	73	6	1	27	39	33	20	3	17
Antibiotics	More sensitive	93				67			
	No change	141				162			
	More tolerant	6				11			

◎: Similar growth to the parent strain, ○: Delayed growth but same cell mass,
△: Delayed growth and small cell mass, ×: No growth

Furthermore, the chemical sensitivity assay showed 93 of 240 antimicrobials inhibit the survival of the RR mutant in lower concentration than the parent strain (Table 4-7, Appendix Figure 2H, and Appendix Table 8). On the contrary, the deletion of RRs increased the tolerance of 6 compounds (Lomefloxacin, Enoxacin, Cefuroxime, Furaltadone, Cinoxacin, and Oxytetracycline) (Table 4-8 and Appendix Table 8). These six compounds have a similar or different mode of actions (Table 4-8). Lomefloxacin and Enoxacin affect DNA topoisomerase and inhibit DNA synthesis. Furaltadone inhibits DNA synthesis and is also estimated to inhibit the initial step of carbohydrate metabolisms through repression of acetyl-CoA. Cinoxacin interferes with the synthesis of DNA and RNA, resulting in the prevention of protein synthesis. Cefuroxime is involved in the inhibition of cell wall synthesis. Oxytetracycline is a kind of tetracycline-type antimicrobials. It binds to 30S ribosomal protein and inhibits translation. The RR mutant also showed smaller cell mass in most cultural conditions even though the growth delay was not severe. On the other hand, the SK mutant was more sensitive in 67 inhibitory conditions and more tolerant in 11 states (Tables 4-7, 4-8, and Appendix Table 8). Among the 11 antimicrobials, three compounds (Lomefloxacin, Cefuroxime,

and Oxytetracycline) are shown in both RR- and SK-knockout strains as resistant. Altogether, the RR gene-deprived strain shows the severely limited viability, and the lack of RR genes causes both of a slower growth rate and a smaller cell population. The effect of SK deprivation is milder than the RR deprivation and induces the initial growth delay.

Table 4-8. List of compounds the mutants showed high resistance.

Antibiotics	Plate/Well	Mode of Action
Δ34 RR		
Lomefloxacin	PM11/B12	DNA topoisomerase, quinolone
Enoxacin	PM11/E08	DNA topoisomerase, quinolone
Cefuroxime	PM13/D04	wall, cephalosporin second generation
Furaltadone	PM14/A08	DNA synthesis, nitro-compound, multiple sites
Cinoxacin	PM16/D11	protein synthesis
Oxytetracycline	PM20/F08	protein synthesis, tetracycline
Δ30 SK		
Lomefloxacin	PM11/B12	DNA topoisomerase, quinolone
Minocycline	PM11/C11, C12	protein synthesis, tetracycline
Dodecyltrimethyl Ammonium Bromide	PM12/H11	membrane, detergent, cationic
Cefuroxime	PM13/D04	wall, cephalosporin second generation
Sanguinarine	PM14/A12	ATPase, Na^+/K^+ and Mg^{++}
Sodium Metaborate	PM14/E12	transport, toxic anion
Niaproof	PM17/E04	membrane, detergent, anionic
Thioglycerol	PM19/H08	reducing agent, thiol, adenosyl methionine antagonist
Amitriptyline	PM20/A03	membrane, transport
Oxytetracycline	PM20/F08	protein synthesis, tetracycline
Captan	PM20/G03	fungicide, carbamate, multisite

4-4. Discussion

4-4-1. The advantages of HoSeI method

Bacteria are unicellular organisms. Individual cells are known to start growth under rich nutrient conditions by operating metabolic networks. On the other hand, bacterial cells that survive have a proper memory for the function of genetic stress response systems. Thus, multi-genetic factors function for bacterial growth. To analyze the function of several genes, I developed the CRISPR-Cas9-based HoSeI method to knock out genes without antibiotic resistance gene markers. The HoSeI method is a genetic marker-less genome editing approach and introduces base substitutions in the target sequence on the original genome by screening dead or alive cells. I repeated the HoSeI method in the *E. coli* K-12 genome and isolated multi-gene knockout strains, even all RR- or SK- deprived strains. The genome sequence analysis confirmed the generated mutants retained the integrated nonsense codon in all target genes. Surprisingly, the RR-deprived

strain contained only four spontaneous mutations, and these were mostly small changes, such as 1-nt substitution (Table 4-5). Moreover, the SK-deprived strain had no unexpected mutations (Table 4-4). These results denoted that the HoSeI method should be a powerful strategy to edit genome sequences, e.g., knockout of multiple genes and artificial introduction of mutations, which are useful experimental demonstrations of bacterial genome-wide epistatic phenomena.

4-4-2. Relationship of sgRNA sequences and the cleavage efficiency

The dead phenotype caused by the Cas9 protein-sgRNA complex depends on the designed sgRNA. Then I investigated the relationship of sgRNA sequence and efficiency of genome cleavage. In this study, more than 200 sgRNAs were designed and introduced into *E. coli* harboring pCas. The efficiency of genome cleavage by sgRNA and Cas9 evaluated by the number of transformants of 2 plasmids (pCas and psgRNA). The efficiency of transformation evaluated genome cleavage by CRISPR-Cas9, showing that 99 of designed sgRNAs were lethal, whereas 106 sgRNAs were not. As a result of the comparison of target positions of sgRNAs on the *E. coli* genome, the efficiency of cleavage has no relation with their positions on the genome (Fig. 4-4A).

Next, to get the insight into functional sgRNAs, primary, secondary, and tertiary structures of sgRNA were analyzed in comparison with non-functional sgRNAs. As a result of primary and secondary structures analysis, primary sequence alignments of both cleaving sgRNA and uncleaving sgRNA with their downstream PAM have no conserved sequence (Fig. 4-4B). Secondary structures of 100-nt full-length sgRNAs were predicted by the CentroidFold software (http://rtools.cbrc.jp/centroidfold/, Sato *et al.* 2009). sgRNAs used in this study consist of three parts; 5'- common sequence, 20-nt of designed crRNA, and 3'- common tracrRNA (Fig. 4-4C). Predicted secondary structures of all of 109 sgRNAs were classified into 3 groups. However, there were no specific structures for cleaving the genome effectively from the comparison of secondary structures of sgRNAs. Finally, tertiary structure predictions were performed using CentroidFold and Rascal (Yamasaki *et al.* 2014). This comparison of the two pairs of sgRNAs, which showed opposite genome cleaving efficiencies with 1- or 2-nt differences of the recognition sequences, suggested that the secondary and tertiary structures of sgRNA were strongly affected its sequence difference even if it differs by 1-nt (Fig. 4-4D). Taken together, these conformation changes and the stability of sgRNA are deduced to contribute to the formation and stability of Cas9-sgRNA complex.

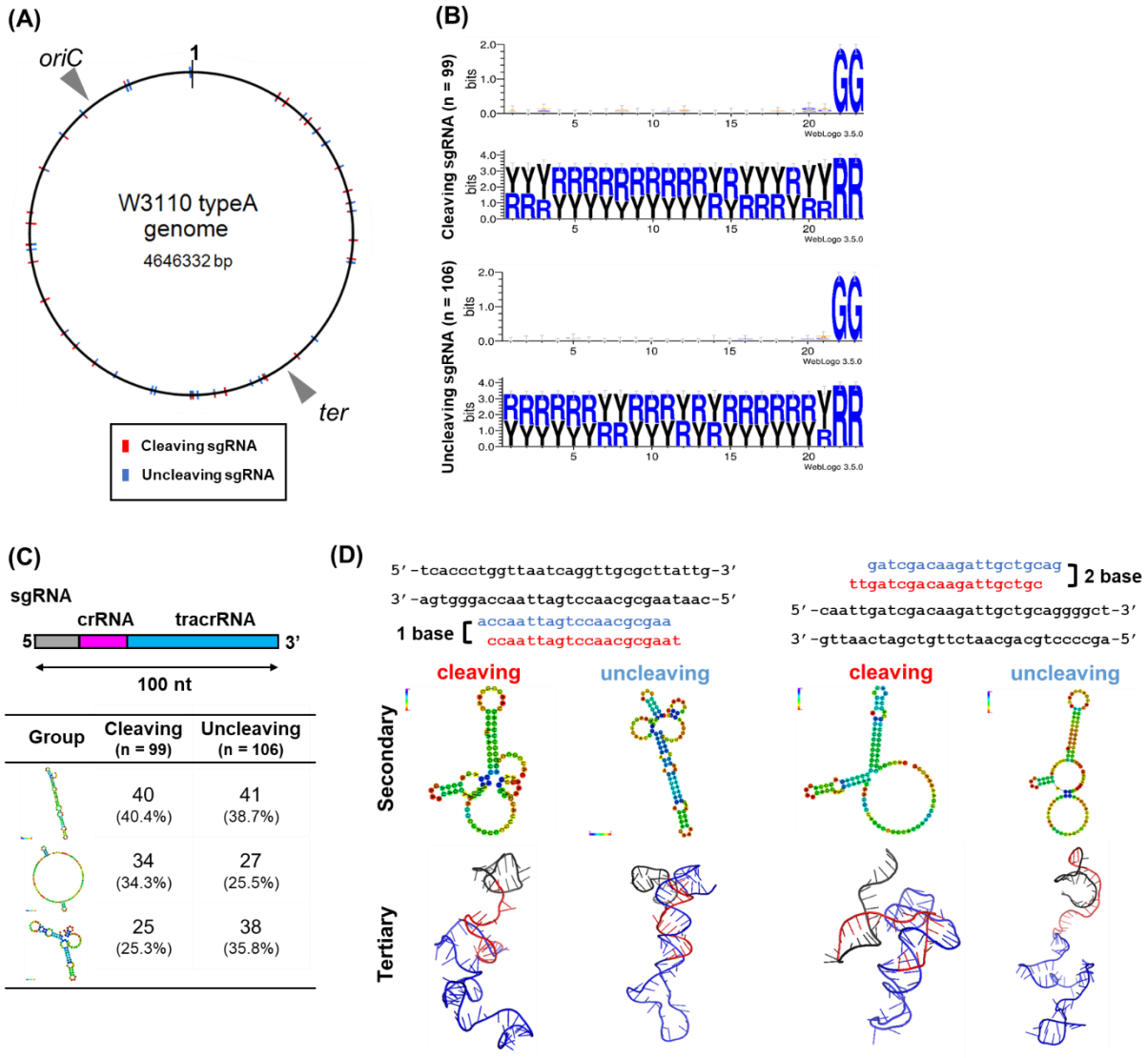

Figure 4-4. Relationship of sgRNA sequences and efficiency of cleavage. [A] The sgRNA recognition positions were mapped on the *E. coli* W3110 genome (4.6 Mb). The recognition sequences resulting in a dead phenotype (cleaving sgRNA) are shown in red, and the sequences resulting in a living phenotype (uncleaving sgRNA) are shown in blue on the genome. Two gray triangles show the positions of *oriC* and *ter*, respectively. **[B]** The multiple sequence alignment of the 20-nt of sgRNA recognition sequences with the 3-nt downstream PAMs were generated with ClustalW. The results of alignment are shown as the stacks of symbols using WebLogo 3 (http://weblogo.threeplusone.com/, Crooks *et al.* 2004). For both cleaving sgRNAs and uncleaving sgRNAs, the alignment of the nitrogenous bases (A, T, G, and C) is shown in the upper logo, and the alignment of purines (R) and pyrimidines (Y) is shown in the lower logo. The number of analyzed sgRNA recognition sequences (n) are shown on the left side of the logos. **[C]** The result of the secondary structure prediction of full-length sgRNAs using CentroidFold (http://rtools.cbrc.jp/centroidfold/, Sato *et al.* 2009). Each sgRNA used in this study consists of three parts; the 5'-consensus sequence (shown in gray), the 20-nt of recognition sequence (crRNA, shown in pink), and the 3'-consensus sequence (tracrRNA, shown in blue). Three distinctive structure groups, the number of sgRNA, and its ratio are shown in the Table. The number of analyzed sgRNA recognition sequences (n) are also shown in the Table. **[D]** The result of the secondary and tertiary structure predictions of full-length sgRNAs using CentroidFold (http://rtools.cbrc.jp/centroidfold/, Sato *et al.* 2009) and Rascal (Yamasaki *et al.* 2014). The structure predictions were performed using the two pairs of sgRNAs, which showed opposite genome cleaving efficiencies with 1- or 2-nt differences of the recognition sequences. In the tertiary structure, gray represents the 5'-consensus sequence, red represents the 20-nt of recognition sequence (crRNA), and blue represents the 3'-consensus sequence (tracrRNA).

4-4-3. Characterization of the parent strain *E. coli* K-12 W3110 type A

E. coli K-12 has been studied as a model bacterium from the initial stage of biology. As wild-type strains of *E. coli* K-12, MG1655 and W3110 were widely used for understanding a cell. These two strains had been derived from the same ancestral strain W1485 through curing of λ phage and the F^+ factor (Bachmann, 1972 and 1996; Guyer *et al.* 1981). Determination and comparison of the complete MG1655 (Guyer *et al*. 1981; Blattner *et al*. 1997) and W3110 (Hayashi *et al.* 2006) genome sequences revealed many differences, including insertions or deletions of short sequences or base substitutions (Hayashi *et al*. 2006). In addition, 13 of IS elements or defective phage were determined in only MG1655 or W3110. It is noteworthy that only W3110 has some IS elements in the intragenic regions, such as *gatA* (galactitol-specific enzyme IIA component of PTS), *rcsC* (hybrid sensory kinase in a two-component regulatory system with RcsB and RcsD), and *tnaB* (tryptophan transporter of low affinity). W3110 also contains a nonsense codon in ORF of *rpoS* (RNA polymerase, sigma S (sigma 38) factor). Also, MG1655 has one defective phage CPZ-55 (Hayashi *et al*. 2006).

In the *E. coli* genome, seven sigma subunit genes have been identified (Ishihama 2000). The analysis of the sigma subunit composition between different stocks of W3110 revealed that there are five types (A-E) of W3110 depends on the patterns of two sigma factors, sigma 28 (the *rpoF* gene product) and sigma 38 (the *rpoS* gene product) (Jishage and Ishihama 1997). The type A strain used as the parent strain in this study contains both two sigma factors of intact sizes. It is in good agreement with the result of the whole-genome sequencing of W3110 type A, which has the full-length of the *rpoS* gene (Table 4-3). Interestingly, the defective phage CPZ-55 was detected, and some of W3110 specific IS elements, such as in the *rcsC* gene, were lost in the W3110 type A genome. Since the CPZ-55 phage has been estimated in ancestral *E. coli* K-12 and was lost in the W3110 reference genome (GenBank: AP009048.1), W3110 type A might be closer to MG1655 than other types of W3110.

Rac prophage conserved in both MG1655 and W3110 and seven genes, *ynaJ* (putative DUF2534 domain-containing protein), *uspE* (universal stress protein with a role cellular motility), *fnr* (DNA-binding transcriptional dual regulator, global regulator of anaerobic growth), *ogt* (O-6-alkylguanine-DNA: cysteine-protein methyltransferase), *abgT* (p-aminobenzoyl-glutamate transporter; membrane protein), *abgB* (p-aminobenzoyl-glutamate hydrolase, B subunit), and *abgA* (p-aminobenzoyl-glutamate hydrolase, A subunit), nearby Rac prophage region were lost in W3110 type A (Table 4-3). The lack of these seven genes possibly affects metabolism, especially under anaerobic conditions. FNR, the product of the *fnr* gene, and ArcA (DNA-binding response regulator in a two-component regulatory system with ArcB) are the major transcription factors of anaerobic metabolism and regulates numerous genes (Salmon *et al*. 2003; Kang *et al*. 2005; Iuchi *et al*. 1989;

Iuchi and Lin 1992). It indicates that a two-component RR ArcA probably plays more important roles in W3110 type A under anaerobiosis.

4-4-4. The features of the TCS-deprived strains

TCSs regulate various response systems for environmental changes in the cell. The function of TCS genes in the *E. coli* genome is divided into 4 response groups, the stress response group, the metabolic response group, the metal response group, and the respiration response group (Yamamoto 2014). The whole-genome sequencing revealed four spontaneous mutations in the RR mutant genome. Two of them were in the intergenic regions, and the rest of mutations were a silent mutation in the *lolE* gene (Leu328, CTG to TTG) and a missense mutation in the *yihQ* gene (Ser528Cys, AGC to TGC). The *yihQ* gene encodes sulfoquinovosidase, which belongs to the glycosyl hydrolase 31 family. YihQ, the product of the *yihQ* gene, degrade sulfoquinovosyl diacylglycerides and sulfoquinovosyl glycerol in the sulfoglycolysis pathway, resulting in the *E. coli* cell gains a carbon and sulfur sources (Speciale *et al*. 2016). The structure of YihQ has been solved and revealed the catalytic domain (Speciale *et al*. 2016; Abayakoon *et al*. 2018). According to the structural information, YihQ forms an $(\alpha\beta)_8$ barrel. The active site consists of D405A, D405N, D472A, and D472N residue. The Ser528 is the last residue of the 10^{th} α-helix domain. These insights suggest that the amino acid substitution of 528^{th} serine might not affect the catalytic activity.

Next, I analyzed the phenotype of the isolated RR- or SK-deprived strains to reveal the contribution of TCSs for the growth of *E. coli*. According to the results of growth assays, TCS deprivation decreased both the growth rate and the maximum cell population under poor nutrient conditions. In the comparison of the RR mutant and the SK mutant, the growth rate of the RR mutant was much slower than the SK mutant at 27℃. The SK mutant growing at 27℃ showed a reduction in the cell mass at 120 hours after incubation, but the initial growth rate within 48 hours looked like as rapid as the parent strain. At 42℃, however, the growth rate of the RR mutant was faster than the SK mutant even though the maximum cell population of two mutants was close to each other. These differences suggest that *E. coli* cells may conceivably carry the rapid initial growth by using RRs at low temperatures and by using SKs at high temperatures. Also, the insights of the maximum cell density proposed that TCSs make the cell possible to form the larger cell mass.

In addition to the general growth kinetics, the RR gene-knockout strain showed a growth defect in various nutrients, osmolytes, pH, and inhibitors. Conversely, the SK-knockout strain did not display a severe restriction in growth capacity under any conditions included in the PM testing. For the most part, the SK mutant could grow in the conditions which did not cultivate the RR mutant. As the results of chemical sensitivity testing, six or eleven antimicrobials were identified as more insensitive in the RR- or the SK-deprived strain, respectively. However, the other compounds which

belonged to the same groups of them, did not show an increase of resistance in the mutants. Further analysis could clarify whether these high tolerances of mutants only appear on the specific inhibitors. Together, these insights proposed the *E. coli* cell survives and performs adaptive growth using the signal transduction systems, especially response regulators when the cell survives in minimal nutrient conditions.

As unexpected, the growth of the RR- and SK-knockout mutants was similar to the parent strain under the nutrient-rich condition. I compared the parent and TCS mutants in the profile of more than 500 cellular proteins detected by LC-MS analysis and in the gene-expression profile by RNA-seq analysis at log phase in LB medium. The profile of proteins and transcripts were both appreciably different between the parent and the mutants (data not shown). According to the transcriptomic analysis, the TCS deprivation seems to induce the expression of metabolic pathway- and ABC-transporter-related genes. Furthermore, although the features of the strains deficient in RRs or SKs partially overlapped, the level of changes was mostly divergent. Therefore, I speculate the absence of TCS variegates the regulation of the multiple processes in the *E. coli* cell, increasing its population in a signal-response independent manner under the eutrophic conditions. It should be mentioned that TCSs are dispensable in *E. coli*, one of gram-negative bacteria, unlike in one of gram-positive bacteria, *Staphylococcus aureus* contains an essential TCS WalRK in the genome (Villanueva *et al*. 2018).

CHAPTER 5. EPISTATIC EFFECT OF RESPONSE REGULATORS TO THE ADAPTIVE GROWTH OF *E. COLI*

5-1. Introduction

Bacteria survive and then increase their population by binary cell division in a timely manner. Individual bacterial cells sense changing environmental signals, transduce those environmental signals into biological responses, and adapt to the environmental change by biological responses. Successful integration of these biological stress responses must induce adaptive growth to increase cell population.

According to recent massive amounts of genomic information, a genome consists of the core genome, a set of species-specific genes, and pan genome, representing non-conserved genes (Touchon *et al.* 2009). Within the core genome, there is a set of genes involved in central and secondary metabolism, cell cycle, and gene expression, many of which are essential for growth (Touchon *et al.* 2009). In addition to genes coding for essential biological functions, regulatory genes are conserved in the core genome but are not essential for growth (Touchon *et al.* 2009). One of the core-genome regulatory genes is the RR gene, which is a unique signal transduction component that is only conserved among prokaryotes. Several TFs are autoregulated during the response to environmental signals. Positive autoregulation leads to a fast response and impacts the response dynamics (Gao and Stock. 2018; Maeda and Sano. 2006). Among ~30 positively autoregulated TFs in the *E. coli* genome (Hermsen *et al.* 2010), 10 of those are RRs of TCSs. A recent report showed that coupled positive and negative feedback allowed both a fast response and optimal RR protein levels in the PhoB/PhoR system in *E. coli* (Gao and Stock. 2018). However, the contribution of coupled autoregulation for continuous bacterial growth is poorly understood.

In this study, I found a correlation of the RR family with bacterial genome size, speculating that the main RR genes (*phoP*, *phoB*, *ompR*) affect *E. coli* growth. To gain insight into the effect of RR genes on growth, the set of gene knockout strains are isolated by using the HoSeI method (see Chapter 4). The differences of elapsed time until the first cell division and initial growth rate of the isolated strains were measured and analyzed with statistics, indicating that a particular pair of main RR genes of *E. coli* K-12 are required for adaptive growth via genetic epistasis.

5-2. Materials and Methods

5-2-1. *E. coli* strains, plasmids, and oligonucleotides

The used *E. coli* strains, plasmids, and oligonucleotides are listed in Table 5-1, Table 4-2, Table 5-2 and Appendix Table 3 and 4, respectively. *E. coli* K-12 W3110 type A strain was used as a parent type (Jishage and Ishihama. 1997).

Table 5-1. Bacterial strains used in this study.

Name	Characterization	Reference
W3110 typeA	Parent strain, complete σ set	Jishage *et al.* 1997
W3110ΔphoP	W3110, Δ*phoP* (W3110 typeA←Δ*phoP*)	This study
W3110ΔphoB	W3110, Δ*phoB* (W3110 typeA←Δ*phoB*)	This study
W3110ΔcitB	W3110, Δ*citB* (W3110 typeA←Δ*citB*)	This study
W3110ΔompR	W3110, Δ*ompR* (W3110 typeA←Δ*ompR*)	This study
W3110ΔnarL	W3110, Δ*narL* (W3110 typeA←Δ*narL*)	This study
W3110ΔcpxR	W3110, Δ*cpxR* (W3110 typeA←Δ*cpxR*)	This study
W3110ΔuhpA	W3110, Δ*uhpA* (W3110 typeA←Δ*uhpA*)	This study
W3110ΔrstA	W3110, Δ*rstA* (W3110 typeA←Δ*rstA*)	This study
W3110ΔevgA	W3110, Δ*evgA* (W3110 typeA←Δ*evgA*)	This study
W3110ΔkdpE	W3110, Δ*kdpE* (W3110 typeA←Δ*kdpE*)	This study
W3110ΔtorR	W3110, Δ*torR* (W3110 typeA←Δ*torR*)	This study
W3110ΔuvrY	W3110, Δ*uvrY* (W3110 typeA←Δ*uvrY*)	This study
W3110ΔqseB	W3110, Δ*qseB* (W3110 typeA←Δ*qseB*)	This study
W3110ΔarcA	W3110, Δ*arcA* (W3110 typeA←Δ*arcA*)	This study
W3110ΔatoC	W3110, Δ*atoC* (W3110 typeA←Δ*atoC*)	This study
W3110ΔbaeR	W3110, Δ*baeR* (W3110 typeA←Δ*baeR*)	This study
W3110ΔntrC	W3110, Δ*ntrC* (W3110 typeA←Δ*ntrC*)	This study
W3110ΔrcsB	W3110, Δ*rcsB* (W3110 typeA←Δ*rcsB*)	This study
W3110ΔpyrR	W3110, Δ*pyrR* (W3110 typeA←Δ*pyrR*)	This study
W3110ΔbtsR	W3110, Δ*btsR* (W3110 typeA←Δ*btsR*)	This study
W3110ΔcreB	W3110, Δ*creB* (W3110 typeA←Δ*creB*)	This study
W3110ΔbasR	W3110, Δ*basR* (W3110 typeA←Δ*basR*)	This study
W3110ΔcusR	W3110, Δ*cusR* (W3110 typeA←Δ*cusR*)	This study
W3110ΔnarP	W3110, Δ*narP* (W3110 typeA←Δ*narP*)	This study
W3110ΔzraR	W3110, Δ*zraR* (W3110 typeA←Δ*zraR*)	This study
W3110ΔrssB	W3110, Δ*rssB* (W3110 typeA←Δ*rssB*)	This study
W3110ΔglrR	W3110, Δ*glrR* (W3110 typeA←Δ*glrR*)	This study
W3110ΔfimZ	W3110, Δ*fimZ* (W3110 typeA←Δ*fimZ*)	This study
W3110ΔygeK	W3110, Δ*ygeK* (W3110 typeA←Δ*ygeK*)	This study
W3110ΔdcuR	W3110, Δ*dcuR* (W3110 typeA←Δ*dcuR*)	This study
W3110ΔyhjB	W3110, Δ*yhjB* (W3110 typeA←Δ*yhjB*)	This study
W3110ΔcheB	W3110, Δ*cheB* (W3110 typeA←Δ*cheB*)	This study
W3110ΔcheY	W3110, Δ*cheY* (W3110 typeA←Δ*cheY*)	This study
W3110ΔhprR	W3110, Δ*hprR* (W3110 typeA←Δ*hprR*)	This study

The *E. coli* strains constructed in this study would be provided from National BioResourse Project (NBRP) *E. coli* of Japan.

Table 5-1. Bacterial strains used in this study. (Continued.)

Name	Characterization	Reference
W3110ΔompRΔphoB	W3110, Δ*ompR*, Δ*phoB* (W3110ΔphoB←Δ*ompR*)	This study
W3110ΔompRΔphoP	W3110, Δ*ompR*, Δ*phoP* (W3110ΔphoP←Δ*ompR*)	This study
W3110ΔphoBΔphoP	W3110, Δ*phoB*, Δ*phoP* (W3110ΔphoB←Δ*phoP*)	This study
W3110ΔompRΔphoBΔphoP	W3110, Δ*ompR*, Δ*phoB*, Δ*phoP* (W3110ΔphoBΔphoP←Δ*ompR*)	This study
W3110ΔompRΔenvZ	W3110, Δ*ompR*, Δ*envZ* (W3110ΔompR←Δ*envZ*)	This study
W3110ΔphoBΔphoR	W3110, Δ*phoB*, Δ*phoR* (W3110ΔphoB←Δ*phoR*)	This study
W3110ΔphoPΔphoQ	W3110, Δ*phoP*, Δ*phoQ* (W3110ΔphoP←Δ*phoQ*)	This study
W3110ΔphoPΔkdpE	W3110, Δ*phoP*, Δ*kdpE* (W3110ΔphoP←Δ*kdpE*)	This study
W3110ΔphoBΔcreB	W3110, Δ*phoB*, Δ*creB* (W3110ΔphoB←Δ*creB*)	This study
W3110ΔompRΔcpxR	W3110, Δ*ompR*, Δ*cpxR* (W3110ΔompR←Δ*cpxR*)	This study
W3110ΔompRΔrstA	W3110, Δ*ompR*, Δ*rstA* (W3110ΔompR←Δ*rstA*)	This study
W3110ΔrstAΔcusR	W3110, Δ*rstA* (W3110ΔrstA←Δ*cusR*)	This study
W3110ΔrstAΔcusRΔhprR	W3110, Δ*rstA*, Δ*cusR*, Δ*hprR* (W3110ΔrstAΔcusR←Δ*hprR*)	This study
W3110ΔcusS	W3110, Δ*cusS* (W3110 typeA←Δ*cusS*)	This study
W3110ΔzraS	W3110, Δ*zraS* (W3110 typeA←Δ*zraS*)	This study
W3110ΔkdpD	W3110, Δ*kdpD* (W3110 typeA←Δ*kdpD*)	This study
W3110ΔphoQ	W3110, Δ*phoQ* (W3110 typeA←Δ*phoQ*)	This study
W3110ΔbasS	W3110, Δ*basS* (W3110 typeA←Δ*basS*)	This study
W3110ΔbaeS	W3110, Δ*baeS* (W3110 typeA←Δ*baeS*)	This study
W3110ΔcpxA	W3110, Δ*cpxA* (W3110 typeA←Δ*cpxA*)	This study
W3110ΔenvZ	W3110, Δ*envZ* (W3110 typeA←Δ*envZ*)	This study
W3110ΔevgS	W3110, Δ*evgS* (W3110 typeA←Δ*evgS*)	This study
W3110ΔglrK	W3110, Δ*glrK* (W3110 typeA←Δ*glrK*)	This study
W3110ΔqseC	W3110, Δ*qseC* (W3110 typeA←Δ*qseC*)	This study
W3110ΔrcsC	W3110, Δ*rcsC* (W3110 typeA←Δ*rcsC*)	This study
W3110ΔrcsD	W3110, Δ*rcsD* (W3110 typeA←Δ*rcsD*)	This study
W3110ΔrstB	W3110, Δ*rstB* (W3110 typeA←Δ*rstB*)	This study
W3110ΔhprS	W3110, Δ*hprS* (W3110 typeA←Δ*hprS*)	This study
W3110ΔatoS	W3110, Δ*atoS* (W3110 typeA←Δ*atoS*)	This study
W3110ΔbarA	W3110, Δ*barA* (W3110 typeA←Δ*barA*)	This study
W3110ΔcreC	W3110, Δ*creC* (W3110 typeA←Δ*creC*)	This study
W3110ΔntrB	W3110, Δ*ntrB* (W3110 typeA←Δ*ntrB*)	This study
W3110ΔphoR	W3110, Δ*phoR* (W3110 typeA←Δ*phoR*)	This study
W3110ΔuhpB	W3110, Δ*uhpB* (W3110 typeA←Δ*uhpB*)	This study
W3110ΔbtsS	W3110, Δ*btsS* (W3110 typeA←Δ*btsS*)	This study
W3110ΔpyrS	W3110, Δ*pyrS* (W3110 typeA←Δ*pyrS*)	This study
W3110ΔarcB	W3110, Δ*arcB* (W3110 typeA←Δ*arcB*)	This study
W3110ΔcitA	W3110, Δ*citA* (W3110 typeA←Δ*citA*)	This study
W3110ΔdcuS	W3110, Δ*dcuS* (W3110 typeA←Δ*dcuS*)	This study
W3110ΔnarQ	W3110, Δ*narQ* (W3110 typeA←Δ*narQ*)	This study
W3110ΔnarX	W3110, Δ*narX* (W3110 typeA←Δ*narX*)	This study
W3110ΔtorS	W3110, Δ*torS* (W3110 typeA←Δ*torS*)	This study
W3110ΔcheA	W3110, Δ*cheA* (W3110 typeA←Δ*cheA*)	This study
W3110ΔenvZΔphoR	W3110, Δ*envZ*, Δ*phoR* (W3110ΔphoR←Δ*envZ*)	This study
W3110ΔenvZΔphoQ	W3110, Δ*envZ*, Δ*phoQ* (W3110ΔphoQ←Δ*envZ*)	This study

The *E. coli* strains constructed in this study would be provided from National BioResource Project (NBRP) *E. coli* of Japan.

Table 5-1. Bacterial strains used in this study. (Continued.)

Name	Characterization	Reference
W3110ΔphoRΔphoQ	W3110, Δ*phoR*, Δ*phoQ* (W3110ΔphoQ←Δ*phoR*)	This study
W3110ΔenvZΔphoRΔphoQ	W3110, Δ*envZ*, Δ*phoR*, Δ*phoQ* (W3110ΔphoQΔphoR←Δ*envZ*)	This study
W3110Δ34RR	W3110, Δ*phoP*, Δ*phoB*, Δ*citB*, Δ*ompR*, Δ*narL*, Δ*cpxR*, Δ*uhpA*, Δ*rstA*, Δ*evgA*, Δ*kdpE*, Δ*torR*, Δ*uvrY*, Δ*qseB*, Δ*arcA*, Δ*atoC*, Δ*baeR*, Δ*ntrC*, Δ*rcsB*, Δ*pyrR*, Δ*btsR*, Δ*creB*, Δ*basR*, Δ*cusR*, Δ*narP*, Δ*zraR*, Δ*rssB*, Δ*glrR*, Δ*fimZ*, Δ*ygeK*, Δ*dcuR*, Δ*yhjB*, Δ*cheB*, Δ*cheY*, Δ*hprR*	This study
W3110Δ30SK	W3110, Δ*cusS*, Δ*zraS*, Δ*kdpD*, Δ*phoQ*, Δ*basS*, Δ*baeS*, Δ*cpxA*, Δ*envZ*, Δ*evgS*, Δ*glrK*, Δ*qseC*, Δ*rcsC*, Δ*rcsD*, Δ*rstB*, Δ*hprS*, Δ*atoS*, Δ*barA*, Δ*creC*, Δ*ntrB*, Δ*phoR*, Δ*uhpB*, Δ*btsS*, Δ*pyrS*, Δ*arcB*, Δ*citA*, Δ*dcuS*, Δ*narQ*, Δ*narX*, Δ*torS*, Δ*cheA*	This study

The *E. coli* strains constructed in this study would be provided from National BioResource Project (NBRP) *E. coli* of Japan.

Table 5-2. Plasmids and oligonucleotides used in this study.

Name	Characterization	Reference
Plasmids		
pLUX	*kan* , *luxCDABE* , STOP codons, ribosome binding site	Burton *et al*. 2010
pLUX-mgtA	pLUX, *mgtA* promoter-*luxCDABE*	This study
pLUX-pstS	pLUX, *pstS* promoter-*luxCDABE*	This study
pLUX-ompC	pLUX, *ompC* promoter-*luxCDABE*	This study
pBAD33	pACYC184 derived, P_{BAD} Cm^r	Guzman *et al*. 1995
pBADPhoP-FLAG	pBAD33, FLAG-tagged PhoP at C-terminus	This study
pBADPhoB-FLAG	pBAD33, FLAG-tagged PhoB at C-terminus	This study
pBADOmpR-FLAG	pBAD33, FLAG-tagged OmpR at C-terminus	This study
Oligonucleotides		
For luciferase reporter plasmid		
mgtA_Lux_F	TCGTCTTCACCTCGACTACGCCGTCGATATTACGCCGTTT	This study
mgtA_Lux_R	ACTAACTAGAGGATCAAGGAGTCCCTCCGCACTGTCTGAA	This study
pstS_Lux_F	TCGTCTTCACCTCGATGTGGAAGAGGTGATTGCACCGATC	This study
pstS_Lux_R	ACTAACTAGAGGATCAATGTCTCCTGGGAGGATTCATAAA	This study
ompC_Lux_F	TCGTCTTCACCTCGAAAACAAAGATTGCTGGAAATTATGC	This study
ompC_Lux_R	ACTAACTAGAGGATCCCTGCTACCAGCAGAGCTGGGACCA	This study
pLux_R	CCGTCCATTTGTGATAATAGTGG	This study
For RR expression plasmid		
PHOPF-1	TAGCGAATTCGAGCTAGGAGGAATTCACCATGCGCGTACTGGTTGTTGA	This study
PHOPR-1	CAAAACAGCCAAGCTTTACTATTTATCGTCGTCATCTTTGTAGTCGCGCAATTCGAACAGATAGC	This study
PHOBF-1	TAGCGAATTCGAGCTAGGAGGAATTCACCATGGCGAGACGTATTCTGGT	This study
PHOBR-1	CAAAACAGCCAAGCTTTACTATTTATCGTCGTCATCTTTGTAGTCAAAGCGGCTTGAAAAACGAT	This study
OMPRF-1	TAGCGAATTCGAGCTAGGAGGAATTCACCATGCAAGAGAACTACAAGATTCT	This study
OMPRR-1	CAAAACAGCCAAGCTTTACTATTTATCGTCGTCATCTTTGTAGTCTGCTTTAGAGCCGTCCGGTA	This study

The plasmids constructed in this study would be provided from National BioResource Project (NBRP) *E. coli* of Japan.

5-2-2. Growth condition of *E. coli*

E. coli cells were grown at 30℃ in M9-glucose medium.

5-2-3. Multi-gene knockout in the *E. coli* genome by the HoSeI method

The W3110 type A strain harboring pCas was grown in LB medium containing 1% arabinose and 50 μg/mL kanamycin to logarithmic phase and then was collected and suspended in a solution of 0.1 M $CaCl_2$. This suspension of *E. coli* was subjected to transformation by the psgRNA-target and DNA fragment to recover the digested site by CRISPR-Cas9. psgRNA-ompR, psgRNA-phoB, psgRNA-phoP, psgRNA-envZ, psgRNA-phoR, psgRNA-phoQ, psgRNA-kdpE, psgRNA-creB, psgRNA-cpxR, psgRNA-rstA, psgRNA-cusR, psgRNA-hprR, psgRNA-arcA, psgRNA-basR, psgRNA-baeR, psgRNA-qseB, and psgRNA-torR were used as psgRNA-target plasmids (Table 4-2). The 83-bp DNA fragments were prepared by hybridization of a pair of complementary synthetic oligonucleotides (see the DNA sequences shown in Appendix Table 4). In comparison with no colonies observed on LB agar containing 100 μg/mL ampicillin by transformation with only psgRNA-target, the addition of the DNA fragment produced transformants that grew on LB agar containing ampicillin. To verify the introduction of a stop codon on the target gene of the genome, genomic DNA was prepared from the transformant and used as a template for amplification of the target sequence by PCR using a pair of oligonucleotides, as shown in Appendix Table 3. The introduction of a stop codon on the target gene was confirmed by DNA sequencing of the amplified DNA.

5-2-4. Time-lapse observation on microscope

Strains were inoculated in M9 glucose medium and shaken overnight at 37℃. The cultures were washed with M9 medium three times and diluted 10-fold into the medium. The diluted cultures were spread on an M9 glucose plate. Next, the plates were cut and placed on a slide glass. The preparation was sealed on a glass coverslip with nail polish. The cells were imaged with a microscope (IX81, Olympus) using a 100x/NA 1.4 objective lens (M Plan Apochromat MPLAPON-Oil, Olympus) and a Retiga EXi Fast1394 CCD camera (Q Imaging). The temperature was maintained at 30℃ using a closed circulation system (EYELA). Image acquisition and microscope control were performed with Image Pro Plus (Nippon roper). The elapsed time until cell division and growth rate of each *E. coli* strain were measured by ImageJ.

5-2-5. Construction of RR protein expression plasmid

I constructed the OmpR, PhoB, and PhoP expression plasmids as well as arabinose-inducible expression system of NarL family RR as previously described (Yoshida *et al.* 2015). In brief, the protein-coding regions of *phoP*, *phoB*, and *ompR* gene with an artificial SD sequence were amplified by PCR using specific primers (Table 5-2). Each amplified DNA fragment was inserted

into the linear pBAD33 vector by In Fusion system (Takara Bio, Japan), resulting in construction of the FLAG-tagged RR protein expression plasmids, pBADPhoP-FLAG, pBADPhoB-FLAG, and pBADOmpR-FLAG (Table 5-2).

5-2-6. Luciferase reporter assay in *E. coli*

I performed luciferase reporter assay in *E. coli* to evaluate activity of TCS-target promoters *in vivo* as previously described (Yamanaka *et al.* 2018; Yamanaka *et al.* 2020). In brief, the *ompC*, *mgtA*, *pstS* promoters were amplified by PCR using W3110 type A genome as a template, a pair of primers (see DNA sequence shown in Table 5-2), and Ex Taq DNA polymerase (Takara Bio, Japan). The promoter DNA was inserted into the *Bam* HI and *Xho* I sites of pLUX vector (Burton *et al.* 2010) by the In-Fusion system (Takara Bio, Japan). The inserted DNA sequence on the resulting plasmid was confirmed by DNA sequencing (Table 5-2). The constructed pLux-mgtA, pLux-pstS, and pLux-ompC were transformed into each strain. Transformants were grown in the M9-glucose medium at 37℃ with shaking for overnight. Then, overnight culture was transferred into fresh M9-glucose medium and OD_{600} and a total intensity of luminescence of culture were measured with a plate reader (Corona). The ratio of luminescence to OD_{600} (LUX/OD) was evaluated as a specific activity of the promoter.

5-2-7. Cluster analysis

Cluster analysis was performed with R software (https://www.R-project.org/). The obtained data of the elapsed time and the growth rate were prepared for Ward's method. A hierarchical clustering dendrogram was calculated using Euclidean distances.

5-2-8. Correlation of the number of COGs and the genome size with the Gompertz function

I used all of the genome sequences of 628 species of bacteria registered in the COG databank. TCS genes and RNA polymerase genes were isolated, and the number of these genes was counted for each bacterial genome. The number of COGs involved in TCSs and the RNA polymerase subunit was analyzed in comparison with the genome size, and the average number of COGs was calculated for each genome size of 0.5, 1, 2, 3, 4, 5, 6, 7, 8, 9, 10, 12, and 15 Mb. The calculated data were fitted by the Gompertz curve $y = ab^{e^{-cx}}$, where y is the number of COGs and x is the genome size.

5-3. Results

5-3-1. Estimation of highly conserved response regulator genes in the bacterial genome

The Clusters of Orthologous Groups of proteins (COGs) database has been designed to classify proteins on the basis of orthology (Tatusov *et al.* 1997). Twelve groups are detected as two-component response regulators from the genomes of 628 bacteria species in the COG database (Tatusov *et al.* 2000) as follows: OmpR family as COG0745, NarL/FixJ family as COG2197, PleD family as COG3706, NtrC family as COG2204, CheB family as COG2201, LytR/AlgR family as COG3279, AmiR/NasT family as COG3707, FixJ family as COG4566, ActR/RegA family as COG4567, YesN/AraC family as COG4753, CriR family as COG4565, and SAPR family as COG3947. I found a correlation between the number of RR COGs and genome size, as fitted by the Gompertz curve (Fig. 5-1A). Bacterial genomes less than 5 Mbp in size contained the relative RR COG number of 2 RR COGs per Mbp of genome, while bacterial genomes more than 5 Mbp in size contained 8 RR COGs (Fig. 5-1A). Bacterial RNA polymerase core enzyme consists of 2α, β, β', ω (Murakami. 2015), which were featured by COG0202, COG0085, COG0086, and COG1758 (Tatusov *et al.* 2000). The COG0202, COG0085, and COG0086 were almost completely conserved among more than 99% of bacteria registered in COG database (Tatusov *et al.* 2000). In addition of four COGs featuring bacterial RNA polymerase core subunits, the 8 COGs of RNA polymerase subunits were similarly analyzed, resulting that bacterial genomes contained at least 4 RNA polymerase COGs relating RNA polymerase core subunits and major sigma factor and bacterial genomes more than 3 Mbp in size contained 7 RNA polymerase COGs by the addition of COGs relating minor sigma factors (Fig. 5-1B). Among the 628 species of bacteria, conservation of RR COGs is the highest in the OmpR family, at 95%, and the lowest in the SAPR family, at 8.4% (Fig. 5-1C), suggesting that the OmpR family is extensively conserved in bacteria as a member of the core genome.

The copy number of RR genes of the *E. coli* K-12 genome was evaluated in detail. The genome sequence of *E. coli* K-12, which is 4.6 Mbp in size, has 34 predicted response regulator genes, of which 6 are classified as RR COGs (Mizuno. 1997; Yamamoto *et al.* 2005). Among all 34 RR genes, OmpR family genes are the most prevalent, with 14 genes, *arcA*, *phoB*, *cusR*, *kdpE*, *torR*, *phoP*, *rstA*, *hprR*, *basR*, *qseB*, *ompR*, *cpxR*, *creB*, and *baeR*, and the CriR family and LytT family have the smallest number, at 2 genes, with *citB* and *dcuR* and with *btsR* and *pyrR*, respectively (Figs. 5-1C and 5-2A). Six RR genes of the OmpR family are known to be positively self-activated (Fig. 5-1D) (Yamamoto *et al.* 2002; Yamamoto and Ishihama. 2006; Ogasawara *et al.* 2012; Pukklay *et al.* 2013; Gao and Stock. 2013; Sperandio *et al.* 2002). In good agreement with the positive feedback regulation of the OmpR family RRs of *E. coli* K-12, OmpR, PhoB, and PhoP are abundant regulators in *E. coli* through the growth phase in rich and poor medium, with

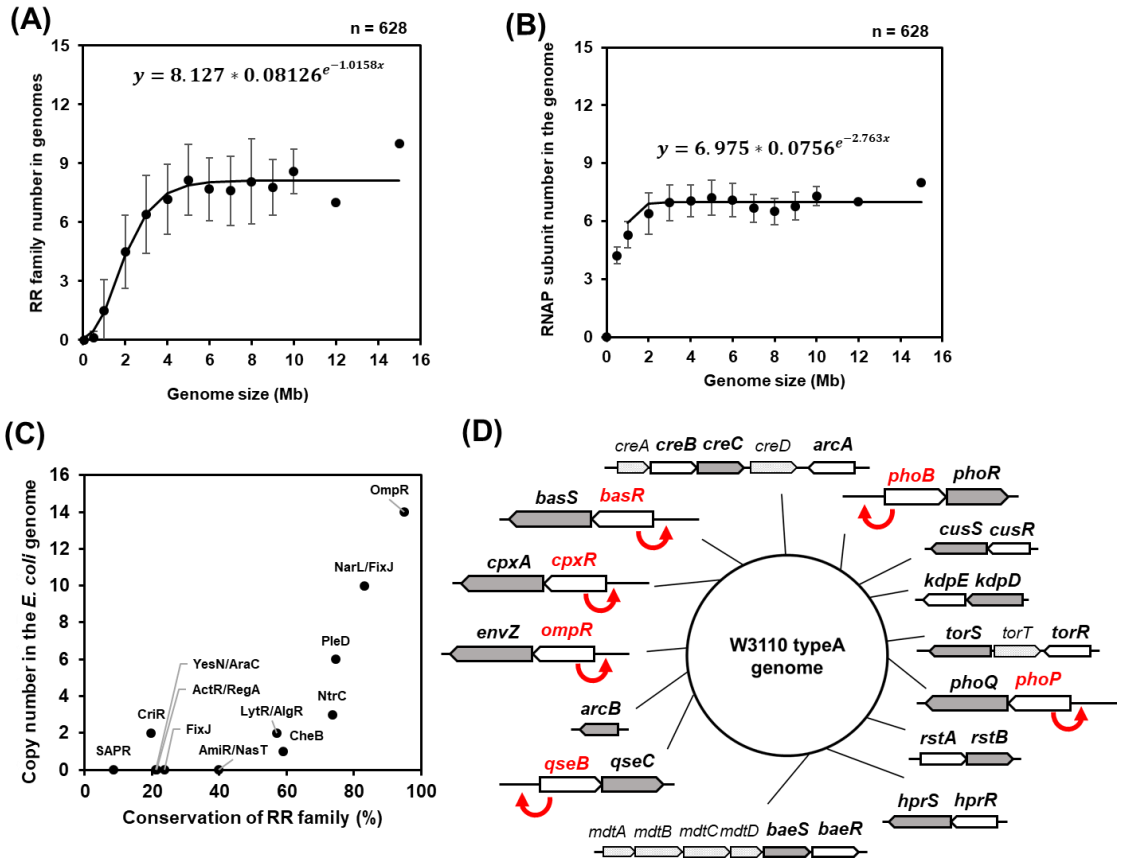

Figure 5-1. Conservation of two-component system response regulator families in bacterial genomes. [A] The correlation between genome size and the number of RR families in the genomes. Twelve groups are detected as two-component response regulators from the bacterial genomes of 628 species in the COG database as follows: OmpR family as COG0745, NarL/FixJ family as COG2197, PleD family as COG3706, NtrC family as COG2204, CheB family as COG2201, LytR/AlgR family as COG3279, AmiR/NasT family as COG3707, FixJ family as COG4566, ActR/RegA family as COG4567, YesN/AraC family as COG4753, CriR family as COG4565, and SAPR family as COG3947. The number of COGs involved in the RR family (y-axis) was analyzed in comparison with the genome size (x-axis). The average number of COGs (black circle) and standard deviation (SD, error bar) were calculated for each genome size of 0.5, 1, 2, 3, 4, 5, 6, 7, 8, 9, 10, 12, and 15 Mb. The calculated data were fitted by the Gompertz curve $y = ab^{e^{-cx}}$, where y is the number of COGs and x is the genome size. The formula of the fitted Gompertz curve is shown in the graph. **[B]** The correlation between genome size and the number of RNA polymerase subunit in bacterial genomes. Eight groups are detected as RNA polymerase subunit from 628 species bacteria genomes in COG database (Tatusov *et al.* 2000) as the following; beta subunit as COG0085, beta' subunit as COG0086, sigma70/sigma32 subunit as COG0568, alpha subunit as COG0202, sigma24 subunit as COG1595, K/omega subunit as COG1758, sigma54 subunit as COG1508, and sigma subunit as COG1191. I used all of genome sequence of 628 species of bacteria registered in COG databank. The number of COGs involved in RNA polymerase subunit (y axis) was analyzed in comparison with genome size (x axis). The average of the number of COGs (black circle) and standard deviation (SD, error bar) was calculated for each genome size of 0.5, 1, 2, 3, 4, 5, 6, 7, 8, 9, 10, 12, and 15 Mb. The calculated data fitted Gompertz curve $y = ab^{e^{-cx}}$ with y is the number of COGs and x is the genome size. The formula of fitted Gompertz curve are shown in the graph. **[C]** Conservation of RR families in the bacterial genomes and gene copy number in the *E. coli* genome. Based on the calculated data shown in **A**, the conservation (%) of each COG was calculated on all genomes of 628 species of bacteria (x-axis). The y-axis shows the gene copy number of each RR family in the *E. coli* K-12 genome. **[D]** OmpR family RR genes in the *E. coli* K-12 genome. *E. coli* K-12 W3110 has 14 OmpR family response regulator genes in its genome. Each arrow shows OmpR family response regulators (white), their cognate sensor kinases (gray), and other genes in the operon (light gray). The direction of arrows shows the direction of genes in the *E. coli* genome. Red letters and arrows show the genes known as positive feedback regulators.

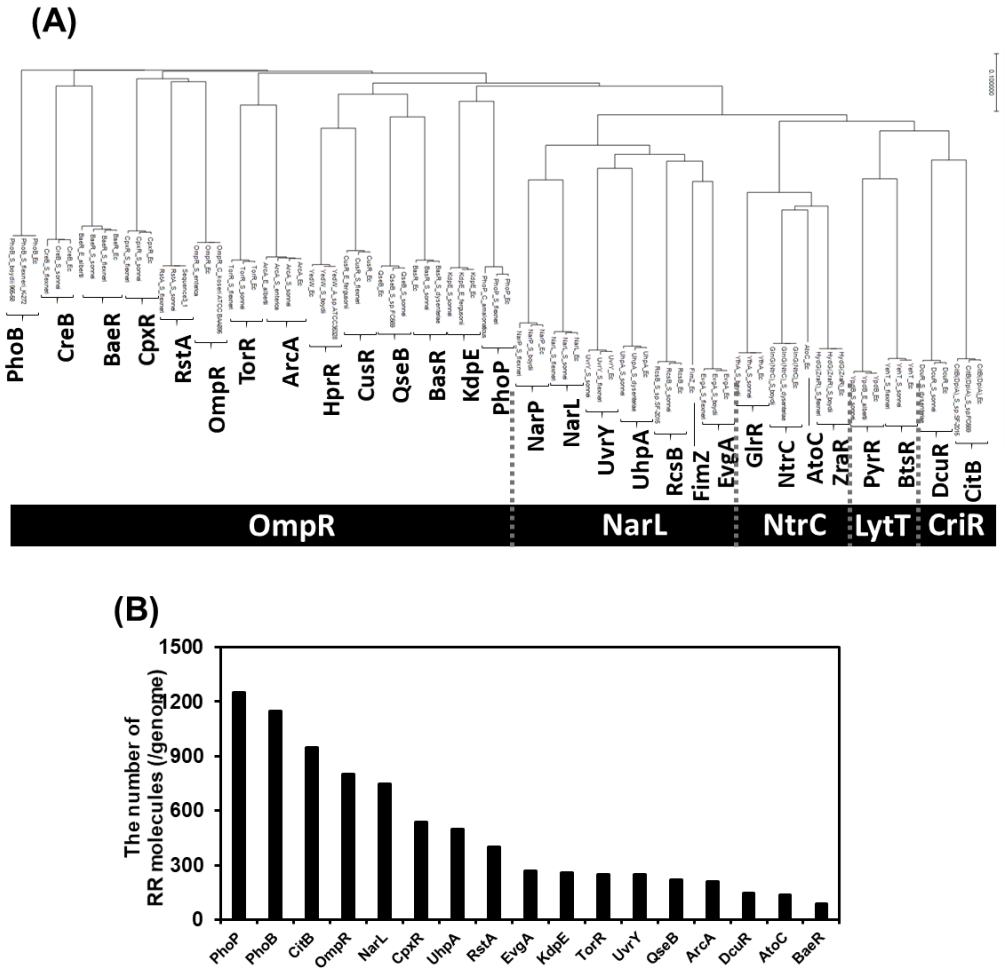

Figure 5-2. Classification of two-component system RRs in *E. coli*. [A] The dendrogram of response regulators of *E. coli*. Cluster analysis was performed for RRs of *E. coli* and two of related species (*E. albertii*, *S. enterica*, *S. sonnei*, *S. flexneri* K-272, *S. dysenteriae*, *S. boydii* 965-58, *C. freundii*, *E. fergusonii*, and *C. koseri* ATCC BAA895) with ClustalW software, resulting in each of RR family shown in the right side. **[B]** The amount of intracellular RR molecules in the *E. coli* K-12 cell. The intracellular levels of 65 species of transcription factor with known function in *E. coli* K-12 W3110 at various phases of cell growth has showed the order of intracellular response regulators. (Ishihama *et al.* 2014). Y axis shows the number of RR molecules per genome as arranged from Ishihama *et al.* (2014).

approximately 1,000 copies per genome (Fig. 5-2B) (Ishihama *et al.* 2014). Taking these observations together, I suspected that OmpR, PhoB, and PhoP play important roles in the adaptive growth of fast-growing *E. coli* as main RR factors.

5-3-2. Construction of multi RR or SK-gene knockout strains using HoSeI method

All single knockouts of the 14 OmpR family RRs and all strains of seven combinations of main RR gene knockout for PhoB, PhoP, and OmpR (Table 5-1) were bred using the newly developed HoSeI method (see Chapter 4). For knockout of each gene, I constructed sgRNA-expressing plasmids (Table 4-2) and designed DNA fragments, including the nonsense codon for

the target gene. The proper introduction of the nonsense codon, TAA, was confirmed by Sanger sequencing in all cases (Fig. 4-2). The psgRNA-free transformant was isolated by IPTG-inducible sgRNA for the psgRNA plasmid from pCas as previously described (Jiang *et al.* 2015). The isolated psgRNA-free transformant was subjected to further gene knockout by repeating the HoSeI method.

5-3-3. Contribution of the optimum adaptive growth of *E. coli* by RR genes

Bacteria are able to grow both in liquid and solid conditions. In both cases, the number of bacteria cells similarly increases (Koga *et al.* 2004). To measure the elapsed time until cell division and growth rate of single *E. coli* cells, time-lapse observation of single cells growing on solid medium was adopted in a 30 min range for 8 h with light microscopy. At the end of observation after 8 hours, 70.8% of the parent strain, W3110 type A, cells formed micro-colonies including 4 to 8 cells, while 8.3% of the cells were not completely divided (Fig. 5-3A). The majority of parent cells started cell division 0.5 - 4.5 hours after incubation (80.2%) and showed a growth rate of 0.5 - 1.1 divisions/hour (75.0%) (Figs. 5-3AP). Fourteen single OmpR family RR gene knockout strains isolated in this study were subjected to time-lapse observation, as was the parent strain. Most of the single RR gene knockouts, except for Δ*ompR*, showed that the percentage of non-growing cells was in the range of 17% to 1.5% at the end of observation after 8 hours, with a maximum of 17% for Δ*rstA* and a minimum of 1.5% for Δ*cpxR* (Fig. 5-3). All of the Δ*ompR* strain cells formed micro-colonies (Figs. 5-3KP). For all of the single RR gene knockout strains, more than 75% of cells started cell division in the time range of 0.5 - 4.5 hours, similar to the parent strain, with several deviations (Fig. 5-3P). The growth rates were divided into three groups with comparison to the parent strain: the faster growth rate mutants were Δ*phoB*, Δ*cusR*, Δ*torR*, Δ*rstA*, Δ*hprR*, Δ*baeR*, Δ*qseB*, Δ*ompR*, Δ*cpxR*, Δ*basR*, and Δ*arcA*; the similar growth rate mutants were Δ*phoP* and Δ*creB*; and the slow growth rate mutant was Δ*kdpE* (Fig. 5-3Q).

5-3-4. The adaptive growth of *E. coli* defected by a knockout of an arbitrary pair of *phoP*, *phoB*, and *ompR* genes

Next, three double main RR gene knockout strains, Δ*phoP*Δ*phoB*, Δ*phoP*Δ*ompR*, and Δ*phoB*Δ*ompR*, were isolated from two single RR knockout strains, Δ*phoB* and Δ*phoP* (Table 5-1) subjected to time-lapse observation to determine the elapsed time until cell division and the growth rate. Most of the cells of the three double RR gene knockout strains did not significantly grow at the end of observation after 8 hours (Fig. 5-4E-G), resulting in a long-elapsed time and slow growth rate (Figs. 5-5A and 5-4). However, all three double RR gene knockout strains formed colonies after incubation for more than 48 hours under the same conditions (data not shown). Surprisingly,

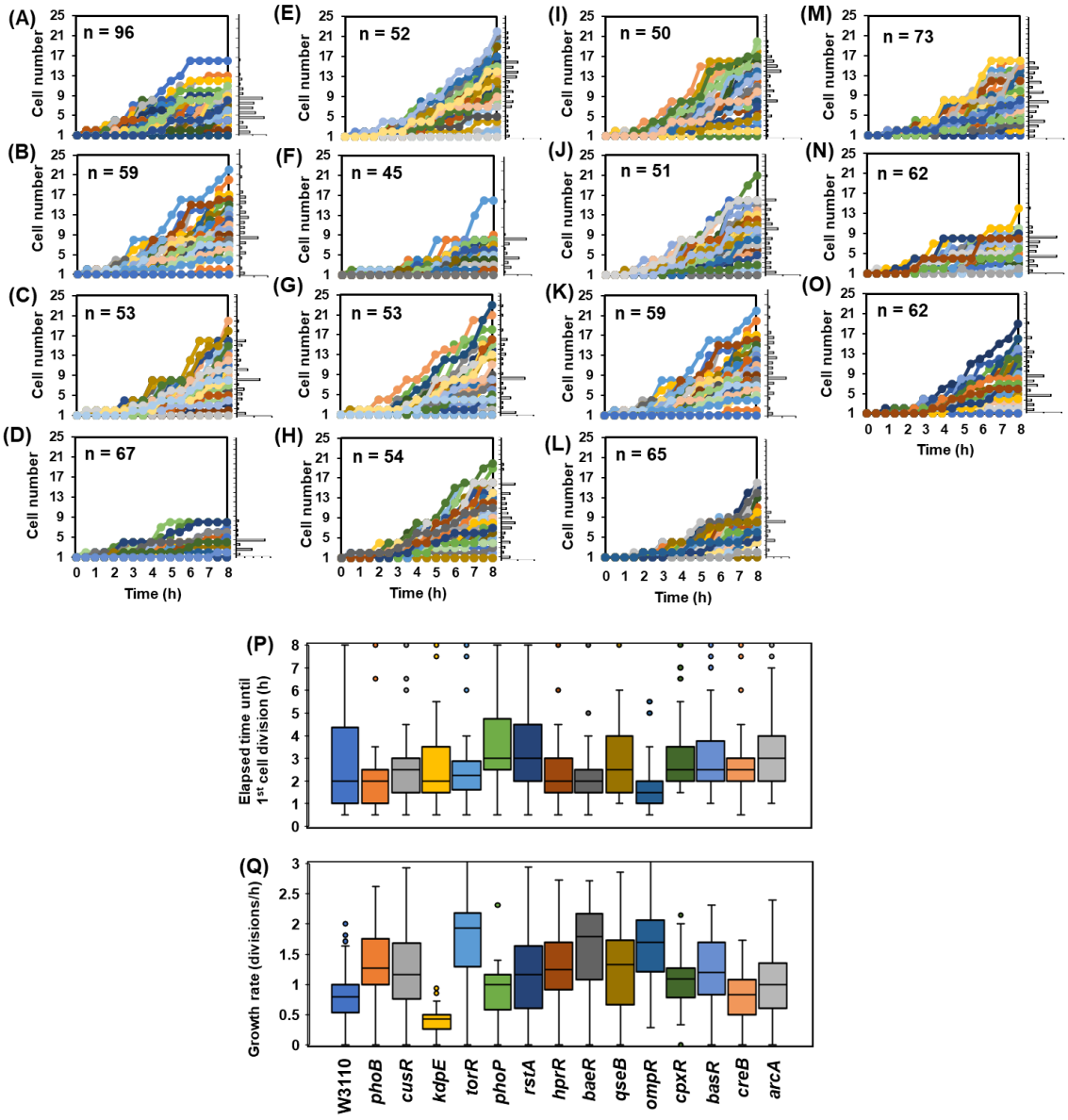

Figure 5-3. Contribution of OmpR family RRs to the adaptive growth of *E. coli* cells. [A-O] Single cell analysis of adaptive growth of single RR gene knockout *E. coli* strains. Strains were inoculated in M9 glucose medium and shaken overnight at 37°C. The cultures were washed with M9 medium three times and diluted 10-fold into the medium. The diluted cultures were spread on M9 glucose agar plate. The piece of agar from the plates were cut and put on a slide glass. The preparation was sealed on a glass coverslip with nail polish. The cells were imaged on a microscope (IX81, Olympus) using 100x/NA 1.4 objective lens (M Plan Apochromat MPLAPON-Oil, Olympus) and Retiga EXi Fast1394 CCD camera (Q Imaging) every 30 min until 8 hours. Temperature was maintained at 30°C using a closed circulation system (EYELA). Image acquisition and microscope control were performed with Image Pro Plus (Nippon roper). The cell division of each *E. coli* cell (hours, showed in x axis) and the population of cell in each microcolony (y axis) were measured by ImageJ. The histograms of cell population in a microcolony at after 8 hrs were showed on the right side of each graph. Each graph shows the parent strain W3110 **(A)**, Δ*phoB* **(B)**, Δ*cusR* **(C)**, Δ*kdpE* **(D)**, Δ*torR* **(E)**, Δ*phoP* **(F)**, Δ*rstA* **(G)**, Δ*hprR* **(H)**, Δ*baeR* **(I)**, Δ*qseB* **(J)**, Δ*ompR* **(K)**, Δ*cpxR* **(L)**, Δ*basR* **(M)**, Δ*creB* **(N)**, and Δ*arcA* **(O)**. The number of measured cell (n) are shown in each graph. **[P, Q]** Time-lapse observation of single cells growing on solid medium was adopted in the 30 min range for 8 hours with a light microscope. Based on the measured data (**A-O**), the elapsed time until cell division (hours, shown in **P**) and growth rate of single *E. coli* cells (divisions/hour, shown in **Q**) were calculated and are shown as box plots with error bars and outliers.

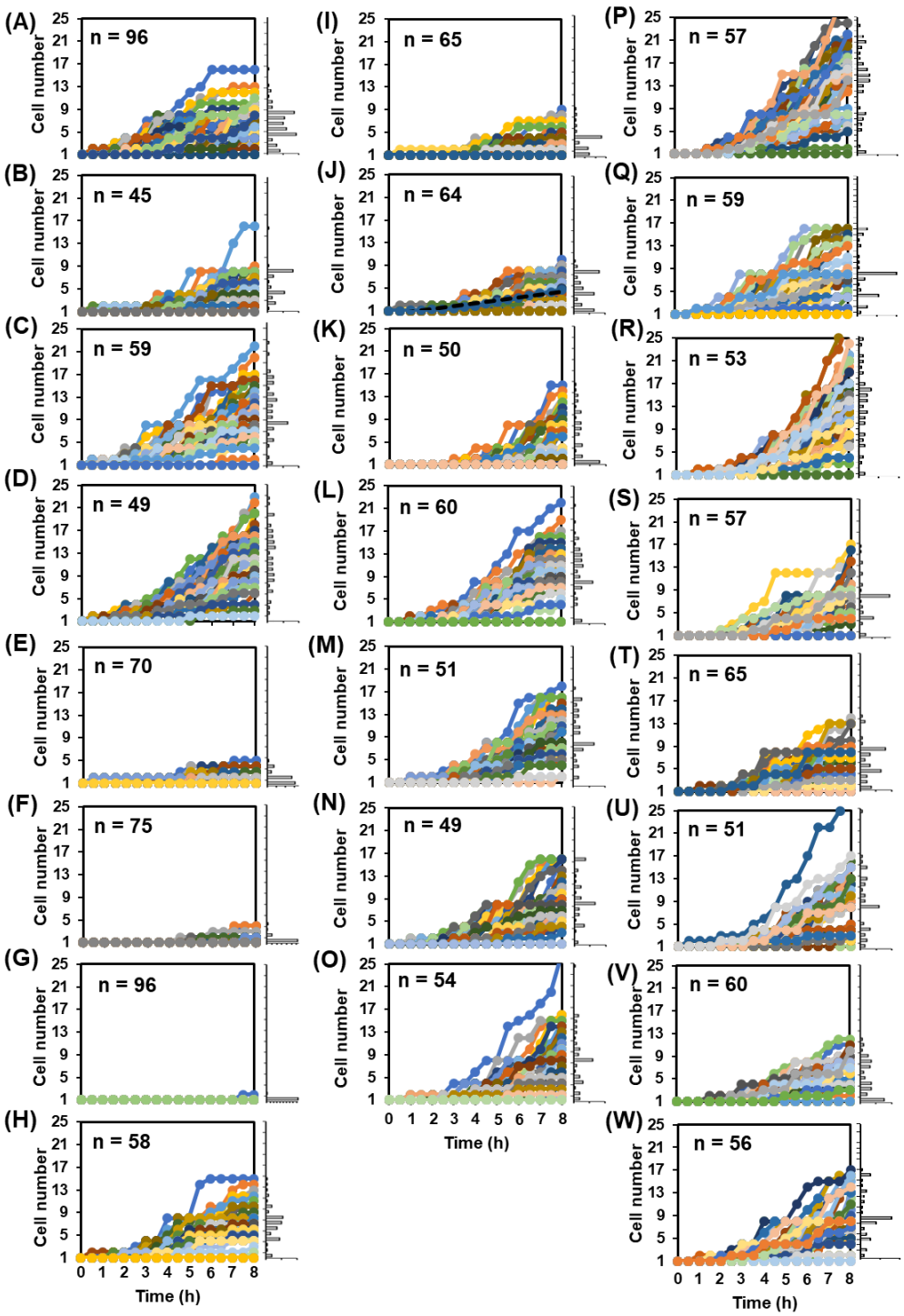

Figure 5-4. Single cell analysis of adaptive growth of multi-gene knockout *E. coli* strains. Strains were cultured, spread on M9 glucose agar plate, and imaged on a microscope as described in **Fig. 5-3**. The cell division (hours, showed in x axis) and the population of cell in each microcolony (y axis) were measured and the histograms of cell population in a microcolony at after 8 hrs were showed on the right side of each graph. Each graph shows the parent strain W3110 **(A)**, Δ*phoP* **(B)**, Δ*phoB* **(C)**, Δ*ompR* **(D)**, Δ*phoP* Δ *phoB* **(E)**, Δ*phoP*Δ*ompR* **(F)**, Δ*phoB*Δ*ompR* **(G)**, Δ*phoP*Δ*phoB*Δ*ompR* **(H)**, Δ*phoQ* **(I)**, Δ*phoR* **(J)**, Δ*envZ* **(K)**, Δ*phoQ*Δ*phoR* **(L)**, Δ*phoQ*Δ*envZ* **(M)**, Δ*phoR*Δ*envZ* **(N)**, Δ*phoQ*Δ*phoR*Δ*envZ* **(O)**, Δ*phoP*Δ*phoQ* **(P)**, Δ*phoB*Δ*phoR* **(Q)**, Δ*ompR*Δ*envZ* **(R)**, Δ*phoP*Δ*kdpE* **(S)**, Δ*phoB*Δ*creB* **(T)**, Δ*ompR*Δ*cpxR* **(U)**, Δ*ompR*Δ*rstA* **(V)**, and Δ*rstA*Δ*cusR*Δ*hprR* **(W)**. The number of measured cell (n) are shown in each graph.

the triple RR gene knockout strain showed similar behavior to that of the parent strain. At the end of observation after 8 hours, 93.1% of Δ*phoP*Δ*phoB*Δ*ompR* strain cells formed micro-colonies, while 6.9% of them were not totally divided (Fig. 5-4H). The majority of the Δ*phoP*Δ*phoB*Δ*ompR* strain cells started cell division at 1.5 - 3.5 hours after incubation (86.2%) and showed a growth rate of 0.6 - 1.4 divisions/hour (79.3%), as did the parent strain (Figs. 5-4H, 5-5A, and 5-6).

I examined to confirm gene knockout of an arbitrary pair of *phoP*, *phoB*, and *ompR* genes, defecting the adaptive growth, by genetic complement test using luciferase reporter system (Fig. 5-5B). The *ompC*, *pstS*, and *mgtA* promoters were employed as target promoters by EnvZ-OmpR, PhoQ-PhoP, PhoR-PhoB. The activation of *ompC* promoter requires the phosphorylated OmpR to upstream of *ompC* gene, which is stimulated by the cognate SK EnvZ at high osmolarity (Egger *et al.* 1997). The activation of *pstS* and *mgtA* promoters requires the phosphorylated PhoB and PhoP to upstream of each gene, respectively (Hsieh and Wanner. 2010; Groisman 2010). The intracellular level of phosphorylated PhoB is decreased by PhoR at high level of inorganic orthophosphate (Hsieh and Wanner. 2010) and the level of phosphorylated PhoP is decreased by PhoQ at high level of magnesium (Groisman 2010). Each lux reporter plasmid, pLUX-ompC, pLUX-pstS, and pLUX-mgtA, was introduced into all strains of seven combinations of main RR gene knockout for OmpR, PhoB, and PhoP (Tables 5-1 and 5-2) and then the luciferase activity was measured in each culture of M9 glucose. As expected, the activity of *ompC* promoter was detected in the parent strain but not in the knockout strains defecting only *ompR* gene (Fig. 5-5B). The defect of *ompC* promoter activity was recovered by expression of *ompR* gene in all of the knockout strains defecting only *ompR* gene (Fig. 5-5B). As well as the activation of *ompC* promoter by *ompR* gene, the activities of *pstS* and *mgtA* promoters were defected in the knockout strains defecting only *phoB* and *phoP* genes, respectively (Fig. 5-5B). The activities of *pstS* and *mgtA* promoters in mutants were recovered by expression of *phoB* and *phoP* genes, respectively (Fig. 5-5B).

Taking all these observations together, OmpR, PhoP, and PhoB each slightly contribute to the growth of *E. coli*, while the disappearance of any two OmpR, PhoP, and PhoB proteins seriously disrupts the adaptive growth of fast-growing *E. coli*.

5-3-5. The adaptive growth of *E. coli* not defected by a knockout of an arbitrary pair of *envZ*, *phoR*, and *phoQ* genes

EnvZ, PhoR, and PhoQ are the cognate SKs of OmpR, PhoB, and PhoP, respectively. Three single SK gene knockout strains, Δ*envZ*, Δ*phoR*, and Δ*phoQ*, were subjected to time-lapse observation as described above. At the end of observation after 8 hours, the percentages of non-growing cells of Δ*envZ*, Δ*phoR*, and Δ*phoQ* were 32.0%, 20.3%, and 21.5%, respectively (Fig. 5-6). In the case of Δ*envZ*, 54.0% of cells started cell division 4.0 - 6.5 hours after incubation, and

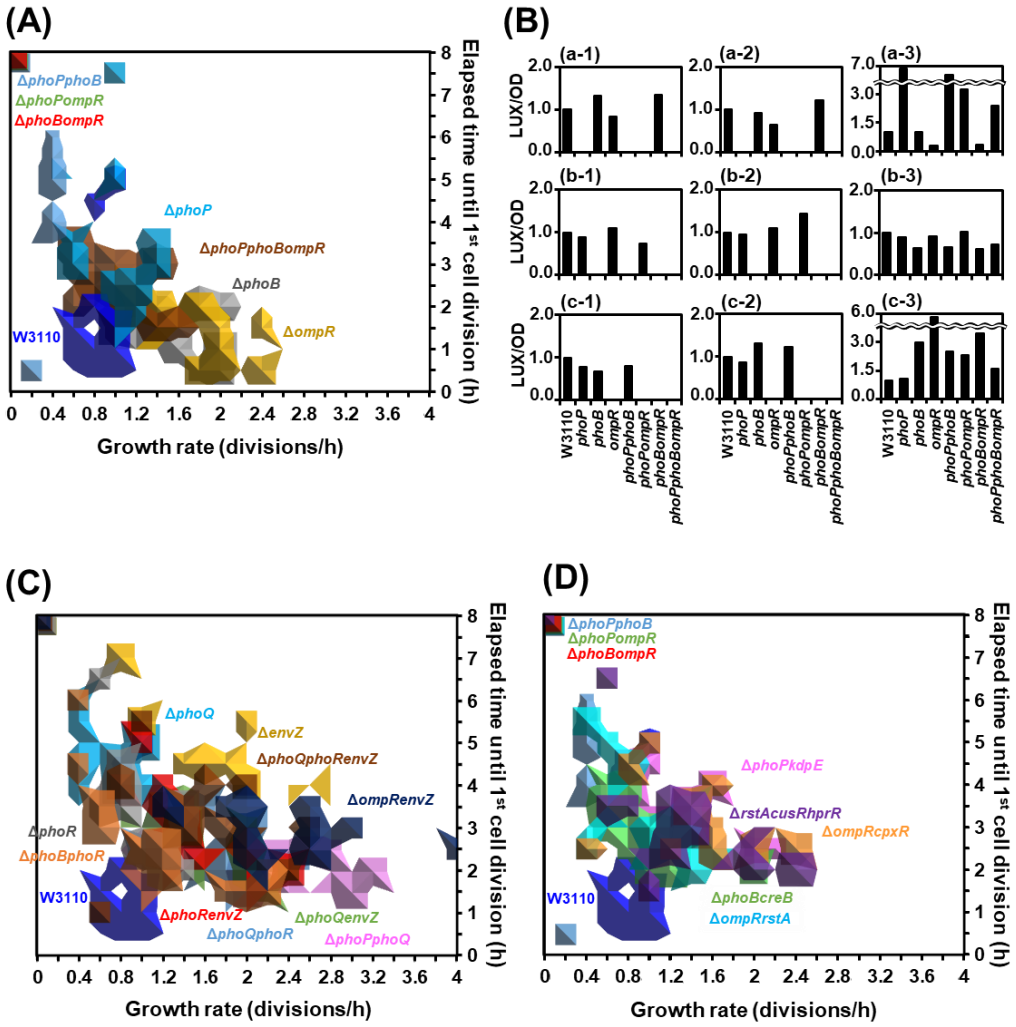

Figure 5-5. Contribution of main two-component RRs to the adaptive growth of *E. coli* cells. Time-lapse observation of single cells growing on solid medium was adopted in the 30 min range for 8 hours with a light microscope (Fig. 5-4). Based on the measured data (Fig. 5-4), the elapsed time until cell division (hours, shown on the y-axis) and growth rate of a single *E. coli* cell (divisions/hour, shown on the x-axis) were calculated and are shown as contour graphs. **[A]** The parent strain (blue) and three of the main RR (*phoP*, *phoB*, and *ompR*) gene knockout strains, Δ*phoP* (light blue), Δ*phoB* (gray), Δ*ompR* (yellow), Δ*phoP*Δ*phoB* (pale blue), Δ*phoP*Δ*ompR* (yellowish green), Δ*phoB*Δ*ompR* (red), and Δ*phoP*Δ*phoB*Δ*ompR* (dark brown). **[B]** The constructed pLUX-mgtA (a), pLUX-pstS (b), and pLUX-ompC (c), shown in Table 5-2, were transformed into each strain (a-1, b-1, and c-1) and each strain carrying either RR protein expression plasmids, pBADPhoP-FLAG (a-3), pBADPhoB-FLAG (b-3), or pBADOmpR-FLAG (c-3) or the empty pBAD33 vector (a-2, b-2, and c-2). Transformants were grown in the M9-glucose medium including 50 mg/mL kanamycin for pLUX plasmid and 20 mg/mL chloramphenicol for pBAD plasmid at 37°C with shaking for overnight. And then, overnight culture was diluted 100-fold by fresh M9-glucose medium with (a-2 and 3, b-2 and 3, and c-2 and 3) and without (a-1, b-1, and c-1) 0.002% arabinose for RR protein expression from pBAD plasmid and incubated at 37°C with shaking. OD_{600} and a total intensity of luminescence were measured and the ratio of luminescence to OD_{600} (LUX/OD) of each strain was calculated. The specific activity for each promoter was normalized with the parent strain W3110. **[C]** The parent strain (blue), cognate SK genes of main RR (*phoP*, *phoB*, and *ompR*) knockout strains Δ*phoQ* (light blue), Δ*phoR* (gray), Δ*envZ* (yellow), Δ*phoQ*Δ*phoR* (pale blue), Δ*phoQ*Δ*envZ* (yellowish green), Δ*phoR*Δ*envZ* (red), and Δ*phoQ*Δ*phoR*Δ*envZ* (dark brown); and cognate pairs of SK-RR knockout strains Δ*phoP*Δ*phoQ* (pink), Δ*phoB*Δ*phoR* (light brown), and Δ*ompR*Δ*envZ* (navy). **[D]** The parent strain (blue), double RR gene knockout strains Δ*phoP*Δ*phoB* (pale blue), Δ*phoP*Δ*ompR* (yellowish green), Δ*phoB*Δ*ompR* (red), Δ*phoP*Δ*kdpE* (pink), Δ*phoB*Δ*creB* (green), Δ*ompR*Δ*cpxR* (orange), and Δ*ompR*Δ*rstA* (light blue), and a triple RR gene knockout strain Δ*rstA*Δ*cusR*Δ*hprR* (purple).

50.0% showed a growth rate of 0.8 - 2.0 divisions/hour, similar to the parent strain (Figs. 5-4K, 5-5C, and 5-6). In the case of Δ*phoQ*, 61.5% of cells started cell division 4.0 - 5.5 hours after incubation, and 67.7% showed a growth rate of 0.3 - 1.0 divisions/hour, similar to the parent strain (Figs. 5-4I, 5-5C, and 5-6). In the case of Δ*phoR*, 62.5% of cells started cell division 1.5 - 4.5 hours after incubation, and 73.4% showed a growth rate of 0.4 - 1.4 divisions/hour, similar to the parent strain (Figs. 5-4J, 5-5C, and 5-6). Overall, three single SK gene mutants showed slightly delayed elapsed times, but their growth rate was similar to that of the parent strain.

Next, three double SK gene knockout strains, Δ*phoQ*Δ*phoR*, Δ*phoQ*Δ*envZ*, and Δ*phoR*Δ*envZ*, were subjected to time-lapse observation to determine the elapsed time until cell division and the growth rate. Most of the cells of the three double SK gene knockout strains grew significantly at the end of observation after 8 hours (Fig. 5-4L-N). All three double SK gene knockout strains showed an elapsed time in the range of 2.0 – 3.5 hours, and the growth rate varied in the range of 0.8 - 2.4 divisions/hour (Figs. 5-4L-N, 5-5C, and 5-6). In addition, for the triple SK gene knockout strain, 92.6% of cells formed micro-colonies (Fig. 5-4O). The majority of the Δ*phoQ*Δ*phoR*Δ*envZ* strain cells started cell division 1.5 - 4.5 hours after incubation (77.8%) and showed a growth rate of 0.4 - 2.0 divisions/hour (74.1%) (Figs. 5-4O, 5-5C, and 5-6). Taking all these observations together, the disappearance of any two OmpR, PhoP, and PhoB proteins seriously disrupts the adaptive growth of fast-growing *E. coli*, while the disappearance of any two EnvZ, PhoR, and PhoQ, the cognate SKs for OmpR, PhoB, and PhoQ, proteins slightly affect the adaptive growth of fast-growing *E. coli*.

5-3-6. A specific arbitrary pair of *phoP*, *phoB*, and *ompR* genes for the optimum adaptive growth of *E. coli*

All three double RR gene knockout strains, Δ*phoP*Δ*phoB*, Δ*phoP*Δ*ompR*, and Δ*phoB*Δ*ompR*, almost disrupted the adaptive growth. I examined whether double RR gene knockout of other combinations. Cluster analysis with all RRs of *E. coli* K-12 showed that PhoP, PhoB, and OmpR were highly similar RRs (Fig. 5-2). Therefore, I knocked out a pair of similar genes and isolated four double RR knockout strains of Δ*phoP*Δ*kdpE*, Δ*phoB*Δ*creB*, Δ*ompR*Δ*cpxR*, and Δ*ompR*Δ*rstA* (see above) (Table 5-1 and Fig. 4-2A). Most of the cells of the Δ*phoP*Δ*kdpE*, Δ*phoB*Δ*creB*, Δ*ompR*Δ*cpxR*, and Δ*ompR*Δ*rstA* strains grew significantly at the end of observation after 8 hours (Fig. 5-4S-V). Three double RR gene knockout strains, Δ*phoP*Δ*kdpE*, Δ*phoB*Δ*creB*, and Δ*ompR*Δ*cpxR*, showed an elapsed time in the range of 2.5 – 4.0 hours, and the growth rate varied in the range of 0.75 - 1.5 divisions/hour (Figs. 5-4S-U, 5-5D, and 5-6). On the other hand, Δ*ompR*Δ*rstA* strains showed an elapsed time in the range of 2.5 – 7.5 hours, and the growth rate varied in the range of 0.05 - 1.2 divisions/hour (Figs. 5-4V, 5-5D, and 5-6). Furthermore, another

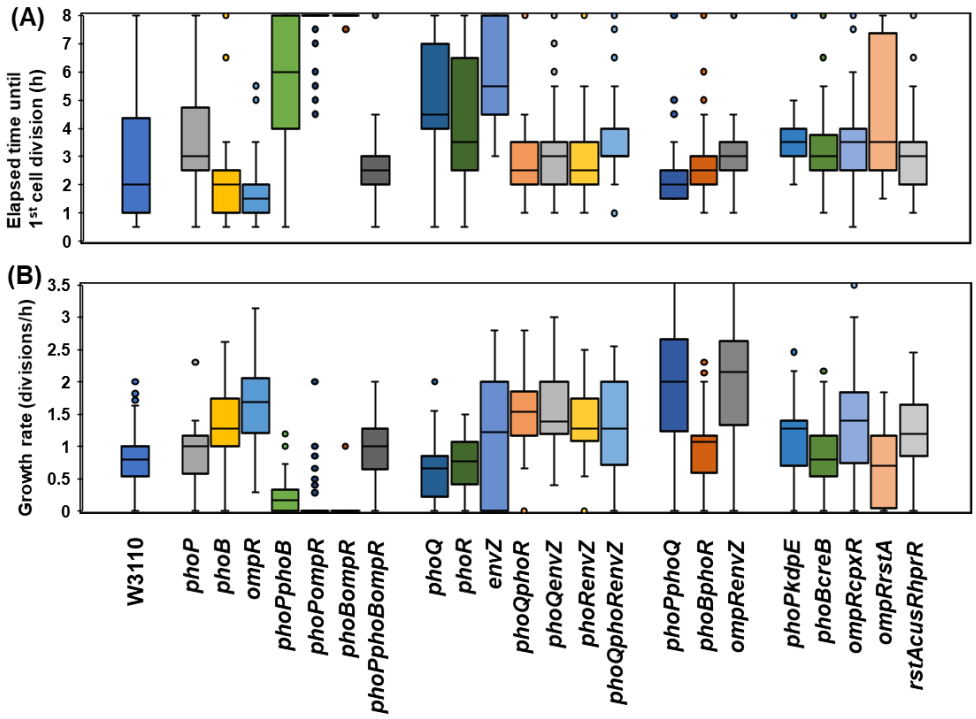

Figure 5-6. The distribution of cell growth values of *E. coli* strains. Based on the measured data (Fig. 5-4), the elapsed time until cell division **(A)** and growth rate of single *E. coli* cell **(B)** were calculated and shown as box plots with error bars and outliers.

triple RR gene knockout strain, Δ*rstA*Δ*cusR*Δ*hrpR*, also presented micro-colony formation in 92.6% of the population, starting cell division 1.5 - 4.5 hours after incubation (83.9%) and showing a growth rate of 0.6 - 2.0 divisions/hour (69.6%), as did the Δ*phoQ*Δ*phoR*Δ*envZ* strain (Figs. 5-4W, 5-5D, and 5-6).

I next examined three cognate pair double gene knockout strains, Δ*phoP*Δ*phoQ*, Δ*phoB*Δ*phoR*, and Δ*ompR*Δ*envZ*, for adaptive growth. Most of the cells of the three cognate pair double gene knockout strains grew significantly at the end of observation after 8 hours (Fig. 5-4P-R). These three strains showed an elapsed time in the range of 1.0 – 3.5 hours, but their growth rates varied (Figs. 5-4P-R, 5-5C, and 5-6). The Δ*phoP*Δ*phoQ* and Δ*ompR*Δ*envZ* strains showed growth rates in the range of 1.3 - 2.7 divisions/hour (70%) and 1.3 - 2.7 divisions/hour (70%), respectively, whereas 70% of cells of the Δ*phoB*Δ*phoR* strain showed growth rates of 0.4 - 1.4 divisions/hour, similar to the parent strain (Figs. 5-5C and 5-6). In agreement with observations of single knockout strains as shown above, these observations showed that the roles of PhoP, PhoB, and OmpR did not completely correspond with their cognate SKs, PhoQ, PhoR, and EnvZ, respectively, in adaptive growth.

To demonstrate the genetic involvement of TCSs for adaptive growth, cluster analysis was performed with the elapsed time and the growth rate on solid medium (Fig. 5-7). The dendrogram of the elapsed time showed two groups, each divided into two sub-groups (Fig. 5-7A). The parent strain was assigned to Group-Ib, which included not only all single RR gene knockout strains but also all double SK gene knockout strains and triple RR and SK gene knockout strains (Fig. 5-7A). Additionally, all cognate pair gene knockout strains were assigned to Group-Ia (Fig. 5-7A). All of the single SK gene knockout strains were assigned to Group II, in which all of the double RR gene knockout strains were part of Group IIb (Fig. 5-7A). The dendrogram of the growth rate also showed two groups (Fig. 5-7B). The parent strain was assigned to Group II, which included most of the knockout strains, whereas all of the double RR gene knockout strains were isolated in Group I (Fig. 5-7B).

Cluster analysis of the elapsed time showed that all four of the double RR gene knockout strains studied were assigned to Group-Ia but not to Group-II (Fig. 5-7A). Additionally, clustering for the growth rate showed that all four of the double RR gene knockout strains were not assigned to Group I (Fig. 5-7B). Taken together, knockout of the double RR gene among *ompR*, *phoP*, and *phoB*, specifically caused a long delay in the start of growth and a lower growth rate (Fig. 5-5).

5-3-7. The adaptive growth of the TCS gene-deprived strains

The *E. coli* K-12 strain has 34 conserved RR genes and 30 conserved SK genes in the genome. To reveal the contribution of these RRs on the adaptive growth of *E. coli*, I performed the time-lapse observation using every single RR- and SK-gene knockout strains and the all 34 RR gene- and 30 SK gene-deprived strain bred by the HoSeI system in Chapter 4. The elapsed time until cell division and the growth rate were determined based on the observation of single cells. At the end of observation, after 8 hours, 70.8% of the parent strain, W3110 type A, cells formed micro-colonies, including 4 to 8 cells, while 8.3% of the cells were not completely divided (Fig. 5-8A). The majority of parent cells started cell division 0.5 - 4.5 hours after incubation (80.2%) and showed a growth rate of 0.5 - 1.1 divisions/hour (75.0%) (Figs. 5-8DE).

Thirty-four single RR gene knockout strains isolated in this study were also subjected to time-lapse observation, as was the parent strain (Appendix Figure 3A). Most of the single RR gene knockouts, except for Δ*ompR* and Δ*evgA*, showed that the percentage of non-growing cells was in the range of 17% to 1.5% at the end of observation after 8 hours, with a maximum of 17% for Δ*rstA* and a minimum of 1.5% for Δ*cpxR* (Appendix Figure 3A). All of the Δ*ompR* and Δ*evgA* strain cells formed micro-colonies. For all of the single RR gene knockout strains, more than 75% of cells started cell division in the time range of 0.5 – 5.0 hours, similar to the parent strain, with several deviations (Fig. 5-8D). The growth rates were divided into three groups with comparison to the

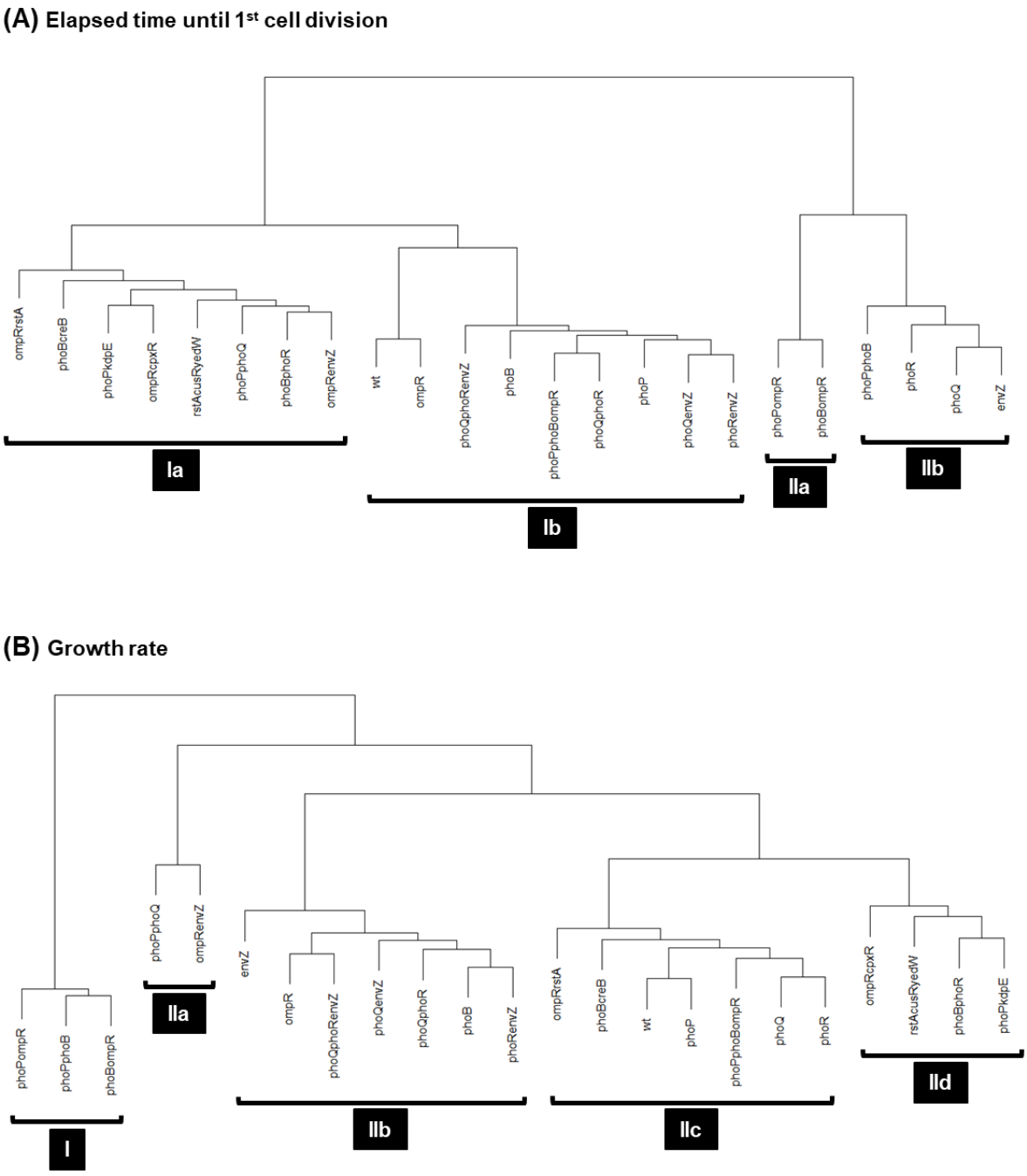

Figure 5-7. Cluster analysis using values for *E. coli* cell growth of strains. Cluster analysis was performed with R software (https://www.R-project.org/). The presenting data of the elapsed time **(A)** and the growth rate **(B)** were prepared for Ward's method. Hierarchical clustering dendrogram was calculated using Euclidean distances.

parent strain: the faster growth rate mutants were Δ*phoB*, Δ*fimZ,* Δ*cusR*, Δ*torR*, Δ*rstA*, Δ*cheY,* Δ*uvrY*, Δ*hprR*, Δ*baeR*, Δ*rcsB,* Δ*evgA*, Δ*pyrR*, Δ*ygeK*, Δ*qseB*, Δ*ompR*, Δ*yhjB*, Δ*ntrC*, Δ*cpxR*, Δ*zraR,* Δ*basR*, Δ*dcuR*, and Δ*arcA*; the similar growth rate mutants were Δ*citB*, Δ*phoP,* Δ*narL*, Δ*rssB,*

Δ*cheB*, Δ*btsR*, Δ*narP*, Δ*atoC*, Δ*glrR*, Δ*uhpA*, and Δ*creB*; and the slow growth rate mutant was Δ*kdpE* (Fig. 5-8E). There was a similar tendency to increase the variation of growth rate in the 22 mutants growing faster than the parent strain. The difference did not appear to correlate with the intracellular level or the number of regulated genes.

In contrast, in the RR-deprived strain, Δ34RR, 66.7% of cells formed micro-colonies, including 2 to 4 cells at the end of observation after 8 hours. However, 30.0% of the cells were not completely divided (Fig. 5-8B). The majority of the Δ34RR cells started cell division 2.5 - 6.6 hours after incubation (70.0%) and showed a growth rate of 0.14 – 0.68 divisions/hour (70.0%) (Figs. 5-8DE). The Δ34RR strain exhibited the delayed 1st cell division and the slower growth rate (both showed $p < 0.01$, tested using the Mann-Whitney U test) (Fig. 5-8DEH). Although the elapsed time until cell division showed a broader distribution in the Δ34RR strain, the variation of growth rate was not significantly different from the parent strain. These results suggested that the lack of RRs decreases the prompt adaptation and start of growth.

Next, thirty single SK gene knockout strains isolated in this study were also subjected to time-lapse observation, as was the parent strain (Appendix Figure 3B). Most of the single SK gene knockouts, except for Δ*citA*, Δ*hprS*, Δ*rcsC*, and Δ*creC* showed that the percentage of non-growing cells was in the range of 32% to 1.75% at the end of observation after 8 hours, with a maximum of 32% for Δ*envZ* and a minimum of 1.75% for Δ*cusS* (Appendix Figure 3B). All of the Δ*citA*, Δ*hprS*, Δ*rcsC*, and Δ*creC* strain cells formed micro-colonies. For most of the single SK gene knockout strains, more than 75% of cells started cell division in the time range of 0.5 – 5.0 hours, similar to the parent strain, with several deviations (Fig. 5-8F). Five strains, Δ*phoR*, Δ*phoQ*, Δ*btsS*, Δ*envZ*, and Δ*uhpB*, prolonged the elapsed time until 1st cell division (Fig. 5-8F). The growth rates were divided into three groups with comparison to the parent strain: the faster growth rate mutants were Δ*cusS*, Δ*citA*, Δ*kdpD*, Δ*torS*, Δ*narX*, Δ*rstB*, Δ*hprS*, Δ*baeS*, Δ*atoC*, Δ*rcsC*, Δ*rcsD*, Δ*evgS*, Δ*pyrS*, Δ*narQ*, Δ*glrK*, Δ*barA*, Δ*ntrB*, Δ*zraS*, and Δ*dcuS*; the similar growth rate mutants were Δ*phoR*, Δ*cheA*, Δ*arcB*, Δ*envZ*, Δ*cpxA*, Δ*basS*, and Δ*creC*; and the slow growth rate mutant was Δ*phoQ*, Δ*btsS*, Δ*qseC*, and Δ*uhpB* (Fig. 5-8G). There was a similar tendency to increase the variation of growth rate in the 15 of 19 mutants growing faster than the parent strain. As with the insights in the adaptive growth of knockout strains of the arbitrary pair of three RRs (*phoP*, *phoB*, *ompR*) or their cognate SKs (*phoQ*, *phoR*, *envZ*), the characteristics of single knockouts were discordant between the specific pair of SK and RR (Fig. 5-8D-G).

In the SK-deprived strain, Δ30SK, about 80% of cells formed micro-colonies, including 2 to 16 cells at the end of observation after 8 hours. However, 20.8% of the cells were wholly undivided (Fig. 5-8B). The majority of the Δ30SK cells started cell division 2.5 – 7.0 hours after incubation (70.0%) and showed a growth rate of 0.1 – 1.3 divisions/hour (80.0%) (Figs. 5-8FG).

Like the Δ34RR strain, the Δ30SK strain exhibited the delayed 1st cell division ($p < 0.01$, tested using the Mann-Whitney U test). However, there was no significant difference in the growth rate between the Δ30SK strain the parent ($p > 0.05$, tested using the Mann-Whitney U test) (Fig. 5-8GH). Although the growth rate showed a wider distribution in the Δ30SK strain, it was not remarkably different from the parent strain. These findings proposed that the deprivation of SKs mainly affects the start of growth, but not on the growth rate.

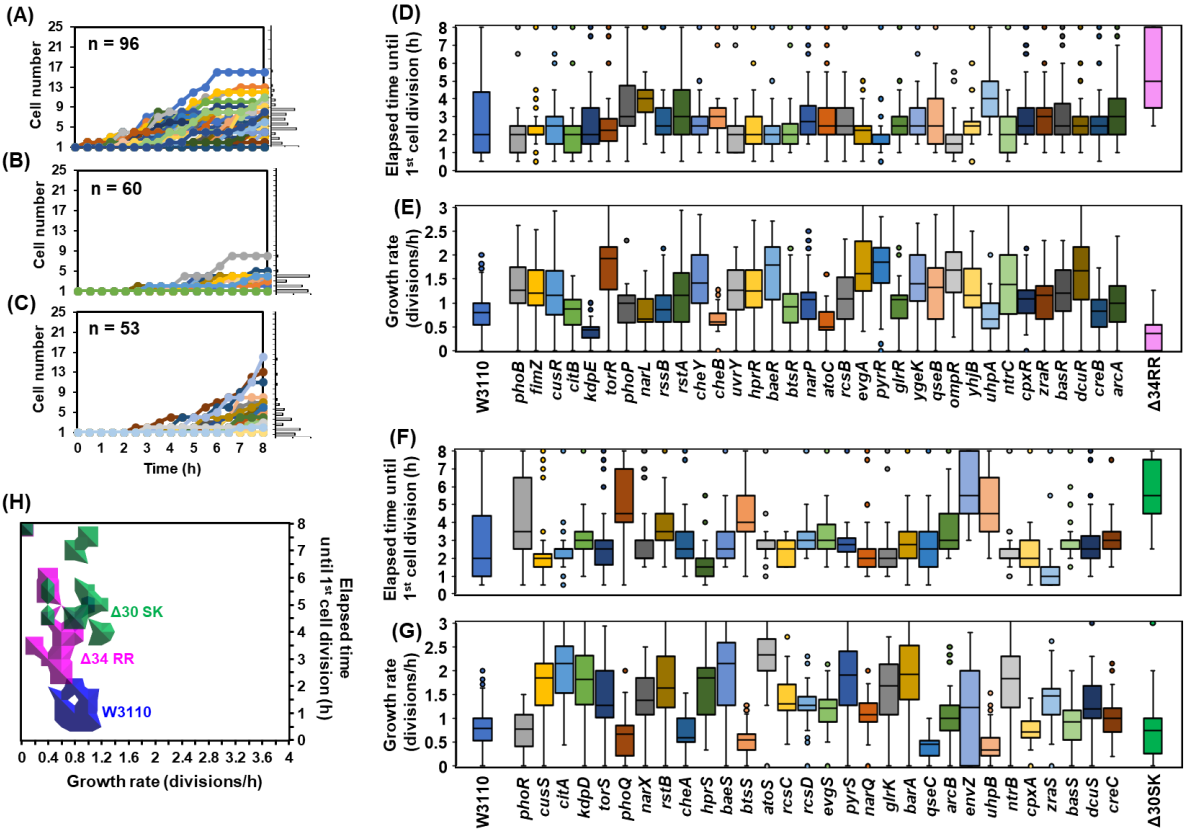

Figure 5-8. The distribution of cell growth values of TCS knockout strains. Strains were cultured, spread on M9 glucose agar plate, and imaged on a microscope as described in **Fig. 5-3**. The cell division (hours, showed in x axis) and the population of cell in each microcolony (y axis) were measured. Based on the measured data (**A-C** and **Appendix Figure 3**), the elapsed time until cell division (**D** and **F**) and growth rate of single *E. coli* cell (**E** and **G**) were calculated and shown as box plots with error bars and outliers. **[A-C]** The cell division (hours, showed in x axis) and the population of cell in each microcolony (y axis) were measured and the histograms of cell population in a microcolony at after 8 hrs were showed on the right side of each graph. Each graph shows the parent strain W3110 type A (**A**), RR-deprived strain Δ34RR (**B**), and SK-deprived strain Δ30SK (**C**). The number of measured cell (n) are shown in each graph. **[H]** Based on the measured data (**A-C**), the elapsed time until cell division (hours, shown on the y-axis) and growth rate of a single *E. coli* cell (divisions/hour, shown on the x-axis) were calculated and are shown as contour graphs. The parent strain (blue), Δ34RR strain (magenta), and Δ30SK strain (green).

5-4. Discussion

5-4-1. Importance of OmpR family genes in bacteria

An OmpR family comparison of *Haemophilus influenzae* Rd KW20, *Corynebacterium glutamicum* ATCC 13032, *Bacillus subtilis* subsp. subtilis str. 168, *Mycobacterium tuberculosis* H37Rv, *Shigella dysenteriae* 1617, *Escherichia coli* str. K-12 substr. MG1655, *Salmonella enterica* subsp. enterica serovar Typhimurium str. LT2, and *Pseudomonas aeruginosa* PAO1 reveals that the four sub-families actually divided PhoP, PhoB, and OmpR (Fig. 5-9B and Appendix Table 9). OmpR family proteins of *E. coli* were classified into 3 sub-families, except for sub-family D, and PhoP, PhoB, and OmpR were divided into sub-families C, B, and A, respectively. The result of the OmpR family comparison was mostly identical to the result of cluster analysis with all RRs of *E. coli* K-12 (Figs. 5-9B and 5-2A). Additionally, OmpR family RRs are conserved not only in closely related bacteria with genome sizes similar to that of *E. coli* but also in bacteria with smaller (*H. influenzae*) or larger (*P. aeruginosa*) genomes than that of *E. coli*. A genome comparison of *E. coli* strains reveals that the predicted pan-genome comprises 15,741 gene families and that the core genome comprises only 993 (6%) of the families, as represented in every genome (Lukjancenko *et al.* 2010). OmpR family genes are included in the *E. coli* core genome and increase their number in the genome. I found that the OmpR family includes conserved TCS genes withing the bacterial genome. The number of the OmpR family gene is also correlated with the size of the genome (Fig. 5-9A). The *E. coli* K-12 genome has 14 genes of the OmpR family, occupying more than 40% of the total number of RR genes. The intracellular levels of 65 species of transcription factors with known function in *E. coli* K-12 W3110 typeA at various phases of cell growth showed the following decreasing order for the intracellular response regulators: PhoP -> PhoB -> CitB -> OmpR -> NarL -> CpxR -> UhpA -> RstA -> EvgA -> KdpE -> TorR -> UvrY -> QseB -> ArcA (Ishihama *et al.* 2014). Among these 14 more abundant species, 9 species of RRs belong to the OmpR family (PhoP, PhoB, OmpR, CpxR, RstA, KdpE, TorR, QseB, and ArcA). I isolated all of 14 OmpR family single RR gene knockout strains by HoSeI method, indicating that none of them was essential for growth under the used conditions in good agreement with previous works (Oshima *et al.* 2002; Zhou *et al.* 2003). Time-lapse live cell imaging with microscope indicated that 14 single RR gene knockout strains were divided into three groups, the faster growth rate mutants, the normal growth rate mutants, and the slow growth rate mutant (Fig. 5-3Q). The difference did not appear to correlate with the intracellular level or the number of regulated genes. Despite having different initial growth times, all single RR gene knockout strains showed similar growth curves in liquid M9 glucose and LB media, as did the parent strain (data not shown). These results suggest that each RR gene could cause fluctuations of the initial growth rate in the range of 0.5 - 2.0 divisions/hour among the bacterial populations. However, it is unclear how each RR gene changes the homogeneity of the initial growth rate in the bacterial population.

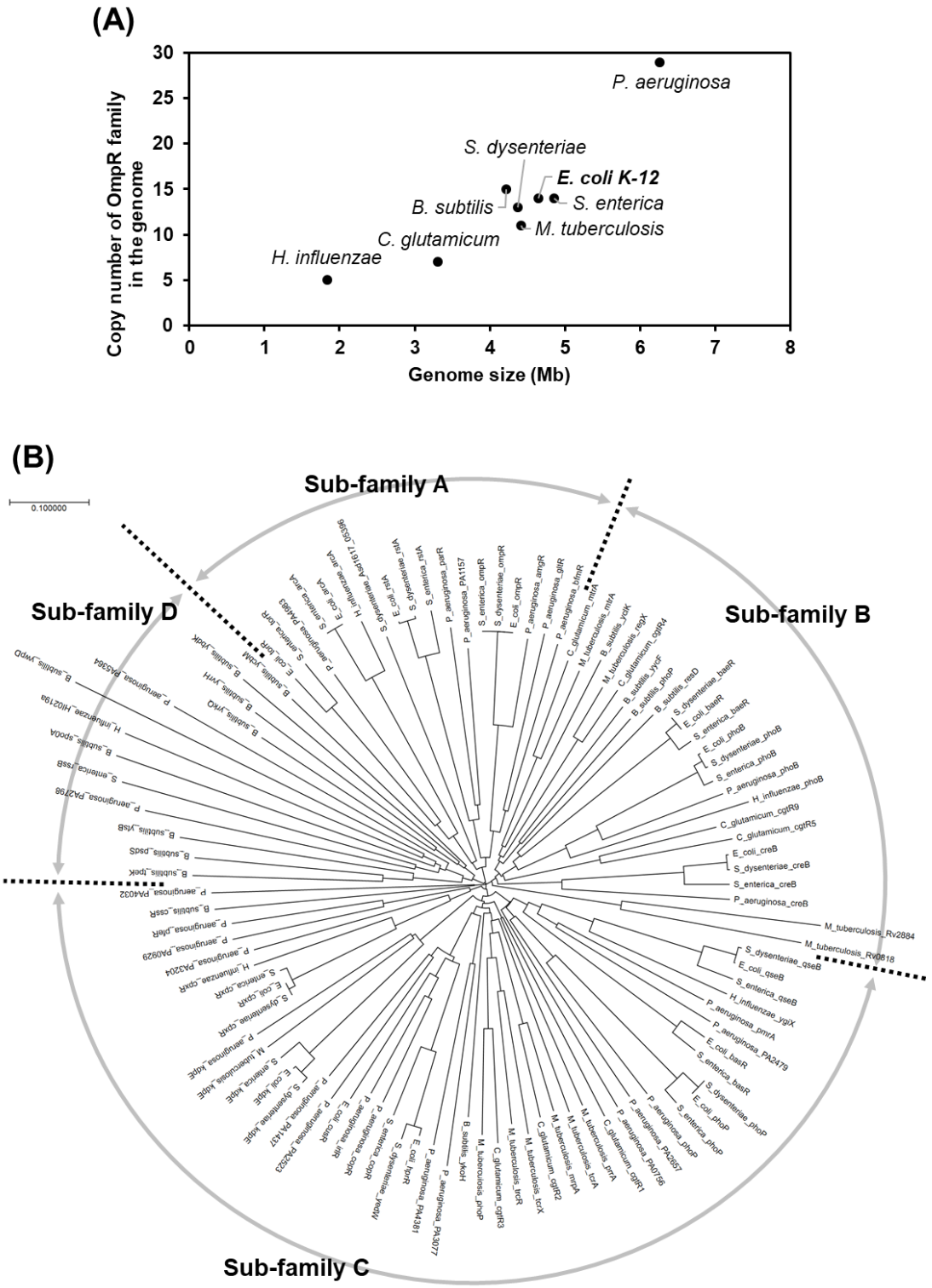

Figure 5-9. Comparison of OmpR family RRs among several bacteria. [A] OmpR family RR gene copy number of several bacteria. On the basis of the data shown in **Fig. 5-1**, the copy number of OmpR family RR genes (y-axis) in eight bacterial genomes was compared with the respective genome size (x-axis). The eight bacterial strains are *Haemophilus influenzae* Rd KW20, *Corynebacterium glutamicum* ATCC 13032, *Bacillus subtilis* subsp. subtilis str. 168, *Mycobacterium tuberculosis* H37Rv, *Shigella dysenteriae* 1617, *Escherichia coli* str. K-12 substr. MG1655, *Salmonella enterica* subsp. enterica serovar Typhimurium str. LT2, and *Pseudomonas aeruginosa* PAO1. **[B]** Phylogenetic analysis of the amino acid sequence of OmpR family RRs. All of the amino acid sequences of the OmpR family RRs in 8 bacteria shown in **[A]** were compared and analysed with ClustalW software. The result divided the RRs into four sub-families. The amino acid sequence of the used OmpR family RRs was compiled in **Appendix Table 9**.

5-4-2. Epistatic requirement of the arbitrary pair of PhoP, PhoB, and OmpR

As unexpected, I found that knockout of the arbitrary pair of *phoP*, *phoB*, and *ompR* are shown as an epistatic inhibition for *E. coli* adaptive growth (Fig. 5-5). When the species of three genes knockout was introduced into single *phoP* knockout strain (Table 5-1), only double defect with *ompR* gene dramatically inhibited the adaptive growth of *E. coli* (Fig. 5-5). When the species of four genes knockout was introduced into single *phoB* knockout strain (Table 5-1), only double defect with either *ompR* or *phoP* gene dramatically inhibited the adaptive growth of *E. coli* (Fig. 5-5). Besides, the knockout for *citB* gene, one of NarL family RR gene of *E. coli*, was introduced into both single *phoB* and single *phoP* knockout strains, resulting that both double gene knockout strains, Δ*citB*Δ*phoB* and Δ*citB*Δ*phoP*, did not show significant inhibition of the adaptive growth of *E. coli* (data not shown). Despite different genetic backgrounds, the genetic defect of an arbitrary pair of *phoP*, *phoB*, and *ompR* largely delays initiation of growth and dramatically reduces the initial growth rate, the results of which were entirely different from not only *phoP*, *phoB*, and *ompR* RR single knockouts but also their triple knockouts (Figs. 5-5 and 5-7). In good agreement with the most abundant RRs, PhoP, PhoB, and OmpR (Ishihama *et al.* 2014), a memory of expression of genes below cytotoxic levels exists for positively autoregulated systems of the genes *phoP*, *phoB*, and *ompR* in *E. coli*. Each OmpR family member, including *E. coli* PhoP, PhoB, and OmpR, contains an N-terminal receiver domain (RD) and a C-terminal DNA-binding domain (DBD), which are connected by a linker. To date, the molecular structure of the truncated RD and DBD and the full-length active and inactive form of OmpR family proteins have been solved by X-ray crystallography and NMR spectroscopy (Bucker *et al.* 2002; Blanco *et al.* 2002; Robinson *et al.* 2003; Nowak *et al.* 2006; Friedland *et al.* 2007; King-Scott *et al.* 2007; Barbieri *et al.* 2010; Menon *et al.* 2011; Choudhury *et al.* 2013). Among these proteins, dimerization or higher-order multimerization is commonly observed, and at least three surfaces have been observed for intermolecules. Two surfaces, the $\alpha 1\alpha 5$ and the $\alpha 4\beta 5\alpha 5$ faces, conserve the RD and one surface the DBD. PhoP, PhoB, and OmpR are known to bind to at least 15 promoters *in vivo*, as denoted in RegulonDB (http://regulondb.ccg.unam.mx/index.jsp), indicating that the intracellular level of approximately 1,000 copies of PhoP, PhoB, and OmpR each per genome is clearly too high, and thus, these proteins could play a role except in the stress response. These are in good agreement with the observation of the adaptive growth of *E. coli* of a knockout of an arbitrary pair of *envZ*, *phoR*, and *phoQ* genes, the cognate SK genes for OmpR, PhoR, and PhoP (Figs. 5-4L-N, 5-5C, and 5-6). PhoB and OmpR are also known to bind to more than 100 genomic sites *in vitro* denoted in TEC (https://shigen.nig.ac.jp/E.coli/tec/top/), suggesting that PhoP, PhoB, and OmpR each basically function as a DNA-binding protein. Genome-wide binding profiles have indicated the recognized DNA sequences TTTAnnnnTTTA as the PhoP-binding consensus (Harai *et al.* 2010), TTTGTTACAT as the OmpR-binding consensus (Seo *et al.* 2017), and TGTnAnAAAnnTGTnA

as the PhoB-binding consensus (Yang *et al.* 2012). The tandem triplet of A or T, found as a common sequence among the genes, could be weakly recognized by every one of PhoB, PhoP, and OmpR. Thus, *E. coli* cells could show adaptive growth when a total of 3,000 intracellular proteins of PhoP, PhoB, and OmpR have become associated with the genome. *E. coli* cells, however, could not properly grow, if insignificant occupation of the genome by 1,000 intracellular proteins of either PhoP, PhoB, or OmpR.

The triple RR gene knockout strain, however, recovered the elapsed time and the growth rate to values similar to those for the parent strain (Fig. 5-5A). This observation showed that a total of 3,000 intracellular proteins of PhoP, PhoB, and OmpR was not essential for adaptive growth of *E. coli*. One possible reason that normal growth of the triple RR gene knockout strain is the existence of excess intracellular RRs in place of PhoP, PhoB, and OmpR. I did not, however, find a significant difference in the profile of cellular proteins, with more than 200 proteins detected with LC-MS, between the parent strain and the triple RR gene knockout strain (data not shown). Additionally, the promoter activities of all TCS genes in the *E. coli* genome were measured using the luciferase reporter system, indicating that three double RR gene knockout strains and a triple RR gene knockout strain were mostly similar to the parent strain with respect to these promoter activities (data not shown).

These findings suggest that the mode of action for inhibition of adaptive growth by knockout of the arbitrary pair of *phoP*, *phoB*, and *ompR* is important for the bacterial cell cycle, genome replication and/or cell division but not for general metabolism and stress responses. The epistatic inhibition for *E. coli* adaptive growth by an arbitrary pair of *phoP*, *phoB*, and *ompR* was obscure on LB agar (data not shown). All of the isolated knockout strains also showed a similar adaptive growth to the parent strain on LB agar (data not shown). One possible is that only either PhoP, PhoB, or OmpR at a high intracellular level bias genome expression profile and inhibit the optimum adaptive growth in *E. coli* grown in M9 glucose that contains less amino acids than LB broth. Another is that a high concentration of only one species of OmpR family severely affect bacterial growth by an unknown molecular mechanism, which could be suppressed by a high concentration of another species of OmpR family. These findings suggest that RRs contribute to the optical high level of the intracellular RRs, resulting in a fitness advantage for growth. The results are in good agreement with the idea of fitness advantages being conferred for both positive and negative feedback in both dynamic and stable environments. Taken together, in *E. coli*, PhoP, PhoB, and OmpR are autoregulated at the optimal intracellular level and balance of their intracellular level play an important role in survival for repeatable growth fitness under the evaluated experimental conditions.

5-4-3. The role of TCSs on the adaptive growth

The all RR gene knockout strain showed both the delayed start of proliferation and the slow growth rate (Fig. 5-8). These features were not found in the adaptive growth of thirty-four single RR gene knockout strains. The elapsed time until cell division of the RR-deprived strain was longer than that of the *uhpA* mutant, which showed the most delayed elapsed time in single gene-knockout mutants. The RR-deprived mutant also exhibited the slowest growth rate. One of the single RR mutants, *kdpE* mutant, also represented the slower growth rate than the parent strain; however, the start of growth was not significantly different from the parent strain. The feature of adaptive growth found in the RR-deprived strain was not the sum of thirty-four single RR gene mutants. This result is a good agreement with the results which the genetic defect of an arbitrary pair of *phoP*, *phoB*, and *ompR* causes considerable adaptive growth delay, whereas the triple RR gene knockout strain recovered the adaptive growth as well as the parent strain (Fig. 5-5A). Therefore, I speculate that the combination of RRs plays a role in the adaptive growth of *E. coli* with a different level of contribution.

Five single SK mutants, Δ*phoR*, Δ*phoQ*, Δ*btsS*, Δ*envZ*, and Δ*uhpB*, prolonged the 1st cell division whereas the cognate RRs of PhoR, PhoQ, BtsS, EnvZ, and UhpB did not show a significant delay on starting cell division. It indicates that these five SKs contribute the start of cell division in a RR independent manner in the cell and might cause delayed 1st cell division in the all SK-deprived mutant. Even so, it should be noted that the double- and triple-gene knockout strains of *phoQ*, *phoR* and *envZ* recuperated the delayed elapsed time appeared in the single-gene knockouts. Hence, likewise the RRs, the contribution level of multi-SK knockouts probably fluctuates depends on the combination. Based on the fact that the SK-deprived mutant contains no unexpected mutations in the genome according to the complete genome sequence determined in Chapter 4, the parent-like initial growth rate of the strain suggests that the depletion of whole SKs causes a long time lag for adaptation because of the lack of sensitivity, but the cell can drive the adaptive growth without SKs after the successful start of the 1st cell division.

Together, these findings proposed that a set of TCSs acts as a mediator in the adaptive growth of *E. coli* by regulating the stress-dependent adaptation and epistasis effects. The further analysis of the RR- and SK-deprived strains is still needed to explain the mechanisms of the function of TCSs in the adaptive growth of *E. coli*. I anticipate the genetic complementation tests using the TCS defective mutant could identify other essential combinations of RRs and SKs, which the *E. coli* cell uses for adaptive growth.

CHAPTER 6. CONCLUSIONS

In this study, I have focused on revealing the role of TCSs on the adaptive growth of bacteria, which the proper rapid proliferation driven by the adapting-cell. To get the insight of the entire role of TCSs on the adaptive growth, I first worked on understanding each TCS. The PyrSR system was estimated to play a role in the reutilization of extracellular pyruvate, known as an exometabolite of *E. coli*. I newly identified 7 regulatory target genes of PyrR in addition to the known-target gene *yhjX*. Also, two pyruvate-sensing TCSs PyrSR and BtsSR showed the cross-talk at stage 1 and 2 for recognition of a single and the same exometabolite, pyruvate between two SKs (PyrS and BtsS), and for indirect regulation of *btsT* promoter by PyrS.

The analysis of the TCS promoter expression profile in *E. coli* indicated that *E. coli* could induce the biosynthesis of more than one TCS factors to respond and adapt to the environment. Then, I developed the novel genome editing technology, the HoSeI (Homologous Sequence Integration) method, based on CRISPR-Cas9. This systematic gene-editing method generated a set of gene-knockout strains, including the 34 RR- and 30 SK-knockout strains.

The RR- and SK-deprived strains exhibited some unique phenotype. The RR deprivation impacted both the growth rate and the maximum cell population under poor nutrient conditions, indicating that RRs makes the cell possible to drive the fast growth and to form the larger cell mass. In addition, the RR-knockout strain showed limited viability and high sensitivity to environmental changes. On the other hand, phenotype characterization showed that the SK-deprivation mostly caused the initial growth delay, but not the reduction of the cell mass. Interestingly, under the nutrient-rich condition, the growth of these two mutants was similar to the parent. These insights proposed the *E. coli* cell survives and performs adaptive growth using the signal transduction systems under severe environmental conditions. I speculated the *E. coli* cell might be able to increase its population in a signal-response independent manner under the eutrophic conditions.

As the results of single-cell observation, the arbitrary pair of *phoP*, *phoB,* and *ompR* are shown as an epistatic requirement for *E. coli* adaptive growth. Their cognate SK-independent feature provided that the arbitrary pairs of three main RRs play a signal-sensing independent role in an adaptive growth. Also, TCS-deprived strains showed the delayed 1st cell division and a slow growth rate. However, the TCS-deprived strain did not show the growth defect appeared in the double main RR gene-knockout strains. Thus, I speculate that the combination of RRs plays a role in the adaptive growth of *E. coli* with a different level of contribution. These findings demonstrated that TCSs acts as a mediator in the adaptive growth of *E. coli* by regulating the stress-dependent adaptation and epistasis effects. Further analysis of the TCS-deprived strain could explain the role of TCSs in the adaptive growth of *E. coli* and identify other essential combinations of TCSs which the *E. coli* cell uses for proper growth.

REFERENCES

Abayakoon P, Jin Y, Lingford JP, Petricevic M, John A, Ryan E, Wai-Ying Mui J, Pires DEV, Ascher DB, Davies GJ, Goddard-Borger ED, Williams SJ. (2018)
Structural and Biochemical Insights into the Function and Evolution of Sulfoquinovosidases. *ACS Cent Sci*. 4(9):1266-1273.

Amemura M, Makino K, Shinagawa H, Nakata A. (1986)
Nucleotide sequence of the phoM region of *Escherichia coli*: four open reading frames may constitute an operon. *J Bacteriol*. 168(1):294-302.

Ashenberg O, Keating AE, Laub MT. (2013)
Helix bundle loops determine whether histidine kinases autophosphorylate in *cis* or in *trans*. *J Mol Biol.* 425:1198-209.

Baba T, Ara T, Hasegawa M, Takai Y, Okumura Y, Baba M, Datsenko KA, Tomita M, Wanner BL, Mori H. (2006)
Construction of *Escherichia coli* K-12 in-frame, single-gene knockout mutants: the Keio collection. *Mol Syst Biol.* 2;2006.0008.

Bachmann BJ. (1972)
Pedigrees of some mutant strains of *Escherichia coli* K-12. *Bacteriol Rev.* 36: 525–557.

Bachmann BJ. (1996)
Derivations and genotypes of some mutant derivatives of *Escherichia coli* K-12. *In Escherichia coli and Salmonella typhimurium Cellular and Molecular Biology*, Neidhardt FC, Curtiss III R, Ingraham JL, Lin ECC, Low Jr KB, Magasanik B, Reznikoff WS, Riley M, Schaechter M, Umbarger HE (eds), 2 edn, pp 2460–2488.

Barbieri CM, Mack TR, Robinson VL, Miller MT, Stock AM. (2010)
Regulation of response regulator autophosphorylation through interdomain contacts. *J. Biol. Chem.* 285, 32325–32335.

Behr S, Brameyer S, Witting M, Schmitt-Kopplin P, Jung K. (2017a)
Comparative analysis of LytS/LytR-type histidine kinase/response regulator systems in gamma-proteobacteria. *PLoS One*. 12:e0182993.

Behr S, Fried L, Jung K. (2014)
Identification of a novel nutrient-sensing histidine kinase/response regulator network in *Escherichia coli*. *J Bacteriol*. 196:2023–2029.

Behr S, Heermann R, Jung K. (2016)
Insights into the DNA-binding mechanism of a LytTR-type transcription regulator. *Biosci Res.* 36:e00326.

Behr S, Kristoficova I, Witting M, Breland EJ, Eberly AR, Sachs C, Schmitt-Kopplin P, Hadjifrangiskou M, Jung K. (2017b)
Identification of a high-affinity pyruvate receptor in *Escherichia coli*. *Sci Rep.* 7:1388.

Bettenbrock K, Fischer S, Kremling A, Jahreis K, Sauter T, Gilles ED. (2006)
A quantitative approach to catabolite repression in *Escherichia coli*. *J Biol Chem.* 281:2578–2584.

Blanco AG, Sola M, Gomis-Rüth FX, Coll M. (2002)
Tandem DNA recognition by PhoB, a two-component signal transduction transcriptional activator. *Struct.* 10, 701–713.

Blattner FR, Plunkett G 3rd, Bloch CA, Perna NT, Burland V, Riley M, Collado-Vides J, Glasner JD, Rode CK, Mayhew GF, Gregor J, Davis NW, Kirkpatrick HA, Goeden MA, Rose DJ, Mau B, Shao Y. (1997)
The complete genome sequence of *Escherichia coli* K-12. *Science*. 277(5331):1453-1462.

Blouin K, Walker SG, Smit J, Turner R. (1996)
Characterization of *in vivo* reporter systems for gene expression and biosensor applications based on luxAB luciferase genes. *Appl Environ Microb* 62:2013–2021.

Booth IR. (2005)
Glycerol and Methylglyoxal Metabolism. *EcoSal Plus*. 1.

Buckler DR, Zhou Y, Stock AM. (2002)
Evidence of intradomain and interdomain flexibility in an OmpR/PhoB homolog from Thermotoga maritima. *Struct.* 10, 153–164.

Burton NA, Johnson MD, Antczak P, Robinson A, Lund PA. (2010)
Novel aspects of the acid response network of *E. coli* K-12 are revealed by a study of transcriptional dynamics. *J Mol Biol*. 401(5):726-742.

Camacho MI, Alvarez AF, Chavez RG, Romeo T, Merino E, Georgellis D. (2015)
Effects of the global regulator CsrA on the BarA/UvrY two component signaling system. *J Bacteriol.* 197:983-991.

Casino P, Miguel-Romero L, Huesa J, García P, García-Del Portillo F, Marina A. (2018)
Conformational dynamism for DNA interaction in the Salmonella RcsB response regulator. *Nucleic Acids Res.* 46:456-472.

Chavez RG, Alvarez AF, Romeo T, Georgellis D. (2010)
The physiological stimulus for the BarA sensor kinase. *J Bacteriol*. 192(7):2009-2012.

Choudhury HG, Konstantinos B. (2013)
The dimeric form of the unphosphorylated response regulator BaeR. *Protein Sci*. 22, 1287–1293.

Coornaert A, Chiaruttini C, Springer M, Guillier M. (2013)
Post-transcriptional control of the *Escherichia coli* PhoQ-PhoP two component system by multiple sRNAs involves a novel pairing region of GcvB. *PLoS Genet.* 9:e1003156.

Coornaert A, Lu A, Mandin P, Springer M, Gottesman S, Guillier M. (2010)
MicA sRNA links the PhoP regulon to cell envelope stress. *Mol Microbiol.* 76:467-479.

Crooks GE, Hon G, Chandonia JM, Brenner SE. (2004)
WebLogo: A sequence logo generator. *Genome Research.* 14:1188-1190.

Datsenko KA, Wanner BL. (2000)
One-step inactivation of chromosomal genes in *Escherichia coli* K-12 using PCR products. *Proc Natl Acad Sci USA.* 97:6640-6645.

Delauné A, Dubrac S, Blanchet C, Poupel O, Mäder U, Hiron A, Leduc A, Fitting C, Nicolas P, Cavaillon JM, Adib-Conquy M, Msadek T. (2012)
The WalKR system controls major staphylococcal virulence genes and is involved in triggering the host inflammatory response. *Infect Immun*. 80(10):3438-3453.

Deutscher J, Francke C, Postma PW. (2006)

How phosphotransferase system-related protein phosphorylation regulates carbohydrate metabolism in bacteria. *Microbiol Mol Biol Rev.* 70:939–1031.

Domka J, Lee J, Bansal T, Wood TK. (2007)
Temporal gene-expression in *Escherichia coli* K-12 biofilms. *Environ Microbiol*. 9(2):332-346.

Dubrac S, Msadek T. (2004)
Identification of genes controlled by the essential YycG/YycF two-component system of *Staphylococcus aureus*. *J Bacteriol*. 186(4):1175-1181.

Dubrac S, Boneca IG, Poupel O, Msadek T. (2007)
New insights into the WalK/WalR (YycG/YycF) essential signal transduction pathway reveal a major role in controlling cell wall metabolism and biofilm formation in *Staphylococcus aureus*. *J Bacteriol*. 189(22):8257-8269.

Egger LA, Park H, Inouye M. (1997)
Signal transduction via the histidyl-aspartyl phosphorelay. *Genes to Cells.* 2, 167–184.

Fabret, C, Hoch JA. (1998)
A two-component signal transduction system essential for growth of *Bacillus subtilis*: implications for anti-infective therapy. *J Bacteriol*. 180:6375-6383.

Franke S, Grass G, Nies DH. (2001)
The product of the ybdE gene of the *Escherichia coli* chromosome is involved in detoxification of silver ions. *Microbiology*. 147(Pt 4):965-972.

Fried L, Behr S, Jung K. (2013)
Identification of a target gene and activating stimulus for the YpdA/YpdB histidine kinase/response regulator system in *Escherichia coli*. *J Bacteriol*. 195:807–815.

Friedland N, Mack TR, Yu M, Hung LW, Terwilliger TC, Waldo GS, Stock AM. (2007)
Domain orientation in the inactive response regulator Mycobacterium tuberculosis MtrA provides a barrier to activation. *Biochem.* 46, 6733–6743.

Gao R, Bouillet S, Stock AM. (2019)
Structural Basis of Response Regulator Function. *Annu Rev Microbiol.* 73:175-197.

Gao R, Stock AM. (2009)
Biological insights from structures of two-component proteins. *Annu. Rev. Microbiol*. 63, 133–154.

Gao R, Stock AM. (2013)
Evolutionary tuning of protein expression levels of a positively autoregulated two-component system. *PLoS Genet*. 9, e1003927.

Gao R, Stock AM. (2018)
Overcoming the cost of positive autoregulation by accelerating the response with a coupled negative feedback. *Cell Reports*. 24, 3061–3071.e6.

Goulian M. (2010)
Two-component signaling circuit structure and properties. *Curr. Opin. Microbiol.* 13, 184–189.

Groisman EA. (2001)
The pleiotropic two-component regulatory system PhoP-PhoQ. *J. Bacteriol*. 183, 1835–1842.

Groisman EA. (2016)
Feedback Control of Two Component Regulatory Systems. *Annu Rev Microbiol.* 70:103-124.

Guillier M, Gottesman S. (2008)
The 5’ end of two redundant sRNAs is involved in the regulation of multiple targets, including their own regulator. *Nucleic Acids Res.* 36:6781–6794.

Guyer MS, Reed RR, Steitz JA, Low KB. (1981)
Identification of a sex-factor-affinity site in *E. coli* as γδ. *Cold Spring Harbor Symp Quant Biol.* 45: 135–140.

Harari O, Park SY, Huang H, Groisman EA, Zwir I. (2010)
Defining the plasticity of transcription factor binding sites by deconstructing DNA consensus sequences: the PhoP-binding sites among gamma/enterobacteria. *PLoS Comput. Biol.* 6, e1000862.

Hayashi K, Morooka N, Yamamoto Y, Fujita K, Isono K, Choi S, Ohtsubo E, Baba T, Wanner BL, Mori H, Horiuchi T. (2006)
Highly accurate genome sequences of *Escherichia coli* K-12 strains MG1655 and W3110. *Mol Syst Biol*. 2:2006.0007.

Hermsen R, Ursem B, Wolde PR. (2010)
Combinatorial gene regulation using auto-regulation. *PLoS Comput. Biol.* 6, 1–13.

Hirakawa H, Nishino K, Hirata T, Yamaguchi A. (2003)
Comprehensive studies of drug resistance mediated by overexpression of response regulators of two-component signal transduction systems in *Escherichia coli*. *J Bacteriol*. 185(6):1851-1856.

Hirakawa H, Nishino K, Yamada J, Hirata T, Yamaguchi A. (2003a)
Beta-lactam resistance modulated by the overexpression of response regulators of two-component signal transduction systems in *Escherichia coli*. *J Antimicrob Chemother*. 52(4):576-582.

Hoch JA. (2000)
Two-component and phosphorelay signal transduction. *Curr Opin Microbiol.* 3(2):165-170.

Holms H. (1996)
Flux analysis and control of the central metabolic pathways in *Escherichia coli*. *FEMS Microbiol Rev*. 19:85–116.

Hsieh YJ, Wanner BL. (2010)
Global regulation by the seven-component pi signaling system. *Curr. Opin. Microbiol*. 13, 198–203.

Hwang S, Choe D, Yoo M, Cho S, Kim SC, Cho S, Cho BK. (2018)
Peptide transporter CstA imports pyruvate in *Escherichia coli* K-12. *J Bacteriol.* 200:e00771–17.

Ishihama A, Kori A, Koshio E, Yamada K, Maeda H, Shimada T, Makinoshima H, Iwata A, Fujita N. (2014)
Intracellular concentrations of 65 species of transcription factors with known regulatory functions in *Escherichia coli*. *J Bacteriol.* 196(15):2718-2727.

Ishihama A, Shimada T, Yamazaki Y. (2016)
Transcription profile of *Escherichia coli*: genomic SELEX search for regulatory targets of transcription factors. *Nucleic Acids Res*. 44: 2058–2074.

Ishihama A. (2000)
Functional modulation of *Escherichia coli* RNA polymerase. *Annu Rev Microbiol*. 54:499-518.

Ishihama A. (2010)
Prokaryotic genome regulation: multifactor promoters, multitarget regulators and hierarchic networks. *FEMS Microbiol Rev*. 34(5):628-645.

Ishihama A. (2012)
Prokaryotic genome regulation: a revolutionary paradigm. *Proc Jpn Acad Ser B Phys Biol Sci*. 2012;88(9):485-508.

Iuchi S, Cameron DC, Lin EC. (1989)
A second global regulator gene (*arcB*) mediating repression of enzymes in aerobic pathways of *Escherichia coli*. *J Bacteriol*. 171(2):868-873.

Iuchi S, Lin EC. (1992)
Mutational analysis of signal transduction by ArcB, a membrane sensor protein responsible for anaerobic repression of operons involved in the central aerobic pathways in *Escherichia coli*. *J Bacteriol*. 174(12):3972-3980.

Jacob-Dubuisson F, Mechaly A, Betton JM, Antoine R. (2018)
Structural insights into the signaling mechanisms of two-component systems. *Nat Rev Microbiol*. 16(10):585-593.

Jiang Y, Chen B, Duan C, Sun B, Yang J, Yang S. (2015)
Multigene editing in the *Escherichia coli* genome via the CRISPR-Cas9 system. *Appl. Environ. Microbiol*. 81, 2506–2514.

Jishage M, Ishihama A. (1997)
Variation in RNA polymerase sigma subunit composition within different stocks of *Escherichia coli* W3110. *J Bacteriol*. 179:959-963

Kang Y, Weber KD, Qiu Y, Kiley PJ, Blattner FR. (2005)
Genome-wide expression analysis indicates that FNR of *Escherichia coli* K-12 regulates a large number of genes of unknown function. *J Bacteriol*. 187(3):1135-60.

King-Scott J, Nowak E, Mylonas E, Panjikar S, Roessle M, Svergun DI, Tucker PA. (2007)
The structure of a full-length response regulator from Mycobacterium tuberculosis in a stabilized three- dimensional domain-swapped, activated state. *J. Biol. Chem.* 282, 37717-37729.

Koga K, Nishizawa Y, Matsumoto Y, Hara T, Takahashi K. (2004)
Evaluation of the growth activity of *Escherichia coli* and Staphylococcus aureus colonies on solid medium using microbial calorimetry. *Biocontrol Sci*. 9, 21–28.

Kraxenberger T, Fried L, Behr S, Jung K. (2012)
First insights into the unexplored two-component system YehU/YehT in *Escherichia coli*. *J Bacteriol*. 194:4272–4284.

Krin E, Danchin A, Soutourina O. (2010)
Decrypting the H-NS-dependent regulatory cascade of acid stress resistance in *Escherichia coli*. *BMC Microbiol*. 10:273.

Kristoficova I, Vilhena C, Behr S, Jung K. (2018)
BtsT - a novel and specific pyruvate/H+ symporter in *Escherichia coli*. *J Bacteriol*. 200:e00599–17.

Kurata T, Katayama A, Hiramatsu M, Kiguchi Y, Takeuchi M, Watanabe T, Ogasawara H, Ishihama A, Yamamoto K. (2013)
Identification of the set of genes, including non-annotated morA, under the direct control of ModE in *Escherichia coli*. *J Bacteriol*. 195:4496–4505.

Lang VJ, Leystra-Lantz C, Cook RA. (1987)
Characterization of the specific pyruvate transport system in *Escherichia coli* K-12. *J Bacteriol*. 169:380–385.

Lange R, Wagner C, de Saizieu A, Flint N, Molnos J, Stieger M, Caspers P, Kamber M, Keck W, Amrein KE. (1999)
Domain organization and molecular characterization of 13 two-component systems identified by genome sequencing of *Streptococcus pneumoniae*. Gene, 237(1):223-234.

Laub MT, Goulian M. (2007)
Specificity in two-component signal transduction pathways. *Annu Rev Genet*. 41:121–145.

Lin EC. (1976)
Glycerol dissimilation and its regulation in bacteria. *Annu Rev Microbiol.* 30:535-578.

Lukjancenko O, Wassenaar TM, Ussery DW. (2010)
Comparison of 61 sequenced *Escherichia coli* genomes. *Microb. Ecol*. 60, 708–720.

Maeda YT, Sano M. (2006)
Regulatory dynamics of synthetic gene networks with positive feedback. *J. Mol. Biol.* 359, 1107–1124.

Martin PK, Li T, Sun D, Biek DP, Schmid MB. (1999)
Role in cell permeability of an essential two-component system in *Staphylococcus aureus*. *J Bacteriol*. 181(12):3666-3673.

Menon S, Wang S. (2011)
Structure of the response regulator PhoP from Mycobacterium tuberculosis reveals a dimer through the receiver domain. *Biochem.* 50, 5948-5957.

Minagawa S, Ogasawara H, Kato A, Yamamoto K, Eguchi Y, Oshima T, Mori H, Ishihama A, Utsumi R. (2003)
Identification and molecular characterization of the Mg2+ stimulon of *Escherichia coli*. *J Bacteriol*. 185(13):3696-3702.

Miyake Y, Inaba T, Watanabe H, Teramoto J, Yamamoto K, Ishihama A. (2019)
Regulatory roles of pyruvate-sensing two-component system PyrSR (YpdAB) in *Escherichia coli* K-12. *FEMS Microbiol Lett*. 366(2).

Miyake Y, Yamamoto K. (2020)
Epistatic Effect of Regulators to the Adaptive Growth of *Escherichia coli*. *Sci Rep.* 10;3661.

Mizuno T. (1997)
Compilation of all genes encoding two-component phosphotransfer signal transducers in the genome of *Escherichia coli*. *DNA Res.* 4(2):161-168.

Munson GP, Lam DL, Outten FW, O'Halloran TV. (2000)
Identification of a copper-responsive two-component system on the chromosome of *Escherichia coli* K-12. *J Bacteriol*. 182(20):5864-5871.

Murakami, S. K. (2015)
Structural biology of bacterial RNA polymerase. *Biomolecules* 5, 848–864.

Nonaka G, Blankschien M, Herman C, Gross CA, Rhodius VA. (2006)
Regulon and promoter analysis of the *E. coli* heat-shock factor, sigma32, reveals a multifaceted cellular response to heat stress. *Genes Dev*. 20(13):1776-1789.

Nowak E, Panjikar S, Konarev P, Svergun DI, Tucker PA. (2006)
The structural basis of signal transduction for the response regulator PrrA from Mycobacterium tuberculosis. *J. Biol. Chem*. 281, 9659–9666.

Ogasawara H, Hasegawa A, Kanda E, Miki T, Yamamoto K, Ishihama A. (2007)
Genomic SELEX search for target promoters under the control of the PhoQP-RstBA signal relay cascade. *J Bacteriol*. 189(13):4791-4799.

Ogasawara H, Ishida Y, Yamada K, Yamamoto K, Ishihama A. (2007)
PdhR (pyruvate dehydrogenase complex regulator) controls the respiratory electron transport system in *Escherichia coli*. *J Bacteriol*. 189:5534–5541

Ogasawara H, Shinohara S, Yamamoto K, Ishihama A. (2012)
Novel regulation targets of the metal-response BasS-BasR two-component system of *Escherichia coli*. *Microbiology*. 158(Pt 6):1482-1492.

Oshima T, Aiba H, Masuda Y, Kanaya S, Sugiura M, Wanner BL, Mori H, Mizuno T. (2002)
Transcriptome analysis of all two-component regulatory system mutants of *Escherichia coli* K-12. *Moleuclar Microbiol*. 46, 281–291.

Paczia N, Nilgen A, Lehmann T, Gätgens J, Wiechert W, Noack S. (2012)
Extensive exometabolome analysis reveals extended overflow metabolism in various microorganisms. *Microb Cell Fact*. 11:122.

Postma PW, Lengeler JW, Jacobson GR. (1993)
Phosphoenolpyruvate:carbohydrate phosphotransferase systems of bacteria. *Microbiol Rev.* 57:543–594.

Pukklay P, Nakanishi Y, Nitta M, Yamamoto K, Ishihama A, Shiratsuchi A. (2013)
Involvement of EnvZ–OmpR two-component system in virulence control of *Escherichia coli* in Drosophila melanogaster. *Biochem. Biophys. Res. Commun.* 438, 306–311.

Pulvermacher SC, Stauffer LT, Stauffer GV. (2009)
Role of the sRNA GcvB in regulation of *cycA* in *Escherichia coli*. *Microbiology*. 155(Pt 1):106-114.

Rabin RS, Stewart V. (1993)
Dual response regulators (NarL and NarP) interact with dual sensors (NarX and NarQ) to control nitrate- and nitrite-regulated gene expression in *Escherichia coli* K-12. *J Bacteriol*. 175(11):3259-3268.

Reichenbach B, Göpel Y, Görke B. (2009)
Dual control by perfectly overlapping sigma 54- and sigma 70- promoters adjusts small RNA GlmY expression to different environmental signals. *Mol Microbiol*. 74(5):1054-1070.

Robinson VL, Wu T, Stock AM. (2003)
Structural analysis of the domain interface in DrrB, a response regulator of the OmpR/PhoB subfamily. *J Bacteriol*. 185(14):4186-4194.

Saini S, Pearl JA, Rao CV. (2009)
Role of FimW, FimY, and FimZ in regulating the expression of type I fimbriae in *Salmonella enterica* serovar Typhimurium. *J Bacteriol*. 191(9):3003-3010.

Salmon K, Hung SP, Mekjian K, Baldi P, Hatfield GW, Gunsalus RP. (2003)
Global gene expression profiling in *Escherichia coli* K12. The effects of oxygen availability and FNR. *J Biol Chem*. 278(32):29837-55.

Sato K, Hamada M, Asai K, Mituyama T. (2009)
CENTROIDFOLD: a web server for RNA secondary structure prediction. *Nucleic Acids Res*. 37(Web Server issue):W277-80.

Sauer U, Eikmanns BJ. (2005)
The PEP-pyruvate-oxalacetate node as the switch point for carbon flux distribution in bacteria. *FEMS Microbiol Rev*. 29:765–794.

Seo SW, Gao Y, Kim D, Szubin R, Yang J, Cho BK, Palsson BO. (2017)
Revealing genome-scale transcriptional regulatory landscape of OmpR highlights its expanded regulatory roles under osmotic stress in *Escherichia coli* K-12 MG1655. *Sci. Reports* 7, 2181.

Shimada T, Fujita N, Maeda M, Ishihama A. (2005)
Systematic search for the Cra-binding promoters using genomic SELEX system. *Genes Cells*. 10:907–918.

Shimada T, Fujita N, Yamamoto K, Ishihama A. (2011)
Novel roles of cAMP receptor protein (CRP) in regulation of transport and metabolism of carbon sources. *PLoS One.* 6:e20081.

Shimada T, Ogasawara H, Ishihama A. (2018)
Genomic SELEX screening of regulatory targets of *Escherichia coli* transcription factors. *Meth Mol Biol*. 1837:49–69.

Shimada T, Tanaka K. (2016)
Use of a bacterial luciferase monitoring system to estimate real-time dynamics of intracellular metabolism in *Escherichia coli*. *Appl Environ Microb*. 82:5960–5968.

Speciale G, Jin Y, Davies GJ, Williams SJ, Goddard-Borger ED. (2016)
YihQ is a sulfoquinovosidase that cleaves sulfoquinovosyl diacylglyceride sulfolipids. *Nat Chem Biol*. 12(4):215-217.

Sperandio V, Torres AG, Kaper JB. (2002)
Quorum sensing *Escherichia coli* regulators B and C (QseBC): A novel two-component regulatory system involved in the regulation of flagella and motility by quorum sensing in *E. coli*. *Mol. Microbiol*. 43, 809–821.

Steiner BD, Eberly AR, Hurst MN, Zhang EW, Green HD, Behr S, Jung K, Hadjifrangiskou M. (2018)
Evidence of crossregulation in two closely related pyruvate-sensing systems in uropathogenic *Escherichia coli*. *J Memb Biol*. 251(1):65–74.

Stock JB, Ninfa AJ, Stock AM. (1989)
Protein phosphorylation and regulation of adaptive responses in bacteria. *Microbiol Rev*. 53;450–490.

Stock JB, Stock AM, Mottonen JM. (1990)
Signal transduction in bacteria. *Nature*. 344(6265):395-400.

Studier FW, Rosenberg AH, Dunn JJ, Dubendorff JW. (1990)
Use of T7 RNA polymerase to direct expression of cloned genes. *J Mol Biol.* 185:60-89.

Stülke J, Hillen W. (1999)
Carbon catabolite repression in bacteria. *Curr Opin Microbiol.* 2:195–201.

Suzuki K, Wang X, Weilbacher T, Pernestig AK, Melefors O, Georgellis D, Babitzke P, Romeo T. (2002)
Regulatory circuitry of the CsrA/CsrB and BarA/UvrY systems of *Escherichia coli*. *J Bacteriol*. 184(18):5130-5140.

Tanabe H, Yamasaki K, Katoh A, Yoshioka S, Utsumi R. (1998)
Identification of the promoter region and the transcriptional regulatory sequence of the evgAS operon of *Escherichia coli*. *Biosci Biotechnol Biochem*. 62(2):286-290.

Tatusov RL, Galperin MY, Natale DA, Koonin EV. (2000)
The COG database: A tool for genome-scale analysis of protein functions and evolution. *Nucleic Acids Res*. 28, 33–36.

Tatusov RL, Koonin EV, Lipman DJ. (1997)
A genomic perspective on protein families. *Science*. 278(5338):631-637.

Throup JP, Koretke KK, Bryant AP, Ingraham KA, Chalker AF, Ge Y, Marra A, Wallis NG, Brown JR, Holmes DJ, Rosenberg M, Burnham MK. (2000)
A genomic analysis of two-component signal transduction in *Streptococcus pneumoniae*. *Mol Microbiol*. 35(3):566-576.

Tian ZX, Li QS, Buck M, Kolb A, Wang YP. (2001)
The CRP-cAMP complex and downregulation of the glnAp2 promoter provides a novel regulatory linkage between carbon metabolism and nitrogen assimilation in *Escherichia coli*. *Mol Microbiol*. 41(4):911-924.

Touchon M, Hoede C, Tenaillon O, Barbe V, Baeriswyl S, Bidet P, Bingen E, Bonacorsi S, Bouchier C, Bouvet O, Calteau A, Chiapello H, Clermont O, Cruveiller S, Danchin A, Diard M, Dossat C, Karoui ME, Frapy E, Garry L, Ghigo JM, Gilles AM, Johnson J, Le Bouguénec C, Lescat M, Mangenot S, Martinez-Jéhanne V, Matic I, Nassif X, Oztas S, Petit MA, Pichon C, Rouy Z, Ruf CS, Schneider D, Tourret J, Vacherie B, Vallenet D, Médigue C, Rocha EP, Denamur E. (2009)
Organised genome dynamics in the *Escherichia coli* species results in highly diverse adaptive paths. *PLoS Genet*. 5, e1000344.

Vemuri GN, Altman E, Sangurdekar DP, Khodursky AB, Eiteman MA. (2006)
Overflow metabolism in *Escherichia coli* during steady-state growth: transcriptional regulation and effect of the redox ratio. *Appl Environ Microb*. 72(5):3653–3661.

Verhamme DT, Arents JC, Postma PW, Crielaard W, Hellingwerf KJ. (2001)
Glucose-6-phosphate-dependent phosphoryl flow through the Uhp two-component regulatory system. *Microbiology.* 147(Pt 12):3345-3352.

Vilhena C, Kaganovitch E, Shin JY, Grünberger A, Behr S, Kristoficova I, Brameyer S, Kohlheyer D, Jung K. (2017)
A single-cell view of the BtsSR/YpdAB pyruvate sensing network in *Escherichia coli* and its biological relevance. *J Bacteriol*. 200:e00536–17.

Villanueva M, García B, Valle J, Rapún B, Ruiz de Los Mozos I, Solano C, Martí M, Penadés JR, Toledo-Arana A, Lasa I. (2018)
Sensory deprivation in *Staphylococcus aureus*. *Nat Commun*. 9(1):523.

Wagner C, Saizieu Ad Ad, Schönfeld HJ, Kamber M, Lange R, Thompson CJ, Page MG. (2002)
Genetic analysis and functional characterization of the *Streptococcus pneumoniae vic* operon. *Infect Immun*. 70(11):6121-6128.

Yamamoto K, Hirao K, Oshima T, Aiba H, Utsumi R, Ishihama A. (2005)
Functional characterization *in vitro* of all two-component signal transduction systems from *Escherichia coli*. *J Biol Chem*. 280(2):1448-1456.

Yamamoto K, Ishihama A. (2006)
Characterization of copper-inducible promoters regulated by CpxA/CpxrRin *Escherichia coli*. *Biosci. Biotechnol. Biochem*. 70, 1688–1695.

Yamamoto K, Ogasawara H, Fujita N, Utsumi R, Ishihama A. (2002)
Novel mode of transcription regulation of divergently overlapping promoters by PhoP, the regulator of two-component system sensing external magnesium availability. *Mol. Microbiol.* 45, 423–438.

Yamamoto K. (2014)
The hierarchic network of metal-response transcription factors in *Escherichia coli*. *Biosci Biotechnol Biochem*. 78(5):737-747.

Yamanaka Y, Oshima T, Ishihama A, Yamamoto K. (2014)
Characterization of the YdeO regulon in *Escherichia coli*. *PLoS One*. 9: e111962.

Yamanaka Y, Winardhi RS, Yamauchi E, Nishiyama SI, Sowa Y, Yan J, Kawagishi I, Ishihama A, Yamamoto K. (2018)
Dimerization site 2 of the bacterial DNA-binding protein H-NS is required for gene silencing and stiffened nucleoprotein filament formation. *J. Biol. Chem.* 293, 9496–9505.

Yamanaka Y, Watanabe H, Yamauchi E, Miyake Y, Yamamoto K. (2020)
Measurement of the promoter activity in *Eschrichia coli* by using a luciferase reporter. *Bio-prot.* 10(2): e3500.

Yamasaki S, Hirokawa T, Asai K, Fukui K. (2014)
Tertiary structure prediction of RNA-RNA complexes using a secondary structure and fragment-based method. *J Chem Inf Model*. 54(2):672-682.

Yang C, Huang TW, Wen SY, Chang CY, Tsai SF, Wu WF, Chang CH. (2012)
Genome-wide PhoB binding and gene expression profiles reveal the hierarchical gene regulatory network of phosphate starvation in *Escherichia coli. PLoS One*. 7, e47314.

Yao R, Xiong D, Hu H, Wakayama M, Yu W, Zhang X, Shimizu K. (2016)
Elucidation of the co-metabolism of glycerol and glucose in Escherichia coli by genetic engineering, transcription profiling, and (13)C metabolic flux analysis. *Biotechnol Biofuels.* 9:175.

Yasid NA, Rolfe MD, Green J, Williamson MP. (2016)
Homeostasis of metabolites in *Escherichia coli* on transition from anaerobic to aerobic conditions and the transient secretion of pyruvate. *R Soc Open Sci*. 3:160187.

Yoshida M, Ishihama A, Yamamoto K. (2015)
Cross talk in promoter recognition between six NarL-family response regulators of *Escherichia coli* two-component system. *Genes Cells.* 20(7):601-612.

Zere TR, Vakulskas CA, Leng Y, Pannuri A, Potts AH, Dias R, Tang D, Kolaczkowski B, Georgellis D, Ahmer BMM, Romeo T. (2015)
Genomic Targets and Features of BarA-UvrY (-SirA) Signal Transduction Systems. *PLoS One*. 10(12):e0145035.

Zhou L, Lei XH, Bochner BR, Wanner BL. (2003)
Phenotype microarray analysis of *Escherichia coli* K-12 mutants with deletions of all two-component systems. *J. Bacteriol*. 185, 4956–4972.

Zschiedrich CP, Keidel V, Szurmant H. (2016)
Molecular Mechanisms of Two-Component Signal Transduction. *J Mol Biol*. 428(19):3752-3775.

LIST OF PUBLICATIONS

1. Miyake Y, Yamamoto K. (2020)

   Epistatic Effect of Regulators to the Adaptive Growth of *Escherichia coli*, *Sci Rep.* 10;3661.

2. Yamanaka Y, Watanabe H, Yamauchi E, Miyake Y, Yamamoto K. (2020)

   Measurement of the Promoter Activity in *Escherichia coli* by Using a Luciferase Reporter, *Bio-prot.* 10(2): e3500.

3. Miyake Y, Inaba T, Watanabe H, Teramoto J, Yamamoto K, Ishihama A. (2019)

   Regulatory roles of pyruvate-sensing two-component system PyrSR (YpdAB) in *Escherichia coli* K-12, *FEMS Microbiol Lett.* Volume 366, Issue 2, fnz009.

4. Maruyama H, Kimura T, Liu H, Ohtsuki S, Miyake Y, Isogai M, Arai F, Honda A. (2018)

   Influenza virus replication raises the temperature of cells. *Virus Res*. 257:94-101.

5. Miyake Y, Ishii K, Honda A. (2017)

   Influenza Virus Infection Induces Host Pyruvate Kinase M Which Interacts with Viral RNA-Dependent RNA Polymerase. *Front Microbiol*. 8:162.

6. Cho J, Miyake Y, Honda A, Kushiro K, Takai M. (2016)

   Analysis of the Changes in Expression Levels of Sialic Acid on Influenza-Virus-Infected Cells Using Lectin-Tagged Polymeric Nanoparticles. *Front Microbiol*. 7:1147.

ACKNOWLEDGEMENTS

Over the last three years, I have benefitted greatly from my interactions with many people of Hosei University. I appreciate principal investigators, department of Frontier Bioscience Hosei University, for their professional assistance and coaching. My deepest gratitude goes to my supervisor, Professor Dr. Kaneyoshi Yamamoto. Without his guidance and persistent help, this dissertation would not have been possible. He also gave me many experiences for my growth as a scientist.

Special thanks are due to Dr. Hideaki Nojiri (Tokyo University), Dr. Ikuro Kawagishi, Dr. Tsutomu Sato, and Dr. Kenro Oshima, Hosei University, for reading the entire text in its original form.

For the study in Chapter 2, I would like to sincerely thank Dr. Akira Ishihama, Hosei University, for his grateful suggestion, discussion, and technical advice. I am thankful to Mr. Tatsuya Inaba (Hosei University) and Dr. Jun Teramoto (Kobe University) for sharing their data with me. I also thank Ms. Ayako Kori and Ms. Kayoko Yamada (Hosei University) for expression and purification of PyrR protein, Dr. Tomohiro Shimada (Meiji University) for tilling array assay of gSELEX fragments, and National Bioresource Project (NBRP) NIG (National Institute of Genetics) center for providing *E. coli* strains.

I appreciate Dr. Myu Yoshida, Mr. Hiroki Watanabe, Ms. Asami Sato, and Mr. Naoki Wakayama, Hosei University, for construction of pLUX reporter plasmids used in Chapter 3.

I also profoundly thank Mr. Shingo Sugawara and Ms. Misaki Sudo, Hosei University, for technical assistance with experiments, especially the construction of psgRNA plasmids and TCS mutants used in Chapters 4 and 5. I am thankful to Dr. Akira Katayama (Nippon Medical School) and Ms. Kumiko Tajima (Hosei University) for technical assistance.

Finally, I would like to thank the members of the Laboratory of Genomic Biology, Hosei University. They always encouraged me in my studies and gave me lots of invaluable support.

This work was supported by the Research Fellowship for Young Scientists from the Japan Society for the Promotion of Science (JP18J14641).

APPENDIX

Appendix Table 1. Oligonucleotides for pLUX cloning.

Name	Sequence (5' to 3')	Reference
arcA_LUX_F	TCGTCTTCACCTCGATAATGATATTTCGCCCGACTGCGCG	This study
arcA_LUX_R	ACTAACTAGAGGATCGTTTGCTACCTAAATTGCCAACTAA	This study
arcB LUX F	TCGTCTTCACCTCGAAGCGAGTGGTTGAAACCGGCGTGGA	This study
arcB LUX R	ACTAACTAGAGGATCTAGGGAATTCCTTCACGACAACCTG	This study
atoSC_Lux_F	TCGTCTTCACCTCGAAACAATCGGAGTCGGCAAACAGCGG	This study
atoSC_Lux_R	ACTAACTAGAGGATCGCTGAAATCCACTAGTCTTGTCCGG	This study
mdtA_LUX_F	TCGTCTTCACCTCGATGGCAGGATCGCAGACTACAAAGCC	This study
mdtA_LUX_R	ACTAACTAGAGGATCCGTTAAGAGTTTCTCTTCCTGAAAC	This study
barA LUX F	TCGTCTTCACCTCGAAAACCCCATCTGAAGTTGCTGTGTT	This study
barA LUX R	ACTAACTAGAGGATCGGAGTTCCGTTATGGGACAATTAAG	This study
uvrY_LUX_F	TCGTCTTCACCTCGAGTCATGTTGCAATGAAAATTTGCGG	This study
uvrY_LUX_R	ACTAACTAGAGGATCAGGAATATCTCCAGAAATAGGGATA	This study
basR_LUX_F	TCGTCTTCACCTCGAACCATCGGCAGCCACGGTCCGACCT	This study
basR_LUX_R	ACTAACTAGAGGATCTCACTCACTCTCCTGCAAGTTTGCA	This study
DPIB_LL_F	TCGTCTTCACCTCGACGCTCAAATCATTTTCATGC	This study
DPIB_LL_R	ACTAACTAGAGGATCTTCTCGTTAAGCTGCAACAT	This study
CPXR_LL_F	TCGTCTTCACCTCGAGTTATCGCCTGAACCGACTT	This study
CPXR_LL_R	ACTAACTAGAGGATCACTAACAGGATTTTATTCAT	This study
creA-lux-F	TCGTCTTCACCTCGAGGTAAATGTCTGTTG	This study
creA-lux-R	ACTAACTAGAGGATCCATATTGTTACCATT	This study
CUSR_LL_F	TCGTCTTCACCTCGATGCCGGACGCTGATAATCCG	This study
CUSR_LL_R	ACTAACTAGAGGATCTCGACAATCAACAGTTTCAT	This study
DCUS_LL_F	TCGTCTTCACCTCGAAATAGACATCGATCTTTTCG	This study
DCUS_LL_R	ACTAACTAGAGGATCTAGGGCAATGAATGTCTCAT	This study
OMPR_LL_F	TCGTCTTCACCTCGACAGACGCTTTTTATTATACT	This study
OMPR_LL_R	ACTAACTAGAGGATCATCTTGTAGTTCTCTTGCAT	This study
evgA_LUX_F	TCGTCTTCACCTCGATGACCAATAGGCATAGGCACCTGAA	This study
evgA_LUX_R	ACTAACTAGAGGATCAGATTATTCCCTTTGCAATGAAGCA	This study
fimZ_LUX_F	TCGTCTTCACCTCGAGATTCAGTCAGGCGTCCCATTATCA	This study
fimZ_LUX_R	ACTAACTAGAGGATCAGTTACCAGTCTCATAGGAGCGGAC	This study
zraSR_Lux_F	TCGTCTTCACCTCGAGTGCGCTGCTTTGAGCGTAAAAGTC	This study
zraSR_Lux_R	ACTAACTAGAGGATCCTTCTTCTTTGCCTGCTCATCCCTT	This study
kdpD_LUX_F	TCGTCTTCACCTCGACCCGCTGCTGACCACCGTACTGGGG	This study
kdpD_LUX_R	ACTAACTAGAGGATCCAAGTTTATCCAGCGCCAGATTGAG	This study
narQ LUX F	TCGTCTTCACCTCGACGTGGCTTTTACTTTTCCTGCCGCG	This study
narQ LUX R	ACTAACTAGAGGATCGCGTCTTCTCCACAAAAAATCATTA	This study
narP_LUX_F	TCGTCTTCACCTCGAGGCGAAGGTAAGTTGATGACTCATG	This study
narP_LUX_R	ACTAACTAGAGGATCAGTAGTCTCCTGAGGTTTTATTAGA	This study
NARX_LL_F	TCGTCTTCACCTCGAGACAGCTCCAGTAGCCCTTT	This study
NARX_LL_R	ACTAACTAGAGGATCGAGAGACAACGTTTAAGCAT	This study
glnA_Lux_F	TCGTCTTCACCTCGAGATGTTGATACGGTAATCATTCCAT	This study
glnA_Lux_R	ACTAACTAGAGGATCACTTTAACTCTCCTGGATTGGTCAT	This study
PHOP_LL_F	TCGTCTTCACCTCGAAAGCAGTTTATCGATGGTCT	This study
PHOP_LL_R	ACTAACTAGAGGATCTCAACAACCAGTACGCGCAT	This study
phoB-lux-F	TCGTCTTCACCTCGAACTGTAGAAGTTCTG	This study

Appendix Table 1. Oligonucleotides for pLUX cloning. (Continued.)

Name	Sequence (5' to 3')	Reference
phoB-lux-R	ACTAACTAGAGGATCCATGATTTGCCCTGT	This study
QSEB_LL_F	TCGTCTTCACCTCGATCTACAGTCGTTACGCTGCC	This study
QSEB_LL_R	ACTAACTAGAGGATCTCTATCAGTAAAATTCGCAT	This study
RCSD_LL_F	TCGTCTTCACCTCGACTTGTTAACTATTTCACAAA	This study
RCSD_LL_R	ACTAACTAGAGGATCGTTGTCTCTTTCTGACGCAT	This study
rcsB_LUX_F	TCGTCTTCACCTCGAGCCTGACGTTCCGCATTCTGGACAC	This study
rcsB_LUX_R	ACTAACTAGAGGATCAGTAGTCTCCTGAGGTTTTATTAGA	This study
rcsC LUX F	TCGTCTTCACCTCGATTATCGCATCCAGCATTTTGTTGTA	This study
rcsC LUX R	ACTAACTAGAGGATCAGGGGCGAAGCTCCGCCTCAGGTGA	This study
RSTA_LL_F	TCGTCTTCACCTCGAGCAAAGGTCGGGAAAAGTGG	This study
RSTA_LL_R	ACTAACTAGAGGATCACAAATACGATAGTGTTCAT	This study
torS LUX F	TCGTCTTCACCTCGATCACCTGGGGAGCATCAATAGCATT	This study
torS LUX R	ACTAACTAGAGGATCGGTCGGTGCACTTTAGGTGAAAAAG	This study
torR_LUX_F	TCGTCTTCACCTCGAAGATATCATTGCTCGCTTCCAGTTT	This study
torR_LUX_R	ACTAACTAGAGGATCCAGAGGGTTTTACTCATTCTGTTCA	This study
IVBL_LL_F(uhpA)	TCGTCTTCACCTCGACAAAATTCGTGCCGAAATTG	This study
IVBL_LL_R(uhpA)	ACTAACTAGAGGATCTTGAGCATGGAAGTAGTCAT	This study
YEDW_LL_F	TCGTCTTCACCTCGATAAGAATGTTTTGTTGTGCG	This study
YEDW_LL_R	ACTAACTAGAGGATCTCAATAAGTAGAATCTTCAT	This study
YEHU_LL_F	TCGTCTTCACCTCGACACTTCACCAATTGTGTAAA	This study
YEHU_LL_R	ACTAACTAGAGGATCACCAGATTAAAATCGTACAT	This study
glrK_Lux_F	TCGTCTTCACCTCGAAGTGGCTCATTCACCGACTTATGTC	This study
glrK_Lux_R	ACTAACTAGAGGATCGGTGTTACTCTCGTCAGACGCGAAT	This study
glrR_LUX_F	TCGTCTTCACCTCGAAACCAATCCGCTTTACTGGCTGCGG	This study
glrR_LUX_R	ACTAACTAGAGGATCCAGGAGTGACCTCATGGGTGGATGG	This study
YPDA_LL_F	TCGTCTTCACCTCGACACCGTCCGGGTTACCCATG	This study
YPDA_LL_R	ACTAACTAGAGGATCATGTTGAATATTTCGTGCAC	This study

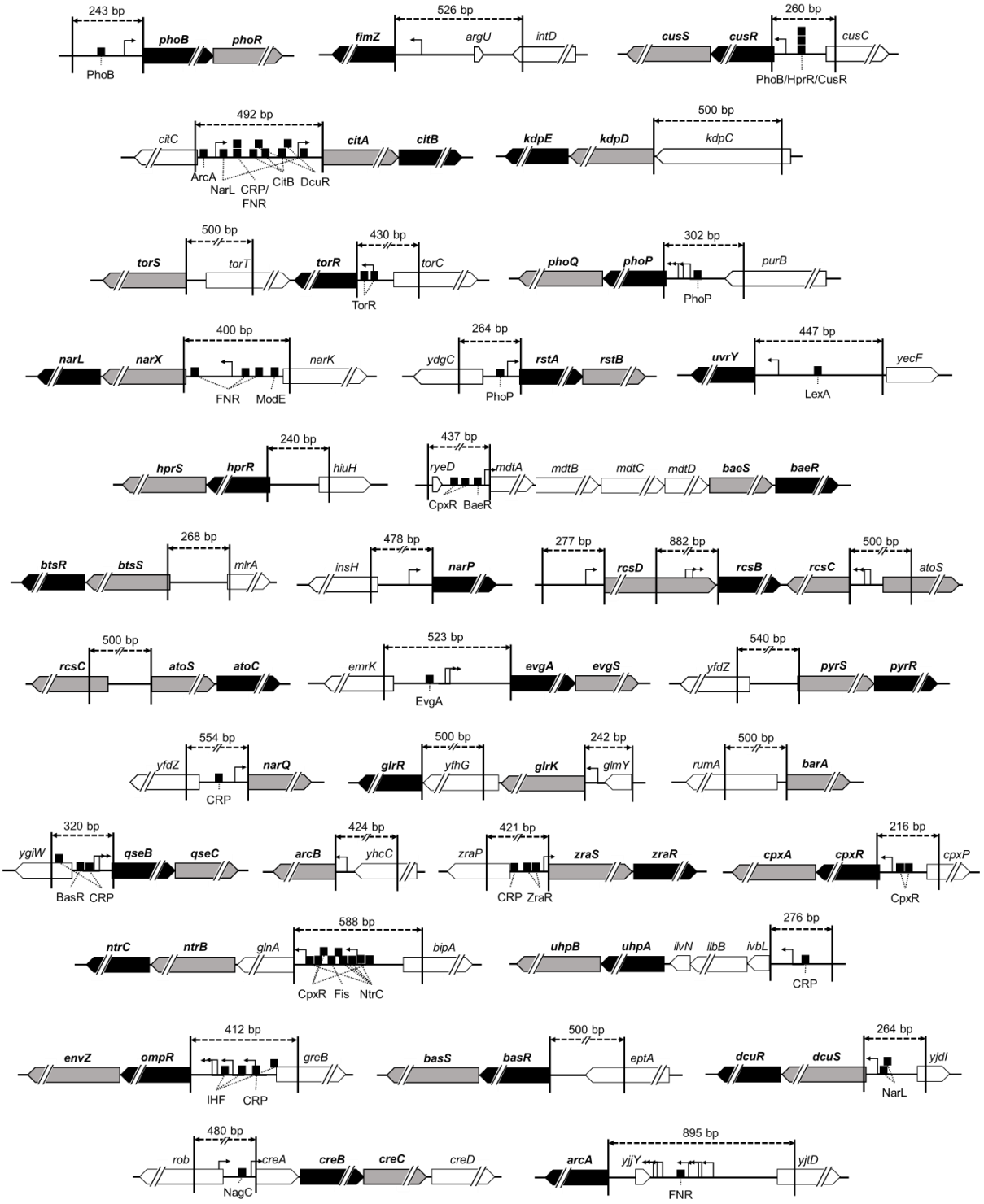

Appendix Figure 1. Two-component gene promoters for lux reporter plasmids. All two-component system genes and their promoter regions in the *E. coli* K-12 W3110 genome (4.6 Mb) are shown with arrows and length (bp). Each arrow shows sensor kinase genes (gray), response regulator genes (black), and other genes (white). The direction of arrows indicates the direction of genes in the *E. coli* genome. The dashed double arrow shows the promoter region that was inserted into the pLUX vector, and it shows the promoter length (bp). RegulonDB (http://regulondb.ccg.unam.mx/) was used to identify the promoter region for each gene. Each promoter region contains one or more transcription start sites and transcription factor (TF) binding site(s). In the case of genes without consensus sequences and TF-binding sites, I identified the promoter region as 500 bp upstream of the start codon of the gene. The thin arrow marks the transcription start site, and the black box marks the identified transcription factor binding site. As described in the Materials and Methods, the promoter regions of each TCS gene (operon) were PCR amplified and inserted into pLUX vectors (Burton *et al.* 2010). The DNA sequences of each inserted gene in the resulting plasmids are shown in **Appendix Table 2**.

Appendix Table 2. Promoter sequences of TCS genes in the *E. coli* K-12 genome.

Promoter	Sequence (5'-3')
PphoB	ACTGTAGAAGTTCTGGCCGAGATGCCAGTCTGAGGTGTGAAGGATGCGCATAACGGTTCCCTGGCGAAAAAGCATGGGCGCGATTATACCCAAACAGATG TGCCATTTGCTTTTTTCTGCGCCACGGAAATCAATAACCTGAAGATATGTGCGACGAGCTTTTCATAAATCTGTCATAAATCTGACGCATAATGACGTCGC ATTAATGATCGCAACCTATTTATTACAACAGGGCAAATCATG
PfimZ	GATTCAGTCAGGCGTCCCATTATCAGTGCTTCAGGAAATGGGCGGATGGGAGTCCATAGAAATGGTTCGTAGGTATGCTCACCTTGCGCCTAATCATTTGA CAGAGCATGCGAGGAAAATAGACGACATTTTTGGTGATAATGTCCCAAATATGTCCCACTCTGAAATTATGGAGGATATAAAGAAGGCGTAACTGATTGA ATTGTAATGGCGCGCCCTGCAGGATTCGAACCTGCGGCCCACGACTTAGAAGGTCGTTGCTCTATCCAACTGAGCTAAGGGCGCGTTGATACCGCAATGCG GTGTAATCGCGTGAATTATACGGTCAACCCTTGCTGAGTCAATGGCTTTTGATCTGGTTGCTGAACAAGTGAACGACCGCGTCTGATTTTCTGATTTATTTC GCTATAGCGGCAAACAAACGCACACCGCTGCGCGTCTGAATCAAGAAAACCCGTATTTTCATGTATCAAAGTACAATTTCCCGACCTAACGGAAAATTGT CCGCTCCTATGAGACTGGTAACT
PcusR	TGCCGGACGCTGATAATCCGGTGCCAGTGAACAACCGGTTAGCGCAAGGGCCACACAAAATGGCAGAAGTTTACAAGGAGACATAGGCTCATAATTTCTG GTGATTTTATGCCGCCAACTTTACTCGCCAGGCTCTGATTTTCCGGTGACAGAAAAATGACAAAATTGTCATTTTGCCAATAAGCGATTGCCATCTGATCC CGCTACTCTAGAATTGCCCGGGCAACATGCGGAGGAAATATGAAACTGTTGATTGTCGA
PcitA	CGCTCAAATCATTTTCATGCAGGAATTGGGCGATTTCCGCCATTTTTTTATTTTCTGAACGTTTTACGCGGGTGAAAATATCATTGCCGAACATAATAAATA GTATCCTGAAGGTGCATGTTGTTATCGATTTGCAACGAATGTTGTTCAATGTTGCAAACTGATAACCTTTTATTTTCACTTGGGAGAAAGGGGGTGATCGAG GTATATCTTTTTCTCCTTTCGCTATACATCCTAAGGAGTATTTCGGCGTGAAATTTTGATTTATTTCACATAGAGTTAGTGGTTTTTTATTTATTTAATGATTT TAAGTTTTTTAATTAATGTAATTACGAAATGACTCGCAGGTTTAAGTGATTTAATTGATTTAATGAATAAAATTTGCCACGATCATAATTAATATCTATGT ATTTTGATTCAACATTTTAATTACATCCGTCAAAGAGGCTCGGGACAACCCGCAAGGAAAACAATGTTGCAGCTTAACGAGAA
PkdpD	CCCGCTGCTGACCACCGTACTGGGGCAATGGTGGTTTCCCTGGCAGGCCAATGGTTCGTTGATTCGTGAAGGTGATACGGTGCGCGGTTCGGCATTAATCGG GCAGAATTTTACCGGCAACGGCTATTTTCATGGTCGCCCGTCGGCAACGGCAGAAATGCCCTATAATCCACAGGCTTCTGGCGGGAGCAATCTGGCGGTCA GTAACCCTGAGCTGGATAAACTAATAGCCGCACGCGTTGCTGCATTACGGGCCGCTAACCCGGATGCCAGCGCGAGCGTTCCGGTTGAACTGGTGACGGCA TCGGCAAGCGGGCTGGACAATAATATCACCCCGCAAGCGGCGGCCTGGCAAATCCCACGCGTGGCGAAAGCGCGTAATCTCAGCGTTGAACAGCTCACGC AACTGATCGCAAAATACAGCCAACAACCGCTGGTGAAATATATCGGCCAGCCGGTTGTCAACATTGTTGAACTCAATCTGGCGCTGGATAAACTTG
PtorS	TCACCTGGGGAGCATCAATAGCATTTACCAGTTCGATCACCGGCAGACTTGCTACCTGCTTTTGCAGGTCGGGAAATGAGGTCGTGCTACTACCGAGCAAA ATGGCCTCTGCGCCCCACTGTTTACACTGGTCGATTTGTGCTTGCTGGGTAGCCAACTGGCTGTAGCCGCCTGCCTCCAGCACTTTTAAATCCACACCGTAG CGGCGAGCAGCCTCCTGCATACCATAGTTCAACGATAACCAATATGAATCTTTCAGGCTGGGATAAAGCGCGCACAGTTTCCATGCGCGTTTGGCTTTAAG CGGCGTAGAGGCTTGCACCGTGAAATGCTGCGCATCATGCCAGCGCAACAGGTTATCAGCCGAAAATGCCGGCAACATGAAAAGGGAAAGAAGTAAAAA TAGCAGTACGCGCATGATAGCCTCATCAATAATAAGGCTTTATGCTAGATGCATTCCGCTTTGCGACTCAACCTTTTTCACCTAAAGTGCACCGACC
PtorR	AGATATCATTGCTCGCTTCCAGTTTGCGCTTCACCATGCCTGGAATATCCGGCGGGATATGACAGTCATGGCATTCAGCTCGCACGCCGGAGGCGTTCTGG AAATGCACCGACTGTTTATATTCTTCATACACCGGTTGCATACTGTGGCAACTGACACAAAATTCGGTTGTGCTGGTGACTTTGATCCCAACGTGTGGCAA TACAATCAGCGCAATGCCAATCACAATCCCAATTGCGACCAGCGCCAGTACCGACCAACGAGCACTGGGTCGGCGTAGCGCGTTCCAGAGTTTCCGCATA ATAACCCCTGTAGAATTATGGTTTAGTGAAGCGATCTTAATGAGCAAATATGAACAGCGGCACTGGTCAGGATGAACGGCTTACGGCAGAATATGAACAG ATATGAACAGAATGAGTAAAACCCTCTG
PphoP	AAGCAGTTTATCGATGGTCTGGCGTTGCCAGAAGAAGAGAAAGCCCGCCTGAAAGCGATGACGCCGGCTAACTATATTGGTCGAGCTATCACGATGGTTG ATGAGCTGAAATAAACCTCGTATCAGTGCCGGATGGCGATGCTGTCCGGCCTGCTTATTAAGATTATCCGCTTTTTATTTTTTCACTTTACCTCCCCTCCCC GCTGGTTTATTTAATGTTTACCCCCATAACCACATAATCGCGTTACACTATTTTAATAATTAAGACAGGGAGAAATAAAAATGCGCGTACTGGTTGTTGA
PnarX	GACAGCTCCAGTAGCCCTTTCGGGGGCGGATGAGTGACTCATAGACACCTCTGATACTCGTTTCGATGTCTGCCACCTTAGTGTCTGTAGCTAAAGGCAAT TTGATGTAAATCAAACGATAAGATAACTTTATCTATCATTGATATTTATCATTACCCATAGTGAGTACAGTGACTTCATAAAAATTATGAGATTTTTCACG GTGCTGTAAAATCCCTACCCTTACCGATGTAAAGCGACTAACCACACGGCAAATAAGGAGTAACTCTTTCCGGGTATGGGTATACTTCAGCCAATAGCCG AGAATACTGCCATTCCAGAATGTATCGTCACATTCATTAAGGTTATTGCTCATTTAAAGCCTGAAGGAAGAGGTTTACATGCTTAAACGTTGTCTCTC
PrstA	GCAAAGGTCGGGAAAAGTGGAATCAGCCCGGCGATATAATAATTTTTCGTTTTTGCTAAAACACCAATCAACAGCACTACCAGCGCACCGAGCGCGGCTT TGATTACCAGCCCCATCTTTTTACCTTAACACTTCCATAACAAGTCATCAGTAGAATACCTGATGAAAACTTGTTTAGAAACGATTGATAGTAAGTAAAA ACAGCGCGGTGTATTGTGACGTTTTTATATCTACCGTGAATGTTATGAACACTATCGTATTTGT
PuvrY	GTCATGTTGCAATGAAAATTTGCGGTGAAAAATGTTAAGGCGGCGGAGTATACCATAAGCTTTGCTAAAAATAGCAGTGGTTGTTTTTTGAGCGTGATATC GGCAGTGCTATAAAATACGTTAATATAATGACCAATAAATATTTTTATCATGAATGTTTTTTGCCCGTATTGTTCGGGTTAATTAATGTTACATATTCAGCG GGCTGATTTTCATTTTTGCTGAATAAAGTCAATTTTTGTCACATTTCATCGTAGGGCTTACTGTGAAACGATCCGGTAAGCCGTTGGTGACGGGCGTGACCA TAACTGTGGACAATCGAATTGACAAAAACGAGAGAAAAATCGAATACCCACCATTTTTAACGTTTCAAAGTTGCAATAAAAACCGCTAATATACGAATG ACTAACTATCAGTAGCGTTATCCCTATTTCTGGAGATATTCCT
PhprR	TAAGAATGTTTTGTTGTGCGGCATTAACCAAAGAAGGTAATGAAAATGCTGCCGTTGCTACCGAGAGTACTAAATAACGCTTTAACATGTTTATATCCTTG TCATGTGAATGAGTTTTGAGGATAGCGAAAAAGCGTCCAGGGTAACCTTACAGCAGCATTACAATTTTGTAATGAACCAGGCTGTTTCTATAACATATGAT TTATGGCATATTATTTTCATGAAGATTCTACTTATTGA
PmdtA	TGGCAGGATCGCAGACTACAAAGCCTGCGGATTGACAATCTTATCGTGAAGGCATACTTTCAGGAGTGAGGGTAGAGCGGGGTTTCCCCCGCCCTGGTAGT CTTAGTAAGCGGGGAAGCTTATGACTAAGAGCACCACGATGATGAGTAGCTTCATCATGACCCTTTCCTTATTTATGGCCCCTTCCTCGGGAGGGGCTTTCC CGTTTCAGCGTCCCGCTGAAATCGTCGGCTTACCTCCTTTCGCCATGCAAGCAGTCTATCGCTAACGCGTAGATAAAATAGTTTCCTGTGTTATTACTGGAT GCGTGCTCGCAAATGTGCCCGTCATTCAGACGATTCCAGACAGTGTTTCATAATTCCTCCATTTTTCTCCCTTATTGGCTGGCTACACTAGTATCATTCCGC GAAACGTTTCAGGAAGAGAAACTCTTAACG
PbtsS	CACTTCACCAATTGTGTAAAGCGCCATCGTCTCACCCTTGCTCGCGAGGTCCCGGTTTAACTTTAGACGCAGTTTTGCGAACCAGGTAGTTTTGCCCGTTTT TTGTGCATCTATAGGGTGATTTTATTTTTGCCAGGCGATTTTGAGTGATCGTACTCACGAATTCTCATTTTTCTGCAAGAGTTCAAAGAAAGTTAAACGCAG GCAATGTATGTTACGCGTTTTAAAGGGAAGTGTGGTTTGCGGGTATGTACGATTTTAATCTGGT
PnarP	GGCGAAGGTAAGTTGATGACTCATGATGAACCCTGTTCTATGGCTCCAGATGACAAACATGATCTCATATCAGGGACTTGTTCGCACCTTCCATAACGCTG TAGCCACCAGAACAGATATTGCGGAACGACAAAGAGAAACAGAACCAGATTGATGCATTGAGCTTTCATCCTATGAAATTAATTGCTGTTAAAAGCATT GGGTACAGAAAATACCCATAGCTCCATACCCGGAGTCAGTTTTTAAAAACTGTTTAAAGAAATGCACAAGTATTGTGATTGATTTTTTAGTTGTTTTTCTT GATGAGAAGCTGATGCAAAATTCCGTCTTTATAATGAAAATGATGCCAAAGCGAACGACAAGGTTGTAGTTTTCACTACATGTCCATACATAAAATGGGG TAACATTCACGCGCCTGGTAGCGTTACCAACGCTACGCTCAAACATAATGATTCTAATAAAACCTCAGGAGACTACT
PrcsC	TTATCGCATCCAGCATTTTGTTGTAATAACCAGCACCGATGCCAGGGAAGGCGTGAGTGATATTTTCGGTAATGGGGGCAAGTTCTGCATTTAATGCGCGG ATACGCTCCTCACGTGGTAAGTCGATGTAGAGATCATAGCGATCGCCTAGTGCCTGATTAAGCAGGTTGACCACGGCAGAAAGTTTTTTCTCTTTTTCAGA TAAGACTGCTGAACGTCCTTCCGTTTCTACGATATAACCAATAGTAAGCGTTGGGACAATGACCATCAGGATTGCCATCAGGATCATTTGATTGCGTAAGC GGCGTGGATAAATCCACTTCATATAATGCATGCTGAAATCCACTAGTCTTGTCCGGTATATGACGATTATCAGAGGTTAAGGTGATGATTTCTCGGCGGTG TATCATATTCCAGAGAAGAGAGAACATTGCGGTAACACGCTTTTACCGCTACCTTAACCACACTCCATCGGTCACCTGAGGCGGAGCTTCGCCCCT
PrcsB	GCCTGACGTTCCGCATTCTGGACACGGGAGAAGGCGTAAGTATTCATGAAATGGATAATTTGCACTTCCCGTTTATCAACCAGACCCAAAACGATCGCTA TGGCAAGGCGGACCCGCTGGCATTCTGGCTGAGCGATCAACTGGCACGTAAACTGGGCGGTCATTTAAACATCAAAACGCGGGATGGGCTTGGTACACGC TACTCTGTGCATATCAAAATGCTCGCAGCTGACCCGGAAGTTGAAGAGGAAGAAGAGCGTTTACTGGATGATGTCTGCGTAATGGTGGATGTTACTTCGGC AGAAATTCGGAATATTGTCACTCGCCAGTTAGAAAATTGGGGTGCAACCTGTATCACACCCGATGAAAGATTAATTAGTCAAGATTATGATATCTTTTTA ACGGATAATCCGTCTAATCTTACTGCCTCTGGCTTGCTTTTAAGCGATGATGAGTCTGGCGTACGGGAAATTGGGCCTGGTCAATTGTGCGTCAACTTCAAT ATGAGCAACGCTATGCAGGAAGCGGTCTTACAATTAATTGAAGTGCAACTGGCGCAGGAAGAGGTGACAGAATCGCCTCTGGGCGGAGATGAAAATGCGC AACTCCATGCCAGCGGCTATTATGCGCTCTTTGTAGACACAGTACCGGATGATGTTAAGAGGCTGTATACTGAAGCAGCAACCAGTGACTTTGCTGCGTTA GCCCAAACGGCTCATCGTCTTAAAGGCGTATTTGCCATGCTAAATCTGGTACCCGGCAAGCAGTTATGTGAAACGCTGGAACATCTGATTCGTGAGAAGG ATGTTCCAGGAATAGAAAAATACATCAGCGACATTGACAGTTATGTCAAGAGCTTGCTGTAGCAAGGTAGCCTATTAC
PrcsD	CTTGTTAACTATTTCACAAATAATTAACATCCGCATAATTTCCAGCAATCTTTGTTTATTTGCAATTATTTTTGTTGGGCTTTTTGTAGGTTATTTGTACAGC AAAATGGCGCTTGTACATCTATTTCCCCCAATGCAGGATGATAAATATCACGGGAGAATAGAGAATCATCAATCAGGTAAGAGTCTGGAATTTCACACTG TACCCTTTATACTGCCCTATCACTTCGCGAAGTTTTAACAGGTCATAAACACGAATGCGTCAGAAAGAGACAAC

Appendix Table 2. Promoter sequences of TCS genes in the *E. coli* K-12 genome. (Continued.)

Promoter	Sequence (5'-3')
PatoS	AACAATCGGAGTCGGCAAACAGCGGTTCAAACGCAGGCACATCCGCCTGCGTTTCTCGTCCACGCGGGGAAAGCACACCGTTTTCTGCCGATAAGCGATTTTCGGCGATGTACTTCAGC TCTTTCATCACATCAGAGGTGCGTTGAATAAAGCGCTGAGCCTGATCGGAACTCAGATTAAATTCCTGACGAATTTCCGATTCTCGCTGATGTAACGCATTAACGATGTAAAAAACGGA TGAAAAAGCAATCAACAGCCAGAGCACTAACGCCAATGCTCTGAACATGTAGCGCGAGGCTTTCAGGGTTGTACGAAAAGAAGCAAGGTATTTCAAAGGGGCGAAGCTCCGCCTCAG GTGACCGATGGAGTGTGGTTAAGGTAGCGGTAAAAGCGTGTTACCGCAATGTTCTCTCTTCTCTGGAATATGATACACCGCCGAGAAATCATCACCTTAACCTCTGATAATCGTCATAT ACCGGACAAGACTAGTGGATTTCAGC
PevgA	TGACCAATAGGCATAGGCACCTGAAAACGCAATAAATAAAACTACCGCCAATAAAGAAAAGTATTTTCTTCTGTTAGAATGTTTTTTATTTGAATTAATCTGTTCCACTATTATCTCTC ATTTCTCATAGATGAAATTTATGAATTGAATGAAAAGAGCATTCATTCTTCATATCAAACACAGTGCATGTGTTGCACATTATCCCAGGAACGTTGGAGGCCTAATTTAAATGAGGTGC AAAAAAAACAACAGAGGACTAAACCGTGGCTTTTGCAATACAATTCTTACGCCTGTAGGATTAGTAAGAAGACTTATAGTGCCAACTTGAAACTATAAATCATCGGTACAATCCCTG ATTTTATTGTTGACATTTCATTTATGCCGACTATTTATATGGTATACTTGTCGAATTATCTTAAAGGAAGCTCAGATTTTCTTATTTTTATTGAGAAAATGAGATGACGCCTTATGTCTGT ATTACTACAGGGAGAAGGGAGATGCTTCATTGCAAAGGGAATAATCT
PpyrS	CACCGTCCGGGTTACCCATGCTGAAATCGATAATATCTTCGCCGCGCCGACGCGCAGCCATTTTCAGTTCAGCGGTGATGTTAAAAACGTAGGGCGGGAGACGATCAATGCGCGTAAAG CGACGTTCAGGGCGAGTGTCAGCCATAATTTCCTCAGATTAACGTTAGCGCCCGGACCGTCCGAGCGACGCTGCCACGATGGTGGCTGTTTTGAAAATAGCCTGATTAATTTCTGTCTGT CCAGCGTTTTAGAACATTTTATTAATGACGTTAAATGAGGAACTCTGCTTTAAAAACAGGAAATTTATCTGCGCTAACAAGAAAATTACCACTCATTTTATTAACATAATAATTTCAA TAAATTTACTAACCAGAAGTGCATTATCAAGAGATGCATTGCTAATACACCATTTATCTATCAATCCCCTTTTAAAATTGTGGTTTTTCCTCAAAAACGGCCTGCTGGTCATCAGCCTT CAGGTTACCTATCATAGAGGTTTAATCCTTATTCAGAGTCACCCGTGCACGAAATATTCAACAT
PnarQ	CGTGGCTTTTACTTTTCCTGCCGCGACGGGTGTCAGGACGATTTGCATCGTACCAAAAGGACAGGCCACCACGCAGGATTTACAGCCAATACACTTTTGCTGATTGACCTGAATGCTGTC ATCAACGTGGCTGATTGCGCCATTAGGGCAGCTACGGGCGCAGGGCGCATCTTCACAATGGTGACAGGTCACTGCACTACGTTGCTGTTGATGTTTGATAACCGTAATTCGGGGATGAA AATGGTGTTGGCTCAGGACATGTTGCTCATCATTGTGAGCCATGACACAGGCGATTTCACAAGCATGACAACCCAGACATTGCTGACTGTTGGCCATAATAAAACGATTCATAACGAC CTTCTTTTTTGGTTGTAAAAACCTTATTCTTTATATGAGTGTTGTTATTACCCGACTTACAGGGGAATCGGCAATGTTCATGTGCCCAGAATAAGTAACTATTTCGCTATAAACTGTGGC AGATCAAATAATCCCATCACTGACTAAATTGCGTTTCAGCGAACTGGAACATTAATGATTTTTTGTGGAGAAGACGC
PglrK	GGTGTTACTCTCGTCAGACGCGAATAGCCTGATGCTAACCGAGGGAAGTTCAGATACAACAAAGCCGGGAATTACCCGGCTTTGTTATGGAATAAGGCGGTGCCTAACTCGACGTTTC GCCCGATGGTTGATATAGCTACGCTGATATCAGAAGTTGGACGGCAGGCACCTTGTTGTGCGTCATTCGTATTTTATGTAGCACGTCCCGAAGGGGCTGACATAAGTCGGTGAATGAGCC ACT
PglrR	AACCAATCCGCTTTACTGGCTGCGGGCGATGGATTGTGCTGATCGTTTAATGCCTGCGCAGTCGCGTCAGCAAGCTCGCCAATATGACGACGGCAGCTGGCAAAATACCTTTAAACAAG GGATTTTGCTCGCCGACGCCAAAATTACGCCGTATGAGCGCCGCCAGCTGGTCGCGCGTATTGAAGCGTTAAGTACCGAGATCCCGGCACAGGTTCGCCCACTGTATCAACTCTGGCGC GATGGTCAGGCGCTGCAACTGCAACTGGCGGAAGAGCGCCAACGTTACAGTAAACTCCAGCAGTCCAGCGACAGCGAGCTGGATACATTGCGCCAGCAACATCACGTTCTACAGCAGC AACTGGAACTCACCACCCGCAAGCTGGAAAACCTGACCGATATTGAACGCCAGCTCTCGACCCGCAAACCGGCTGGAAATTTCTCGCCGGATACGCCGCACGAGAGTGAAAAGCCCG CGCCATCCACCCATGAGGTCACTCCTG
PbarA	AAACCCCATCTGAAGTTGCTGTGTTTTCGGTAAGTAGTTCAGACTTAAACGCGCGCGACGGCGATAGCCCCAGGGAACATCGGCGATCACTTCAGAGACATCGTGTTTCATTAATCGGG CGAGTGCCGCACTTTTGCTTCGCTGCTGTAAATCCACGCTGGCGTGTTGTTGCTGACAGCCACCGCATACGCCAAAATGAGGACAGCGTGGCGTTTCGCGTTCCGGGCTATCGCTTAACC GGCGTACGACTTTAGCGCGGGCATACTGTTTTTTATCTTCAGTAACAGTAACTTCCGCGTTTTCCTGCGGCAATAATCCGGGGATAAATAGCGTTTTGCCGTTATGTCGCGCCACGCCCT GACCAAAAGAGTCGAGGTCGTTGACTGAAACGGTTATGATCTGACGCGTCGTCGTGCGTCGTTTTGCAGAGTAGAATTGCGCCATTGGCGAGACTTTCTCAATTTAACAGTGTGACCTTA ATTGTCCCATAACGGAACTCC
PqseB	TCTACAGTCGTTACGCTGCCGTTCGGCCCCTGGAATCCTCCGGCCTGACTTTGCGTTGCCGATGGGCCAGAAAAACCGCCCTGCTCTGCTGCCATCACCGGTGCGCTGCACAGGGCCATT ACTGCGATTACTGCTGCGAATTTTTTCATGTTTATTACTCCCTTTAATGTCTGTTTCCGAGCATTTAACAAGATAGTCCTTAACAACTTCTTAAGGGAAAAAAATAAAATTTAGTGCTGT ACAGAGCGCGTTACAACACGGTTTACTGGCAGCAAATACGGTTATCGCAGGGATGAAAAAATGCGAATTTTACTGATAGA
ParcB	AGCGAGTGGTTGAAACCGGCGTGGACGGCATAAAGCTGCATCCGCTGCATATTGTGAAAGGCAGCATTATGGCGAAAGCCTGGGAAGCGGGGCGTTTGAACGGTATTGAACTGGAGGA TTACACGCTCACTGCCGGAGAAATGATTCGCCATACGCCACCGGAAGTGATCTACCACCGCATTTCCGCCAGCGCCCGTCGCCCGACGCTGCTTGCTCCGCTGTGGTGCGAAAATCGAT GGACGGGAATGGTCGAGCTGGATCGCTATCTGAATGAACATGGCGTACAGGGATCGGCGCTGGGACGTCCGTGGCTACCTCCAACGGAGTAGGTCGTTGAGGGGAATTCCGCATTTCTC ACACAATTTATAACGTAACTGTCAGAATTGGGTATTATTGGGGCAGGTTGTCGTGAAGGAATTCCCTA
PzraS	GTGCGCTGCTTTGAGCGTAAAAGTCATTATGGATTTTCTGCCACGCTGTCTGTTGTTCGCTGGTCAAAGGCGCGGCATTTTGCTGCCACATACCGTGTCCGCCGTGAGCAAATGCAGATG TCGATCCCATCGCCATTGCTGAAAGCGCCATCATTACCAGGGCAATTTTCGTGTTCCGTTTCATGGTTAATCCTCCAGTGGTTGTCTTACTTCGGGTATTGCATCTTCCGTGCCAACGATG AAACGCTGATATGACGGGTAATCTGGCATGATAAACGAGTAAAAATGACTCGCCTGCTGCGGGTAGCGAGTCATTTTTACTCATTGAAACTTAAGCCTTTGTGTTACAGCGCAGGGTAA GCGCTGATAAAAGATGGCATGATTTCTGCTGTCAGAAAGGGATGAGCAGGCAAAGAAGAAG
PcpxR	GTTATCGCCTGAACCGACTTCAGCAGCGTGGCTTAATGAACTGACTGCCAGCGTTGAGGCCATGACGGCAGCGGTAACTATGCGCATCATTTGCTCCCAAAATCTTTCTGTCGCGATTC AACGATAGAGAGTTTACGATTCAGGCTGCAAACATGCGTCAGGGGGTGTAAAACAACGTAAAGTCATGGATTAGCGACGTCTGATGACGTAATTTCTGCCTCGGAGGTATTTAAACAA TGAATAAAATCCTGTTAGT
PglnA	GATGTTGATACGGTAATCATTCCATTTGATAGCGGTGTTTTTCGCGAGGATGGTAATCCCACGCTCTTTCTCCAAATCGTTGGAGTCCATCACGCGCTCTTGGGTTTCGGCACGAGAGTCG AACGTACCGGATTGTTGGAGCAGCTTGTCTACCAGGGTGGTTTTACCATGGTCTACGTGCGCGATGATGGCGATATTACGCAATTTTTCGATCACAACTTTGCCTCAGGCATTAGAAATA GCGCGTTATTGTACACGGATTAATCGCACTACAAAACAGGATCACAAACATCCTCCGCAAACAAGTATTGCAGAGTCCCTTTGTGATCGCTTTCACGGAGCATAAAAAGGGTTATCCA AAGGTCATTGCACCAACATGGTGCTTAATGTTTCCATTGAAGCACTATATTGGTGCAACATTCACATCGTGGTGCAGCCCTTTTGCACGATGGTGCGCATGATAACGCCTTTTAGGGGCA ATTTAAAAGTTGGCACAGATTTCGCTTTATCTTTTTTACGGCGACACGGCCAAAATAATTGCAGATTTCGTTACCACGACGACCATGACCAATCCAGGAGAGTTAAAGT
PivbL	CAAAATTCGTGCCGAAATTGCGCGTTCTGCGCGGAACACGTATACTTTCAGTGTTGACATAATACAGTGTGCTTTGCGGTTACCAGCCGCAGGCGACTGACGAAACCTCGCTCCGGCGG GGTTTTTTGTTATCTGCAATTCAGTACAAAACGTGATCAACCCCTCAATTTTCCCTTGCTGAAAAATTTTCCATTGTCTCCCCTGTAAAGCTGTGCTTGTATAAATATTGTTAAACACAA AACCAACAAGGTCCCCAATGACTACTTCCATGCTCAA
PompR	CAGACGCTTTTTATTATACTGATAGTCAGCATTTTCGCTGCGGTCGCCCAGACTTGCGGCCCAGGTCACCTTTTTTGTGACCTCCGGGCGTTCTTCACGCCAGAGATAATTAAGCTCTTGT TTGAGTTTTTCATACCCTTCCCGGGTAACCAGGGGCGTTTTCATCTCGTTGATTCCCTTTGTCTGTTTGATAATGCGCACATTGGGTATAACGTGATCATATCAACAGAATCAATAATGTT TCGCCGAATAAATTGTATACTTAAGCTGCTGTTTAATATGCTTTGTAACAATTTAGGCTGAAATTCATACCAGATTTAGCTGGTGACGAACGTGAGCTTTTTTAAGAATACACGCTTAC AAATTGTTGCGAACCTTTGGGAGTACAAACAATGCAAGAGAACTACAAGAT
PbasR	ACCATCGGCAGCCACGGTCCGACCTATTACAACCGCTATCCGCCTCAGTTCAGGAAATTTACCCCAACCTGCGACACCAATGAGATCCAGACCTGTACCAAAGAGCAACTGGTGAAC ACTTACGACAACACGCTGGTTTACGTCGACTATATTGTTGATAAAGCGATTAATCTGCTGAAAGAACATCAGGATAAATTTACCACCAGCCTGGTTTATCTTTCTGACCACGGTGAATC GTTAGGTGAAAATGGCATCTATCTGCACGGTCTGCCTTATGCCATCGCCCCGGATAGCCAAAAACAGGTGCCGATGCTGCTGTGGCTGTCGGAGGATTATCAAAAACGGTATCAGGTTG ACCAGAACTGCCTGCAAAAACAGGCGCAAACGCAACACTATTCACAAGACAATTTATTCTCCACGCTATTGGGATTAACTGGCGTTGAGACGAAGTATTACCAGGCTGCGGATGATAT TCTGCAAACTTGCAGGAGAGTGAGTGA
PdcuS	AATAGACATCGATCTTTTCGCCGGTATAACAGCGATAACCCCCGTCCAGTAGCGCCTGATCCATGACCTTCCCTCTCTCATCAGTATGATTATCGCTATAAGCATAGCCCCGGAATCTT CATACAGCACTGGCAGTTTCCGTTGCCAGAGTCTCTTCCCCTATATAGCCAATCATTCTTACTCCCTTTGAATTACCCGCCTCATCAGAGATAATGCTTAAGAAATTTGTCACACAAGG AAGCTGATGAGACATTCATTGCCCTA
PcreA	GGTAAATGTCTGTTGAGAGTCGAAGCGGTATTGCAGCGCGATGTCCAGAATCGGACGCGCAGTCAGGCGTAGTGCGACCGCCGATTTCGACAAACGACGAGCACGAATATACGCGCCA ATAGCATGGCCAGTGACATCTTTAAACATTCTCTGTAAGTGCCACTTGGAATAACCTGCTTTCGCCGCTACATTGTCGAGCGACAGGGGCTGATCCAGATGACCTTCCAGCCAGATTAA AAGGTCGCGAATAATGCCGGCCTGATCCATAAAATATCCTCATCCTTTCAACAACGAGCACCTGACATCAGGTAATTGGATAATAGCATTTTTTGCTGTTTTAGCATTCAGTGTTTTTTT CTTAGTAGAGTATGTTTTAGGGCTTGACGGAAATAAAAGTATTGAGATTTTGTTCTTAATCAATATGTTATTTACCGTGACGAACTAATTGCTCGTGTAATAGATAAAAATGGTAACAA TATG
ParcA	TAATGATATTTCGCCCGACTGCGCGCAGTGGTGGCGACAGTGAAATCGACATCGTGTAACGATTCAGCCAATGTCGGGAAAACTTTAATATTATCAATAATATCACCAGATCCATGTGC GACCCAGCGGGTGGCTGGCTCCAGGTGTGCCTGACTATCGACAATCCGCAGATCGCTAAACCCCATCGTTTTCATTGCCCGCGCCGCTGCCCCAATATTTTCTGCTCTGGCGGGTGCGAC CAGAATAATCGTTATACGCATATTGCCACTCTTCTTGATCAAATAACCGCGAACCGGGTGATCACTGTCAACTTATTACGCGGTGCGAATTTACAAATTCTTAACGTAAGTCGCAGAAA AAGCCCTTTACTTAGCTTAAAAAAGGCTAAACTATTTCCTGACTGTACTAACGGTTGAGTTGTTAAAAAATGCTACATATCCTTCTGTTTACTTAGGATAATTTTATAAAAAATAAATC TCGACAATTGGATTCACCACGTTTATTAGTTGTATGATGCAACTAGTTGGATTATTAAAATAATGTGACGAAAGCTAGCATTTAGATACGATGATTTCATCAAACTGTTAACGTGCTAC AATTGAACTTGATATATGTCAACGAAGCGTAGTTTTATTGGGTGTCCGGCCCCTCTTAGCCTGTTATGTTGCTGTTAAAATGGTTAGGATGACAGCCGTTTTTGACACTGTCGGGTCCTGA GGGAAAGTACCCACGACCAAGCTAATGATGTTGTTGACGTTGATGGAAAGTGCATCAAGAACGCAATTACGTACTTTAGTCATGTTACGCCGATCATGTTAATTTGCAGCATGCATCAG GCAGGTCAGGGACTTTTGTACTTCCTGTTTCGATTTAGTTGGCAATTTAGGTAGCAAAC

Appendix Table 3. Oligonucleotides for psgRNA cloning and DNA amplification in the HoSeI method.

Name	Sequence (5' to 3')
For psgRNA cloning	
pEX_For	GGAGCAGACAAGCCCGTCAGG
pEX_Rev	CAGGCTTTACACTTTATGCTTCCGGC
phoP_sgRNA_N20	CCGCAGCGGTTTCAGGATATTGCGATTGTCGATCTGTTTTAGAGCTAGAA
phoP_sgRNA_com	TTCTAGCTCTAAAACAGATCGACAATCGCAATATCCTGAAACCGCTGCGG
phoB_sgRNA_N20	CCGCAGCGGTTTCAGCGAACAAAATGGCTTTCAGCGTTTTAGAGCTAGAA
phoB_sgRNA_com	TTCTAGCTCTAAAACGCTGAAAGCCATTTTGTTCGCTGAAACCGCTGCGG
citB_sgRNA_N20	CCGCAGCGGTTTCAGCGTTGAGGACGAAACGCCGCGTTTTAGAGCTAGAA
citB_sgRNA_com	TTCTAGCTCTAAAACGCGGCGTTTCGTCCTCAACGCTGAAACCGCTGCGG
ompR_sgRNA_N20	CCGCAGCGGTTTCAGAACGTTCCAGCAGCGCACGCGTTTTAGAGCTAGAA
ompR_sgRNA_com	TTCTAGCTCTAAAACGCGTGCGCTGCTGGAACGTTCTGAAACCGCTGCGG
narL_sgRNA_com	TTCTAGCTCTAAAACGATGCTGCGAACTGGCGTAACTGAAACCGCTGCGG
narL_sgRNA_N20	CCGCAGCGGTTTCAGTTACGCCAGTTCGCAGCATCGTTTTAGAGCTAGAA
cpxR_sgRNA_N20	CCGCAGCGGTTTCAGTTAATAGGGAAGTCAGCTCTGTTTTAGAGCTAGAA
cpxR_sgRNA_com	TTCTAGCTCTAAAACAGAGCTGACTTCCCTATTAACTGAAACCGCTGCGG
uhpA_sgRNA_N20	CCGCAGCGGTTTCAGGATCACCTCATCGTCCGCTCGTTTTAGAGCTAGAA
uhpA_sgRNA_com	TTCTAGCTCTAAAACGAGCGGACGATGAGGTGATCCTGAAACCGCTGCGG
rstA_sgRNA_N20	CCGCAGCGGTTTCAGTTCACTGATTGCCGCGTACCGTTTTAGAGCTAGAA
rstA_sgRNA_com	TTCTAGCTCTAAAACGGTACGCGGCAATCAGTGAACTGAAACCGCTGCGG
evgA_sgRNA_com	TTCTAGCTCTAAAACGCTGAACGGCACTTCCGCCTCTGAAACCGCTGCGG
evgA_sgRNA_N20	CCGCAGCGGTTTCAGAGGCGGAAGTGCCGTTCAGCGTTTTAGAGCTAGAA
kdpE_sgRNA_N20	CCGCAGCGGTTTCAGTATTCGTCGCTTTCTGCGCAGTTTTAGAGCTAGAA
kdpE_sgRNA_com	TTCTAGCTCTAAAACTGCGCAGAAAGCGACGAATACTGAAACCGCTGCGG
torR_sgRNA_N20	CCGCAGCGGTTTCAGTGTTATTGTTGAAGATGAGCGTTTTAGAGCTAGAA
torR_sgRNA_com	TTCTAGCTCTAAAACGCTCATCTTCAACAATAACACTGAAACCGCTGCGG
uvrY_sgRNA_com	CCGCAGCGGTTTCAGATAAAGGGTATAAAAGTCGTGTTTTAGAGCTAGAA
uvrY_sgRNA_N20	TTCTAGCTCTAAAACACGACTTTTATACCCTTTATCTGAAACCGCTGCGG
qseB_sgRNA_N20	CCGCAGCGGTTTCAGAGCGTCGACTGGTTTACACAGTTTTAGAGCTAGAA
qseB_sgRNA_com	TTCTAGCTCTAAAACTGTGTAAACCAGTCGACGCTCTGAAACCGCTGCGG
arcA_sgRNA_N20	CCGCAGCGGTTTCAGGTTGAAAAGTATTTTCGAAGGTTTTAGAGCTAGAA
arcA_sgRNA_com	TTCTAGCTCTAAAACCTTCGAAAATACTTTTCAACCTGAAACCGCTGCGG
atoC_sgRNA_N20	CCGCAGCGGTTTCAGTATCCATCAACACCACATCAGTTTTAGAGCTAGAA
atoC_sgRNA_com	TTCTAGCTCTAAAACTGATGTGGTGTTGATGGATACTGAAACCGCTGCGG
baeR_sgRNA_N20	CCGCAGCGGTTTCAGTCTTCCACGATCAAAATACGGTTTTAGAGCTAGAA
baeR_sgRNA_com	TTCTAGCTCTAAAACCGTATTTTGATCGTGGAAGACTGAAACCGCTGCGG
ntrC_sgRNA_com	TTCTAGCTCTAAAACGCGAGCGCACGTTCAAGCACCTGAAACCGCTGCGG
ntrC_sgRNA_N20	CCGCAGCGGTTTCAGGTGCTTGAACGTGCGCTCGCGTTTTAGAGCTAGAA
rcsB_sgRNA_com	TTCTAGCTCTAAAACATAGTCTTGTTCGGTATTCGCTGAAACCGCTGCGG
rcsB_sgRNA_N20	CCGCAGCGGTTTCAGCGAATACCGAACAAGACTATGTTTTAGAGCTAGAA
pyrR_sgRNA_N20	CCGCAGCGGTTTCAGAATTAAAGAGCACAGCCAGAGTTTTAGAGCTAGAA
pyrR_sgRNA_com	TTCTAGCTCTAAAACTCTGGCTGTGCTCTTTAATTCTGAAACCGCTGCGG
btsR_sgRNA_N20	CCGCAGCGGTTTCAGCGCAGGTTCTCCCGTGCTAAGTTTTAGAGCTAGAA
btsR_sgRNA_com	TTCTAGCTCTAAAACTTAGCACGGGAGAACCTGCGCTGAAACCGCTGCGG
creB_sgRNA_N20	CCGCAGCGGTTTCAGGCAAGGGATAGCCGACACGCGTTTTAGAGCTAGAA
creB_sgRNA_com	TTCTAGCTCTAAAACGCGTGTCGGCTATCCCTTGCCTGAAACCGCTGCGG

Appendix Table 3. Oligonucleotides for psgRNA cloning and DNA amplification in the HoSeI method. (Continued.)

Name	Sequence (5' to 3')
For psgRNA cloning	
basR_sgRNA_N20	CCGCAGCGGTTTCAGATTCTGGCGGCGCAAACCGAGTTTTAGAGCTAGAA
basR_sgRNA_com	TTCTAGCTCTAAAACTCGGTTTGCGCCGCCAGAATCTGAAACCGCTGCGG
cusR_sgRNA_N20	CCGCAGCGGTTTCAGACCGGAGAATACTTGACCAAGTTTTAGAGCTAGAA
cusR_sgRNA_com	TTCTAGCTCTAAAACTTGGTCAAGTATTCTCCGGTCTGAAACCGCTGCGG
narP_sgRNA_N20	CCGCAGCGGTTTCAGCTCTGAAGTGGTCGCCGAAGGTTTTAGAGCTAGAA
narP_sgRNA_com	TTCTAGCTCTAAAACCTTCGGCGACCACTTCAGAGCTGAAACCGCTGCGG
zraR_sgRNA_N20	CCGCAGCGGTTTCAGAAGCCTGCAAAATAGTGCAGGTTTTAGAGCTAGAA
zraR_sgRNA_com	TTCTAGCTCTAAAACCTGCACTATTTTGCAGGCTTCTGAAACCGCTGCGG
rssB_sgRNA_N20	CCGCAGCGGTTTCAGTTCGCTCGCTTCTGGATTCAGTTTTAGAGCTAGAA
rssB_sgRNA_com	TTCTAGCTCTAAAACTGAATCCAGAAGCGAGCGAACTGAAACCGCTGCGG
glrR_sgRNA_N20	CCGCAGCGGTTTCAGATTATTGGTCGATGACGATCGTTTTAGAGCTAGAA
glrR_sgRNA_com	TTCTAGCTCTAAAACGATCGTCATCGACCAATAATCTGAAACCGCTGCGG
fimZ_sgRNA_N20	CCGCAGCGGTTTCAGTCAATAGACATTCTGATGATGTTTTAGAGCTAGAA
fimZ_sgRNA_com	TTCTAGCTCTAAAACATCATCAGAATGTCTATTGACTGAAACCGCTGCGG
ygeK_sgRNA_N20	CCGCAGCGGTTTCAGATTATCCCATCAATCATAAAGTTTTAGAGCTAGAA
ygeK_sgRNA_com	TTCTAGCTCTAAAACTTTATGATTGATGGGATAATCTGAAACCGCTGCGG
dcuR_sgRNA_N20	CCGCAGCGGTTTCAGGTTCCACAGCATTGAAAGCCGTTTTAGAGCTAGAA
dcuR_sgRNA_com	TTCTAGCTCTAAAACGGCTTTCAATGCTGTGGAACCTGAAACCGCTGCGG
yhjB_sgRNA_N20	CCGCAGCGGTTTCAGAGTTTACAGCAGCGTATTCCGTTTTAGAGCTAGAA
yhjB_sgRNA_com	TTCTAGCTCTAAAACGGAATACGCTGCTGTAAACTCTGAAACCGCTGCGG
cheB_sgRNA_N20	CCGCAGCGGTTTCAGGGTGTTATCTGTCGATGATTGTTTTAGAGCTAGAA
cheB_sgRNA_com	TTCTAGCTCTAAAACAATCATCGACAGATAACACCCTGAAACCGCTGCGG
cheY_sgRNA_N20	CCGCAGCGGTTTCAGGTTACGCACTATGCGTCGCAGTTTTAGAGCTAGAA
cheY_sgRNA_com	TTCTAGCTCTAAAACTGCGACGCATAGTGCGTAACCTGAAACCGCTGCGG
hprR_sgRNA_N20	CCGCAGCGGTTTCAGTGAAGATAATCAAAGGACCCGTTTTAGAGCTAGAA
hprR_sgRNA_com	TTCTAGCTCTAAAACGGGTCCTTTGATTATCTTCACTGAAACCGCTGCGG
cusS_sgRNA_N20	CCGCAGCGGTTTCAGGGCTGATAAAAAAGGTCAGGGTTTTAGAGCTAGAA
cusS_sgRNA_com	TTCTAGCTCTAAAACCCTGACCTTTTTTATCAGCCCTGAAACCGCTGCGG
zraS_sgRNA_N20	CCGCAGCGGTTTCAGGTTAAGCGCGATCCTCCCCGGTTTTAGAGCTAGAA
zraS_sgRNA_com	TTCTAGCTCTAAAACCGGGGAGGATCGCGCTTAACCTGAAACCGCTGCGG
kdpD_sgRNA_N20	CCGCAGCGGTTTCAGTCCCGACCCCGATCGTCTGCGTTTTAGAGCTAGAA
kdpD_sgRNA_com	TTCTAGCTCTAAAACGCAGACGATCGGGGTCGGGACTGAAACCGCTGCGG
phoQ_sgRNA_N20	CCGCAGCGGTTTCAGGTTTCGATAAAACTACGTTTGTTTTAGAGCTAGAA
phoQ_sgRNA_com	TTCTAGCTCTAAAACAAACGTAGTTTTATCGAAACCTGAAACCGCTGCGG
basS_sgRNA_N20	CCGCAGCGGTTTCAGTTGAGCTGATCAGCGTCTTCGTTTTAGAGCTAGAA
basS_sgRNA_com	TTCTAGCTCTAAAACGAAGACGCTGATCAGCTCAACTGAAACCGCTGCGG
baeS_sgRNA_N20	CCGCAGCGGTTTCAGTATTACCGGCAAACTGTTTCGTTTTAGAGCTAGAA
baeS_sgRNA_com	TTCTAGCTCTAAAACGAAACAGTTTGCCGGTAATACTGAAACCGCTGCGG
cpxA_sgRNA_N20	CCGCAGCGGTTTCAGCGCGCATCTTCGCCATCTTCGTTTTAGAGCTAGAA
cpxA_sgRNA_com	TTCTAGCTCTAAAACGAAGATGGCGAAGATGCGCGCTGAAACCGCTGCGG
envZ_sgRNA_N20	CCGCAGCGGTTTCAGGACGATGAGCAATAACGTACGTTTTAGAGCTAGAA
envZ_sgRNA_com	TTCTAGCTCTAAAACGTACGTTATTGCTCATCGTCCTGAAACCGCTGCGG
evgS_sgRNA_N20	CCGCAGCGGTTTCAGATCTTCGTCTGCGAAACTTAGTTTTAGAGCTAGAA
evgS_sgRNA_com	TTCTAGCTCTAAAACTAAGTTTCGCAGACGAAGATCTGAAACCGCTGCGG

Appendix Table 3. Oligonucleotides for psgRNA cloning and DNA amplification in the HoSeI method. (Continued.)

Name	Sequence (5' to 3')
For psgRNA cloning	
glrK_sgRNA_N20	CCGCAGCGGTTTCAGATTACGACAACTGGTAATGCGTTTTAGAGCTAGAA
glrK_sgRNA_com	TTCTAGCTCTAAAACGCATTACCAGTTGTCGTAATCTGAAACCGCTGCGG
qseC_sgRNA_N20	CCGCAGCGGTTTCAGGTTATCCGTTGTTTGTTTCCGTTTTAGAGCTAGAA
qseC_sgRNA_com	TTCTAGCTCTAAAACGGAAACAAACAACGGATAACCTGAAACCGCTGCGG
rcsC_sgRNA_N20	CCGCAGCGGTTTCAGCATGTAGCGCGAGGCTTTCAGTTTTAGAGCTAGAA
rcsC_sgRNA_com	TTCTAGCTCTAAAACTGAAAGCCTCGCGCTACATGCTGAAACCGCTGCGG
rcsD_sgRNA_N20	CCGCAGCGGTTTCAGACTGTTGATCATTGTGTTACGTTTTAGAGCTAGAA
rcsD_sgRNA_com	TTCTAGCTCTAAAACGTAACACAATGATCAACAGTCTGAAACCGCTGCGG
rstB_sgRNA_N20	CCGCAGCGGTTTCAGCTTCCTTGTGATGTCTCTGCGTTTTAGAGCTAGAA
rstB_sgRNA_com	TTCTAGCTCTAAAACGCAGAGACATCACAAGGAAGCTGAAACCGCTGCGG
hprS_sgRNA_N20	CCGCAGCGGTTTCAGATATTGCTACTGTCTGTTGCGTTTTAGAGCTAGAA
hprS_sgRNA_com	TTCTAGCTCTAAAACGCAACAGACAGTAGCAATATCTGAAACCGCTGCGG
atoS_sgRNA_N20	CCGCAGCGGTTTCAGACGCAATCAAATGATCCTGAGTTTTAGAGCTAGAA
atoS_sgRNA_com	TTCTAGCTCTAAAACTCAGGATCATTTGATTGCGTCTGAAACCGCTGCGG
barA_sgRNA_N20	CCGCAGCGGTTTCAGACGCATGATGATTCTGATCCGTTTTAGAGCTAGAA
barA_sgRNA_com	TTCTAGCTCTAAAACGGATCAGAATCATCATGCGTCTGAAACCGCTGCGG
creC_sgRNA_N20	CCGCAGCGGTTTCAGTTTAACTTCTTTGACAAAAAGTTTTAGAGCTAGAA
creC_sgRNA_com	TTCTAGCTCTAAAACTTTTTGTCAAAGAAGTTAAACTGAAACCGCTGCGG
ntrB_sgRNA_N20	CCGCAGCGGTTTCAGGGTTGGCGTAATGGATCGCCGTTTTAGAGCTAGAA
ntrB_sgRNA_com	TTCTAGCTCTAAAACGGCGATCCATTACGCCAACCCTGAAACCGCTGCGG
phoR_sgRNA_N20	CCGCAGCGGTTTCAGCACCCAGGATGAAAGCCGGGGTTTTAGAGCTAGAA
phoR_sgRNA_com	TTCTAGCTCTAAAACCCCGGCTTTCATCCTGGGTGCTGAAACCGCTGCGG
uhpB_sgRNA_N20	CCGCAGCGGTTTCAGACTCCACAGGCAAAACCATGGTTTTAGAGCTAGAA
uhpB_sgRNA_com	TTCTAGCTCTAAAACCATGGTTTTGCCTGTGGAGTCTGAAACCGCTGCGG
btsS_sgRNA_N20	CCGCAGCGGTTTCAGATTATTCATACCGTTAATGCGTTTTAGAGCTAGAA
btsS_sgRNA_com	TTCTAGCTCTAAAACGCATTAACGGTATGAATAATCTGAAACCGCTGCGG
pyrS_sgRNA_N20	CCGCAGCGGTTTCAGGGATACGGATGAGAAAGAACGTTTTAGAGCTAGAA
pyrS_sgRNA_com	TTCTAGCTCTAAAACGTTCTTTCTCATCCGTATCCCTGAAACCGCTGCGG
arcB_sgRNA_N20	CCGCAGCGGTTTCAGCCTGATGATGAAGTTAGGTCGTTTTAGAGCTAGAA
arcB_sgRNA_com	TTCTAGCTCTAAAACGACCTAACTTCATCATCAGGCTGAAACCGCTGCGG
citA_sgRNA_N20	CCGCAGCGGTTTCAGAATATTTGTCATTGCAGCCCGTTTTAGAGCTAGAA
citA_sgRNA_com	TTCTAGCTCTAAAACGGGCTGCAATGACAAATATTCTGAAACCGCTGCGG
dcuS_sgRNA_N20	CCGCAGCGGTTTCAGACTGTGGTACTCAATTTCATGTTTTAGAGCTAGAA
dcuS_sgRNA_com	TTCTAGCTCTAAAACATGAAATTGAGTACCACAGTCTGAAACCGCTGCGG
narQ_sgRNA_N20	CCGCAGCGGTTTCAGCGTCTCGGCCAGTCTGGCCCGTTTTAGAGCTAGAA
narQ_sgRNA_com	TTCTAGCTCTAAAACGGGCCAGACTGGCCGAGACGCTGAAACCGCTGCGG
narX_sgRNA_N20	CCGCAGCGGTTTCAGTCCGCTCACCCTGGTTAATCGTTTTAGAGCTAGAA
narX_sgRNA_com	TTCTAGCTCTAAAACGATTAACCAGGGTGAGCGGACTGAAACCGCTGCGG
torS_sgRNA_N20	CCGCAGCGGTTTCAGTCAGGGTTAACAGCGCCATCGTTTTAGAGCTAGAA
torS_sgRNA_com	TTCTAGCTCTAAAACGATGGCGCTGTTAACCCTGACTGAAACCGCTGCGG
cheA_sgRNA_N20	CCGCAGCGGTTTCAGTGATGAAGCGGACGAACTGTGTTTTAGAGCTAGAA
cheA_sgRNA_com	TTCTAGCTCTAAAACACAGTTCGTCCGCTTCATCACTGAAACCGCTGCGG

Appendix Table 3. Oligonucleotides for psgRNA cloning and DNA amplification in the HoSeI method. (Continued.)

Name	Sequence (5' to 3')
For DNA amplification	
phoP_LL_F	TCGTCTTCACCTCGAAAGCAGTTTATCGATGGTCT
phoP_check_R	CTATTACGCCGCATTAATGCCTGCA
phoB_K030S	GAGGCAAGATCTGCGGCGCATGTCCGGCGC
phoB_check_R	TTTCAAGGCCGCGCACGCGATCTTC
CITA_LL_F	TCGTCTTCACCTCGACGCTCAAATCATTTTCATGC
citB_check_R	AACACCACGTCGCCGGGATAATGCG
ompR_K306T	CAGCCAGATCTAGGAGGTTAAGACTCTTCC
ompR_check_R	GTCACCATAATGATCGGCATCGGGT
narL_K427T	CGTAACGAAGATCTTGCATCCTGGGCGCAG
narL_check_R	ATGCGCCCTGAGAGGGACTTTTCGC
cpxR_K365T	CCCACAGATCTTGGGGGAAGACAGGGATGG
cpxR_check_R	GCATCAACTTCCAGTGTCGGTGAAC
uhpA_K334T	ATGATAGATCTTCAGGAGATGGCGACCGCC
uhpA_check_R	CTGTCGTGAACGGAGAGCATAATCG
rstA_LL_F	TCGTCTTCACCTCGAGCAAAGGTCGGGAAAAGTGG
rstA_check_R	GCTTTGTAGGGAGTCAGAGACGTTT
evgA_K227S	GAGTGAGATCTTGGCATCAGTTTTATCCAG
evgA_check_R	TTCATGCCTTCTTTTTTACTCACGA
kdpE_K425S	TCAGGCAGAGATCTTAACGCTCGATCTGGC
kdpE_check_R	TCGCTCTCTTCGCTGCGTGCGGAAA
torR_K097T	ACTGCAGATCTAAGCCGCTACTCATATCCG
torR_check_R	ACCAGAATAATCCCCACCGTTGAGC
uvrY_K179T	GCCGGAGATCTATTACTGACGGTAGGCTTG
uvrY_check_R	ATGATTTTGACATCAGCTGTGGAAC
qseB_K283S	TTCGCAGATCTGTAGTTGAGCAATTCAGGG
qseB_check_R	CACAGATAATCGTCAGCTCCCAGAC
arcA_K421T	CCATCGAGATCTTTGCCCGCGCCGCTGCCC
arcA_check_R	AGGAACATCAACGCAACATTCGCCT
atoC_K213S	GCATTTAGATCTTTATTGATGCGTTCATGC
atoC_check_R	ACGATTAAATTCAACTCATCGAGAT
baeR_K190S	TGGGCAGATCTGCGCAAGACTTCAACCAGC
baeR_check_R	CGACGAATTTCCCGGCACAGCGTCA
ntrC_K360T	GTTTCCCAGATCTGGCAGCTAACCCGTACC
ntrC_check_R	CTGACGGCAGCATCCAGATCGGAAT
rcsB_K211S	CGGGAAGATCTTGGTACACGCTACTCTGTG
rcsB_check_R	CTTGGGAAATGGCGCTTGATGTACT
pyrR_K432S	CTGTCGCAGATCTTCTCCACGCAACTGGAG
pyrR_check_R	TCTTTCCACGCGGTGATGAACACAA
btsR_K430T	CGGCGCAGATCTTTGCCGGGCAATATGAGC
btsR_check_R	ACAATATACGGGCGATGTTCCGGGT
creB_K420S	GCACCAGATCTCAGGTAATTGGATAATAGC
creB_check_R	TCACTTCGGGCCGTCAGGAACAGTA
basR_K389T	AGGCGAGATCTATATCATTCAGCGAGCGGG
basR_check_R	GCGATTTTGTCGGTCAGCGTATCGC

Appendix Table 3. Oligonucleotides for psgRNA cloning and DNA amplification in the HoSeI method. (Continued.)

Name	Sequence (5' to 3')
For DNA amplification	
cusR_K052T	GCGCATAGATCTGTTGCTGATTGAAATAGC
cusR_check_R	GCGGTAAGCAACAGAATCGGCATCC
narP_K204S	CGCGCCAGATCTCAGGTTGTACCAATGCTG
narP_check_R	CGAATATGTACTTTTACTGTCTGCT
zraR_K438S	CGCTGGGAGATCTTGCGGCAGGCGTTGCCC
zraR_check_R	GTCATAATCAGCACCGGAATTGCCG
rssB_K116S	GATCGAGATCTGTTCCCGTCGCTTTGCGGC
rssB_check_R	TCTGCCATATTTTCAGTGGCAGATA
glrR_K244T	GCGACAGATCTTTCAACGATTATTGCCCCG
glrR_check_R	ATAATTACCGGCATTCCCGGCTGCA
fimZ_K049T	GTGATAGATCTGGCAAGCATCACAAATGGG
fimZ_check_R	ACTTTCACTGTGCTCTGGATTTGTT
ygeK_K422T	CCTGTAGATCTCCATATACCTACCAGTTTC
ygeK_check_R	TGAGCATCTATCTTATGCGATTTAA
dcuR_K440T	GACTCGAAGATCTGGTCAACTATGCTGACG
dcuR_check_R	TCACTTTTGCAACGCGCGTTATGCA
yhjB_K320T	TCATGAGATCTGGCGTGAGTTTGACCCGTC
yhjB_check_R	ATAACTTCCTGTAACCACCGTTTAT
cheB_K173T	CCGACTAGATCTTCGTTTGCGTTCGCTGGG
cheB_check_R	ACGGGCATTGGACGCAAACGCATTA
cheY_K428T	GTACGGCAGATCTGGCGAGCCTTGCAGCAC
cheY_check_R	ACTGGCAATGCCGACATCGCGCCAT
hprR_K182T	TACATAGATCTGCATTAACTGCCACGATAG
hprR_check_R	CTTGCAGTAAGGCAAATAACAGGGG
cusS_K423T	CCGGAGAGATCTTGACCAAAGGGTTAACCG
cusS_check_R	CCACTGACGATATCTTCCAGCGTCA
zraS_K373S	TGGCAAGATCTGATTTCTGTCGCTGGCAAC
zraS_check_R	GGCTGTCCCGCCATCTCTTCCAGAA
kdpD_K068T	GCGTGAGATCTAAACCGCTTACCGCTTCTG
kdpD_check_R	TTTAACGGCAGAACAGCCAGCCCTT
phoQ_PHOP_LL_F	TCGTCTTCACCTCGAAAGCAGTTTATCGATGGTCT
phoQ_check_R	TTCGATTTCAGCCAGTCAGGCTGGA
basS_K439T	GGGACTAGATCTGGCGGCGCAAACCGAAGG
basS_check_R	TGCAGCTCCGCCAGCGGGCGGGTGA
baeS_K189S-2	GTGCTAGATCTGCTGCACGCCAGAAATAAC
baeS_check_R	ATCTGAAAGACAAAGCGATCATTGT
cpxA_K437T	ATGACCGAGATCTGACTTCCCTATTAAAGG
cpxA_check_R	GGCGGTGCCCACTTATCAATCGCCC
envZ_K434T	TGCAAGAGATCTACAAGATTCTGGTGGTCG
envZ_check_R	ATCTCCCGACGGAAAGCGGGAGGCA
evgS_K431S	CTTAGCAGATCTGACTGAAGGCGGAAGTGC
evgS_check_R	GCATTAATACCACGAACCCGTTGCT
glrK_K245T-2	GGAACGAGATCTCCGTACTGTCAGCAACTC
glrK_check_R	GCCAGGGTTGGGTCGTCCAGCACGC

Appendix Table 3. Oligonucleotides for psgRNA cloning and DNA amplification in the HoSeI method. (Continued.)

Name	Sequence (5' to 3')
For DNA amplification	
qseC_K433S	GATAGAAGATCTCATGCTGATTGGCGACGG
qseC_check_R	AGGACCATTCTGCCGTCGTGGGTAA
rcsC_K212T	CCGAGGAGATCTCCATTACGCTCAATGGGG
rcsC_check_R	GCGATGTACTTCAGCTCTTTCATCA
rcsD_K210S	CATACAGATCTACCCTCATTAATCAGTCGG
rcsD_check_R	TCCTGTTTCAGGCGCGTCTCTTGTA
rstB_K471S	GATGCAGATCTCGGTTCACTGATTGCCGCG
rstB_check_R	TCATCAAGATGGTATTTACTCAGTG
hprS_K429T	GCTGGCAGATCTTACAAACGTTAAGAACAG
hprS_check_R	TTATTGATGCTATCACCATGAATAA
atoS_K213S	GCATTTAGATCTTTATTGATGCGTTCATGC
atoS_check_R	GCAAGTTCTGCATTTAATGCGCGGA
barA_K262S	ATCTGCAGATCTTAGCGGTGCGGTATGGCG
barA_check_R	ATATCGGAATGGCGACGATGCAGTA
creC_K441S	GGGAAAAGATCTGGTTAGTGGAAGATGAGC
creC_check_R	TTGCGCACTTTGTTAATGCCACCGA
ntrB_K360T	GTTTCCCAGATCTGGCAGCTAACCCGTACC
ntrB_check_R	ACAGAAAGGATATGCGAGCGCCCGT
phoR_K031S	GGCTTAGATCTGGTCGAAGCGGAAGATTAT
phoR_check_R	TTTCGCAGCTGCATCTGGTGTAAGC
uhpB_K435T	TATAGAAGATCTCCTCATCGTCCGCTCCGG
uhpB_check_R	ATCAATAACGGAAAATGGGTTAAAC
YEHU_LL_F	TCGTCTTCACCTCGACACTTCACCAATTGTGTAAA
btsS_check_R	ATCGAATATCGATGTAAGCCGCCGG
YPDA_LL_F	TCGTCTTCACCTCGACACCGTCCGGGTTACCCATG
pyrR_check_R	ACCCACGGGCCAAACAGAATCCCGC
arcB_K293T	GTGTGAGATCTCGCCCGGACTGCGTGCCGG
arcB_check_R	AGACGTTGTCGTGACTCCTCCAGTT
citA_K062S	AGATGAGATCTGTGCCGCTCATAGGCGAGG
citA_check_R	GCGATGGTCGCCAGCCGTTTGTAGT
dcuS_K392T	CCCATAGATCTCGAATATCATCATACTCCC
dcuS_check_R	CCACTCTCCTGCGGTTTTTTCTGCA
narQ_K238S	CACGGTAGATCTTCCTGACGCGCGGTGCGC
narQ_check_R	GAATGCAGTGCCTGCTGAAATAACT
narX_K114T	GCCAGAGATCTGGAATAATCAGAATACCGG
narX_check_R	GCCGTTTGTTCCATCTCTTTAATTA
torS_K096T	CCGGCAGATCTTGCGCGAAAACCTTCGACC
torS_check_R	CCCTGCGCCTGCCACATCTTTTCGT
cheA_K174T	GGCGGAGATCTCATTTCTAATAGTGAAAGC
cheA_check_R	ATGTCGGTGTTGAGTTGCATCTCAC

Appendix Table 4. Oligonucleotides for DNA fragment preparation in HoSeI method.

Name	Sequence (5' to 3')
phoP_PAMstop	TCTCAATGAACATATACCGGATATTGCGATTGTCGATCTCTAATTGCCAGACGAGGACGGTCTGTCACTGATTCGCCGCTGGC
phoP_PAMstop_com	GCCAGCGGCGAATCAGTGACAGACCGTCCTCGTCTGGCAATTAGAGATCGACAATCGCAATATCCGGTATATGTTCATTGAGA
phoB_PAMstop	CGAAATGGTCTGCTTCGTGCTCGAACAAAATGGCTTTCAGTAAGTCGAAGCGGAAGATTATGACAGTGCTGTGAATCAACTGA
phoB_PAMstop_com	TCAGTTGATTCACAGCACTGTCATAATCTTCCGCTTCGACTTACTGAAAGCCATTTTGTTCGAGCACGAAGCAGACCATTTCG
citB_PAMstop	AGCTCCATTAACCCTATTGATCGTTGAGGACGAAACGCCGTAAGCAGAGATGCATGCGGAATATATTCGTCACATTCCCGGAT
citB_PAMstop_com	ATCCGGGAATGTGACGAATATATTCCGCATGCATCTCTGCTTACGGCGTTTCGTCCTCAACGATCAATAGGGTTAATGGAGCT
ompR_PAMstop	AGAGAACTACAAGATTCTGGTGGTCGATGACGACATGCGCTAACGTGCGCTGCTGGAACGTTATCTCACCGAACAAGGCTTCC
ompR_PAMstop_com	GGAAGCCTTGTTCGGTGAGATAACGTTCCAGCAGCGCACGTTAGCGCATGTCGTCATCGACCACCAGAATCTTGTAGTTCTCT
narL_PAMstop	TAATCAGGAACCGGCTACTATCCTGCTGATTGACGATCACTAAATGCTGCGAACTGGCGTAAAACAGCTTATCAGTATGGCAC
narL_PAMstop_com	GTGCCATACTGATAAGCTGTTTTACGCCAGTTCGCAGCATTTAGTGATCGTCAATCAGCAGGATAGTAGCCGGTTCCTGATTA
cpxR_PAMstop	TATTTAAACAATGAATAAAATCCTGTTAGTTGATGATGACTAAGAGCTGACTTCCCTATTAAAGGAGCTGCTCGAGATGGAAG
cpxR_PAMstop_com	CTTCCATCTCGAGCAGCTCCTTTAATAGGGAAGTCAGCTCTTAGTCATCATCAACTAACAGGATTTTATTCATTGTTTAAATA
uhpA_PAMstop	CACCGTTGCCCTTATAGACGATCACCTCATCGTCCGCTCCTAATTTGCGCAGCTGCTGGGGCTGGAACCTGATTTGCAGGTAG
uhpA_PAMstop_com	CTACCTGCAAATCAGGTTCCAGCCCCAGCAGCTGCGCAAATTAGGAGCGGACGATGAGGTGATCGTCTATAAGGGCAACGGTG
rstA_PAMstop	GGAAGATGATGCGGAAGTCGGTTCACTGATTGCCGCGTACTAAGCAAAACATGATATGCAGGTTACCGTAGAGCCGCGCGGCG
rstA_PAMstop_com	CGCCGCGCGGCTCTACGGTAACCTGCATATCATGTTTTGCTTAGTACGCGGCAATCAGTGAACCGACTTCCGCATCATCTTCC
evgA_PAMstop	AATCTTAGCAGAGTTGACTGAAGGCGGAAGTGCCGTTCAGTAAGTGGAAACACTTAAGCCTGATATCGTCATCATTGATGTCG
evgA_PAMstop_com	CGACATCAATGATGACGATATCAGGCTTAAGTGTTTCCACTTACTGAACGGCACTTCCGCCTTCAGTCAACTCTGCTAAGATT
kdpE_PAMstop	GATTGTTGAAGATGAACAGGCTATTCGTCGCTTTCTGCGCTAAGCGCTGGAGGGCGACGGGATGCGCGTCTTTGAGGCCGAAA
kdpE_PAMstop_com	TTTCGGCCTCAAAGACGCGCATCCCGTCGCCCTCCAGCGCTTAGCGCAGAAAGCGACGAATAGCCTGTTCATCTTCAACAATC
torR_PAMstop	CCCTCTGATGCCACATCACATTGTTATTGTTGAAGATGAGTAAGTTACCCAGGCGCGATTACAATCCTACTTCACTCAGGAGG
torR_PAMstop_com	CCTCCTGAGTGAAGTAGGATTGTAATCGCGCCTGGGTAACTTACTCATCTTCAACAATAACAATGTGATGTGGCATCAGAGGG
uvrY_PAMstop	ACGACGCATTCTGGAAGATATAAAGGGTATAAAAGTCGTCTAAGAGGCATCGTGCGGTGAAGACGCCGTTAAGTGGTGCCGGA
uvrY_PAMstop_com	TCCGGCACCACTTAACGGCGTCTTCACCGCACGATGCCTCTTAGACGACTTTTATACCCTTTATATCTTCCAGAATGCGTCGT
qseB_PAMstop	CCTTAGTAAAATGGGTTTTAGCGTCGACTGGTTTACACAATAACGTCAGGGAAAAGAGGCGCTTTATAGCGCACCTTATGATG
qseB_PAMstop_com	CATCATAAGGTGCGCTATAAAGCGCCTCTTTTCCCTGACGTTATTGTGTAAACCAGTCGACGCTAAAACCCATTTTACTAAGG
arcA_PAMstop	CGAGTTGGTAACACGCAACACGTTGAAAAGTATTTTCGAATAAGAAGGCTATGATGTTTTCGAAGCGACAGATGGCGCGGAAA
arcA_PAMstop_com	TTTCCGCGCCATCTGTCGCTTCGAAAACATCATAGCCTTCTTATTCGAAAATACTTTTCAACGTGTTGCGTGTTACCAACTCG
atoC_PAMstop	CAACGGACGCACAGCATTACACCTGTTTGCCGATATTCACTAAGATGTGGTGTTGATGGATATCCGCATGCCAGAGATGGACG
atoC_PAMstop_com	CGTCCATCTCTGGCATGCGGATATCCATCAACACCACATCTTAGTGAATATCGGCAAACAGGTGTAATGCTGTGCGTCCGTTG
baeR_PAMstop	AGAGAGAAGTATGACCGAGTTACCAATCGACGAAAACACATAACGTATTTTGATCGTGGAAGATGAACCGAAGCTGGGGCAGT
baeR_PAMstop_com	ACTGCCCCAGCTTCGGTTCATCTTCCACGATCAAAATACGTTATGTGTTTTCGTCGATTGGTAACTCGGTCATACTTCTCTCT
ntrC_PAMstop	CGATAGTTCCATCCGTTGGGTGCTTGAACGTGCGCTCGCTTAAGCAGGTTTAACCTGTACGACGTTTGAGAACGGCGCAGAAG
ntrC_PAMstop_com	CTTCTGCGCCGTTCTCAAACGTCGTACAGGTTAAACCTGCTTAAGCGAGCGCACGTTCAAGCACCCAACGGATGGAACTATCG
rcsB_PAMstop	TTACATGAACAATATGAACGTAATTATTGCCGATGACCATTAAATAGTCTTGTTCGGTATTCGCAAATCACTTGAGCAAATTG
rcsB_PAMstop_com	CAATTTGCTCAAGTGATTTGCGAATACCGAACAAGACTATTTAATGGTCATCGGCAATAATTACGTTCATATTGTTCATGTAA
ypdB_PAM_stop	GGCACAACAGGAACTGAGCTGGCTAATTAAAGAGCACAGCTAAATGGAGATTGTCGGCACCTTTGACGACGGTCTGGACGTGT
ypdB_PAM_stop_com	ACACGTCCAGACCGTCGTCAAAGGTGCCGACAATCTCCATTTAGCTGTGCTCTTTAATTAGCCAGCTCAGTTCCTGTTGTGCC
yehT_PAM_stop	GGGACGAGGCATGATTAAAGTCTTAATTGTCGATGATGAATAATTAGCACGGGAGAACCTGCGTGTATTTTTGCAGGAGCAGA
yehT_PAM_stop_com	TCTGCTCCTGCAAAAATACACGCAGGTTCTCCCGTGCTAATTATTCATCATCGACAATTAAGACTTTAATCATGCCTCGTCCC
creB_PAMstop	GGTCTGGTTAGTGGAAGATGAGCAAGGGATAGCCGACACGTAAGTCTACATGTTGCAGCAGGAAGGTTTTGCCGTCGAGGTCT
creB_PAMstop_com	AGACCTCGACGGCAAAACCTTCCTGCTGCAACATGTAGACTTACGTGTCGGCTATCCCTTGCTCATCTTCCACTAACCAGACC
basR_PAMstop	CGATACGCTGTTATTGCAGGGACTGATTCTGGCGGCGCAATAAGAAGGCTACGCGTGCGATAGCGTGACAACCGCGCGGATGG
basR_PAMstop_com	CCATCCGCGCGGTTGTCACGCTATCGCACGCGTAGCCTTCTTATTGCGCCGCCAGAATCAGTCCCTGCAATAACAGCGTATCG
cusR_PAMstop	TGTCGAAGATGAAAAGAAAACCGGAGAATACTTGACCAAATAATTAACCGAAGCCGGTTTTGTGGTCGATTTGGCCGACAACG
cusR_PAMstop_com	CGTTGTCGGCCAAATCGACCACAAAACCGGCTTCGGTTAATTATTTGGTCAAGTATTCTCCGGTTTTCTTTTCATCTTCGACA
narP_PAMstop	GTTACTGGAGCTTGATCCTGGCTCTGAAGTGGTCGCCGAATAAGGCGACGGCGCGAGCGCTATCGATCTGGCGAATAGACTGG
narP_PAMstop_com	CCAGTCTATTCGCCAGATCGATAGCGCTCGCGCCGTCGCCTTATTCGGCGACCACTTCAGAGCCAGGATCAAGCTCCAGTAAC
zraR_PAMstop	CGATAATATCGATATTCTGGTGGTGGATGATGACATTAGCTAATGCACTATTTTGCAGGCTTTACTGCGCGGCTGGGGCTATA
zraR_PAMstop_com	TATAGCCCCAGCCGCGCAGTAAAGCCTGCAAAATAGTGCATTAGCTAATGTCATCATCCACCACCAGAATATCGATATTATCG
rssB_PAMstop	TGTTGAAGATGAGCAGGTATTTCGCTCGCTTCTGGATTCATAATTTTCCTCATTGGGAGCGACAACGGTACTGGCGGCTGATG
rssB_PAMstop_com	CATCAGCCGCCAGTACCGTTGTCGCTCCCAATGAGGAAAATTATGAATCCAGAAGCGAGCGAAATACCTGCTCATCTTCAACA
glrR_PAMstop	GAGCCATAAACCTGCGCATTTATTATTGGTCGATGACGATTAAGGATTGCTGAAACTGCTTGGCCTGCGCCTGACCAGCGAAG
glrR_PAMstop_com	CTTCGCTGGTCAGGCGCAGGCCAAGCAGTTTCAGCAATCCTTAATCGTCATCGACCAATAATAAATGCGCAGGTTTATGGCTC
fimZ_PAMstop	AACTATGAAACCAACGTCGGTGATCATTATGGATACTCATTAAATCATCAGAATGTCTATTGAAGTTCTGTTGCAAAAAAACA
fimZ_PAMstop_com	TGTTTTTTTGCAACAGAACTTCAATAGACATTCTGATGATTTAATGAGTATCCATAATGATCACCGACGTTGGTTTCATAGTT
ygeK_PAMstop	ATATATGGGAAAAATTAAAATTGTAGTTTCAGATCAGCAGTAATTTATGATTGATGGGATAATTGGATTTCTCGGACATTATC
ygeK_PAMstop_com	GATAATGTCCGAGAAATCCAATTATCCCATCAATCATAAATTACTGCTGATCTGAAACTACAATTTTAATTTTTCCCATATAT
dcuR_PAMstop	AATGGTCGCGGAGCTGAATCGCCGATACGTAGCACAAATCTAAGGCTTTCAATGCTGTGGAACAGCCTCGACGCTGGAGAAAG
dcuR_PAMstop_com	CTTTCTCCAGCGTCGAGGCTGTTCCACAGCATTGAAAGCCTTAGATTTGTGCTACGTATCGGCGATTCAGCTCCGCGACCATT
yhjB_PAMstop	TATTCATGGAATGAAAATCAGTTTACAGCAGCGTATTCCATAAGTGAGTATTCAGGGGGCCAGTCAGGCAGACGAGTTATGGC
yhjB_PAMstop_com	GCCATAACTCGTCTGCCTGACTGGCCCCCTGAATACTCACTTATGGAATACGCTGCTGTAAACTGATTTTCATTCCATGAATA
cheB_PAMstop	ATTAACGATGAGCAAAATCAGGGTGTTATCTGTCGATGATTAAGCACTGATGCGCCAGATCATGACAGAAATCATCAACAGCC
cheB_PAMstop_com	GGCTGTTGATGATTTCTGTCATGATCTGGCGCATCAGTGCTTAATCATCGACAGATAACACCCTGATTTTGCTCATCGTTAAT

Appendix Table 4. Oligonucleotides for DNA fragment preparation in HoSeI method. (Continued.)

Name	Sequence (5' to 3')
cheY_PAMstop	GGATAAAGAACTTAAATTTTTGGTTGTGGATGACTTTTCCTAAATGCGACGCATAGTGCGTAACCTGCTGAAAGAGCTGGGAT
cheY_PAMstop_com	ATCCCAGCTCTTTCAGCAGGTTACGCACTATGCGTCGCATTTAGGAAAAGTCATCCACAACCAAAAATTTAAGTTCTTTATCC
hprR_PAMstop	TTTCATGAAGATTCTACTTATTGAAGATAATCAAAGGACCTAAGAATGGGTAACGCAGGGGCTTTCCGAAGCGGGTTATGTCA
hprR_PAMstop_com	TGACATAACCCGCTTCGGAAAGCCCCTGCGTTACCCATTCTTAGGTCCTTTGATTATCTTCAATAAGTAGAATCTTCATGAAA
cusS_PAM_stop	GGTCAGTAAGCCATTTCAGCGCCCGTTTTCGCTGGCAACCTAACTGACCTTTTTTATCAGCCTGGCCACCATCGCGGCGTTTT
cusS_PAM_stop_com	AAAACGCCGCGATGGTGGCCAGGCTGATAAAAAAGGTCAGTTAGGTTGCCAGCGAAAACGGGCGCTGAAATGGCTTACTGACC
zraS_PAM_stop	TAAAGACTCCTTAGCTAAATGGTTAAGCGCGATCCTCCCCTAAGTCATTGTTGGGCTGGTGGGATTGTTTGCGGTAACTGTGA
zraS_PAM_stop_com	TCACAGTTACCGCAAACAATCCCACCAGCCCAACAATGACTTAGGGGAGGATCGCGCTTAACCATTTAGCTAAGGAGTCTTTA
kdpD_PAM_stop	GATGAATAACGAACCCTTACGTCCCGACCCCGATCGTCTGTAAGAACAAACTGCCGCGCCGCATCGGGGGAAGCTGAAAGTTT
kdpD_PAM_stop_com	AAACTTTCAGCTTCCCCCGATGCGGCGCGGCAGTTTGTTCTTACAGACGATCGGGGTCGGGACGTAAGGGTTCGTTATTCATC
phoQ_PAMstop_F	GCTGATCGGTTATAGCGTCAGTTTCGATAAAACTACGTTTTAACTGTTACGTGGCGAGAGCAATCTGTTCTATACCCTTGCGA
phoQ_PAMstop_R	TCGCAAGGGTATAGAACAGATTGCTCTCGCCACGTAACAGTTAAAACGTAGTTTTATCGAAACTGACGCTATAACCGATCAGC
basS_PAMstop_F	CGGGGCCATTTTGTTGGTGTTTGAGCTGATCAGCGTCTTCTAACTATGGCATGAAAGTACCGAGCAGATTCAGCTGTTTGAGC
basS_PAMstop_R	GCTCAAACAGCTGAATCTGCTCGGTACTTTCATGCCATAGTTAGAAGACGCTGATCAGCTCAAACACCAACAAAATGGCCCCG
baeS_PAM_stop	AATGAAGTTCTGGCGACCCGGTATTACCGGCAAACTGTTTTAAGCGATTTTCGCCACCTGCATTGTCTTGCTGATCAGTATGC
baeS_PAM_stop_com	GCATACTGATCAGCAAGACAATGCAGGTGGCGAAAATCGCTTAAAACAGTTTGCCGGTAATACCGGGTCGCCAGAACTTCATT
cpxA_PAM_stop	CATGATAGGCAGCTTAACCGCGCGCATCTTCGCCATCTTCTAACTGACGCTGGCGCTGGTGTTGATGTTGGTTTTGATGTTAC
cpxA_PAM_stop_com	GTAACATCAAAACCAACATCAACACCAGCGCCAGCGTCAGTTAGAAGATGGCGAAGATGCGCGCGGTTAAGCTGCCTATCATG
envZ_PAMstop_F	AAGCATGAGGCGATTGCGCTTCTCGCCACGAAGTTCATTTTAACGTACGTTATTGCTCATCGTCACCTTGCTGTTCGCCAGCC
envZ_PAMstop_R	GGCTGGCGAACAGCAAGGTGACGATGAGCAATAACGTACGTTAAAATGAACTTCGTGGCGAGAAGCGCAATCGCCTCATGCTT
evgS_PAM_stop	TTTACCCTATATTTTTCTTCTCTGTTGTGGTCTTTGGTCGTAAATAAGTTTCGCAGACGAAGATTACATCGAATATCGTGGCA
evgS_PAM_stop_com	TGCCACGATATTCGATGTAATCTTCGTCTGCGAAACTTATTTACGACCAAAGACCACAACAGAGAAGAAAAATATAGGGTAAA
glrK_PAM_stop	CTGGCCCGTTTTTCCCCGCTCATTACGACAACTGGTAATGTAAGCATTTTTGCTGATTCTGCTGCCCCTGTTGGTGCTGGCAT
glrK_PAM_stop_com	ATGCCAGCACCAACAGGGGCAGCAGAATCAGCAAAAATGCTTACATTACCAGTTGTCGTAATGAGCGGGGAAAAACGGGCCAG
qseC_PAMstop_F	AATTCTGGCCTCGGTGACCTGGCTGCTTTCCAGCTTTGTCTAATGGAAACAAACAACGGATAACGTCGATGAATTGTTCGACA
qseC_PAMstop_R	TGTCGAACAATTCATCGACGTTATCCGTTGTTTGTTTCCATTAGACAAAGCTGGAAAGCAGCCAGGTCACCGAGGCCAGAATT
rcsC_PAM_stop	GAGCTTCGCCCCTTTGAAATACCTTGCTTCTTTTCGTACATAACTGAAAGCCTCGCGCTACATGTTCAGAGCATTGGCGTTAG
rcsC_PAM_stop_com	CTAACGCCAATGCTCTGAACATGTAGCGCGAGGCTTTCAGTTATGTACGAAAAGAAGCAAGGTATTTCAAAGGGGCGAAGCTC
rcsD_PAM_stop	GAGCATTACCCGCTTCTTTTTACTGTTGATCATTGTGTTATAAGTGACGATGGGTGTAATGGTACAAAGCGCCGTTAACGCCT
rcsD_PAM_stop_com	AGGCGTTAACGGCGCTTTGTACCATTACACCCATCGTCACTTATAACACAATGATCAACAGTAAAAAGAAGCGGGTAATGCTC
rstB_PAM_stop	TTACCTGTTATTGTTTGTCTGCTTCCTTGTGATGTCTCTGTAAGTTGGGCTGGTGTACAAATTTACCGCCGAACGCGCGGGCA
rstB_PAM_stop_com	TGCCCGCGCGTTCGGCGGTAAATTTGTACACCAGCCCAACTTACAGAGACATCACAAGGAAGCAGACAAACAATAACAGGTAA
hprS_PAM_stop	CCGTTTAACCTTGCTTTTTATATTGCTACTGTCTGTTGCTTAAGCCGGAATTGTCTGGACTCTCTATAATGGCCTGGCAAGTG
hprS_PAM_stop_com	CACTTGCCAGGCCATTATAGAGAGTCCAGACAATTCCGGCTTAAGCAACAGACAGTAGCAATATAAAAAGCAAGGTTAAACGG
atoS_PAM_stop	GTGGATTTATCCACGCCGCTTACGCAATCAAATGATCCTGTAAGCAATCCTGATGGTCATTGTCCCAACGCTTACTATTGGTT
atoS_PAM_stop_com	AACCAATAGTAAGCGTTGGGACAATGACCATCAGGATTGCTTACAGGATCATTTGATTGCGTAAGCGGCGTGGATAAATCCAC
barA_PAM_stop	GACCAACTACAGCCTGCGCGCACGCATGATGATTCTGATCTAAGCACCGACCGTCCTTATTGGTTTATTGCTGAGTATCTTTT
barA_PAM_stop_com	AAAAGATACTCAGCAATAAACCAATAAGGACGGTCGGTGCTTAGATCAGAATCATCATGCGTGCGCGCAGGCTGTAGTTGGTC
creC_PAM_stop	CTATTTTTTACTGGTGGCGGTGGCAGCCTGGTTCGTACTGTAAATTTTTGTCAAAGAAGTTAAACCGGGCGTGCGAAGAGCAA
creC_PAM_stop_com	TTGCTCTTCGCACGCCCGGTTTAACTTCTTTGACAAAAATTTACAGTACGAACCAGGCTGCCACCGCCACCAGTAAAAAATAG
ntrB_PAM_stop	CAACTCGCTGATTAACAGTATTTTGTTAATCGATGACAACTAAGCGATCCATTACGCCAACCCTGCCGCGCAACAACTGCTCG
ntrB_PAM_stop_com	CGAGCAGTTGTTGCGCGGCAGGGTTGGCGTAATGGATCGCTTAGTTGTCATCGATTAACAAAATACTGTTAATCAGCGAGTTG
phoR_PAMstop_F	GTCGTGGAAAAGGCTGGTGCTGGAGCTGCTACTTTGCTGCTAACCGGCTTTCATCCTGGGTGCATTTTTTGGTTACCTGCCCT
phoR_PAMstop_R	AGGGCAGGTAACCAAAAAATGCACCCAGGATGAAAGCCGGTTAGCAGCAAAGTAGCAGCTCCAGCACCAGCCTTTTCCACGAC
uhpB_PAMstop_F	CCGCTTAATTACCGTTATTGCCTGCTTTTTTATCTTCTCTTAAGCATGGTTTTGCCTGTGGAGTATCAGCCTGCATCTGGTTG
uhpB_PAMstop_R	CAACCAGATGCAGGCTGATACTCCACAGGCAAAACCATGCTTAAGAGAAGATAAAAAAGCAGGCAATAACGGTAATTAAGCGG
btsS_PAM_stop	ATGGTTAATGAGTAAAACGCCATTATTCATACCGTTAATGTAAGTCACGGTTCGTCTGCCGCATAAATTTCTCTGCTACATCG
btsS_PAM_stop_com	CGATGTAGCAGAGAAATTTATGCGGCAGACGAACCGTGACTTACATTAACGGTATGAATAATGGCGTTTTACTCATTAACCAT
pyrS_PAM_stop	GCTGGCGGTCTTCGATCGGGCAGCGTTAATGCTTATCTGCTAATTCTTTCTCATCCGTATCCGCCTGTTTCGCGAACTGTTGC
pyrS_PAM_stop_com	GCAACAGTTCGCGAAACAGGCGGATACGGATGAGAAAGAATTAGCAGATAAGCATTAACGCTGCCCGATCGAAGACCGCCAGC
arcB_PAM_stop	GCTGGCGCAGTATTATGTTGACCTGATGATGAAGTTAGGTTAAGTGCGCTTCTCAATGTTGCTGGCGCTGGCCCTCGTCGTTC
arcB_PAM_stop_com	GAACGACGAGGGCCAGCGCCAGCAACATTGAGAAGCGCACTTAACCTAACTTCATCATCAGGTCAACATAATACTGCGCCAGC
citA_PAMstop	TTTGCTGATTCTGGTGTTCTCAATATTTGTCATTGCAGCCTAAGCGCAATATTTTACGGCCAGTTTTGAGGACTATTTAACGC
citA_PAMstop_com	GCGTTAAATAGTCCTCAAAACTGGCCGTAAAATATTGCGCTTAGGCTGCAATGACAAATATTGAGAACACCAGAATCAGCAAA
dcuS_PAM_stop	GATGAGACATTCATTGCCCTACCGCATGTTACGCAAACGTTAAATGAAATTGAGTACCACAGTGATCTTAATGGTCAGTGCGG
dcuS_PAM_stop_com	CCGCACTGACCATTAAGATCACTGTGGTACTCAATTTCATTTAACGTTTGCGTAACATGCGGTAGGGCAATGAATGTCTCATC
narQ_PAM_stop	GCGTGTGATTGTTAAACGACCCGTCTCGGCCAGTCTGGCCTAAGCCTTTTTTTACATTGTGCTGCTGTCGATTCTTTCCACGG
narQ_PAM_stop_com	CCGTGGAAAGAATCGACAGCAGCACAATGTAAAAAAAGGCTTAGGCCAGACTGGCCGAGACGGGTCGTTTAACAATCACACGC
narX_PAM_stop	CATGCTTAAACGTTGTCTCTCTCCGCTCACCCTGGTTAATTAAGTTGCGCTTATTGTGTTGCTTTCTACTGCTATTGGACTGG
narX_PAM_stop_com	CCAGTCCAATAGCAGTAGAAAGCAACACAATAAGCGCAACTTAATTAACCAGGGTGAGCGGAGAGAGACAACGTTTAAGCATG
torS_PAM_stop	GAATTTAACCCTGACCCGAAGACTCTGGATGGGCTTTGCCTAAATGGCGCTGTTAACCCTGACCAGTACCCTGGTGGGATGGT
torS_PAM_stop_com	ACCATCCCACCAGGGTACTGGTCAGGGTTAACAGCGCCATTTAGGCAAAGCCCATCCAGAGTCTTCGGGTCAGGGTTAAATTC
cheA_PAM_stop	CGATTTTTATCAGACATTTTTTGATGAAGCGGACGAACTGTAAGCTGACATGGAGCAGCATTTGCTGGTTTTGCAGCCGGAAG
cheA_PAM_stop_com	CTTCCGGCTGCAAAACCAGCAAATGCTGCTCCATGTCAGCTTACAGTTCGTCCGCTTCATCAAAAAATGTCTGATAAAAATCG

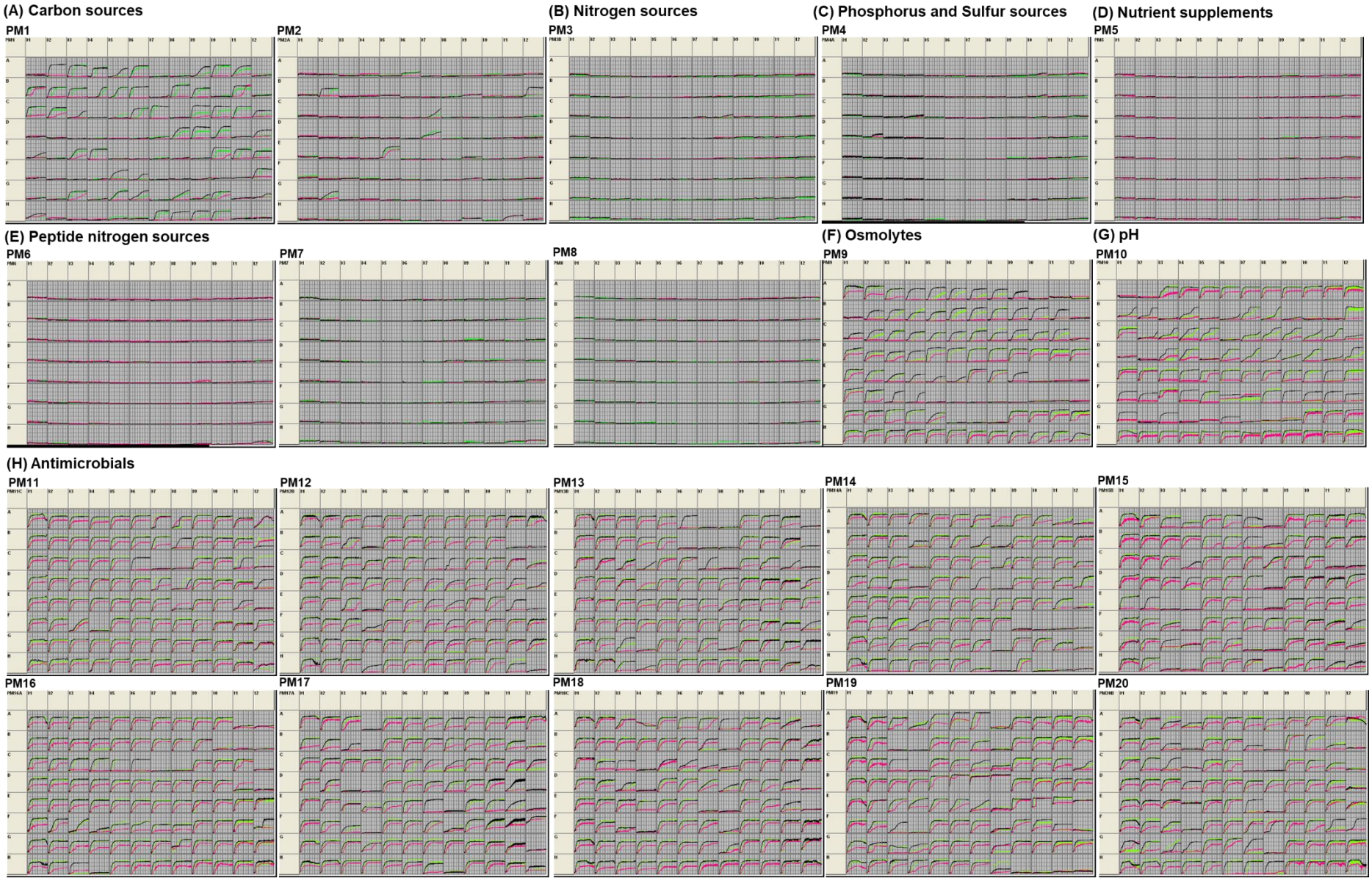
(A) Carbon sources
PM1
PM2
(B) Nitrogen sources
PM3
(C) Phosphorus and Sulfur sources
PM4
(D) Nutrient supplements
PM5
(E) Peptide nitrogen sources
PM6
PM7
PM8
(F) Osmolytes
PM9
(G) pH
PM10
(H) Antimicrobials
PM11
PM12
PM13
PM14
PM15
PM16
PM17
PM18
PM19
PM20

Appendix Figure 2. The growth capacity of the RR- and SK-knockout strain. The Phenotype Microarray testing was performed to characterize the growth capacity of the RR mutant (magenta), the SK mutant (green), and the parent strain (black). Each strain was inoculated for 96 hours at 37℃ under 1920 environmental conditions. Each graph shows the growth of three strains (x-axis; incubate time, y-axis; the level of reduced dye) under various culture conditions such as carbon sources **[A]**, nitrogen sources **[B]**, phosphorus and sulfur sources **[C]**, nutrient supplements **[D]**, peptide nitrogen sources **[E]**, osmolytes **[F]**, pH **[G]**, and inhibitory compounds **[H]**. The more detailed information is shown in **Appendix Table 5, 6, 7, and 8**.

Appendix Table 5. Carbon source utilization of Δ34 RR and Δ30 SK strains.

Carbon source	Plate/Well	Parent	Δ34 RR	Δ30 SK
Negative Control	PM01/A01	×	×	×
L-Arabinose	PM01/A02	◎	×	×
N-Acetyl-D-Glucosamine	PM01/A03	◎	×	○
D-Saccharic Acid	PM01/A04	◎	×	○
Succinic Acid	PM01/A05	△	×	×
D-Galactose	PM01/A06	◎	×	◎
L-Aspartic Acid	PM01/A07	×	×	×
L-Proline	PM01/A08	×	×	×
D-Alanine	PM01/A09	○	×	×
D-Trehalose	PM01/A10	◎	×	○
D-Mannose	PM01/A11	◎	×	△
Dulcitol	PM01/A12	×	×	×
D-Serine	PM01/B01	◎	○	◎
D-Sorbitol	PM01/B02	◎	×	○
Glycerol	PM01/B03	◎	×	○
L-Fucose	PM01/B04	○	×	○
D-Glucuronic Acid	PM01/B05	○	×	◎
D-Gluconic Acid	PM01/B06	◎	×	◎
D,L-α-Glycerol- Phosphate	PM01/B07	×	×	×
D-Xylose	PM01/B08	◎	×	○
L-Lactic Acid	PM01/B09	◎	×	○
Formic Acid	PM01/B10	×	×	×
D-Mannitol	PM01/B11	◎	○	△
L-Glutamic Acid	PM01/B12	×	×	×
D-Glucose-6-Phosphate	PM01/C01	◎	×	○
D-Galactonic Acid-γ-Lactone	PM01/C02	◎	×	◎
D,L-Malic Acid	PM01/C03	△	×	×
D-Ribose	PM01/C04	×	×	×
Tween 20	PM01/C05	×	×	△
L-Rhamnose	PM01/C06	◎	×	○
D-Fructose	PM01/C07	◎	×	◎
Acetic Acid	PM01/C08	×	×	×
α-D-Glucose	PM01/C09	◎	×	△
Maltose	PM01/C10	◎	×	△
D-Melibiose	PM01/C11	◎	×	◎
Thymidine	PM01/C12	×	×	×
L-Asparagine	PM01/D01	×	×	×
D-Aspartic Acid	PM01/D02	×	×	×
D-Glucosaminic Acid	PM01/D03	×	×	×
1,2-Propanediol	PM01/D04	×	×	×
Tween 40	PM01/D05	×	×	×
α-Keto-Glutaric Acid	PM01/D06	×	×	×
α-Keto-Butyric Acid	PM01/D07	×	×	×
α-Methyl-D-Galactoside	PM01/D08	◎	×	△
α-D-Lactose	PM01/D09	◎	×	△
Lactulose	PM01/D10	○	×	△
Sucrose	PM01/D11	×	×	×
Uridine	PM01/D12	◎	×	×
L-Glutamine	PM01/E01	△	×	×
m-Tartaric Acid	PM01/E02	×	×	×
D-Glucose-1-Phosphate	PM01/E03	○	△	◎
D-Fructose-6-Phosphate	PM01/E04	◎	×	○

◎: Rapid growth to stationary phase in 24 hours, ○: Delayed growth but same cell mass,
△: Delayed growth and small cell mass, ×: No growth

Appendix Table 5. Carbon source utilization of Δ34 RR and Δ30 SK strains. (Continued.)

Carbon source	Plate/Well	Parent	Δ34 RR	Δ30 SK
Tween 80	PM01/E05	×	×	×
α-Hydroxy Glutaric Acid-γ-Lactone	PM01/E06	×	×	×
α-Hydroxy-Butyric Acid	PM01/E07	×	×	×
β-Methyl-D-Glucoside	PM01/E08	×	×	×
Adonitol	PM01/E09	×	×	×
Maltotriose	PM01/E10	◎	△	△
2`-Deoxy-Adenosine	PM01/E11	◎	×	○
Adenosine	PM01/E12	◎	×	○
Glycyl-L-Aspartic Acid	PM01/F01	×	×	×
Citric Acid	PM01/F02	×	×	×
M-Inositol	PM01/F03	×	×	×
D-Threonine	PM01/F04	×	×	×
Fumaric Acid	PM01/F05	○	×	×
Bromo-Succinic Acid	PM01/F06	△	×	×
Propionic Acid	PM01/F07	×	×	×
Mucic Acid	PM01/F08	×	×	×
Glycolic Acid	PM01/F09	×	×	×
Glyoxylic Acid	PM01/F10	×	×	×
D-Cellobiose	PM01/F11	×	×	×
Inosine	PM01/F12	◎	×	○
Glycyl-L-Glutamic Acid	PM01/G01	×	×	×
Tricarballylic Acid	PM01/G02	×	×	×
L-Serine	PM01/G03	◎	○	○
L-Threonine	PM01/G04	×	×	×
L-Alanine	PM01/G05	○	×	◎
L-Alanyl-Glycine	PM01/G06	○	×	△
Acetoacetic Acid	PM01/G07	×	×	×
N-Acetyl-β-D-Mannosamine	PM01/G08	△	×	◎
Mono Methyl Succinate	PM01/G09	×	×	×
Methyl Pyruvate	PM01/G10	◎	△	○
D-Malic Acid	PM01/G11	×	×	×
L-Malic Acid	PM01/G12	×	×	×
Glycyl-L-Proline	PM01/H01	×	×	×
p-Hydroxy-Phenylacetic Acid	PM01/H02	×	×	×
m-Hydroxy-Phenylacetic Acid	PM01/H03	×	×	×
Tyramine	PM01/H04	×	×	×
D-Psicose	PM01/H05	×	×	×
L-Lyxose	PM01/H06	×	×	×
Glucuronamide	PM01/H07	◎	×	○
Pyruvic Acid	PM01/H08	◎	×	×
L-Galactonic Acid-γ-Lactone	PM01/H09	◎	×	△
D-Galacturonic Acid	PM01/H10	◎	×	○
Phenylethylamine	PM01/H11	×	×	×
Ethanolamine	PM01/H12	×	×	×
Negative Control	PM02/A01	×	×	×
Chondroitin Sulfate C	PM02/A02	×	×	×
α-Cyclodextrin	PM02/A03	×	×	×
β-Cyclodextrin	PM02/A04	×	×	×
γ-Cyclodextrin	PM02/A05	×	×	×
Dextrin	PM02/A06	×	×	×
Gelatin	PM02/A07	×	×	×
Glycogen	PM02/A08	×	×	×
Inulin	PM02/A09	×	×	×

◎: Rapid growth to stationary phase in 24 hours, ○: Delayed growth but same cell mass,
△: Delayed growth and small cell mass, ×: No growth

Appendix Table 5. Carbon source utilization of Δ34 RR and Δ30 SK strains. (Continued.)

Carbon source	Plate/Well	Parent	Δ34 RR	Δ30 SK
Laminarin	PM02/A10	×	×	×
Mannan	PM02/A11	×	×	×
Pectin	PM02/A12	×	×	×
N-Acetyl-D-Galactosamine	PM02/B01	×	×	×
N-Acetyl-Neuraminic Acid	PM02/B02	◎	×	○
β-D-Allose	PM02/B03	×	×	×
Amygdalin	PM02/B04	×	×	×
D-Arabinose	PM02/B05	×	×	×
D-Arabitol	PM02/B06	×	×	×
L-Arabitol	PM02/B07	×	×	×
Arbutin	PM02/B08	×	×	×
2-Deoxy-D-Ribose	PM02/B09	×	×	×
I-Erythritol	PM02/B10	×	×	×
D-Fucose	PM02/B11	×	×	×
3-0-β-D-Galactopyranosyl-D-Arabinose	PM02/B12	◎	×	×
Gentiobiose	PM02/C01	×	×	×
L-Glucose	PM02/C02	×	×	×
D-Lactitol	PM02/C03	×	×	×
D-Melezitose	PM02/C04	×	×	×
Maltitol	PM02/C05	×	×	×
α-Methyl-D-Glucoside	PM02/C06	×	×	×
β-Methyl-D-Galactoside	PM02/C07	○	×	×
3-O-Methyl-Glucose	PM02/C08	×	×	×
β-Methyl-D-Glucuronic Acid	PM02/C09	×	×	×
α-Methyl-D-Mannoside	PM02/C10	×	×	×
β-Methyl-D-Xyloside	PM02/C11	×	×	×
Palatinose	PM02/C12	×	×	×
D-Raffinose	PM02/D01	×	×	×
Salicin	PM02/D02	×	×	×
Sedoheptulosan	PM02/D03	×	×	×
L-Sorbose	PM02/D04	×	×	×
Stachyose	PM02/D05	×	×	×
D-Tagatose	PM02/D06	×	×	×
Turanose	PM02/D07	△	×	◎
Xylitol	PM02/D08	×	×	×
N-Acetyl-D-Glucosaminitol	PM02/D09	×	×	×
γ-Amino-Butyric Acid	PM02/D10	×	×	×
δ-Amino-Valeric Acid	PM02/D11	×	×	×
Butyric Acid	PM02/D12	×	×	×
Capric Acid	PM02/E01	×	×	×
Caproic Acid	PM02/E02	×	×	×
Citraconic Acid	PM02/E03	×	×	×
D,L-Citramalic Acid	PM02/E04	×	×	×
D-Glucosamine	PM02/E05	◎	○	◎
2-Hydroxy-Benzoic Acid	PM02/E06	×	×	×
4-Hydroxy-Benzoic Acid	PM02/E07	×	×	×
β-Hydroxy-Butyric Acid	PM02/E08	×	×	×
γ-Hydroxy-Butyric Acid	PM02/E09	×	×	×
α-Keto-Valeric Acid	PM02/E10	×	×	×
Itaconic Acid	PM02/E11	×	×	×
5-Keto-D-Gluconic Acid	PM02/E12	×	×	×
D-Lactic Acid Methyl Ester	PM02/F01	×	×	×
Malonic Acid	PM02/F02	×	×	×

◎: Rapid growth to stationary phase in 24 hours, ○: Delayed growth but same cell mass,
△: Delayed growth and small cell mass, ×: No growth

Appendix Table 5. Carbon source utilization of Δ34 RR and Δ30 SK strains. (Continued.)

Carbon source	Plate/Well	Parent	Δ34 RR	Δ30 SK
Melibionic Acid	PM02/F03	×	×	×
Oxalic Acid	PM02/F04	×	×	×
Oxalomalic Acid	PM02/F05	×	×	×
Quinic Acid	PM02/F06	×	×	×
D-Ribono-1,4-Lactone	PM02/F07	×	×	×
Sebacic Acid	PM02/F08	×	×	×
Sorbic Acid	PM02/F09	×	×	×
Succinamic Acid	PM02/F10	×	×	×
D-Tartaric Acid	PM02/F11	×	×	×
L-Tartaric Acid	PM02/F12	×	×	×
Acetamide	PM02/G01	×	×	×
L-Alaninamide	PM02/G02	○	×	○
N-Acetyl-L-Glutamic Acid	PM02/G03	×	×	×
L-Arginine	PM02/G04	×	×	×
Glycine	PM02/G05	×	×	×
L-Histidine	PM02/G06	×	×	×
L-Homoserine	PM02/G07	×	×	×
4-Hydroxy-L-Proline (trans)	PM02/G08	×	×	×
L-Isoleucine	PM02/G09	×	×	×
L-Leucine	PM02/G10	×	×	×
L-Lysine	PM02/G11	×	×	×
L-Methionine	PM02/G12	×	×	×
L-Ornithine	PM02/H01	×	×	×
L-Phenylalanine	PM02/H02	×	×	×
L-Pyroglutamic Acid	PM02/H03	×	×	×
L-Valine	PM02/H04	×	×	×
D,L-Carnitine	PM02/H05	×	×	×
Sec-Butylamine	PM02/H06	×	×	×
D,L-Octopamine	PM02/H07	×	×	×
Putrescine	PM02/H08	×	×	×
Dihydroxy-Acetone	PM02/H09	×	×	×
2,3-Butanediol	PM02/H10	×	×	×
2,3-Butanone	PM02/H11	×	×	×
3-Hydroxy-2-Butanone	PM02/H12	×	×	×

◎: Rapid growth to stationary phase in 24 hours, ○: Delayed growth but same cell mass,
△: Delayed growth and small cell mass, ×: No growth

Appendix Table 6. Viability of Δ34 RR and Δ30 SK strains under various osmolytes.

Osmolyte	Plate/Well	Parent	Δ34 RR	Δ30 SK
1% NaCl	PM09/A01	◎	△	◎
2% NaCl	PM09/A02	◎	△	◎
3% NaCl	PM09/A03	◎	×	◎
4% NaCl	PM09/A04	◎	×	×
5% NaCl	PM09/A05	◎	×	△
5.5% NaCl	PM09/A06	◎	×	△
6% NaCl	PM09/A07	◎	×	△
6.5% NaCl	PM09/A08	◎	×	△
7% NaCl	PM09/A09	◎	×	×
8% NaCl	PM09/A10	×	×	×
9% NaCl	PM09/A11	×	×	×
10% NaCl	PM09/A12	×	×	×
6% NaCl	PM09/B01	×	×	×
6% NaCl + Betaine	PM09/B02	◎	×	×
6% NaCl + N-N Dimethyl Glycine	PM09/B03	◎	×	○
6% NaCl + Sarcosine	PM09/B04	◎	×	○
6% NaCl + Dimethyl Sulphonyl Propionate	PM09/B05	◎	×	○
6% NaCl + MOPS	PM09/B06	◎	×	○
6% NaCl + Ectoine	PM09/B07	◎	×	△
6% NaCl + Choline	PM09/B08	◎	×	○
6% NaCl + Phosphorylcholine	PM09/B09	◎	×	×
6% NaCl + Creatine	PM09/B10	◎	×	×
6% NaCl + Creatinine	PM09/B11	◎	×	×
6% NaCl + L-Carnitine	PM09/B12	×	×	×
6% NaCl + KCl	PM09/C01	△	×	×
6% NaCl + L-Proline	PM09/C02	◎	×	△
6% NaCl + N-Acetyl-L-Glutamine	PM09/C03	◎	×	○
6% NaCl + β-Glutamic Acid	PM09/C04	◎	×	○
6% NaCl + γ-Amino-n-Butyric Acid	PM09/C05	◎	×	○
6% NaCl + Glutathione	PM09/C06	◎	×	○
6% NaCl + Glycerol	PM09/C07	◎	×	○
6% NaCl + Trehalose	PM09/C08	◎	×	○
6% NaCl + Trimethylamine-N-Oxide	PM09/C09	◎	×	△
6% NaCl + Trimethylamine	PM09/C10	◎	×	○
6% NaCl + Octopine	PM09/C11	◎	×	△
6% NaCl + Trigonelline	PM09/C12	×	×	×
3% Potassium Chloride	PM09/D01	◎	△	○
4% Potassium Chloride	PM09/D02	◎	△	△
5% Potassium Chloride	PM09/D03	◎	△	△
6% Potassium Chloride	PM09/D04	◎	×	×
2% Sodium Sulfate	PM09/D05	◎	△	○
3% Sodium Sulfate	PM09/D06	◎	×	○
4% Sodium Sulfate	PM09/D07	◎	×	◎
5% Sodium Sulfate	PM09/D08	◎	×	◎
5% Ethylene Glycol	PM09/D09	◎	△	◎
10% Ethylene Glycol	PM09/D10	◎	△	◎
15% Ethylene Glycol	PM09/D11	◎	△	◎
20% Ethylene Glycol	PM09/D12	◎	△	◎
1% Sodium Formate	PM09/E01	◎	△	○
2% Sodium Formate	PM09/E02	◎	×	○
3% Sodium Formate	PM09/E03	△	×	○
4% Sodium Formate	PM09/E04	△	×	×
5% Sodium Formate	PM09/E05	△	×	×

◎: Rapid growth to stationary phase in 24 hours, ○: Delayed growth but same cell mass,
△: Delayed growth and small cell mass, ×: No growth

Appendix Table 6. Viability of Δ34 RR and Δ30 SK strains under various osmolytes. (Continued.)

Osmolyte	Plate/Well	Parent	Δ34 RR	Δ30 SK
6% Sodium Formate	PM09/E06	△	×	×
2% Urea	PM09/E07	◎	○	◎
3% Urea	PM09/E08	◎	○	○
4% Urea	PM09/E09	◎	×	×
5% Urea	PM09/E10	×	×	×
6% Urea	PM09/E11	×	×	×
7% Urea	PM09/E12	×	×	×
1% Sodium Lactate	PM09/F01	◎	◎	◎
2% Sodium Lactate	PM09/F02	◎	×	○
3% Sodium Lactate	PM09/F03	○	×	×
4% Sodium Lactate	PM09/F04	○	×	×
5% Sodium Lactate	PM09/F05	×	×	×
6% Sodium Lactate	PM09/F06	×	×	×
7% Sodium Lactate	PM09/F07	×	×	×
8% Sodium Lactate	PM09/F08	×	×	×
9% Sodium Lactate	PM09/F09	×	×	×
10% Sodium Lactate	PM09/F10	×	×	×
11% Sodium Lactate	PM09/F11	×	×	×
12% Sodium Lactate	PM09/F12	×	×	×
20mM Sodium Phosphate pH 7	PM09/G01	◎	△	◎
50mM Sodium Phosphate pH 7	PM09/G02	◎	△	◎
100mM Sodium Phosphate pH 7	PM09/G03	◎	×	◎
200mM Sodium Phosphate pH 7	PM09/G04	◎	×	◎
20mM Sodium Benzoate pH 5.2	PM09/G05	○	△	○
50mM Sodium Benzoate pH 5.2	PM09/G06	×	×	×
100mM Sodium Benzoate pH 5.2	PM09/G07	×	×	×
200mM Sodium Benzoate pH 5.2	PM09/G08	×	×	×
10mM Ammonium Sulfate pH 8	PM09/G09	◎	△	◎
20mM Ammonium Sulfate pH 8	PM09/G10	◎	△	◎
50mM Ammonium Sulfate pH 8	PM09/G11	◎	△	○
100mM Ammonium Sulfate pH 8	PM09/G12	◎	△	○
10mM Sodium Nitrate	PM09/H01	◎	△	◎
20mM Sodium Nitrate	PM09/H02	◎	△	◎
40mM Sodium Nitrate	PM09/H03	◎	△	◎
60mM Sodium Nitrate	PM09/H04	◎	△	◎
80mM Sodium Nitrate	PM09/H05	◎	△	◎
100mM Sodium Nitrate	PM09/H06	◎	△	◎
10mM Sodium Nitrite	PM09/H07	◎	△	◎
20mM Sodium Nitrite	PM09/H08	◎	△	◎
40mM Sodium Nitrite	PM09/H09	◎	△	◎
60mM Sodium Nitrite	PM09/H10	◎	△	○
80mM Sodium Nitrite	PM09/H11	◎	×	○
100mM Sodium Nitrite	PM09/H12	◎	×	△

◎: Rapid growth to stationary phase in 24 hours, ○: Delayed growth but same cell mass,
△: Delayed growth and small cell mass, ×: No growth

Appendix Table 7. Viability of Δ34 RR and Δ30 SK strains under different pH conditions.

pH	Plate/Well	Parent	Δ34 RR	Δ30 SK
pH 3.5	PM10/A01	×	×	×
pH 4	PM10/A02	×	×	×
pH 4.5	PM10/A03	◎	△	◎
pH 5	PM10/A04	◎	△	◎
pH 5.5	PM10/A05	◎	△	◎
pH 6	PM10/A06	◎	△	◎
pH 7	PM10/A07	◎	△	◎
pH 8	PM10/A08	◎	△	◎
pH 8.5	PM10/A09	◎	△	◎
pH 9	PM10/A10	◎	△	◎
pH 9.5	PM10/A11	◎	◎	◎
pH 10	PM10/A12	◎	◎	◎
pH 4.5	PM10/B01	○	×	×
pH 4.5 + L-Alanine	PM10/B02	○	×	×
pH 4.5 + L-Arginine	PM10/B03	×	×	×
pH 4.5 + L-Asparagine	PM10/B04	○	×	×
pH 4.5 + L-Aspartic Acid	PM10/B05	×	×	×
pH 4.5 + L-Glutamic Acid	PM10/B06	×	×	×
pH 4.5 + L-Glutamine	PM10/B07	○	×	○
pH 4.5 + Glycine	PM10/B08	○	×	○
pH 4.5 + L-Histidine	PM10/B09	×	×	×
pH 4.5 + L-Isoleucine	PM10/B10	×	×	×
pH 4.5 + L-Leucine	PM10/B11	×	×	×
pH 4.5 + L-Lysine	PM10/B12	◎	×	○
pH 4.5 + L-Methionine	PM10/C01	◎	△	◎
pH 4.5 + L-Phenylalanine	PM10/C02	×	×	×
pH 4.5 + L-Proline	PM10/C03	○	×	×
pH 4.5 + L-Serine	PM10/C04	○	×	○
pH 4.5 + L-Threonine	PM10/C05	○	×	○
pH 4.5 + L-Tryptophan	PM10/C06	×	×	×
pH 4.5 + L-Tyrosine	PM10/C07	△	×	◎
pH 4.5 + L-Valine	PM10/C08	○	×	○
pH 4.5 + Hydroxy-L-Proline	PM10/C09	○	×	○
pH 4.5 + L-Ornithine	PM10/C10	○	×	△
pH 4.5 + L-Homoarginine	PM10/C11	○	×	◎
pH 4.5 + L-Homoserine	PM10/C12	×	×	×
pH 4.5 + Anthranilic Acid	PM10/D01	×	×	×
pH 4.5 + L-Norleucine	PM10/D02	×	×	×
pH 4.5 + L-Norvaline	PM10/D03	○	△	○
pH 4.5 + α-Amino-N-Butyric Acid	PM10/D04	○	×	○
pH 4.5 + p-Aminobenzoate	PM10/D05	×	×	×
pH 4.5 + L-Cysteic acid	PM10/D06	○	×	○
pH 4.5 + D-Lysine	PM10/D07	○	×	○
pH 4.5 + 5-Hydroxy-L-Lysine	PM10/D08	○	×	×
pH 4.5 + 5-Hydroxy-L-Tryptophan	PM10/D09	△	◎	◎
pH 4.5 + D,L Diamino pimelic Acid	PM10/D10	○	×	○
pH 4.5 + Trimethylamine-N-Oxide	PM10/D11	×	×	×
pH 4.5 + Urea	PM10/D12	○	×	△
pH 9.5	PM10/E01	◎	△	◎
pH 9.5 + L-Alanine	PM10/E02	◎	◎	◎
pH 9.5 + L-Arginine	PM10/E03	◎	×	◎
pH 9.5 + L-Asparagine	PM10/E04	◎	×	○
pH 9.5 + L-Aspartic Acid	PM10/E05	◎	△	○

◎: Rapid growth to stationary phase in 24 hours, ○: Delayed growth but same cell mass,
△: Delayed growth and small cell mass, ×: No growth

Appendix Table 7. Viability of Δ34 RR and Δ30 SK strains under different pH conditions. (Continued.)

pH	Plate/Well	Parent	Δ34 RR	Δ30 SK
pH 9.5 + L-Glutamic Acid	PM10/E06	◎	×	◎
pH 9.5 + L-Glutamine	PM10/E07	◎	△	○
pH 9.5 + Glycine	PM10/E08	◎	△	○
pH 9.5 + L-Histidine	PM10/E09	◎	×	○
pH 9.5 + L-Isoleucine	PM10/E10	◎	×	○
pH 9.5 + L-Leucine	PM10/E11	◎	×	×
pH 9.5 + L-Lysine	PM10/E12	◎	×	◎
pH 9.5 + L-Methionine	PM10/F01	◎	×	×
pH 9.5 + L-Phenylalanine	PM10/F02	◎	×	×
pH 9.5 + L-Proline	PM10/F03	◎	○	◎
pH 9.5 + L-Serine	PM10/F04	◎	×	×
pH 9.5 + L-Threonine	PM10/F05	◎	×	○
pH 9.5 + L-Tryptophan	PM10/F06	×	×	×
pH 9.5 + L-Tyrosine	PM10/F07	×	×	×
pH 9.5 + L-Valine	PM10/F08	◎	×	○
pH 9.5 + Hydroxy-L-Proline	PM10/F09	◎	×	×
pH 9.5 + L-Ornithine	PM10/F10	◎	×	×
pH 9.5 + L-Homoarginine	PM10/F11	◎	×	×
pH 9.5 + L-Homoserine	PM10/F12	◎	×	×
pH 9.5 + Anthranilic Acid	PM10/G01	◎	×	×
pH 9.5 + L-Norleucine	PM10/G02	×	×	×
pH 9.5 + L-Norvaline	PM10/G03	◎	×	×
pH 9.5 + Agmatine	PM10/G04	×	×	×
pH 9.5 + Cadaverine	PM10/G05	×	×	×
pH 9.5 + Putrescine	PM10/G06	◎	×	×
pH 9.5 + Histamine	PM10/G07	×	×	×
pH 9.5 + Phenylethylamine	PM10/G08	×	×	×
pH 9.5 + Tyramine	PM10/G09	×	×	×
pH 9.5 + Tryptamine	PM10/G10	◎	◎	◎
pH 9.5 + Trimethylamine-N-Oxide	PM10/G11	◎	△	◎
pH 9.5 + Urea	PM10/G12	◎	△	×
X-Caprylate	PM10/H01	◎	△	◎
X-α-D-Glucoside	PM10/H02	◎	△	◎
X-β-D-Glucoside	PM10/H03	◎	△	◎
X-α-D-Galactoside	PM10/H04	◎	△	◎
X-β-D-Galactoside	PM10/H05	◎	△	◎
X-α-D-Glucuronide	PM10/H06	◎	△	◎
X-β-D-Glucuronide	PM10/H07	◎	△	◎
X-β-D-Glucosaminide	PM10/H08	◎	△	◎
X-β-D-Galactosaminide	PM10/H09	◎	△	◎
X-α-D-Mannoside	PM10/H10	◎	△	◎
X-PO4	PM10/H11	◎	◎	◎
X-SO4	PM10/H12	◎	△	△

◎: Rapid growth to stationary phase in 24 hours, ○: Delayed growth but same cell mass,
△: Delayed growth and small cell mass, ×: No growth

Appendix Table 8. The sensitivity of Δ34 RR and Δ30 SK strains to various antimicrobials.

Antibiotics	Plate/Well	Concentration	Mode of Action	Parent	Δ34 RR	Δ30 SK
Amikacin	PM11/A01	1	protein synthesis, aminoglycoside	◎	△	◎
Amikacin	PM11/A02	2	protein synthesis, aminoglycoside	◎	△	◎
Amikacin	PM11/A03	3	protein synthesis, aminoglycoside	◎	△	◎
Amikacin	PM11/A04	4	protein synthesis, aminoglycoside	◎	△	◎
Chlortetracycline	PM11/A05	1	protein synthesis, tetracycline	◎	△	◎
Chlortetracycline	PM11/A06	2	protein synthesis, tetracycline	◎	△	◎
Chlortetracycline	PM11/A07	3	protein synthesis, tetracycline	◎	◎	◎
Chlortetracycline	PM11/A08	4	protein synthesis, tetracycline	○	○	○
Lincomycin	PM11/A09	1	protein synthesis	◎	△	◎
Lincomycin	PM11/A10	2	protein synthesis	◎	△	◎
Lincomycin	PM11/A11	3	protein synthesis	○	◎	◎
Lincomycin	PM11/A12	4	protein synthesis	△	◎	×
Amoxicillin	PM11/B01	1	wall, lactam	◎	△	◎
Amoxicillin	PM11/B02	2	wall, lactam	◎	△	◎
Amoxicillin	PM11/B03	3	wall, lactam	◎	△	◎
Amoxicillin	PM11/B04	4	wall, lactam	◎	△	◎
Cloxacillin	PM11/B05	1	wall, lactam	◎	△	◎
Cloxacillin	PM11/B06	2	wall, lactam	◎	△	◎
Cloxacillin	PM11/B07	3	wall, lactam	◎	△	◎
Cloxacillin	PM11/B08	4	wall, lactam	◎	×	×
Lomefloxacin	PM11/B09	1	DNA topoisomerase, quinolone	◎	△	◎
Lomefloxacin	PM11/B10	2	DNA topoisomerase, quinolone	◎	△	◎
Lomefloxacin	PM11/B11	3	DNA topoisomerase, quinolone	◎	△	◎
Lomefloxacin	PM11/B12	4	DNA topoisomerase, quinolone	×	☆	☆
Bleomycin	PM11/C01	1	DNA polymerase	◎	△	◎
Bleomycin	PM11/C02	2	DNA polymerase	◎	△	◎
Bleomycin	PM11/C03	3	DNA polymerase	◎	△	◎
Bleomycin	PM11/C04	4	DNA polymerase	◎	△	◎
Colistin	PM11/C05	1	membrane, cyclic peptide	◎	△	◎
Colistin	PM11/C06	2	membrane, cyclic peptide	◎	×	×
Colistin	PM11/C07	3	membrane, cyclic peptide	×	×	×
Colistin	PM11/C08	4	membrane, cyclic peptide	×	×	×
Minocycline	PM11/C09	1	protein synthesis, tetracycline	◎	△	◎
Minocycline	PM11/C10	2	protein synthesis, tetracycline	◎	△	◎
Minocycline	PM11/C11	3	protein synthesis, tetracycline	○	×	☆
Minocycline	PM11/C12	4	protein synthesis, tetracycline	×	×	☆
Capreomycin	PM11/D01	1	respiration, Na^+-K^+ ATPase	◎	△	◎
Capreomycin	PM11/D02	2	respiration, Na^+-K^+ ATPase	◎	△	◎
Capreomycin	PM11/D03	3	respiration, Na^+-K^+ ATPase	◎	△	◎
Capreomycin	PM11/D04	4	respiration, Na^+-K^+ ATPase	◎	○	○
Demeclocyline	PM11/D05	1	protein synthesis, tetracycline	◎	△	◎
Demeclocyline	PM11/D06	2	protein synthesis, tetracycline	◎	△	◎
Demeclocyline	PM11/D07	3	protein synthesis, tetracycline	◎	△	◎
Demeclocyline	PM11/D08	4	protein synthesis, tetracycline	×	×	×
Nafcillin	PM11/D09	1	wall, lactam	◎	△	◎
Nafcillin	PM11/D10	2	wall, lactam	◎	△	◎
Nafcillin	PM11/D11	3	wall, lactam	△	○	◎
Nafcillin	PM11/D12	4	wall, lactam	◎	×	×
Cefazolin	PM11/E01	1	wall, cephalosporin	◎	△	◎
Cefazolin	PM11/E02	2	wall, cephalosporin	◎	△	◎
Cefazolin	PM11/E03	3	wall, cephalosporin	◎	△	◎
Cefazolin	PM11/E04	4	wall, cephalosporin	◎	△	◎
Enoxacin	PM11/E05	1	DNA topoisomerase, quinolone	◎	△	◎
Enoxacin	PM11/E06	2	DNA topoisomerase, quinolone	◎	△	◎
Enoxacin	PM11/E07	3	DNA topoisomerase, quinolone	◎	△	◎
Enoxacin	PM11/E08	4	DNA topoisomerase, quinolone	×	☆	×
Nalidixic Acid	PM11/E09	1	DNA topoisomerase	◎	△	◎
Nalidixic Acid	PM11/E10	2	DNA topoisomerase	◎	△	◎
Nalidixic Acid	PM11/E11	3	DNA topoisomerase	○	△	×
Nalidixic Acid	PM11/E12	4	DNA topoisomerase	×	×	×
Cefotaxime	PM11/F01	1	wall, cephalosporin	◎	△	◎
Cefotaxime	PM11/F02	2	wall, cephalosporin	◎	△	◎
Cefotaxime	PM11/F03	3	wall, cephalosporin	○	△	○
Cefotaxime	PM11/F04	4	wall, cephalosporin	×	×	×
Erythromycin	PM11/F05	1	protein synthesis, macrolide	◎	△	◎
Erythromycin	PM11/F06	2	protein synthesis, macrolide	◎	△	◎
Erythromycin	PM11/F07	3	protein synthesis, macrolide	◎	△	◎
Erythromycin	PM11/F08	4	protein synthesis, macrolide	◎	△	◎
Neomycin	PM11/F09	1	protein synthesis, aminoglycoside	◎	△	◎
Neomycin	PM11/F10	2	protein synthesis, aminoglycoside	○	◎	◎
Neomycin	PM11/F11	3	protein synthesis, aminoglycoside	○	◎	◎
Neomycin	PM11/F12	4	protein synthesis, aminoglycoside	○	△	◎
Ceftriaxone	PM11/G01	1	wall, cephalosporin	◎	△	◎
Ceftriaxone	PM11/G02	2	wall, cephalosporin	◎	△	◎
Ceftriaxone	PM11/G03	3	wall, cephalosporin	◎	△	◎
Ceftriaxone	PM11/G04	4	wall, cephalosporin	◎	△	◎
Gentamicin	PM11/G05	1	protein synthesis, aminoglycoside	◎	△	◎
Gentamicin	PM11/G06	2	protein synthesis, aminoglycoside	◎	△	◎
Gentamicin	PM11/G07	3	protein synthesis, aminoglycoside	◎	△	◎
Gentamicin	PM11/G08	4	protein synthesis, aminoglycoside	◎	△	◎
Norfloxacin	PM11/G09	1	DNA topoisomerase, quinolone	◎	△	◎
Norfloxacin	PM11/G10	2	DNA topoisomerase, quinolone	◎	○	◎
Norfloxacin	PM11/G11	3	DNA topoisomerase, quinolone	○	◎	◎
Norfloxacin	PM11/G12	4	DNA topoisomerase, quinolone	○	◎	◎
Cephalothin	PM11/H01	1	wall, cephalosporin	◎	△	◎
Cephalothin	PM11/H02	2	wall, cephalosporin	◎	△	○
Cephalothin	PM11/H03	3	wall, cephalosporin	◎	△	○
Cephalothin	PM11/H04	4	wall, cephalosporin	◎	△	○

◎: Rapid growth to stationary phase in 24 hours, ○: Delayed growth but same cell mass, △: Delayed growth and small cell mass, ×: No growth, ☆: Faster growth than the parent strain.

Appendix Table 8. The sensitivity of Δ34 RR and Δ30 SK strains to various antimicrobials. (Continued.)

Antibiotics	Plate/Well	Concentration	Mode of Action	Parent	Δ34 RR	Δ30 SK
Kanamycin	PM11/H05	1	protein synthesis, aminoglycoside	◎	△	○
Kanamycin	PM11/H06	2	protein synthesis, aminoglycoside	◎	△	○
Kanamycin	PM11/H07	3	protein synthesis, aminoglycoside	◎	△	○
Kanamycin	PM11/H08	4	protein synthesis, aminoglycoside	◎	△	△
Ofloxacin	PM11/H09	1	DNA topoisomerase, quinolone	◎	△	◎
Ofloxacin	PM11/H10	2	DNA topoisomerase, quinolone	◎	△	◎
Ofloxacin	PM11/H11	3	DNA topoisomerase, quinolone	◎	△	◎
Ofloxacin	PM11/H12	4	DNA topoisomerase, quinolone	△	◎	×
Penicillin G	PM12/A01	1	wall, lactam	◎	△	◎
Penicillin G	PM12/A02	2	wall, lactam	◎	△	◎
Penicillin G	PM12/A03	3	wall, lactam	◎	△	○
Penicillin G	PM12/A04	4	wall, lactam	◎	×	×
Tetracycline	PM12/A05	1	protein synthesis, tetracycline	◎	△	◎
Tetracycline	PM12/A06	2	protein synthesis, tetracycline	◎	△	◎
Tetracycline	PM12/A07	3	protein synthesis, tetracycline	◎	△	◎
Tetracycline	PM12/A08	4	protein synthesis, tetracycline	◎	△	◎
Carbenicillin	PM12/A09	1		◎	△	◎
Carbenicillin	PM12/A10	2		◎	△	◎
Carbenicillin	PM12/A11	3		◎	△	○
Carbenicillin	PM12/A12	4		◎	△	○
Oxacillin	PM12/B01	1	wall, lactam	◎	△	◎
Oxacillin	PM12/B02	2	wall, lactam	◎	△	◎
Oxacillin	PM12/B03	3	wall, lactam	○	△	△
Oxacillin	PM12/B04	4	wall, lactam	×	×	×
Penimepicycline	PM12/B05	1	protein synthesis, tetracycline	◎	△	◎
Penimepicycline	PM12/B06	2	protein synthesis, tetracycline	◎	△	◎
Penimepicycline	PM12/B07	3	protein synthesis, tetracycline	◎	△	◎
Penimepicycline	PM12/B08	4	protein synthesis, tetracycline	◎	△	◎
Polymyxin B	PM12/B09	1	membrane, outer	◎	△	◎
Polymyxin B	PM12/B10	2	membrane, outer	◎	△	◎
Polymyxin B	PM12/B11	3	membrane, outer	×	×	×
Polymyxin B	PM12/B12	4	membrane, outer	×	×	×
Paromomycin	PM12/C01	1	protein synthesis, aminoglycoside	◎	△	◎
Paromomycin	PM12/C02	2	protein synthesis, aminoglycoside	◎	△	◎
Paromomycin	PM12/C03	3	protein synthesis, aminoglycoside	◎	△	◎
Paromomycin	PM12/C04	4	protein synthesis, aminoglycoside	○	△	◎
Vancomycin	PM12/C05	1	protein synthesis	◎	△	◎
Vancomycin	PM12/C06	2	protein synthesis	◎	△	◎
Vancomycin	PM12/C07	3	protein synthesis	◎	×	×
Vancomycin	PM12/C08	4	protein synthesis	○	×	×
D,L-Serine Hydroxamate	PM12/C09	1	tRNA synthetase	◎	△	◎
D,L-Serine Hydroxamate	PM12/C10	2	tRNA synthetase	◎	△	◎
D,L-Serine Hydroxamate	PM12/C11	3	tRNA synthetase	◎	◎	◎
D,L-Serine Hydroxamate	PM12/C12	4	tRNA synthetase	△	○	○
Sisomicin	PM12/D01	1	protein synthesis, aminoglycoside	◎	△	◎
Sisomicin	PM12/D02	2	protein synthesis, aminoglycoside	◎	○	◎
Sisomicin	PM12/D03	3	protein synthesis, aminoglycoside	◎	△	◎
Sisomicin	PM12/D04	4	protein synthesis, aminoglycoside	×	×	×
Sulfamethazine	PM12/D05	1	folate antagonist	◎	△	◎
Sulfamethazine	PM12/D06	2	folate antagonist	◎	△	◎
Sulfamethazine	PM12/D07	3	folate antagonist	○	△	△
Sulfamethazine	PM12/D08	4	folate antagonist	○	△	×
Novobiocin	PM12/D09	1	DNA topoisomerase	◎	△	◎
Novobiocin	PM12/D10	2	DNA topoisomerase	◎	△	◎
Novobiocin	PM12/D11	3	DNA topoisomerase	○	△	△
Novobiocin	PM12/D12	4	DNA topoisomerase	△	×	×
2,4-Diamino-6,7-Diisopropylpteridine	PM12/E01	1		◎	△	◎
2,4-Diamino-6,7-Diisopropylpteridine	PM12/E02	2		◎	△	◎
2,4-Diamino-6,7-Diisopropylpteridine	PM12/E03	3		○	△	○
2,4-Diamino-6,7-Diisopropylpteridine	PM12/E04	4		×	×	×
Sulfadiazine	PM12/E05	1	folate antagonist	◎	○	◎
Sulfadiazine	PM12/E06	2	folate antagonist	◎	△	○
Sulfadiazine	PM12/E07	3	folate antagonist	○	△	×
Sulfadiazine	PM12/E08	4	folate antagonist	○	△	×
Benzethonium Chloride	PM12/E09	1	membrane, detergent, cationic	◎	○	◎
Benzethonium Chloride	PM12/E10	2	membrane, detergent, cationic	◎	△	◎
Benzethonium Chloride	PM12/E11	3	membrane, detergent, cationic	○	×	×
Benzethonium Chloride	PM12/E12	4	membrane, detergent, cationic	×	×	×
Tobramycin	PM12/F01	1	protein synthesis, aminoglycoside	◎	△	◎
Tobramycin	PM12/F02	2	protein synthesis, aminoglycoside	◎	○	◎
Tobramycin	PM12/F03	3	protein synthesis, aminoglycoside	○	△	○
Tobramycin	PM12/F04	4	protein synthesis, aminoglycoside	△	×	×
Sulfathiazole	PM12/F05	1	folate antagonist	◎	○	◎
Sulfathiazole	PM12/F06	2	folate antagonist	◎	○	○
Sulfathiazole	PM12/F07	3	folate antagonist	○	△	×
Sulfathiazole	PM12/F08	4	folate antagonist	○	△	×
5-Fluoroorotic Acid	PM12/F09	1		◎	○	◎
5-Fluoroorotic Acid	PM12/F10	2		◎	○	◎
5-Fluoroorotic Acid	PM12/F11	3		◎	○	◎
5-Fluoroorotic Acid	PM12/F12	4		◎	○	◎
Spectinomycin	PM12/G01	1	protein synthesis	◎	△	◎
Spectinomycin	PM12/G02	2	protein synthesis	◎	△	◎
Spectinomycin	PM12/G03	3	protein synthesis	◎	△	◎
Spectinomycin	PM12/G04	4	protein synthesis	◎	△	◎
Sulfamethoxazole	PM12/G05	1	folate antagonist	◎	△	◎
Sulfamethoxazole	PM12/G06	2	folate antagonist	◎	○	○
Sulfamethoxazole	PM12/G07	3	folate antagonist	○	○	×
Sulfamethoxazole	PM12/G08	4	folate antagonist	○	△	×
L-Aspartic-β-Hydroxamate	PM12/G09	1	tRNA synthetase	◎	◎	◎
L-Aspartic-β-Hydroxamate	PM12/G10	2	tRNA synthetase	◎	△	◎
L-Aspartic-β-Hydroxamate	PM12/G11	3	tRNA synthetase	◎	○	○
L-Aspartic-β-Hydroxamate	PM12/G12	4	tRNA synthetase	○	△	○

◎: Rapid growth to stationary phase in 24 hours, ○: Delayed growth but same cell mass, △: Delayed growth and small cell mass, ×: No growth, ☆: Faster growth than the parent strain.

Appendix Table 8. The sensitivity of Δ34 RR and Δ30 SK strains to various antimicrobials. (Continued.)

Antibiotics	Plate/Well	Concentration	Mode of Action	Parent	Δ34 RR	Δ30 SK
Spiramycin	PM12/H01	1	protein synthesis, macrolide	◎	△	◎
Spiramycin	PM12/H02	2	protein synthesis, macrolide	◎	△	◎
Spiramycin	PM12/H03	3	protein synthesis, macrolide	◎	△	◎
Spiramycin	PM12/H04	4	protein synthesis, macrolide	△	×	×
Rifampicin	PM12/H05	1	RNA polymerase	◎	△	◎
Rifampicin	PM12/H06	2	RNA polymerase	◎	△	◎
Rifampicin	PM12/H07	3	RNA polymerase	◎	△	◎
Rifampicin	PM12/H08	4	RNA polymerase	◎	△	○
Dodecyltrimethyl Ammonium Bromide	PM12/H09	1	membrane, detergent, cationic	◎	△	◎
Dodecyltrimethyl Ammonium Bromide	PM12/H10	2	membrane, detergent, cationic	◎	△	◎
Dodecyltrimethyl Ammonium Bromide	PM12/H11	3	membrane, detergent, cationic	△	×	☆
Dodecyltrimethyl Ammonium Bromide	PM12/H12	4	membrane, detergent, cationic	×	×	×
Ampicillin	PM13/A01	1	wall, lactam	◎	△	◎
Ampicillin	PM13/A02	2	wall, lactam	◎	△	◎
Ampicillin	PM13/A03	3	wall, lactam	◎	△	◎
Ampicillin	PM13/A04	4	wall, lactam	◎	△	◎
Dequalinium	PM13/A05	1	ion channal inhibitor, K^+ (m)	◎	△	◎
Dequalinium	PM13/A06	2	ion channal inhibitor, K^+ (m)	○	×	×
Dequalinium	PM13/A07	3	ion channal inhibitor, K^+ (m)	×	×	×
Dequalinium	PM13/A08	4	ion channal inhibitor, K^+ (m)	×	×	×
Nickel chloride	PM13/A09	1	toxic cation	◎	△	◎
Nickel chloride	PM13/A10	2	toxic cation	◎	△	◎
Nickel chloride	PM13/A11	3	toxic cation	◎	△	◎
Nickel chloride	PM13/A12	4	toxic cation	×	×	×
Azlocillin	PM13/B01	1	wall, lactam	◎	△	◎
Azlocillin	PM13/B02	2	wall, lactam	◎	△	◎
Azlocillin	PM13/B03	3	wall, lactam	◎	△	◎
Azlocillin	PM13/B04	4	wall, lactam	◎	△	△
2,2'-Dipyridyl	PM13/B05	1	chelator, Fe^{++}	◎	△	◎
2,2'-Dipyridyl	PM13/B06	2	chelator, Fe^{++}	×	×	×
2,2'-Dipyridyl	PM13/B07	3	chelator, Fe^{++}	×	×	×
2,2'-Dipyridyl	PM13/B08	4	chelator, Fe^{++}	×	×	×
Oxolinic acid	PM13/B09	1	DNA unwinding, gyrase (GN), topoisomerase (GP), quinolone	◎	△	◎
Oxolinic acid	PM13/B10	2	DNA unwinding, gyrase (GN), topoisomerase (GP), quinolone	◎	△	◎
Oxolinic acid	PM13/B11	3	DNA unwinding, gyrase (GN), topoisomerase (GP), quinolone	○	△	△
Oxolinic acid	PM13/B12	4	DNA unwinding, gyrase (GN), topoisomerase (GP), quinolone	×	×	×
6-Mercaptopurine	PM13/C01	1	nucleic acid analog, purine	◎	◎	◎
6-Mercaptopurine	PM13/C02	2	nucleic acid analog, purine	○	◎	◎
6-Mercaptopurine	PM13/C03	3	nucleic acid analog, purine	○	△	◎
6-Mercaptopurine	PM13/C04	4	nucleic acid analog, purine	△	×	×
Doxycycline	PM13/C05	1	protein synthesis, tetracycline	◎	○	◎
Doxycycline	PM13/C06	2	protein synthesis, tetracycline	◎	○	○
Doxycycline	PM13/C07	3	protein synthesis, tetracycline	○	×	×
Doxycycline	PM13/C08	4	protein synthesis, tetracycline	×	×	×
Potassium chromate	PM13/C09	1	toxic anion	◎	△	◎
Potassium chromate	PM13/C10	2	toxic anion	○	×	◎
Potassium chromate	PM13/C11	3	toxic anion	△	×	×
Potassium chromate	PM13/C12	4	toxic anion	×	×	×
Cefuroxime	PM13/D01	1	wall, cephalosporin second generation	◎	△	◎
Cefuroxime	PM13/D02	2	wall, cephalosporin second generation	◎	△	◎
Cefuroxime	PM13/D03	3	wall, cephalosporin second generation	○	◎	◎
Cefuroxime	PM13/D04	4	wall, cephalosporin second generation	×	☆	☆
5-Fluorouracil	PM13/D05	1	nucleic acid analog, pyrimidine	◎	△	◎
5-Fluorouracil	PM13/D06	2	nucleic acid analog, pyrimidine	◎	△	◎
5-Fluorouracil	PM13/D07	3	nucleic acid analog, pyrimidine	◎	△	◎
5-Fluorouracil	PM13/D08	4	nucleic acid analog, pyrimidine	◎	△	◎
Rolitetracycline	PM13/D09	1	protein synthesis, 30S ribosomal subunit, tetracycline	◎	△	◎
Rolitetracycline	PM13/D10	2	protein synthesis, 30S ribosomal subunit, tetracycline	◎	△	◎
Rolitetracycline	PM13/D11	3	protein synthesis, 30S ribosomal subunit, tetracycline	○	◎	◎
Rolitetracycline	PM13/D12	4	protein synthesis, 30S ribosomal subunit, tetracycline	○	△	○
Cytosine arabinoside	PM13/E01	1	nucleic acid analog, pyrimidine	◎	◎	◎
Cytosine arabinoside	PM13/E02	2	nucleic acid analog, pyrimidine	◎	◎	◎
Cytosine arabinoside	PM13/E03	3	nucleic acid analog, pyrimidine	◎	△	◎
Cytosine arabinoside	PM13/E04	4	nucleic acid analog, pyrimidine	◎	△	△
Geneticin (G418)	PM13/E05	1	protein synthesis, aminoglycoside	◎	△	◎
Geneticin (G418)	PM13/E06	2	protein synthesis, aminoglycoside	◎	△	◎
Geneticin (G418)	PM13/E07	3	protein synthesis, aminoglycoside	◎	△	◎
Geneticin (G418)	PM13/E08	4	protein synthesis, aminoglycoside	○	△	◎
Ruthenium red	PM13/E09	1	respiration, mitochondrial Ca^{++} porter	◎	△	◎
Ruthenium red	PM13/E10	2	respiration, mitochondrial Ca^{++} porter	◎	△	◎
Ruthenium red	PM13/E11	3	respiration, mitochondrial Ca^{++} porter	◎	△	◎
Ruthenium red	PM13/E12	4	respiration, mitochondrial Ca^{++} porter	◎	△	◎
Cesium chloride	PM13/F01	1	toxic cation	◎	△	◎
Cesium chloride	PM13/F02	2	toxic cation	◎	△	◎
Cesium chloride	PM13/F03	3	toxic cation	◎	△	◎
Cesium chloride	PM13/F04	4	toxic cation	◎	△	△
Glycine	PM13/F05	1	wall	◎	△	◎
Glycine	PM13/F06	2	wall	◎	△	◎
Glycine	PM13/F07	3	wall	◎	△	◎
Glycine	PM13/F08	4	wall	◎	△	◎
Thallium (I) acetate	PM13/F09	1	toxic cation	◎	△	◎
Thallium (I) acetate	PM13/F10	2	toxic cation	◎	○	◎
Thallium (I) acetate	PM13/F11	3	toxic cation	○	×	◎
Thallium (I) acetate	PM13/F12	4	toxic cation	○	×	×
Cobalt chloride	PM13/G01	1	toxic cation	◎	△	◎
Cobalt chloride	PM13/G02	2	toxic cation	◎	△	◎
Cobalt chloride	PM13/G03	3	toxic cation	○	×	△
Cobalt chloride	PM13/G04	4	toxic cation	×	×	×
Manganese (II) chloride	PM13/G05	1	toxic cation	◎	○	◎
Manganese (II) chloride	PM13/G06	2	toxic cation	◎	△	◎
Manganese (II) chloride	PM13/G07	3	toxic cation	◎	△	○
Manganese (II) chloride	PM13/G08	4	toxic cation	×	×	×

◎: Rapid growth to stationary phase in 24 hours, ○: Delayed growth but same cell mass, △: Delayed growth and small cell mass, ×: No growth, ☆: Faster growth than the parent strain.

Appendix Table 8. The sensitivity of Δ34 RR and Δ30 SK strains to various antimicrobials. (Continued.)

Antibiotics	Plate/Well	Concentration	Mode of Action	Parent	Δ34 RR	Δ30 SK
Trifluoperazine	PM13/G09	1	cell cycle modulation, DNA synthesis, Ca^{2+}/calmodulin dependent protein phosphorylation and lipid	◎	○	◎
Trifluoperazine	PM13/G10	2	cell cycle modulation, DNA synthesis, Ca^{2+}/calmodulin dependent protein phosphorylation and lipid	◎	○	◎
Trifluoperazine	PM13/G11	3	cell cycle modulation, DNA synthesis, Ca^{2+}/calmodulin dependent protein phosphorylation and lipid	○	△	◎
Trifluoperazine	PM13/G12	4	cell cycle modulation, DNA synthesis, Ca^{2+}/calmodulin dependent protein phosphorylation and lipid	○	×	×
Cupric chloride	PM13/H01	1	toxic cation	◎	◎	◎
Cupric chloride	PM13/H02	2	toxic cation	◎	○	◎
Cupric chloride	PM13/H03	3	toxic cation	○	×	◎
Cupric chloride	PM13/H04	4	toxic cation	△	×	×
Moxalactam	PM13/H05	1	wall, lactam	◎	△	◎
Moxalactam	PM13/H06	2	wall, lactam	◎	△	◎
Moxalactam	PM13/H07	3	wall, lactam	◎	△	◎
Moxalactam	PM13/H08	4	wall, lactam	◎	△	◎
Tylosin	PM13/H09	1	protein synthesis, 50S ribosomal subunit, macrolide	◎	△	◎
Tylosin	PM13/H10	2	protein synthesis, 50S ribosomal subunit, macrolide	◎	△	◎
Tylosin	PM13/H11	3	protein synthesis, 50S ribosomal subunit, macrolide	○	○	◎
Tylosin	PM13/H12	4	protein synthesis, 50S ribosomal subunit, macrolide	△	×	×
Acriflavine	PM14/A01	1	DNA intercalator	◎	△	◎
Acriflavine	PM14/A02	2	DNA intercalator	◎	◎	◎
Acriflavine	PM14/A03	3	DNA intercalator	◎	◎	◎
Acriflavine	PM14/A04	4	DNA intercalator	◎	○	○
Furaltadone	PM14/A05	1	DNA synthesis, nitro-compound, multiple sites	◎	△	○
Furaltadone	PM14/A06	2	DNA synthesis, nitro-compound, multiple sites	◎	△	○
Furaltadone	PM14/A07	3	DNA synthesis, nitro-compound, multiple sites	○	△	○
Furaltadone	PM14/A08	4	DNA synthesis, nitro-compound, multiple sites	×	☆	×
Sanguinarine	PM14/A09	1	ATPase, Na^{+}/K^{+} and Mg^{++}	◎	○	◎
Sanguinarine	PM14/A10	2	ATPase, Na^{+}/K^{+} and Mg^{++}	○	△	◎
Sanguinarine	PM14/A11	3	ATPase, Na^{+}/K^{+} and Mg^{++}	△	×	△
Sanguinarine	PM14/A12	4	ATPase, Na^{+}/K^{+} and Mg^{++}	×	×	☆
9-Aminoacridine	PM14/B01	1	DNA intercalator	◎	△	◎
9-Aminoacridine	PM14/B02	2	DNA intercalator	◎	◎	◎
9-Aminoacridine	PM14/B03	3	DNA intercalator	◎	△	◎
9-Aminoacridine	PM14/B04	4	DNA intercalator	△	×	×
Fusaric Acid	PM14/B05	1	chelator, lipophilic	◎	△	○
Fusaric Acid	PM14/B06	2	chelator, lipophilic	◎	△	○
Fusaric Acid	PM14/B07	3	chelator, lipophilic	○	×	×
Fusaric Acid	PM14/B08	4	chelator, lipophilic	×	×	×
Sodium Arsenate	PM14/B09	1	transport, toxic anion, PO4 analog	◎	△	◎
Sodium Arsenate	PM14/B10	2	transport, toxic anion, PO4 analog	◎	△	◎
Sodium Arsenate	PM14/B11	3	transport, toxic anion, PO4 analog	◎	△	○
Sodium Arsenate	PM14/B12	4	transport, toxic anion, PO4 analog	◎	△	△
Boric Acid	PM14/C01	1	transport, toxic anion	◎	△	◎
Boric Acid	PM14/C02	2	transport, toxic anion	◎	△	◎
Boric Acid	PM14/C03	3	transport, toxic anion	◎	×	◎
Boric Acid	PM14/C04	4	transport, toxic anion	×	×	×
1-Hydroxy-Pyridine-2-thione	PM14/C05	1	chelator, lipophilic	◎	△	○
1-Hydroxy-Pyridine-2-thione	PM14/C06	2	chelator, lipophilic	◎	△	◎
1-Hydroxy-Pyridine-2-thione	PM14/C07	3	chelator, lipophilic	◎	△	◎
1-Hydroxy-Pyridine-2-thione	PM14/C08	4	chelator, lipophilic	○	×	△
Sodium Cyanate	PM14/C09	1	transport, toxic anion	◎	△	◎
Sodium Cyanate	PM14/C10	2	transport, toxic anion	◎	△	◎
Sodium Cyanate	PM14/C11	3	transport, toxic anion	◎	△	○
Sodium Cyanate	PM14/C12	4	transport, toxic anion	△	×	○
Cadmium Chloride	PM14/D01	1	transport, toxic cation	◎	△	◎
Cadmium Chloride	PM14/D02	2	transport, toxic cation	◎	×	◎
Cadmium Chloride	PM14/D03	3	transport, toxic cation	◎	×	◎
Cadmium Chloride	PM14/D04	4	transport, toxic cation	×	×	×
Iodoacetate	PM14/D05	1	oxidation, sulfhydryl	◎	△	○
Iodoacetate	PM14/D06	2	oxidation, sulfhydryl	◎	○	◎
Iodoacetate	PM14/D07	3	oxidation, sulfhydryl	○	×	×
Iodoacetate	PM14/D08	4	oxidation, sulfhydryl	×	×	×
Sodium Dichromate	PM14/D09	1	transport, toxic anion, SO4 analog	◎	△	◎
Sodium Dichromate	PM14/D10	2	transport, toxic anion, SO4 analog	◎	△	◎
Sodium Dichromate	PM14/D11	3	transport, toxic anion, SO4 analog	○	△	◎
Sodium Dichromate	PM14/D12	4	transport, toxic anion, SO4 analog	○	×	○
Cefoxitin	PM14/E01	1	wall, cephalosporin	◎	△	◎
Cefoxitin	PM14/E02	2	wall, cephalosporin	◎	△	◎
Cefoxitin	PM14/E03	3	wall, cephalosporin	◎	△	◎
Cefoxitin	PM14/E04	4	wall, cephalosporin	○	△	◎
Nitrofurantoin	PM14/E05	1	DNA synthesis, nitro-compound, multiple sites	◎	△	○
Nitrofurantoin	PM14/E06	2	DNA synthesis, nitro-compound, multiple sites	◎	△	◎
Nitrofurantoin	PM14/E07	3	DNA synthesis, nitro-compound, multiple sites	◎	△	◎
Nitrofurantoin	PM14/E08	4	DNA synthesis, nitro-compound, multiple sites	○	△	○
Sodium Metaborate	PM14/E09	1	transport, toxic anion	◎	△	◎
Sodium Metaborate	PM14/E10	2	transport, toxic anion	◎	△	○
Sodium Metaborate	PM14/E11	3	transport, toxic anion	○	×	○
Sodium Metaborate	PM14/E12	4	transport, toxic anion	×	×	☆
Chloramphenicol	PM14/F01	1	protein synthesis	◎	△	◎
Chloramphenicol	PM14/F02	2	protein synthesis	◎	△	◎
Chloramphenicol	PM14/F03	3	protein synthesis	○	△	◎
Chloramphenicol	PM14/F04	4	protein synthesis	△	△	△
Piperacillin	PM14/F05	1	wall, lactam	◎	△	○
Piperacillin	PM14/F06	2	wall, lactam	◎	△	◎
Piperacillin	PM14/F07	3	wall, lactam	◎	△	◎
Piperacillin	PM14/F08	4	wall, lactam	◎	○	◎
Sodium Metavanadate	PM14/F09	1	transport, toxic anion, PO4 analog	×	×	×
Sodium Metavanadate	PM14/F10	2	transport, toxic anion, PO4 analog	×	×	×
Sodium Metavanadate	PM14/F11	3	transport, toxic anion, PO4 analog	×	×	×
Sodium Metavanadate	PM14/F12	4	transport, toxic anion, PO4 analog	×	×	×
Chelerythrine	PM14/G01	1	protein kinase C	◎	△	◎
Chelerythrine	PM14/G02	2	protein kinase C	◎	△	◎
Chelerythrine	PM14/G03	3	protein kinase C	○	△	◎
Chelerythrine	PM14/G04	4	protein kinase C	△	△	○

◎: Rapid growth to stationary phase in 24 hours, ○: Delayed growth but same cell mass, △: Delayed growth and small cell mass, ×: No growth, ☆: Faster growth than the parent strain.

Appendix Table 8. The sensitivity of Δ34 RR and Δ30 SK strains to various antimicrobials. (Continued.)

Antibiotics	Plate/Well	Concentration	Mode of Action	Parent	Δ34 RR	Δ30 SK
Carbenicillin	PM14/G05	1	wall, lactam	◎	△	○
Carbenicillin	PM14/G06	2	wall, lactam	◎	△	○
Carbenicillin	PM14/G07	3	wall, lactam	○	○	◎
Carbenicillin	PM14/G08	4	wall, lactam	×	×	×
Sodium Nitrite	PM14/G09	1	transport, toxic anion	◎	△	◎
Sodium Nitrite	PM14/G10	2	transport, toxic anion	◎	△	○
Sodium Nitrite	PM14/G11	3	transport, toxic anion	△	×	○
Sodium Nitrite	PM14/G12	4	transport, toxic anion	×	×	×
EGTA	PM14/H01	1	chelator, Ca^{++}	◎	△	◎
EGTA	PM14/H02	2	chelator, Ca^{++}	◎	×	◎
EGTA	PM14/H03	3	chelator, Ca^{++}	◎	×	◎
EGTA	PM14/H04	4	chelator, Ca^{++}	◎	△	◎
Promethazine	PM14/H05	1	cyclic nucleotide phosphodiesterase	◎	△	○
Promethazine	PM14/H06	2	cyclic nucleotide phosphodiesterase	◎	○	◎
Promethazine	PM14/H07	3	cyclic nucleotide phosphodiesterase	△	×	△
Promethazine	PM14/H08	4	cyclic nucleotide phosphodiesterase	×	×	×
Sodium Orthovanadate	PM14/H09	1	transport, toxic anion, PO4 analog	○	○	○
Sodium Orthovanadate	PM14/H10	2	transport, toxic anion, PO4 analog	×	×	×
Sodium Orthovanadate	PM14/H11	3	transport, toxic anion, PO4 analog	×	×	×
Sodium Orthovanadate	PM14/H12	4	transport, toxic anion, PO4 analog	×	×	×
Procaine	PM15/A01	1	ion channal inhibitor, Na^{+} (m)	◎	△	◎
Procaine	PM15/A02	2	ion channal inhibitor, Na^{+} (m)	◎	○	◎
Procaine	PM15/A03	3	ion channal inhibitor, Na^{+} (m)	◎	×	◎
Procaine	PM15/A04	4	ion channal inhibitor, Na^{+} (m)	△	×	○
Guanidine hydrochloride	PM15/A05	1	membrane, chaotropic agent	◎	△	◎
Guanidine hydrochloride	PM15/A06	2	membrane, chaotropic agent	◎	△	◎
Guanidine hydrochloride	PM15/A07	3	membrane, chaotropic agent	○	×	×
Guanidine hydrochloride	PM15/A08	4	membrane, chaotropic agent	×	×	×
Cefmetazole	PM15/A09	1	wall, cephalosporin second generation	◎	△	◎
Cefmetazole	PM15/A10	2	wall, cephalosporin second generation	◎	△	◎
Cefmetazole	PM15/A11	3	wall, cephalosporin second generation	◎	△	◎
Cefmetazole	PM15/A12	4	wall, cephalosporin second generation	◎	△	○
D-Cycloserine	PM15/B01	1	wall, sphingolipid synthesis	◎	△	◎
D-Cycloserine	PM15/B02	2	wall, sphingolipid synthesis	◎	△	◎
D-Cycloserine	PM15/B03	3	wall, sphingolipid synthesis	◎	△	◎
D-Cycloserine	PM15/B04	4	wall, sphingolipid synthesis	◎	△	◎
EDTA	PM15/B05	1	chelator, hydrophilic	◎	△	◎
EDTA	PM15/B06	2	chelator, hydrophilic	◎	△	○
EDTA	PM15/B07	3	chelator, hydrophilic	◎	×	×
EDTA	PM15/B08	4	chelator, hydrophilic	×	×	×
5,7-Dichloro-8-hydroxy-quinaldine	PM15/B09	1	chelator, lipophilic	◎	△	◎
5,7-Dichloro-8-hydroxy-quinaldine	PM15/B10	2	chelator, lipophilic	◎	△	◎
5,7-Dichloro-8-hydroxy-quinaldine	PM15/B11	3	chelator, lipophilic	○	△	◎
5,7-Dichloro-8-hydroxy-quinaldine	PM15/B12	4	chelator, lipophilic	◎	○	○
5,7-Dichloro-8-hydroxyquinoline	PM15/C01	1	chelator, lipophilic	◎	△	◎
5,7-Dichloro-8-hydroxyquinoline	PM15/C02	2	chelator, lipophilic	◎	△	◎
5,7-Dichloro-8-hydroxyquinoline	PM15/C03	3	chelator, lipophilic	◎	△	◎
5,7-Dichloro-8-hydroxyquinoline	PM15/C04	4	chelator, lipophilic	△	×	×
Fusidic acid	PM15/C05	1	protein synthesis, elongation factor	◎	△	◎
Fusidic acid	PM15/C06	2	protein synthesis, elongation factor	◎	△	◎
Fusidic acid	PM15/C07	3	protein synthesis, elongation factor	○	○	○
Fusidic acid	PM15/C08	4	protein synthesis, elongation factor	○	○	◎
1,10-Phenanthroline	PM15/C09	1	chelator, Fe^{++}, Zn^{++}, divalent metal ions	◎	○	◎
1,10-Phenanthroline	PM15/C10	2	chelator, Fe^{++}, Zn^{++}, divalent metal ions	◎	△	◎
1,10-Phenanthroline	PM15/C11	3	chelator, Fe^{++}, Zn^{++}, divalent metal ions	×	×	×
1,10-Phenanthroline	PM15/C12	4	chelator, Fe^{++}, Zn^{++}, divalent metal ions	×	×	×
Phleomycin	PM15/D01	1	DNA damage, oxidative, ionizing ratiation	◎	△	◎
Phleomycin	PM15/D02	2	DNA damage, oxidative, ionizing ratiation	◎	△	◎
Phleomycin	PM15/D03	3	DNA damage, oxidative, ionizing ratiation	◎	△	○
Phleomycin	PM15/D04	4	DNA damage, oxidative, ionizing ratiation	○	△	×
Domiphen bromide	PM15/D05	1	membrane, detergent, cationic, fungiside	◎	△	◎
Domiphen bromide	PM15/D06	2	membrane, detergent, cationic, fungiside	◎	○	◎
Domiphen bromide	PM15/D07	3	membrane, detergent, cationic, fungiside	○	×	◎
Domiphen bromide	PM15/D08	4	membrane, detergent, cationic, fungiside	×	×	×
Nordihydroguaiaretic acid	PM15/D09	1	lipoxygenase, fungicide	◎	△	◎
Nordihydroguaiaretic acid	PM15/D10	2	lipoxygenase, fungicide	◎	○	◎
Nordihydroguaiaretic acid	PM15/D11	3	lipoxygenase, fungicide	◎	○	◎
Nordihydroguaiaretic acid	PM15/D12	4	lipoxygenase, fungicide	◎	△	◎
Alexidine	PM15/E01	1	membrane, biguanide, electron transport	◎	×	◎
Alexidine	PM15/E02	2	membrane, biguanide, electron transport	○	×	×
Alexidine	PM15/E03	3	membrane, biguanide, electron transport	×	×	×
Alexidine	PM15/E04	4	membrane, biguanide, electron transport	×	×	×
Nitrofurazone	PM15/E05	1	DNA damage, multiple sites, nitrofuran analog	◎	△	◎
Nitrofurazone	PM15/E06	2	DNA damage, multiple sites, nitrofuran analog	◎	△	○
Nitrofurazone	PM15/E07	3	DNA damage, multiple sites, nitrofuran analog	◎	×	×
Nitrofurazone	PM15/E08	4	DNA damage, multiple sites, nitrofuran analog	×	×	×
Methyl viologen	PM15/E09	1	oxidizing agent	◎	△	◎
Methyl viologen	PM15/E10	2	oxidizing agent	◎	△	◎
Methyl viologen	PM15/E11	3	oxidizing agent	◎	△	◎
Methyl viologen	PM15/E12	4	oxidizing agent	◎	△	◎
3, 4-Dimethoxybenzyl alcohol	PM15/F01	1	oxidizing agent, free radical-peroxidase substrate	◎	△	◎
3, 4-Dimethoxybenzyl alcohol	PM15/F02	2	oxidizing agent, free radical-peroxidase substrate	◎	△	◎
3, 4-Dimethoxybenzyl alcohol	PM15/F03	3	oxidizing agent, free radical-peroxidase substrate	△	△	◎
3, 4-Dimethoxybenzyl alcohol	PM15/F04	4	oxidizing agent, free radical-peroxidase substrate	×	×	×
Oleandomycin	PM15/F05	1	protein synthesis, 50S ribosomal subunit, macrolide	◎	△	◎
Oleandomycin	PM15/F06	2	protein synthesis, 50S ribosomal subunit, macrolide	◎	△	◎
Oleandomycin	PM15/F07	3	protein synthesis, 50S ribosomal subunit, macrolide	◎	△	◎
Oleandomycin	PM15/F08	4	protein synthesis, 50S ribosomal subunit, macrolide	◎	×	○
Puromycin	PM15/F09	1	protein synthesis, 30S ribosomal subunit, premature chanin termination	◎	△	◎
Puromycin	PM15/F10	2	protein synthesis, 30S ribosomal subunit, premature chanin termination	◎	△	◎
Puromycin	PM15/F11	3	protein synthesis, 30S ribosomal subunit, premature chanin termination	○	○	◎
Puromycin	PM15/F12	4	protein synthesis, 30S ribosomal subunit, premature chanin termination	○	×	×

◎: Rapid growth to stationary phase in 24 hours, ○: Delayed growth but same cell mass, △: Delayed growth and small cell mass, ×: No growth, ☆: Faster growth than the parent strain.

Appendix Table 8. The sensitivity of Δ34 RR and Δ30 SK strains to various antimicrobials. (Continued.)

Antibiotics	Plate/Well	Concentration	Mode of Action	Parent	Δ34 RR	Δ30 SK
CCCP	PM15/G01	1	respiration, ionophore, H^+	○	○	◎
CCCP	PM15/G02	2	respiration, ionophore, H^+	◎	○	◎
CCCP	PM15/G03	3	respiration, ionophore, H^+	○	×	×
CCCP	PM15/G04	4	respiration, ionophore, H^+	×	×	×
Sodium azide	PM15/G05	1	respiration, uncoupler	◎	△	◎
Sodium azide	PM15/G06	2	respiration, uncoupler	○	△	△
Sodium azide	PM15/G07	3	respiration, uncoupler	×	×	×
Sodium azide	PM15/G08	4	respiration, uncoupler	×	×	×
Menadione	PM15/G09	1	respiration, uncoupler	◎	△	◎
Menadione	PM15/G10	2	respiration, uncoupler	◎	△	◎
Menadione	PM15/G11	3	respiration, uncoupler	○	◎	◎
Menadione	PM15/G12	4	respiration, uncoupler	△	◎	◎
2-Nitroimidazole	PM15/H01	1	ribonucleotide DP reductase	◎	△	◎
2-Nitroimidazole	PM15/H02	2	ribonucleotide DP reductase	◎	△	○
2-Nitroimidazole	PM15/H03	3	ribonucleotide DP reductase	×	×	×
2-Nitroimidazole	PM15/H04	4	ribonucleotide DP reductase	×	×	×
Hydroxyurea	PM15/H05	1	ribonucleotide DP reductase, antifolate (inhibits thymine and methionine synthesis)	◎	△	◎
Hydroxyurea	PM15/H06	2	ribonucleotide DP reductase, antifolate (inhibits thymine and methionine synthesis)	◎	△	◎
Hydroxyurea	PM15/H07	3	ribonucleotide DP reductase, antifolate (inhibits thymine and methionine synthesis)	◎	○	△
Hydroxyurea	PM15/H08	4	ribonucleotide DP reductase, antifolate (inhibits thymine and methionine synthesis)	×	×	×
Zinc chloride	PM15/H09	1	toxic cation	◎	△	◎
Zinc chloride	PM15/H10	2	toxic cation	◎	△	◎
Zinc chloride	PM15/H11	3	toxic cation	△	×	△
Zinc chloride	PM15/H12	4	toxic cation	△	×	×
Cefotaxime	PM16/A01	1	wall, cephalosporin	◎	△	◎
Cefotaxime	PM16/A02	2	wall, cephalosporin	◎	△	◎
Cefotaxime	PM16/A03	3	wall, cephalosporin	◎	△	◎
Cefotaxime	PM16/A04	4	wall, cephalosporin	◎	△	◎
Phosphomycin	PM16/A05	1	wall	◎	△	◎
Phosphomycin	PM16/A06	2	wall	◎	△	◎
Phosphomycin	PM16/A07	3	wall	◎	△	◎
Phosphomycin	PM16/A08	4	wall	◎	△	◎
5-Chloro-7-Iodo-8-Hydroxyquinoline	PM16/A09	1	chelator, lipophilic	◎	△	◎
5-Chloro-7-Iodo-8-Hydroxyquinoline	PM16/A10	2	chelator, lipophilic	◎	△	◎
5-Chloro-7-Iodo-8-Hydroxyquinoline	PM16/A11	3	chelator, lipophilic	×	×	×
5-Chloro-7-Iodo-8-Hydroxyquinoline	PM16/A12	4	chelator, lipophilic	×	×	×
Norfloxacin	PM16/B01	1	DNA topoisomerase, quinolone	◎	△	◎
Norfloxacin	PM16/B02	2	DNA topoisomerase, quinolone	◎	△	◎
Norfloxacin	PM16/B03	3	DNA topoisomerase, quinolone	◎	△	◎
Norfloxacin	PM16/B04	4	DNA topoisomerase, quinolone	◎	△	×
Sulfanilamide	PM16/B05	1	folate antagonist	◎	△	◎
Sulfanilamide	PM16/B06	2	folate antagonist	◎	△	◎
Sulfanilamide	PM16/B07	3	folate antagonist	◎	△	◎
Sulfanilamide	PM16/B08	4	folate antagonist	◎	△	◎
Trimethoprim	PM16/B09	1	folate antagonist, dihyldrofolate reductase	◎	○	◎
Trimethoprim	PM16/B10	2	folate antagonist, dihyldrofolate reductase	×	×	×
Trimethoprim	PM16/B11	3	folate antagonist, dihyldrofolate reductase	×	×	×
Trimethoprim	PM16/B12	4	folate antagonist, dihyldrofolate reductase	×	×	×
Dichlofluanid	PM16/C01	1	fungicide, phenylsulphamide	◎	△	◎
Dichlofluanid	PM16/C02	2	fungicide, phenylsulphamide	◎	△	○
Dichlofluanid	PM16/C03	3	fungicide, phenylsulphamide	◎	×	○
Dichlofluanid	PM16/C04	4	fungicide, phenylsulphamide	○	×	○
Protamine Sulfate	PM16/C05	1	membrane, ATPase	◎	×	◎
Protamine Sulfate	PM16/C06	2	membrane, ATPase	◎	×	×
Protamine Sulfate	PM16/C07	3	membrane, ATPase	×	×	×
Protamine Sulfate	PM16/C08	4	membrane, ATPase	×	×	×
Cetylpyridinium Chloride	PM16/C09	1	membrane, detergent, cationic	◎	△	◎
Cetylpyridinium Chloride	PM16/C10	2	membrane, detergent, cationic	◎	△	◎
Cetylpyridinium Chloride	PM16/C11	3	membrane, detergent, cationic	◎	○	◎
Cetylpyridinium Chloride	PM16/C12	4	membrane, detergent, cationic	×	×	×
1-Chloro-2,4-Dinitrobenzene	PM16/D01	1	oxidation, glutathione	◎	△	◎
1-Chloro-2,4-Dinitrobenzene	PM16/D02	2	oxidation, glutathione	◎	△	◎
1-Chloro-2,4-Dinitrobenzene	PM16/D03	3	oxidation, glutathione	◎	△	◎
1-Chloro-2,4-Dinitrobenzene	PM16/D04	4	oxidation, glutathione	◎	△	◎
Diamide	PM16/D05	1	oxidation, glutathione	◎	△	○
Diamide	PM16/D06	2	oxidation, glutathione	◎	△	○
Diamide	PM16/D07	3	oxidation, glutathione	◎	△	◎
Diamide	PM16/D08	4	oxidation, glutathione	◎	△	◎
Cinoxacin	PM16/D09	1	protein synthesis	◎	△	◎
Cinoxacin	PM16/D10	2	protein synthesis	◎	△	◎
Cinoxacin	PM16/D11	3	protein synthesis	×	☆	×
Cinoxacin	PM16/D12	4	protein synthesis	×	×	×
Streptomycin	PM16/E01	1	protein synthesis, aminoglycoside	◎	△	◎
Streptomycin	PM16/E02	2	protein synthesis, aminoglycoside	◎	△	◎
Streptomycin	PM16/E03	3	protein synthesis, aminoglycoside	◎	△	◎
Streptomycin	PM16/E04	4	protein synthesis, aminoglycoside	◎	△	◎
5-Azacytidine	PM16/E05	1	DNA methyltransferase	◎	△	◎
5-Azacytidine	PM16/E06	2	DNA methyltransferase	◎	△	◎
5-Azacytidine	PM16/E07	3	DNA methyltransferase	◎	△	◎
5-Azacytidine	PM16/E08	4	DNA methyltransferase	◎	△	◎
Rifamycin SV	PM16/E09	1	RNA polymerase	◎	△	○
Rifamycin SV	PM16/E10	2	RNA polymerase	◎	△	○
Rifamycin SV	PM16/E11	3	RNA polymerase	◎	○	○
Rifamycin SV	PM16/E12	4	RNA polymerase	◎	◎	◎
Potassium Tellurite	PM16/F01	1	transport, toxic anion	◎	△	◎
Potassium Tellurite	PM16/F02	2	transport, toxic anion	○	△	◎
Potassium Tellurite	PM16/F03	3	transport, toxic anion	○	×	◎
Potassium Tellurite	PM16/F04	4	transport, toxic anion	×	×	×
Sodium Selenite	PM16/F05	1	transport, toxic anion	◎	△	◎
Sodium Selenite	PM16/F06	2	transport, toxic anion	○	×	◎
Sodium Selenite	PM16/F07	3	transport, toxic anion	○	×	◎
Sodium Selenite	PM16/F08	4	transport, toxic anion	◎	△	◎

◎: Rapid growth to stationary phase in 24 hours, ○: Delayed growth but same cell mass, △: Delayed growth and small cell mass, ×: No growth, ☆: Faster growth than the parent strain.

Appendix Table 8. The sensitivity of Δ34 RR and Δ30 SK strains to various antimicrobials. (Continued.)

Antibiotics	Plate/Well	Concentration	Mode of Action	Parent	Δ34 RR	Δ30 SK
Aluminum Sulfate	PM16/F09	1	transport, toxic cation	◎	△	◎
Aluminum Sulfate	PM16/F10	2	transport, toxic cation	◎	△	◎
Aluminum Sulfate	PM16/F11	3	transport, toxic cation	◎	△	○
Aluminum Sulfate	PM16/F12	4	transport, toxic cation	○	×	×
Chromium Chloride	PM16/G01	1	transport, toxic cation	◎	△	◎
Chromium Chloride	PM16/G02	2	transport, toxic cation	◎	△	◎
Chromium Chloride	PM16/G03	3	transport, toxic cation	◎	△	◎
Chromium Chloride	PM16/G04	4	transport, toxic cation	◎	△	◎
Ferric Chloride	PM16/G05	1	transport, toxic cation	◎	△	◎
Ferric Chloride	PM16/G06	2	transport, toxic cation	◎	△	◎
Ferric Chloride	PM16/G07	3	transport, toxic cation	◎	△	◎
Ferric Chloride	PM16/G08	4	transport, toxic cation	○	×	◎
L-Glutamic-γ-Hydroxamate	PM16/G09	1	tRNA synthetase	◎	△	◎
L-Glutamic-γ-Hydroxamate	PM16/G10	2	tRNA synthetase	◎	△	◎
L-Glutamic-γ-Hydroxamate	PM16/G11	3	tRNA synthetase	◎	○	○
L-Glutamic-γ-Hydroxamate	PM16/G12	4	tRNA synthetase	◎	◎	◎
Glycine Hydroxamate	PM16/H01	1	tRNA synthetase	◎	△	◎
Glycine Hydroxamate	PM16/H02	2	tRNA synthetase	◎	△	◎
Glycine Hydroxamate	PM16/H03	3	tRNA synthetase	◎	×	×
Glycine Hydroxamate	PM16/H04	4	tRNA synthetase	×	×	×
Chloroxylenol	PM16/H05	1	fungicide	◎	△	◎
Chloroxylenol	PM16/H06	2	fungicide	◎	△	◎
Chloroxylenol	PM16/H07	3	fungicide	◎	△	◎
Chloroxylenol	PM16/H08	4	fungicide	◎	△	◎
Sorbic Acid	PM16/H09	1	respiration, ionophore, H^+	◎	○	◎
Sorbic Acid	PM16/H10	2	respiration, ionophore, H^+	◎	△	◎
Sorbic Acid	PM16/H11	3	respiration, ionophore, H^+	◎	△	◎
Sorbic Acid	PM16/H12	4	respiration, ionophore, H^+	◎	◎	◎
D-Serine	PM17/A01	1	inhibits 3PGA dehydrogenase (L-serine and pantothenate synthesis)	◎	◎	◎
D-Serine	PM17/A02	2	inhibits 3PGA dehydrogenase (L-serine and pantothenate synthesis)	◎	◎	◎
D-Serine	PM17/A03	3	inhibits 3PGA dehydrogenase (L-serine and pantothenate synthesis)	◎	△	○
D-Serine	PM17/A04	4	inhibits 3PGA dehydrogenase (L-serine and pantothenate synthesis)	×	×	×
β-Chloro-L-Alanine	PM17/A05	1	amino acid analog, alanine, aminotransferase inhibitor	◎	△	◎
β-Chloro-L-Alanine	PM17/A06	2	amino acid analog, alanine, aminotransferase inhibitor	◎	△	◎
β-Chloro-L-Alanine	PM17/A07	3	amino acid analog, alanine, aminotransferase inhibitor	◎	△	◎
β-Chloro-L-Alanine	PM17/A08	4	amino acid analog, alanine, aminotransferase inhibitor	○	△	◎
Thiosalicylate	PM17/A09	1	anti-capsule, thiol	◎	△	◎
Thiosalicylate	PM17/A10	2	anti-capsule, thiol	◎	△	◎
Thiosalicylate	PM17/A11	3	anti-capsule, thiol	◎	△	◎
Thiosalicylate	PM17/A12	4	anti-capsule, thiol	◎	△	◎
Salicylate	PM17/B01	1	anti-capsule, anti-inflammatory, mar inducer	◎	△	◎
Salicylate	PM17/B02	2	anti-capsule, anti-inflammatory, mar inducer	○	△	○
Salicylate	PM17/B03	3	anti-capsule, anti-inflammatory, mar inducer	△	×	×
Salicylate	PM17/B04	4	anti-capsule, anti-inflammatory, mar inducer	×	×	×
Hygromycin B	PM17/B05	1	protein synthesis, aminoglycoside	◎	△	◎
Hygromycin B	PM17/B06	2	protein synthesis, aminoglycoside	◎	△	◎
Hygromycin B	PM17/B07	3	protein synthesis, aminoglycoside	◎	△	◎
Hygromycin B	PM17/B08	4	protein synthesis, aminoglycoside	◎	△	◎
Ethionamide	PM17/B09	1	anti-tuberculosic	◎	△	◎
Ethionamide	PM17/B10	2	anti-tuberculosic	◎	△	◎
Ethionamide	PM17/B11	3	anti-tuberculosic	○	△	◎
Ethionamide	PM17/B12	4	anti-tuberculosic	×	×	×
4-Aminopyridine	PM17/C01	1	ion channel, K^+	◎	△	◎
4-Aminopyridine	PM17/C02	2	ion channel, K^+	◎	△	◎
4-Aminopyridine	PM17/C03	3	ion channel, K^+	◎	△	◎
4-Aminopyridine	PM17/C04	4	ion channel, K^+	◎	△	◎
Sulfachloropyridazine	PM17/C05	1	folate antagonist	◎	△	◎
Sulfachloropyridazine	PM17/C06	2	folate antagonist	◎	△	○
Sulfachloropyridazine	PM17/C07	3	folate antagonist	○	△	×
Sulfachloropyridazine	PM17/C08	4	folate antagonist	○	△	×
Sulfamonomethoxine	PM17/C09	1	folate antagonist	◎	△	◎
Sulfamonomethoxine	PM17/C10	2	folate antagonist	◎	△	○
Sulfamonomethoxine	PM17/C11	3	folate antagonist	○	○	×
Sulfamonomethoxine	PM17/C12	4	folate antagonist	○	○	×
Oxycarboxin	PM17/D01	1	fungicide, carboxamide, respiratory enzymes	◎	△	◎
Oxycarboxin	PM17/D02	2	fungicide, carboxamide, respiratory enzymes	○	△	○
Oxycarboxin	PM17/D03	3	fungicide, carboxamide, respiratory enzymes	×	×	×
Oxycarboxin	PM17/D04	4	fungicide, carboxamide, respiratory enzymes	×	×	×
Aminotriazole	PM17/D05	1	histidine biosynthesis, catalase	◎	△	◎
Aminotriazole	PM17/D06	2	histidine biosynthesis, catalase	◎	△	◎
Aminotriazole	PM17/D07	3	histidine biosynthesis, catalase	◎	△	◎
Aminotriazole	PM17/D08	4	histidine biosynthesis, catalase	○	×	○
Chlorpromazine	PM17/D09	1	phenothiazine	◎	△	◎
Chlorpromazine	PM17/D10	2	phenothiazine	◎	△	◎
Chlorpromazine	PM17/D11	3	phenothiazine	○	×	×
Chlorpromazine	PM17/D12	4	phenothiazine	×	×	×
Niaproof	PM17/E01	1	membrane, detergent, anionic	◎	◎	◎
Niaproof	PM17/E02	2	membrane, detergent, anionic	◎	△	◎
Niaproof	PM17/E03	3	membrane, detergent, anionic	△	◎	◎
Niaproof	PM17/E04	4	membrane, detergent, anionic	△	○	☆
Compound 48/80	PM17/E05	1	phospholipase C, ADP ribosylation	◎	△	◎
Compound 48/80	PM17/E06	2	phospholipase C, ADP ribosylation	◎	△	◎
Compound 48/80	PM17/E07	3	phospholipase C, ADP ribosylation	◎	×	×
Compound 48/80	PM17/E08	4	phospholipase C, ADP ribosylation	×	×	×
Sodium Tungstate	PM17/E09	1	transport, toxic anion, molybdate analog	◎	△	○
Sodium Tungstate	PM17/E10	2	transport, toxic anion, molybdate analog	○	×	○
Sodium Tungstate	PM17/E11	3	transport, toxic anion, molybdate analog	○	×	△
Sodium Tungstate	PM17/E12	4	transport, toxic anion, molybdate analog	×	×	×
Lithium Chloride	PM17/F01	1	transport, toxic cation	◎	△	◎
Lithium Chloride	PM17/F02	2	transport, toxic cation	◎	△	◎
Lithium Chloride	PM17/F03	3	transport, toxic cation	△	×	○
Lithium Chloride	PM17/F04	4	transport, toxic cation	×	×	×

◎: Rapid growth to stationary phase in 24 hours, ○: Delayed growth but same cell mass, △: Delayed growth and small cell mass, ×: No growth, ☆: Faster growth than the parent strain.

Appendix Table 8. The sensitivity of Δ34 RR and Δ30 SK strains to various antimicrobials. (Continued.)

Antibiotics	Plate/Well	Concentration	Mode of Action	Parent	Δ34 RR	Δ30 SK
D,L-Methionine Hydroxamate	PM17/F05	1	tRNA synthetase	◎	△	◎
D,L-Methionine Hydroxamate	PM17/F06	2	tRNA synthetase	◎	△	◎
D,L-Methionine Hydroxamate	PM17/F07	3	tRNA synthetase	○	○	○
D,L-Methionine Hydroxamate	PM17/F08	4	tRNA synthetase	△	×	○
Tannic acid	PM17/F09	1	antimicrobial, from plants	◎	△	◎
Tannic acid	PM17/F10	2	antimicrobial, from plants	○	△	◎
Tannic acid	PM17/F11	3	antimicrobial, from plants	○	△	○
Tannic acid	PM17/F12	4	antimicrobial, from plants	○	×	×
Chlorambucil	PM17/G01	1		◎	△	◎
Chlorambucil	PM17/G02	2		◎	△	◎
Chlorambucil	PM17/G03	3		◎	◎	◎
Chlorambucil	PM17/G04	4		○	○	◎
Cefamandole	PM17/G05	1	wall, cephalosporin	◎	△	◎
Cefamandole	PM17/G06	2	wall, cephalosporin	◎	△	◎
Cefamandole	PM17/G07	3	wall, cephalosporin	◎	◎	◎
Cefamandole	PM17/G08	4	wall, cephalosporin	◎	△	◎
Cetoperazone	PM17/G09	1	wall, cephalosporin	◎	△	◎
Cetoperazone	PM17/G10	2	wall, cephalosporin	◎	△	◎
Cetoperazone	PM17/G11	3	wall, cephalosporin	○	◎	◎
Cetoperazone	PM17/G12	4	wall, cephalosporin	×	×	×
Cefsulodin	PM17/H01	1	wall, cephalosporin	◎	△	◎
Cefsulodin	PM17/H02	2	wall, cephalosporin	◎	△	◎
Cefsulodin	PM17/H03	3	wall, cephalosporin	◎	△	◎
Cefsulodin	PM17/H04	4	wall, cephalosporin	◎	△	◎
Caffeine	PM17/H05	1	cyclic AMP phosphodiesterase	◎	△	◎
Caffeine	PM17/H06	2	cyclic AMP phosphodiesterase	◎	△	◎
Caffeine	PM17/H07	3	cyclic AMP phosphodiesterase	◎	×	◎
Caffeine	PM17/H08	4	cyclic AMP phosphodiesterase	×	×	×
Phenylarsine Oxide	PM17/H09	1	tyrosine phosphatase	◎	○	◎
Phenylarsine Oxide	PM17/H10	2	tyrosine phosphatase	◎	△	◎
Phenylarsine Oxide	PM17/H11	3	tyrosine phosphatase	◎	△	◎
Phenylarsine Oxide	PM17/H12	4	tyrosine phosphatase	△	×	×
Ketoprofen	PM18/A01	1	anti-capsule	◎	△	◎
Ketoprofen	PM18/A02	2	anti-capsule	◎	◎	◎
Ketoprofen	PM18/A03	3	anti-capsule	○	○	◎
Ketoprofen	PM18/A04	4	anti-capsule	×	×	×
Sodium pyrophosphate decahydrate	PM18/A05	1	chelating agent	◎	△	◎
Sodium pyrophosphate decahydrate	PM18/A06	2	chelating agent	◎	×	◎
Sodium pyrophosphate decahydrate	PM18/A07	3	chelating agent	◎	○	◎
Sodium pyrophosphate decahydrate	PM18/A08	4	chelating agent	◎	×	×
Thiamphenicol	PM18/A09	1	protein synthesis	◎	△	◎
Thiamphenicol	PM18/A10	2	protein synthesis	○	△	○
Thiamphenicol	PM18/A11	3	protein synthesis	○	◎	◎
Thiamphenicol	PM18/A12	4	protein synthesis	×	×	×
Trifluorothymidine	PM18/B01	1	thymidylate synthetase, DNA polymerase	◎	△	◎
Trifluorothymidine	PM18/B02	2	thymidylate synthetase, DNA polymerase	◎	△	◎
Trifluorothymidine	PM18/B03	3	thymidylate synthetase, DNA polymerase	◎	△	◎
Trifluorothymidine	PM18/B04	4	thymidylate synthetase, DNA polymerase	◎	△	◎
Pipemidic Acid	PM18/B05	1	DNA unwinding, gyrase (GN), topoisomerase (GP), quinolone	◎	△	◎
Pipemidic Acid	PM18/B06	2	DNA unwinding, gyrase (GN), topoisomerase (GP), quinolone	◎	△	◎
Pipemidic Acid	PM18/B07	3	DNA unwinding, gyrase (GN), topoisomerase (GP), quinolone	○	△	×
Pipemidic Acid	PM18/B08	4	DNA unwinding, gyrase (GN), topoisomerase (GP), quinolone	×	×	×
Azathioprine	PM18/B09	1	nucleic acid analog, purine	◎	△	◎
Azathioprine	PM18/B10	2	nucleic acid analog, purine	◎	△	◎
Azathioprine	PM18/B11	3	nucleic acid analog, purine	○	◎	◎
Azathioprine	PM18/B12	4	nucleic acid analog, purine	○	△	◎
Poly-L-lysine	PM18/C01	1	membrane, detergent, cationic	◎	◎	◎
Poly-L-lysine	PM18/C02	2	membrane, detergent, cationic	◎	×	◎
Poly-L-lysine	PM18/C03	3	membrane, detergent, cationic	◎	×	×
Poly-L-lysine	PM18/C04	4	membrane, detergent, cationic	×	×	×
Sulfisoxazole	PM18/C05	1	folate synthesis, PABA analog	○	○	×
Sulfisoxazole	PM18/C06	2	folate synthesis, PABA analog	○	△	×
Sulfisoxazole	PM18/C07	3	folate synthesis, PABA analog	△	×	×
Sulfisoxazole	PM18/C08	4	folate synthesis, PABA analog	×	×	×
Pentachlorophenol (PCP)	PM18/C09	1	respiration, ionophore, H^+	◎	△	◎
Pentachlorophenol (PCP)	PM18/C10	2	respiration, ionophore, H^+	◎	◎	◎
Pentachlorophenol (PCP)	PM18/C11	3	respiration, ionophore, H^+	◎	◎	◎
Pentachlorophenol (PCP)	PM18/C12	4	respiration, ionophore, H^+	◎	◎	◎
Sodium m-arsenite	PM18/D01	1	toxic anion	◎	△	◎
Sodium m-arsenite	PM18/D02	2	toxic anion	○	△	◎
Sodium m-arsenite	PM18/D03	3	toxic anion	△	×	○
Sodium m-arsenite	PM18/D04	4	toxic anion	×	×	×
Sodium bromate	PM18/D05	1	toxic anion	◎	△	◎
Sodium bromate	PM18/D06	2	toxic anion	○	△	◎
Sodium bromate	PM18/D07	3	toxic anion	○	△	◎
Sodium bromate	PM18/D08	4	toxic anion	△	×	×
Lidocaine	PM18/D09	1	ion channal inhibitor, Na^+	◎	○	◎
Lidocaine	PM18/D10	2	ion channal inhibitor, Na^+	◎	△	◎
Lidocaine	PM18/D11	3	ion channal inhibitor, Na^+	○	×	×
Lidocaine	PM18/D12	4	ion channal inhibitor, Na^+	×	×	×
Sodium metasilicate	PM18/E01	1	toxic anion	◎	△	◎
Sodium metasilicate	PM18/E02	2	toxic anion	◎	△	◎
Sodium metasilicate	PM18/E03	3	toxic anion	◎	△	○
Sodium metasilicate	PM18/E04	4	toxic anion	◎	×	○
Sodium periodate	PM18/E05	1	toxic anion, oxidizing agent	◎	△	◎
Sodium periodate	PM18/E06	2	toxic anion, oxidizing agent	◎	△	◎
Sodium periodate	PM18/E07	3	toxic anion, oxidizing agent	×	×	×
Sodium periodate	PM18/E08	4	toxic anion, oxidizing agent	×	×	×
Antimony (III) chloride	PM18/E09	1	toxic cation	◎	△	◎
Antimony (III) chloride	PM18/E10	2	toxic cation	○	△	◎
Antimony (III) chloride	PM18/E11	3	toxic cation	○	×	×
Antimony (III) chloride	PM18/E12	4	toxic cation	×	×	×

◎: Rapid growth to stationary phase in 24 hours, ○: Delayed growth but same cell mass, △: Delayed growth and small cell mass, ×: No growth, ☆: Faster growth than the parent strain.

Appendix Table 8. The sensitivity of Δ34 RR and Δ30 SK strains to various antimicrobials. (Continued.)

Antibiotics	Plate/Well	Concentration	Mode of Action	Parent	Δ34 RR	Δ30 SK
Semicarbazide hydrochloride	PM18/F01	1	carbonyl agent, semicarbazide-sensitive amine oxidase, DNA damage	◎	△	◎
Semicarbazide hydrochloride	PM18/F02	2	carbonyl agent, semicarbazide-sensitive amine oxidase, DNA damage	◎	△	◎
Semicarbazide hydrochloride	PM18/F03	3	carbonyl agent, semicarbazide-sensitive amine oxidase, DNA damage	△	×	○
Semicarbazide hydrochloride	PM18/F04	4	carbonyl agent, semicarbazide-sensitive amine oxidase, DNA damage	×	×	×
Tinidazole	PM18/F05	1	Mutagen, nitroimidazole (GP, GN)	◎	△	◎
Tinidazole	PM18/F06	2	Mutagen, nitroimidazole (GP, GN)	◎	△	◎
Tinidazole	PM18/F07	3	Mutagen, nitroimidazole (GP, GN)	○	△	◎
Tinidazole	PM18/F08	4	Mutagen, nitroimidazole (GP, GN)	×	×	×
Aztreonam	PM18/F09	1	wall, lactam	◎	△	◎
Aztreonam	PM18/F10	2	wall, lactam	◎	△	◎
Aztreonam	PM18/F11	3	wall, lactam	◎	◎	◎
Aztreonam	PM18/F12	4	wall, lactam	◎	◎	◎
Triclosan	PM18/G01	1	bacterial fatty acid synthesis, enoyl-acyl carrier protein reductase	◎	△	◎
Triclosan	PM18/G02	2	bacterial fatty acid synthesis, enoyl-acyl carrier protein reductase	◎	△	◎
Triclosan	PM18/G03	3	bacterial fatty acid synthesis, enoyl-acyl carrier protein reductase	◎	△	◎
Triclosan	PM18/G04	4	bacterial fatty acid synthesis, enoyl-acyl carrier protein reductase	◎	△	◎
3,5- Diamino-1,2,4-triazole (Guanazole)	PM18/G05	1	ribonucleotide DP reductase	◎	△	◎
3,5- Diamino-1,2,4-triazole (Guanazole)	PM18/G06	2	ribonucleotide DP reductase	◎	△	◎
3,5- Diamino-1,2,4-triazole (Guanazole)	PM18/G07	3	ribonucleotide DP reductase	○	○	◎
3,5- Diamino-1,2,4-triazole (Guanazole)	PM18/G08	4	ribonucleotide DP reductase	△	△	△
Myricetin	PM18/G09	1	DNA & RNA synthesis, polymerase inhibitor (*E. coli*)	◎	○	◎
Myricetin	PM18/G10	2	DNA & RNA synthesis, polymerase inhibitor (*E. coli*)	◎	○	◎
Myricetin	PM18/G11	3	DNA & RNA synthesis, polymerase inhibitor (*E. coli*)	◎	◎	◎
Myricetin	PM18/G12	4	DNA & RNA synthesis, polymerase inhibitor (*E. coli*)	◎	◎	◎
5-Fluoro-5'-deoxyuridine	PM18/H01	1	pyrimidine antimetabolite: inhibits nucleic acid replication	◎	△	◎
5-Fluoro-5'-deoxyuridine	PM18/H02	2	pyrimidine antimetabolite: inhibits nucleic acid replication	◎	△	◎
5-Fluoro-5'-deoxyuridine	PM18/H03	3	pyrimidine antimetabolite: inhibits nucleic acid replication	◎	△	◎
5-Fluoro-5'-deoxyuridine	PM18/H04	4	pyrimidine antimetabolite: inhibits nucleic acid replication	◎	△	◎
2- Phenylphenol	PM18/H05	1	DNA intercalator	◎	△	◎
2- Phenylphenol	PM18/H06	2	DNA intercalator	◎	△	◎
2- Phenylphenol	PM18/H07	3	DNA intercalator	◎	△	◎
2- Phenylphenol	PM18/H08	4	DNA intercalator	◎	△	◎
Plumbagin	PM18/H09	1	oxidizing agent	◎	△	◎
Plumbagin	PM18/H10	2	oxidizing agent	◎	△	◎
Plumbagin	PM18/H11	3	oxidizing agent	◎	◎	◎
Plumbagin	PM18/H12	4	oxidizing agent	◎	◎	◎
Josamycin	PM19/A01	1	protein synthesis, macrolide	◎	○	◎
Josamycin	PM19/A02	2	protein synthesis, macrolide	◎	△	◎
Josamycin	PM19/A03	3	protein synthesis, macrolide	◎	△	◎
Josamycin	PM19/A04	4	protein synthesis, macrolide	△	×	◎
Gallic Acid	PM19/A05	1	antimicrobial, from plants	◎	△	○
Gallic Acid	PM19/A06	2	antimicrobial, from plants	◎	△	△
Gallic Acid	PM19/A07	3	antimicrobial, from plants	◎	○	◎
Gallic Acid	PM19/A08	4	antimicrobial, from plants	×	×	×
Coumarin	PM19/A09	1	DNA intercalator	◎	△	◎
Coumarin	PM19/A10	2	DNA intercalator	◎	△	◎
Coumarin	PM19/A11	3	DNA intercalator	◎	△	◎
Coumarin	PM19/A12	4	DNA intercalator	◎	△	◎
Methyltrioctylammonium Chloride	PM19/B01	1	membrane, detergent, cationic	◎	△	◎
Methyltrioctylammonium Chloride	PM19/B02	2	membrane, detergent, cationic	◎	△	◎
Methyltrioctylammonium Chloride	PM19/B03	3	membrane, detergent, cationic	×	×	×
Methyltrioctylammonium Chloride	PM19/B04	4	membrane, detergent, cationic	×	×	×
Harmane	PM19/B05	1	imidazoline binding sites, agonist	◎	△	◎
Harmane	PM19/B06	2	imidazoline binding sites, agonist	◎	△	◎
Harmane	PM19/B07	3	imidazoline binding sites, agonist	○	×	○
Harmane	PM19/B08	4	imidazoline binding sites, agonist	×	×	×
2,4-Dintrophenol	PM19/B09	1	respiration, ionophore, H^+	◎	△	◎
2,4-Dintrophenol	PM19/B10	2	respiration, ionophore, H^+	◎	△	◎
2,4-Dintrophenol	PM19/B11	3	respiration, ionophore, H^+	◎	△	◎
2,4-Dintrophenol	PM19/B12	4	respiration, ionophore, H^+	◎	△	△
Chlorhexidine	PM19/C01	1	membrane, biguanide, electron transport	◎	△	◎
Chlorhexidine	PM19/C02	2	membrane, biguanide, electron transport	◎	△	◎
Chlorhexidine	PM19/C03	3	membrane, biguanide, electron transport	◎	×	×
Chlorhexidine	PM19/C04	4	membrane, biguanide, electron transport	×	×	×
Umbelliferone	PM19/C05	1	DNA intercalator	◎	△	◎
Umbelliferone	PM19/C06	2	DNA intercalator	◎	△	◎
Umbelliferone	PM19/C07	3	DNA intercalator	○	×	△
Umbelliferone	PM19/C08	4	DNA intercalator	×	×	×
Cinnamic Acid	PM19/C09	1	respiration, ionophore, H^+	◎	△	◎
Cinnamic Acid	PM19/C10	2	respiration, ionophore, H^+	◎	△	◎
Cinnamic Acid	PM19/C11	3	respiration, ionophore, H^+	◎	△	◎
Cinnamic Acid	PM19/C12	4	respiration, ionophore, H^+	△	×	△
Disulphiram	PM19/D01	1	fungicide	◎	△	◎
Disulphiram	PM19/D02	2	fungicide	◎	△	◎
Disulphiram	PM19/D03	3	fungicide	◎	△	◎
Disulphiram	PM19/D04	4	fungicide	◎	△	◎
Iodonitro Tetrazolium Violet	PM19/D05	1	respiration	◎	○	◎
Iodonitro Tetrazolium Violet	PM19/D06	2	respiration	◎	◎	◎
Iodonitro Tetrazolium Violet	PM19/D07	3	respiration	◎	◎	◎
Iodonitro Tetrazolium Violet	PM19/D08	4	respiration	◎	◎	◎
Phenyl-Methyl-Sulfonyl-Fluoride (PMSF)	PM19/D09	1	protease inhibitor, serine	◎	△	◎
Phenyl-Methyl-Sulfonyl-Fluoride (PMSF)	PM19/D10	2	protease inhibitor, serine	◎	△	△
Phenyl-Methyl-Sulfonyl-Fluoride (PMSF)	PM19/D11	3	protease inhibitor, serine	◎	△	△
Phenyl-Methyl-Sulfonyl-Fluoride (PMSF)	PM19/D12	4	protease inhibitor, serine	◎	△	◎
FCCP	PM19/E01	1	respiration, ionophore, H^+	○	◎	◎
FCCP	PM19/E02	2	respiration, ionophore, H^+	◎	○	◎
FCCP	PM19/E03	3	respiration, ionophore, H^+	○	○	◎
FCCP	PM19/E04	4	respiration, ionophore, H^+	○	△	◎
D,L-Thioctic Acid	PM19/E05	1	oxidizing agent	○	△	◎
D,L-Thioctic Acid	PM19/E06	2	oxidizing agent	○	△	○
D,L-Thioctic Acid	PM19/E07	3	oxidizing agent	○	×	○
D,L-Thioctic Acid	PM19/E08	4	oxidizing agent	×	×	×

◎: Rapid growth to stationary phase in 24 hours, ○: Delayed growth but same cell mass, △: Delayed growth and small cell mass, ×: No growth, ☆: Faster growth than the parent strain.

Appendix Table 8. The sensitivity of Δ34 RR and Δ30 SK strains to various antimicrobials. (Continued.)

Antibiotics	Plate/Well	Concentration	Mode of Action	Parent	Δ34 RR	Δ30 SK
Lawsone	PM19/E09	1	oxidizing agent	◎	○	◎
Lawsone	PM19/E10	2	oxidizing agent	◎	○	○
Lawsone	PM19/E11	3	oxidizing agent	◎	×	◎
Lawsone	PM19/E12	4	oxidizing agent	×	×	×
Phenethicillin	PM19/F01	1	wall, lactam	◎	△	◎
Phenethicillin	PM19/F02	2	wall, lactam	○	△	◎
Phenethicillin	PM19/F03	3	wall, lactam	○	×	×
Phenethicillin	PM19/F04	4	wall, lactam	×	×	×
Blasticidin S	PM19/F05	1	protein synthesis	◎	△	◎
Blasticidin S	PM19/F06	2	protein synthesis	◎	△	◎
Blasticidin S	PM19/F07	3	protein synthesis	◎	△	◎
Blasticidin S	PM19/F08	4	protein synthesis	×	×	×
Sodium Caprylate	PM19/F09	1	respiration, ionophore, H^+	◎	○	◎
Sodium Caprylate	PM19/F10	2	respiration, ionophore, H^+	○	△	△
Sodium Caprylate	PM19/F11	3	respiration, ionophore, H^+	△	×	×
Sodium Caprylate	PM19/F12	4	respiration, ionophore, H^+	×	×	×
Lauryl sulfobetaine	PM19/G01	1	membrane, detergent, zwitterionic	○	△	◎
Lauryl sulfobetaine	PM19/G02	2	membrane, detergent, zwitterionic	○	△	○
Lauryl sulfobetaine	PM19/G03	3	membrane, detergent, zwitterionic	△	×	○
Lauryl sulfobetaine	PM19/G04	4	membrane, detergent, zwitterionic	△	△	△
Dihydrostreptomycin	PM19/G05	1	protein synthesis, aminoglycoside	◎	△	◎
Dihydrostreptomycin	PM19/G06	2	protein synthesis, aminoglycoside	◎	△	◎
Dihydrostreptomycin	PM19/G07	3	protein synthesis, aminoglycoside	◎	△	◎
Dihydrostreptomycin	PM19/G08	4	protein synthesis, aminoglycoside	△	◎	×
Hydroxylamine	PM19/G09	1	DNA damage, mutagen, antifolate (inhibits thymine and methionine synthesis)	◎	△	◎
Hydroxylamine	PM19/G10	2	DNA damage, mutagen, antifolate (inhibits thymine and methionine synthesis)	◎	◎	◎
Hydroxylamine	PM19/G11	3	DNA damage, mutagen, antifolate (inhibits thymine and methionine synthesis)	◎	○	○
Hydroxylamine	PM19/G12	4	DNA damage, mutagen, antifolate (inhibits thymine and methionine synthesis)	◎	△	△
Hexaminecobalt (III) Chloride	PM19/H01	1	DNA synthesis	◎	△	◎
Hexaminecobalt (III) Chloride	PM19/H02	2	DNA synthesis	◎	○	◎
Hexaminecobalt (III) Chloride	PM19/H03	3	DNA synthesis	◎	△	○
Hexaminecobalt (III) Chloride	PM19/H04	4	DNA synthesis	◎	△	○
Thioglycerol	PM19/H05	1	reducing agent, thiol, adenosyl methionine antagonist	◎	△	◎
Thioglycerol	PM19/H06	2	reducing agent, thiol, adenosyl methionine antagonist	◎	△	◎
Thioglycerol	PM19/H07	3	reducing agent, thiol, adenosyl methionine antagonist	◎	◎	◎
Thioglycerol	PM19/H08	4	reducing agent, thiol, adenosyl methionine antagonist	×	×	☆
Polymyxin B	PM19/H09	1	membrane, outer	×	×	×
Polymyxin B	PM19/H10	2	membrane, outer	×	×	×
Polymyxin B	PM19/H11	3	membrane, outer	×	×	×
Polymyxin B	PM19/H12	4	membrane, outer	×	×	×
Amitriptyline	PM20/A01	1	membrane, transport	◎	△	◎
Amitriptyline	PM20/A02	2	membrane, transport	◎	○	◎
Amitriptyline	PM20/A03	3	membrane, transport	○	△	☆
Amitriptyline	PM20/A04	4	membrane, transport	×	×	×
Apramycin	PM20/A05	1	antimicrobial, aminocyclitol	◎	△	◎
Apramycin	PM20/A06	2	antimicrobial, aminocyclitol	◎	△	◎
Apramycin	PM20/A07	3	antimicrobial, aminocyclitol	◎	△	◎
Apramycin	PM20/A08	4	antimicrobial, aminocyclitol	◎	△	○
Benserazide	PM20/A09	1	fungicide	◎	△	◎
Benserazide	PM20/A10	2	fungicide	◎	○	○
Benserazide	PM20/A11	3	fungicide	◎	△	×
Benserazide	PM20/A12	4	fungicide	×	×	×
Orphenadrine	PM20/B01	1	cholinergic antagonist	◎	△	◎
Orphenadrine	PM20/B02	2	cholinergic antagonist	◎	△	◎
Orphenadrine	PM20/B03	3	cholinergic antagonist	△	×	×
Orphenadrine	PM20/B04	4	cholinergic antagonist	×	×	×
D,L-Propranolol	PM20/B05	1	beta-adrenergic blocker	◎	△	◎
D,L-Propranolol	PM20/B06	2	beta-adrenergic blocker	◎	△	◎
D,L-Propranolol	PM20/B07	3	beta-adrenergic blocker	△	×	×
D,L-Propranolol	PM20/B08	4	beta-adrenergic blocker	×	×	×
Tetrazolium Violet	PM20/B09	1	respiration	◎	○	◎
Tetrazolium Violet	PM20/B10	2	respiration	◎	×	○
Tetrazolium Violet	PM20/B11	3	respiration	△	×	◎
Tetrazolium Violet	PM20/B12	4	respiration	×	×	×
Thioridazine	PM20/C01	1	respiration	◎	△	◎
Thioridazine	PM20/C02	2	respiration	○	×	◎
Thioridazine	PM20/C03	3	respiration	○	×	×
Thioridazine	PM20/C04	4	respiration	×	×	×
Atropine	PM20/C05	1	acetylcholine receptor, antagonist	◎	△	○
Atropine	PM20/C06	2	acetylcholine receptor, antagonist	◎	△	◎
Atropine	PM20/C07	3	acetylcholine receptor, antagonist	×	×	×
Atropine	PM20/C08	4	acetylcholine receptor, antagonist	×	×	×
Ornidazole	PM20/C09	1	protein glycosolation	◎	△	◎
Ornidazole	PM20/C10	2	protein glycosolation	◎	△	◎
Ornidazole	PM20/C11	3	protein glycosolation	△	×	◎
Ornidazole	PM20/C12	4	protein glycosolation	×	×	×
Proflavine	PM20/D01	1	RNA synthesis	◎	△	◎
Proflavine	PM20/D02	2	RNA synthesis	◎	△	◎
Proflavine	PM20/D03	3	RNA synthesis	◎	△	◎
Proflavine	PM20/D04	4	RNA synthesis	△	×	×
Ciprofloxacin	PM20/D05	1	DNA topoisomerase, quinolone	◎	△	◎
Ciprofloxacin	PM20/D06	2	DNA topoisomerase, quinolone	◎	△	◎
Ciprofloxacin	PM20/D07	3	DNA topoisomerase, quinolone	◎	△	◎
Ciprofloxacin	PM20/D08	4	DNA topoisomerase, quinolone	◎	△	◎
18-Crown-6-Ether	PM20/D09	1	respiration, ionophore	◎	△	◎
18-Crown-6-Ether	PM20/D10	2	respiration, ionophore	◎	△	◎
18-Crown-6-Ether	PM20/D11	3	respiration, ionophore	◎	×	○
18-Crown-6-Ether	PM20/D12	4	respiration, ionophore	×	×	×
Crystal Violet	PM20/E01	1	respiration	◎	△	◎
Crystal Violet	PM20/E02	2	respiration	◎	△	◎
Crystal Violet	PM20/E03	3	respiration	◎	◎	○
Crystal Violet	PM20/E04	4	respiration	×	×	×

◎: Rapid growth to stationary phase in 24 hours, ○: Delayed growth but same cell mass, △: Delayed growth and small cell mass, ×: No growth, ☆: Faster growth than the parent strain.

Appendix Table 8. The sensitivity of Δ34 RR and Δ30 SK strains to various antimicrobials. (Continued.)

Antibiotics	Plate/Well	Concentration	Mode of Action	Parent	Δ34 RR	Δ30 SK
Dodine	PM20/E05	1	fungicide, guanidine, membrane permeability	◎	△	◎
Dodine	PM20/E06	2	fungicide, guanidine, membrane permeability	◎	○	◎
Dodine	PM20/E07	3	fungicide, guanidine, membrane permeability	◎	×	×
Dodine	PM20/E08	4	fungicide, guanidine, membrane permeability	×	×	×
Hexachlorophene	PM20/E09	1	membrane, electron transport	◎	◎	◎
Hexachlorophene	PM20/E10	2	membrane, electron transport	◎	◎	◎
Hexachlorophene	PM20/E11	3	membrane, electron transport	◎	◎	◎
Hexachlorophene	PM20/E12	4	membrane, electron transport	○	◎	◎
4-Hydroxycoumarin	PM20/F01	1	DNA intercalator	◎	△	◎
4-Hydroxycoumarin	PM20/F02	2	DNA intercalator	◎	△	◎
4-Hydroxycoumarin	PM20/F03	3	DNA intercalator	○	×	○
4-Hydroxycoumarin	PM20/F04	4	DNA intercalator	×	×	×
Oxytetracycline	PM20/F05	1	protein synthesis, tetracycline	◎	△	◎
Oxytetracycline	PM20/F06	2	protein synthesis, tetracycline	◎	△	○
Oxytetracycline	PM20/F07	3	protein synthesis, tetracycline	○	◎	◎
Oxytetracycline	PM20/F08	4	protein synthesis, tetracycline	○	☆	☆
Pridinol	PM20/F09	1	cholinergic antagonist	◎	△	◎
Pridinol	PM20/F10	2	cholinergic antagonist	◎	△	◎
Pridinol	PM20/F11	3	cholinergic antagonist	○	×	×
Pridinol	PM20/F12	4	cholinergic antagonist	○	×	×
Captan	PM20/G01	1	fungicide, carbamate, multisite	○	○	×
Captan	PM20/G02	2	fungicide, carbamate, multisite	◎	×	○
Captan	PM20/G03	3	fungicide, carbamate, multisite	○	×	☆
Captan	PM20/G04	4	fungicide, carbamate, multisite	○	×	×
3,5-Dinitrobenzene	PM20/G05	1	respiration, ionophore, H^+	◎	△	◎
3,5-Dinitrobenzene	PM20/G06	2	respiration, ionophore, H^+	◎	○	◎
3,5-Dinitrobenzene	PM20/G07	3	respiration, ionophore, H^+	○	×	×
3,5-Dinitrobenzene	PM20/G08	4	respiration, ionophore, H^+	×	×	×
8-Hydroxyquinoline	PM20/G09	1	chelator, lipophilic	◎	△	◎
8-Hydroxyquinoline	PM20/G10	2	chelator, lipophilic	◎	△	◎
8-Hydroxyquinoline	PM20/G11	3	chelator, lipophilic	◎	◎	◎
8-Hydroxyquinoline	PM20/G12	4	chelator, lipophilic	◎	△	◎
Patulin	PM20/H01	1	antifungal, tubulin binding	◎	△	◎
Patulin	PM20/H02	2	antifungal, tubulin binding	◎	△	◎
Patulin	PM20/H03	3	antifungal, tubulin binding	◎	△	◎
Patulin	PM20/H04	4	antifungal, tubulin binding	◎	△	◎
Tolylfluanid	PM20/H05	1	fungicide, phenylsulphamide	◎	△	○
Tolylfluanid	PM20/H06	2	fungicide, phenylsulphamide	◎	×	○
Tolylfluanid	PM20/H07	3	fungicide, phenylsulphamide	◎	×	○
Tolylfluanid	PM20/H08	4	fungicide, phenylsulphamide	◎	×	×
Troleandomycin	PM20/H09	1	protein synthesis, macrolide	◎	◎	◎
Troleandomycin	PM20/H10	2	protein synthesis, macrolide	◎	◎	◎
Troleandomycin	PM20/H11	3	protein synthesis, macrolide	◎	◎	◎
Troleandomycin	PM20/H12	4	protein synthesis, macrolide	◎	△	○

◎: Rapid growth to stationary phase in 24 hours, ○: Delayed growth but same cell mass, △: Delayed growth and small cell mass, ×: No growth, ☆: Faster growth than the parent strain.

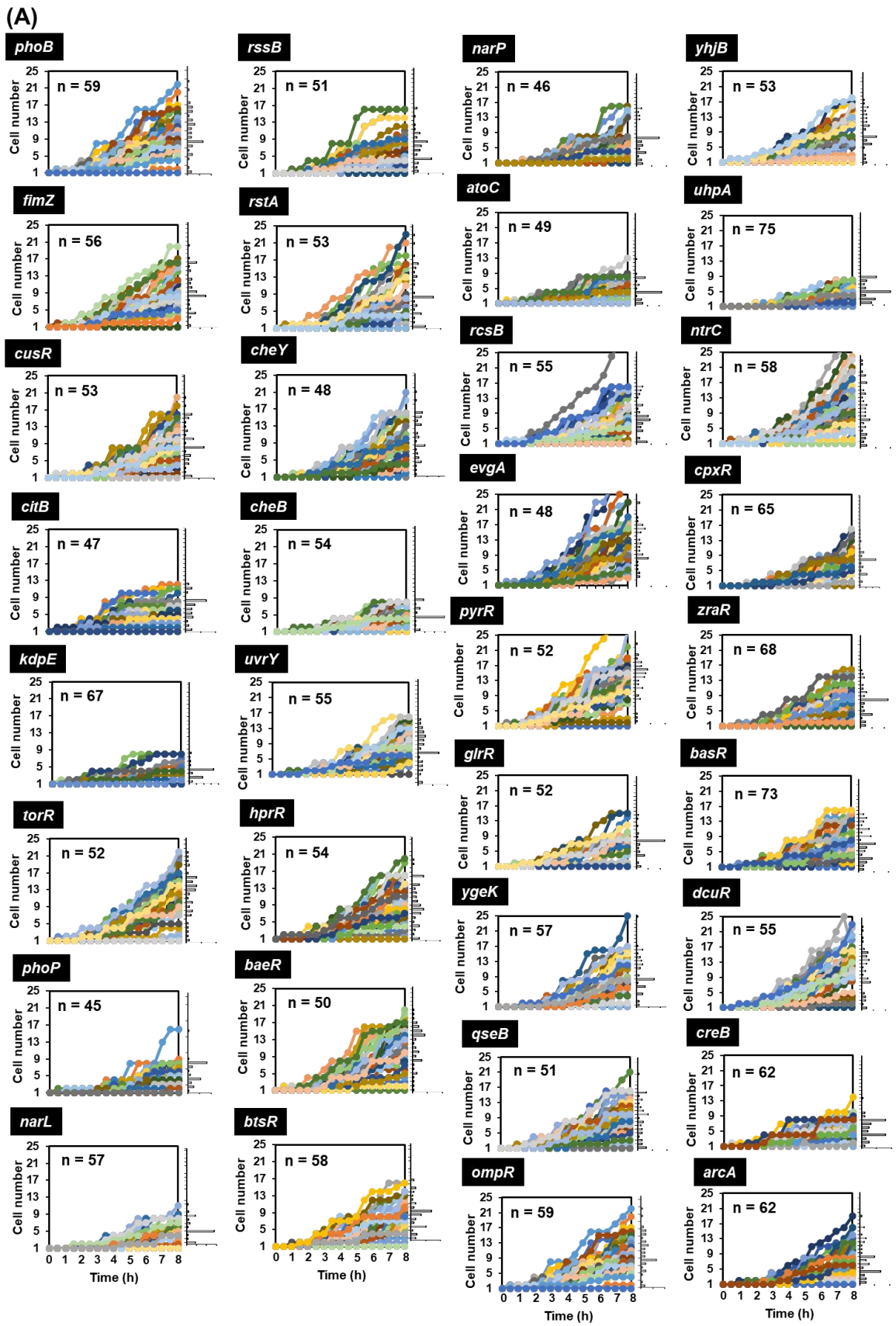
(A)
phoB
n = 59
rssB
n = 51
narP
n = 46
yhjB
n = 53
fimZ
n = 56
rstA
n = 53
atoC
n = 49
uhpA
n = 75
cusR
n = 53
cheY
n = 48
rcsB
n = 55
ntrC
n = 58
citB
n = 47
cheB
n = 54
evgA
n = 48
cpxR
n = 65
kdpE
n = 67
uvrY
n = 55
pyrR
n = 52
zraR
n = 68
torR
n = 52
hprR
n = 54
glrR
n = 52
basR
n = 73
phoP
n = 45
baeR
n = 50
ygeK
n = 57
dcuR
n = 55
narL
n = 57
btsR
n = 58
qseB
n = 51
creB
n = 62
ompR
n = 59
arcA
n = 62
Cell number
Time (h)

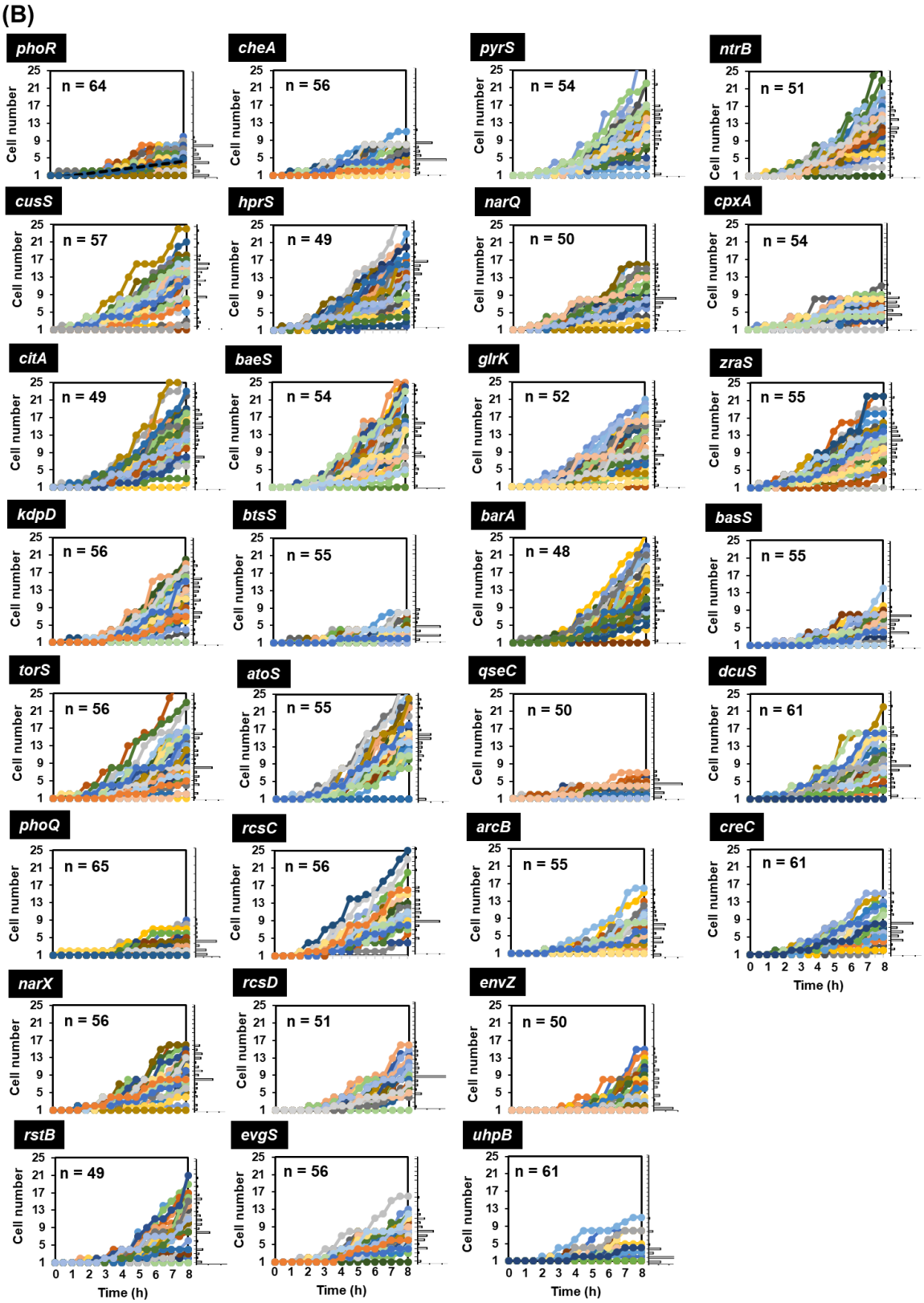

Appendix Figure 3. Single cell analysis of adaptive growth of single gene knockout *E. coli* strains. Strains were cultured, spread on M9 glucose agar plate, and imaged on a microscope as described in **Fig. 5-3**. The cell division (hours, showed in x axis) and the population of cell in each microcolony (y axis) were measured and the histograms of cell population in a microcolony at after 8 hours were showed on the right side of each graph. The number of measured cell (n) are shown in each graph. **[A]** The results of single RR-gene knockout strains. **[B]** The results of single SK-gene knockout strains.

Appendix Table 9. The amino acid sequence of OmpR family RRs.

Sub-family	Bacteral strain	Gene name	Amino acid sequence
A	*Escherichia coli* str. K-12 substr. MG1655	*arcA*	MQTPHILIVEDELVTRNTLKSIFEAEGYDVFEATDGAEMHQILSEYDINLVIMDINLPGKNGLLLAR ELREQANVALMFLTGRDNEVDKILGLEIGADDYITKPFNPRELTIRARNLLSRTMNLGTVSEERRS VESYKFNGWELDINSRSLIGPDGEQYKLPRSEFRAMLHFCENPGKIQSRAELLKKMTGRELKPHD RTVDVTIRRIRKHFESTPDTPEIIATIHGEGYRFCGDLED
A	*Escherichia coli* str. K-12 substr. MG1655	*ompR*	MQENYKILVVDDDMRLRALLERYLTEQGFQVRSVANAEQMDRLLTRESFHLMVLDLMLPGEDG LSICRRLRSQSNPMPIIMVTAKGEEVDRIVGLEIGADDYIPKPFNPRELLARIRAVLRRQANELPGA PSQEEAVIAFGKFKLNLGTREMFREDEPMPLTSGEFAVLKALVSHPREPLSRDKLMNLARGREYS AMERSIDVQISRLRRMVEEDPAHPRYIQTVWGLGYVFVPDGSKA
A	*Escherichia coli* str. K-12 substr. MG1655	*rstA*	MNTIVFVEDDAEVGSLIAAYLAKHDMQVTVEPRGDQAEETILRENPDLVLLDIMLPGKDGMTICR DLRAKWSGPIVLLTSLDSDMNHILALEMGACDYILKTTPPAVLLARLRLHLRQNEQATLTKGLQE TSLTPYKALHFGTLTIDPINRVVTLANTEISLSTADFELLWELATHAGQIMDRDALLKNLRGVSYD GLDRSVDVAISRLRKKLLDNAAEPYRIKTVRNKGYLFAPHAWE
A	*Escherichia coli* str. K-12 substr. MG1655	*torR*	MPHHIVIVEDEPVTQARLQSYFTQEGYTVSVTASGAGLREIMQNQSVDLILLDINLPDENGLMLTR ALRERSTVGIILVTGRSDRIDRIVGLEMGADDYVTKPLELRELVVRVKNLLWRIDLARQAQPHTQ DNCYRFAGYCLNVSRHTLERDGEPIKLTRAEYEMLVAFVTNPGEILSRERLLRMLSARRVENPDL RTVDVLIRRLRHKLSADLLVTQHGEGYFLAADVC
A	*Pseudomonas aeruginosa* PAO1	*parR*	MDCPTLSKVLLVEDDQKLARLIASFLSQHGFEVRQVHRGDAAFAAFLDFKPQVVVLDLMLPGQN GLQVCREIRRVANLPILILTAQEDDLDHILGLESGADDYVIKPIEPPVLLARLRALMRRHAPLPASP ESLTFGKLNIDRRRREAELEGLGIELTTMEFELLWLLASQAGEILSRDEILNQIRGIGFDGLNRSVDV CISKLRNKLKDNPREPVRIKTVWGKGYLFNPLGWEL
A	*Pseudomonas aeruginosa* PAO1	*gltR*	MSANGRSILLVDDDQEIRELLETYLSRAGFQVRSVSRGADFRQALCEEEASLAILDVMLPDEDGFS LCRWIRSHQRLACMPIIMLTASSDEADRVIGLELGADDYLGKPFSPRELLARIKALLRRAQFTQVR GGDVLAFEDWRLDTVSHRLFHEDGEEFFLSGADFALLKLFLDHPQQILDRDTIANATRGREVLPLE RIVDMAVSRLRQRLRDTGKAPRLIQTVRGSGYLLAAQVRPHLQP
A	*Pseudomonas aeruginosa* PAO1	*bfmR*	MEHVDHILIVDDDREIRELVGNYLKKNGLRTTIVADGRQMRAFLEANTVDLIVLDIMMPGDDGL LLCRELRVGKHKATPVLMLTARNDETDRIIGLEMGADDYLTKPFSARELLARINAVLRRTRMLPP NLTVSESSRLIGFGQWQLDTSARHLLDDAGTVVALSGAEYRLLRVFLDHPQRVLSRDQLLNLTQG READIFDRSIDLLVSRLRQRLGDDAREPEYIKTVRSEGYVFSLPVRLVEAHP
A	*Pseudomonas aeruginosa* PAO1	*PA4983*	MAMVPRVLVVDDDPVIRELLQAYLGEEGYDVLCAGNAEQAEACLAECAHLGQPVELVLLDIRL PGKDGLTLTRELRVRSEVGIILITGRNDEIDRIVGLECGADDYVIKPLNPRELVSRAKNLIRRVRHA QASAGPARQALRQFGDWLLDADRRRLIDHAGNETLLTHGEFQLLGAFLRNSGHTLSRDQLMDQI RNREWLPSDRSIDVLVGRLRRKLRDDPAEPQLIITIHGAGYLFTAAASDA
A	*Pseudomonas aeruginosa* PAO1	*PA1157*	MEQEAWRILIVEDDRRLAELTREYLEGNGLKVDIEANGALAAARILAERPDLVVLDLMLPGEDGL SICRQVRPQFDGPILMLTARTDDMDEVLGLEMGADDYVCKPVRPRVLLARIRALLRRSEAPEAG APAADSKRLAFGRLVIDNAMREAWLDGTTIELTSAEFDLLWLLAANAGRILSREEIFNALRGIEYD GQDRSIDVRISRIRPKIGDDPMHPRLIKTVRSKGYLFVGEG
A	*Pseudomonas aeruginosa* PAO1	*amgR*	MSNPAALAEGEKILVVDDDARLRRLLERFLDEQGYRVRAVENTEQMDRLLSRELFQLVVLDLML PGEDGLTACRRLREQNNQVPIIMLTAKGDEGSRIQGLELGADDYLAKPFNPRELLARIKAVLRRQ APLVPGAPAGADEVVTFGDYQLFLATRELKKGDEVHMLTTGEFAVLKALVQHAREPLTRDKLM NLARGREWDALERSIDVQISRLRRLIEPDPSKPRYIQTVWGVGYVFVPDGNARKA
A	*Haemophilus influenzae* Rd KW20	*arcA*	MTTPKILVVEDEIVTRNTLKGIFEAEGYDVFEAENGVEMHHILANHNINLVVMDINLPGKNGLLL ARELREELSLPLIFLTGRDNEVDKILGLEIGADDYLTKPFNPRELTIRARNLLHRAMPHQEKENTFG REFYRFNGWKLDLNSHSLITPEGQEFKLPRSEFRAMLHFCENPGKLQTREELLKKMTGRELKPQD RTVDVTIRRIRKHFEDHPNTPNIIMTIHGEGYRFCGDIE
A	*Salmonella enterica* subsp. Enterica serovar Typhimurium str. LT2	*rstA*	MNRIVFVEDDAEVGSLIAAYLAKHDIDVIVEPRGDRAEDLILTTQPDLVLLDIMLPGKDGMTICRD LRHRWQGPIVLLTSLDSDMNHILALEMGACDYILKTTPPAVLLARLRLHLRQSEQTQQAKSLQES ALTPHKALRFGALTIDPLNRAVQLNGDFISLSTADFELLWELATHAGQIMDRDALLKTLRGVNYD GLDRSVDVAISRLRKKLLDSAAEPYRIKTIRNKGYLFAPHAWDETTG
A	*Salmonella enterica* subsp. Enterica serovar Typhimurium str. LT2	*ompR*	MQENYKILVVDDDMRLRALLERYLTEQGFQVRSVANAEQMDRLLTRESFHLMVLDLMLPGEDG LSICRRLRSQSNPMPIIMVTAKGEEVDRIVGLEIGADDYIPKPFNPRELLARIRAVLRRQANELPGA PSQEEAVIAFGKFKLNLGTREMFREDEPMPLTSGEFAVLKALVSHPREPLSRDKLMNLARGREYS AMERSIDVQISRLRRMVEEDPAHPRYIQTVWGLGYVFVPDGSKA
A	*Salmonella enterica* subsp. Enterica serovar Typhimurium str. LT2	*torR*	MSHHIVIVEDEPVTQARLQAYFEQEGYRVSVTDSGAGLRDIMEHEHVSLILLDINLPDENGLMLTR ALRERSTVGIILVTGRCDQIDRIVGLEMGADDYVTKPLELRELVVRVKNLLWRIDLARPTPQNAS ENCYMFSGYCLNVMNHTLEHNGEAIKLTRAEYELLLAFVTNPGKVLHRERLLRMLSARRVETPD LRTIDVLVRRLRHKITPELLVTQHGEGYFLASEVY
A	*Salmonella enterica* subsp. Enterica serovar Typhimurium str. LT2	*arcA*	MQTPHILIVEDELVTRNTLKSIFEAEGYDVFEATDGAEMHQILSEYDINLVIMDINLPGKNGLLLAR ELREQANVALMFLTGRDNEVDKILGLEIGADDYITKPFNPRELTIRARNLLSRTMNLGTVSEERRS VESYKFNGWELDINSRSLIGPDGEQYKLPRSEFRAMLHFCENPGKIQSRAELLKKMTGRELKPHD RTVDVTIRRIRKHFESTPDTPEIIATIHGEGYRFCGDLQD
A	*Shigella dysenteriae* 1617	*Asd161705396*	MKPVVLVVDDDTAICALLQDVLSEHVFTVSVCHTGQEAILRIEGDPDIALVVLDMMLPDTNGLR VLQQIQKLRPTLPVVMLTGMGSKSDVVVGLEMGADDYICKPFTPRVVVARLKAVLRRVGALAV NDEKSAGLSFNGWYLDTMRCQLHNPLQQHVELTQGEYGLLLALAQNASRVLSREQLLAFTHSDS VEVFDRTIDVLIMRLRRKIELNPHQPMLIKTLRGLGYVFAADVH
A	*Shigella dysenteriae* 1617	*rstA*	MTFFISTVNVMNTIVFVEDDAEVGSLIAAYLAKHDMQVTVEPRGDQAEETILRENPDLVLLDIML PGKDGMTICRDLRAKWSGPIVLLTSLDSDMNHILALEMGACDYMPPAVLLARLRLHLRQNEQAT LTKGLQETSLTPYKALHFGTLTIDPINRVVTLANTEISLSTADFELLWELATHAGQIMDRDALLKN LRGVSYDGLDRSVDVAISRLRKKLLDNAAEPYRIKTVRNKGYLFAPHAWE
A	*Shigella dysenteriae* 1617	*ompR*	MGVQTMQENYKILVVDDDMRLRALLERYLTEQGFQVRSVANAEQMDRLLTRESFHLMVLDLM LPGEDGLSICRRLRSQSNPMPIIMVTAKGEEVDRIVGLEIGADDYIPKPFNPRELLARIRAVLRRQA NELPGAPSQEEAVIAFGKFKLNLGTREMFREDEPMPLTSGEFAVLKALVSHPREPLSRDKLMNLA RGREYSAMERSIDVQISRLRRMVEEDPAHPRYIQTVWGLGYVFVPDGSKA
B	*Escherichia coli* str. K-12 substr. MG1655	*baeR*	MTELPIDENTPRILIVEDEPKLGQLLIDYLRAASYAPTLISHGDQVLPYVRQTPPDLILLDLMLPGT DGLTLCREIRRFSDIPIVMVTAKIEEIDRLLGLEIGADDYICKPYSPREVVARVKTILRRCKPQRELQ QQDAESPLIIDEGRFQASWRGKMLDLTPAEFRLLKTLSHEPGKVFSREQLLNHLYDDYRVVTDRT IDSHIKNLRRKLESLDAEQSFIRAVYGVGYRWEADACRIV
B	*Escherichia coli* str. K-12 substr. MG1655	*creB*	MQRETVWLVEDEQGIADTLVYMLQQEGFAVEVFERGLPVLDKARKQVPDVMILDVGLPDISGFE LCRQLLALHPALPVLFLTARSEEVDRLLGLEIGADDYVAKPFSPREVCARVRTLLRRVKKFSTPSP VIRIGHFELNEPAAQISWFDTPLALTRYEFLLLKTLLKSPGRVWSRQQLMDSVWEDAQDTYDRTV DTHIKTLRAKLRAINPDLSPINTHRGMGYSLRGL
B	*Escherichia coli* str. K-12 substr. MG1655	*phoB*	MARRILVVEDEAPIREMVCFVLEQNGFQPVEAEDYDSAVNQLNEPWPDLILLDWMLPGGSGIQFI KHLKRESMTRDIPVVMLTARGEEEDRVRGLETGADDYITKPFSPKELVARIKAVMRRISPMAVEE VIEMQGLSLDPTSHRVMAGEEPLEMGPTEFKLLHFFMTHPERVYSREQLLNHVWGTNVYVEDRT VDVHIRRLRKALEPGGHDRMVQTVRGTGYRFSTRF
B	*Bacillus subtilis* substr. subtilis str. 168	*yclK*	MKILMIEDNVSVCTMTEMFFFKEGFEAEFVHDGLEGYQRFTEENWDLIILDIMLPSMDGVTICRKI RETSTVPIIMLTAKDTESDQVIGFEMGADDYVTKPFSPLTLVARIKAVIRRYKATGKAVIDEDMIE TECFTINKKTREVLLNGEPVENLTPKEFDLLYYLVQNPRQVFSREQLLEQVWGYQFYGDERTVD VHIKRLRKKLASEDKPFLYTVWGVGYKFDED
B	*Bacillus subtilis* substr. subtilis str. 168	*yycF*	MDKKILVVDDEKPIADILEFNLRKEGYEVHCAHDGNEAVEMVEELQPDLILLDIMLPNKDGVEV CREVRKKYDMPIIMLTAKDSEIDKVIGLEIGADDYVTKPFSTRELLARVKANLRRQLTTAPAEEEP SSNEIHIGSLVIFPDAYVVSKRDETIELTHREFELLHYLAKHIGQVMTREHLLQTVWGYDYFGDVR TVDVTVRRLREKIEDNPSHPNWIVTRRGVGYYLRNPEQD

Appendix Table 9. The amino acid sequence of OmpR family RRs. (Continued.)

Sub-family	Bacteral strain	Gene name	Amino acid sequence
B	*Bacillus subtilis* substr. subtilis str. 168	*resD*	MDQTNETKILVVDDEARIRRLLRMYLERENYAIDEAENGDEAIAKGLEANYDLILLDLMMPGTD GIEVCRQIREKKATPIIMLTAKGEEANRVQGFEAGTDDYIVKPFSPREVVLRVKALLRRASQTSYF NANTPTKNVLVFSHLSIDHDAHRVTADGTEVSLTPKEYELLYFLAKTPDKVYDREKLLKEVWQY EFFGDLRTVDTHVKRLREKLNKVSPEAAKKIVTVWGVGYKFEVGAE
B	*Bacillus subtilis* substr. subtilis str. 168	*phoP*	MNKKILVVDDEESIVTLLQYNLERSGYDVITASDGEEALKKAETEKPDLIVLDVMLPKLDGIEVC KQLRQQKLMFPILMLTAKDEEFDKVLGLELGADDYMTKPFSPREVNARVKAILRRSEIAAPSSEM KNDEMEGQIVIGDLKILPDHYEAYFKESQLELTPKEFELLLYLGRHKGRVLTRDLLLSAVWNYDF AGDTRIVDVHISHLRDKIENNTKKPIYIKTIRGLGYKLEEPKMNE
B	*Mycobacterium tuberculosis* H37Rv	*regX*	MTSVLIVEDEESLADPLAFLLRKEGFEATVVTDGPAALAEFDRAGADIVLLDLMLPGMSGTDVCK QLRARSSVPVIMVTARDSEIDKVVGLELGADDYVTKPYSARELIARIRAVLRRGGDDDSEMSDGV LESGPVRMDVERHVVSVNGDTITLPLKEFDLLEYLMRNSGRVLTRGQLIDRVWGADYVGDTKTL DVHVKRLRSKIEADPANPVHLVTVRGLGYKLEG
B	*Mycobacterium tuberculosis* H37Rv	*Rv0818*	MLELLLLTSELYPDPVLPALSLLPHTVRTAPAEASSLLEAGNADAVLVDARNDLSSGRGLCRLLSS TGRSIPVLAVVSEGGLVAVSADWGLDEILLLSTGPAEIDARLRLVVGRRGDLADQESLGKVSLGEL VIDEGTYTARLRGRPLDLTYKEFELLKYLAQHAGRVFTRAQLLHEVWGYDFFGGTRTVDVHVRR LRAKLGPEHEALIGTVRNVGYKAVRPARGRPPAADPDDEDADPGRDGMQEPLVDPLRSQ
B	*Mycobacterium tuberculosis* H37Rv	*Rv2884*	MPTGPTTGKWHPHEVWRYLLEVLLLTDEADLESALPELESFAQSVQRAPLDDPGAAKGADADV AIIDARADLAAARRVCRRLTTSAPALAVVAVVAPANFVAVDGDWIFDDVLLNAAGGAELQARL RLAITRRRSTLAGTLQFGDLVLHPASYTASLGDRDLGLTLTEFKLMNFLVQHAGRAFTRTRLMRE VWGYECHGRIRTVDVHVRRLRAKLGAEHESMIDTVRGVGYMAVTPPQPRWIISESILNRCK
B	*Mycobacterium tuberculosis* H37Rv	*mtrA*	MDTMRQRILVVDDDASLAEMLTIVLRGEGFDTAVIGDGTQALTAVRELRPDLVLLDLMLPGMNG IDVCRVLRADSGVPIVMLTAKTDTVDVVLGLESGADDYIMKPFKPKELVARVRARLRRNDDEPA EMLSIADVEIDVPAHKVTRNGEQISLTPLEFDLLVALARKPRQVFTRDVLLEQVWGYRHPADTRL VNVHVQRLRAKVEKDPENPTVVLTVRGVGYKAGPP
B	*Pseudomonas aeruginosa* PAO1	*creB*	MPHILIVEDEAAIADTLLYALQAEGFATTWVTLAGEALALQERQPADLLILDVGLPDISGFEACKR LRRFSEVPVIFLTARDAEIDRVVGLEIGADDYVVKPFSPREVAARVKAILKRMAPRPAALEEAAP SGPFQVDEERVRIHYRDTPLNLTRHEFRLLQTLLGQPERVFSREQLLDALGVASEAGYERNIDSHI KSLRAKLRQVNERGEAIQTHRGLGYSYSPDHA
B	*Pseudomonas aeruginosa* PAO1	*phoB*	MVGKTILIVDDEAPIREMIAVALEMAGYECLEAENTQQAHAVIVDRKPDLILLDWMLPGTSGIEL ARRLKRDELTVDIPIIMLTAKGEEDNKIQGLEVGADDYITKPFSPRELVARLKAVLRRTGPGDSEA PIEVGGLLLDPISHRVTIDGKPAEMGPTEYRLLQFFMTHQERAYTRGQLLDQVWGGNVYVEERTV DVHIRRLRKALGEVYENLVQTVRGTGYRFSTKS
B	*Corynebacterium glutamicum* ATCC 13032	*cgtR4*	MTRILIVEDEESLADPLAFLLRKEGFDTIIAGDGPTALVEFSRNEIDIVLLDLMLPGMSGTDVCKEL RSVSTVPVIMVTARDSEIDKVVGLELGADDYVTKPYSSRELIARIRAVLRRRGVTETEAEELPLDD QILEGGRVRMDVDSHTVTVGGEPVSMPLKEFDLLEYLLRNAGRVLTRGQLIDRIWGADYVGDTK TLDVHVKRLRSKIEEEPSRPRYLVTVRGLGYKFEL
B	*Corynebacterium glutamicum* ATCC 13032	*mtrA*	MSQKILVVDDDPAISEMLTIVLSAEGFDTVAVTDGALAVETASREQPDLILLDLMLPGMNGIDICR LIRQESSVPIIMLTAKTDTVDVVLGLESGADDYVNKPFKAKELVARIRARLRATVDEPSEIIEVGD LSIDVPAHTVKRNGAEISLTPLEFDLLLELARKPQQVFTREELLGKVWGYRHASDTRLVNVHVQR LRAKIEKDPENPQIVLTVRGVGYKTGHND
B	*Corynebacterium glutamicum* ATCC 13032	*cgtR5*	MTNPSPALNETLSGRVLIVEDERPLARMISLYLSKAGFDTTTIHDGAAAPDKVAHLRPDVVILDLG LPGLDGLEVCKRIRAFTDCYILMLTARGSERDRITGLEIGADDYITKPFNIRELVIRIQSVMRRPRKI DETIQNGLTLTYGHIELDTLAHEVTVKGVGVTLTRTEFELLQALMHKPGEAVSRRDLVSQVWDTT WVGDERIVDVHIGNLRRKLEAPAPGSHFIDTIRGVGYRMAFK
B	*Corynebacterium glutamicum* ATCC 13032	*cgtR9*	MADRTPTTATPPGRVLVVDDEQPLAQMVASYLIRAGFDTRQAHTGTQAVDEARRFSPDVVVLD LGLPELDGLEVCRRIRTFSDCYILMLTARGSEDDKISGLTLGADDYITKPFSIRELVTRVHAVLRRP RTSTTPPQVTTPLIVGDLILDPVAHQVWVGETTVELTRTEFELLVALALRPGQVLTRHDLITEVWD TTWVGDERIVDVHIGNLRRKLGTDTRGRGFIDTVRGVGYRVGQP
B	*Haemophilus influenzae* Rd KW20	*phoB*	MTRKILIVEDECAIREMIALFLSQKYYDVIEASDFKTAINKIKENPKLILLDWMLPGRSGIQFIQYIK KQESYAAIPIIMLTAKSTEEDCIACLNAGADDYITKPFSPQILLARIEAVWRRIYEQQSQFIQIDELSI DENAQRVFFQQQEINLSSTEFKLLHFFMRHPEKVYSREQLLNRIWHNDLEVEYRTVDSYIRRLRR NLAPFQCEHYIQTVRGSGYRFSSYLRDKQ
B	*Salmonella enterica* subsp. Enterica serovar Typhimurium str. LT2	*phoB*	MARRILVVEDEAPIREMVCFVLEQNGFQPVEAEDYDSAVNKLNEPWPDLILLDWMLPGGSGLQF IKHLKREAMTRDIPVVMLTARGEEEDRVRGLETGADDYITKPFSPKELVARIKAVMRRISPMAVE EVIEMQGLSLDPGSHRVMTGDSPLDMGPTEFKLLHFFMTHPERVYSREQLLNHVWGTNVYVEDR TVDVHIRRLRKALEHSGHDRMVQTVRGTGYRFSTRF
B	*Salmonella enterica* subsp. Enterica serovar Typhimurium str. LT2	*baeR*	MTELPIDENTPRILIVEDEPKLGQLLIDYLRAASYAPTLINHGDKVLPYVRQTPPDLILLDLMLPGT DGLTLCREIRRFSDIPIVMVTAKIEEIDRLLGLEIGADDYICKPYSPREVVARVKTILRRCKPQRELQ QQDAESPLMIDESRFQASWCGKALDLTPAEFRLLKTLSLEPGKVFSREQLLNHLYDDYRVVTDRT IDSHIKNLRRKLESLDAEQSFIRAVYGVGYRWEADACRLV
B	*Salmonella enterica* subsp. Enterica serovar Typhimurium str. LT2	*creB*	MQQPQVWLVEDEQGIADTLIYTLQLEGFTVELFARGLPALEKARQQRPDAVILDVGLPDISGFEL CRQLLERHPALPILFLTARSDEVDRLLGLEIGADDYVAKPFSPREVSARVRTLLRRVKKFAAPSPV VRTGHFELNEPAAQIAWFGTPLSLTRYEFLLLKTLLLSPERVYSRQQLMDIVWSDAQETFDRTVD THIKTLRAKLRAINPELSPINTHRGMGYSLRSV
B	*Shigella dysenteriae* 1617	*phoB*	MARRILVVEDEAPIREMVCFVLEQNGFQPVEAEDYDSAVNQLNEPWPDLILLDWMLPGGSGIQFI KHLKRESMTRDIPVVMLTARGEEEDRVRGLETGADDYITKPFSPKELVARIKAVMRRISPMAVEE VIEMQGLSLDPTSHRVMTGEEPLEMGPTEFKLLHFFMTHPERVYSREQLLNHVWGTNVYVEDRT VDVHIRRLRKALEPGGHDRMVQTVRGTGYRFSTRF
B	*Shigella dysenteriae* 1617	*baeR*	MTELPIDENTPRILIVEDEPKLGQLLIDYLRAASYAPTLISHGDQVLPYVRQTPPDLILLDLMLPGT DGLTLCREIRRFSDIPIVMVTAKIEEIDRLLGLEIGADDYICKPYSPREVVARVKTILRRCKPQRELQ QQDAESPLIIDEGRFQASWRGKMLDLTPAEFRLLKTLSHEPGKVFSREQLLNHLYDDYRVVTDRT IDSHIKNLRRKLESLDAEQSFIRAVYGVGYRWEADACRIV
B	*Shigella dysenteriae* 1617	*creB*	MQRETVWLVEDEQGIADTLVYMLQQEGFAVEVFERGLPVLDKARQQQAPDVMILDVGLPDISGFE LCRQLLALHPALPVLFLTARSEEVDRLLGLEIGADDYVAKPFSPREVCARVRTLLRRVKKFSSPSP VIRIGHFELNEPAAQISWFDTPLTLTRYEFLLLKTLLKSPGRVWSRQQLMDSVWEDAQDTYDRTV DTHIKTLRAKLRAINPDLSPINTHRGMGYSLRGL
C	*Escherichia coli* str. K-12 substr. MG1655	*basR*	MKILIVEDDTLLLQGLILAAQTEGYACDSVTTARMAEQSLEAGHYSLVVLDLGLPDEDGLHFLAR IRQKKYTLPVLILTARDTLTDKIAGLDVGADDYLVKPFALEELHARIRALLRRHNNQGESELIVGN LTLNMGRRQVWMGGEELILTPKEYALLSRLMLKAGSPVHREILYNDIYNWDNEPSTNTLEVHIH NLRDKVGKARIRTVRGFGYMLVANEEN
C	*Escherichia coli* str. K-12 substr. MG1655	*cpxR*	MNKILLVDDDRELTSLLKELLEMEGFNVIVAHDGEQALDLLDDSIDLLLLDVMMPKKNGIDTLK ALRQTHQTPVIMLTARGSELDRVLGLELGADDYLPKPFNDRELVARIRAILRRSHWSEQQQNND NGSPTLEVDALVLNPGRQEASFDGQTLELTGTEFTLLYLLAQHLGQVVSREHLSQEVLGKRLTPF DRAIDMHISNLRRKLPDRKDGHPWFKTLRGRGYLMVSAS
C	*Escherichia coli* str. K-12 substr. MG1655	*cusR*	MKLLIVEDEKKTGEYLTKGLTEAGFVVDLADNGLNGYHLAMTGDYDLIILDIMLPDVNGWDIVR MLRSANKGMPILLLTALGTIEHRVKGLELGADDYLVKPFAFAELLARVRTLLRRGAAVIIESQFQV ADLMVDLVSRKVTRSGTRITLTSKEFTLLEFFLRHQGEVLPRSLIASQVWDMNFDSDTNAIDVAV KRLRGKIDNDFEPKLIQTVRGVGYMLEVPDGQ
C	*Escherichia coli* str. K-12 substr. MG1655	*kdpE*	MTNVLIVEDEQAIRRFLRTALEGDGMRVFEAETLQRGLLEAATRKPDLIILDLGLPDGDGIEFIRDL RQWSAVPVIVLSARSEESDKIAALDAGADDYLSKPFGIGELQARLRVALRRHSATTAPDPLVKFS DVTVDLAARVIHRGEEEVHLTPIEFRLLAVLLNNAGKVLTQRQLLNQVWGPNAVEHSHYLRIYM GHLRQKLEQDPARPRHFITETGIGYRFML

Appendix Table 9. The amino acid sequence of OmpR family RRs. (Continued.)

Sub-family	Bacteral strain	Gene name	Amino acid sequence
C	*Escherichia coli* str. K-12 substr. MG1655	*phoP*	MRVLVVEDNALLRHHLKVQIQDAGHQVDDAEDAKEADYYLNEHIPDIAIVDLGLPDEDGLSLIR RWRSNDVSLPILVLTARESWQDKVEVLSAGADDYVTKPFHIEEVMARMQALMRRNSGLASQVIS LPPFQVDLSRRELSINDEVIKLTAFEYTIMETLIRNNGKVVSKDSLMLQLYPDAELRESHTIDVLM GRLRKKIQAQYPQEVITTVRGQGYLFELR
C	*Escherichia coli* str. K-12 substr. MG1655	*qseB*	MRILLIEDDMLIGDGIKTGLSKMGFSVDWFTQGRQGKEALYSAPYDAVILDLTLPGMDGRDILRE WREKGQREPVLILTARDALAERVEGLRLGADDYLCKPFALIEVAARLEALMRRTNGQASNELRH GNVMLDPGKRIATLAGEPLTLKPKEFALLELLMRNAGRVLSRKLIEEKLYTWDEEVTSNAVEVH VHHLRRKLGSDFIRTVHGIGYTLGEK
C	*Escherichia coli* str. K-12 substr. MG1655	*hprR*	MKILLIEDNQRTQEWVTQGLSEAGYVIDAVSDGRDGLYLALKDDYALIILDIMLPGMDGWQILQT LRTAKQTPVICLTARDSVDDRVRGLDSGANDYLVKPFSFSELLARVRAQLRQHHALNSTLEISGL RMDSVSHSVSRDNISITLTRKEFQLLWLLASRAGEIIPRTVIASEIWGINFDSDTNTVDVAIRRLRAK VDDPFPEKLIATIRGMGYSFVAVKK
C	*Bacillus subtilis* substr. subtilis str. 168	*ykoH*	MEKGHILIVEDEEKIARVLQLELEYEGYSVTIKHNGTEGLDAAAEGGYSLVLLDVMLPGLSGLEVL RRLRKTDSQTPVILLTARDSIPDKVTGLDIGANDYVTKPFEIEELLARIRAALRQNGTKTEDIGTFL TYDDLRVNEKTREVRRGDKEVELTPREFDLLVYMLKHPQQVLTREQILSSVWGFDYIGDTNVVD VYIRYIRKKLDYPYEKQLIHTIRGVGYAIKG
C	*Bacillus subtilis* substr. subtilis str. 168	*cssR*	MSYTIYLVEDEDNLNELLTKYLENEGWNITSFTKGEDARKKMTPSPHLWILDIMLPDTDGYTLIK EIKAKDPDVPVIFISARDADIDRVLGLELGSNDYISKPFLPRELIIRVQKLLQLVYKEAPPVQKNEI AVSSYRVAEDAREVYDENGNIINLTSKEFDLLLLFIHHKGHPYSREDILLKVWGHDYFGTDRVVD DLVRRLRRKMPELKVETIYGFGYRMMSS
C	*Mycobacterium tuberculosis* H37Rv	*tcrA*	MADETTMRAGRGPGRACGRVSGVRILVVEDEPKMTALLARALTEEGHTVDTVADGRHAVAAV DGGDYDAVVLDVMLPGIDGFEVCARLRRQRVWTPVLMLTARGAVTDRIAGLDGGADDYLTKPF NLDELFARLRALSRRGPIPRPPTLEAGDLRLDPSEHRVWRADTEIRLSHKEFTLLEALIRRPGIVHT RAQLLERCWDAAYEARSNIVDVYIRYLRDKIDRPFGVTSLETIRGAGYRLRKDGGRHALPR
C	*Mycobacterium tuberculosis* H37Rv	*phoP*	MRKGVDLVTAGTPGENTTPEARVLVVDDEANIVELLSVSLKFQGFEVVTATNGAQALDRARETR PDAVILDVMMPGMDGFGVLRRLRADGIDAPALFLTARDSLQDKIAGLTLGGDDYVTKPFSLEEV VARLRVILRRAGKGNKEPRNVRLTFADIELDEETHEVWKAGQPVSLSPTEFTLLRYFVINAGTVLS KPKILDHVWRYDFGGDVNVVESYVSYLRRKIDTGEKRLLHTLRGVGYVLREPR
C	*Mycobacterium tuberculosis* H37Rv	*prrA*	MGGMDTGVTSPRVLVVDDDSDVLASLERGLRLSGFEVATAVDGAEALRSATENRPDAIVLDINM PVLDGVSVVTALRAMDNDVPVCVLSARSSVDDRVAGLEAGADDYLVKPFVLAELVARVKALL RRRGSTATSSSETITVGPLEVDIPGRRARVNGVDVDLTKREFDLLAVLAEHKTAVLSRAQLLELV WGYDFAADTNVVDVFIGYLRRKLEAGGGPRLLHTVRGVGFVLRMQ
C	*Mycobacterium tuberculosis* H37Rv	*kdpE*	MTLVLVIDDEPQILRALRINLTVRGYQVITASTGAGALRAAAEHPPDVVILDLGLPDMSGIDVLGG LRGWLTAPVIVLSARTDSSDKVQALDAGADDYVTKPFGMDEFLARLRAAVRRNTAAAELEQPVI ETDSFTVDLAGKKVIKDGAEVHLTPTEWGMLEMLARNRGKLVGRGELLKEVWGPAYATETHYL RVYLAQLRRKLEDDPSHPKHLLTESGMGYRFEA
C	*Mycobacterium tuberculosis* H37Rv	*trcR*	MTTMSGYTRSQRPRQAILGQLPRIHRADGSPIRVLLVDDEPALTNLVKMALHYEGWDVEVAHDG QEAIAKFDKVGPDVLVLDIMLPDVDGLEILRRVRESDVYTPTLFLTARDSVMDRVTGLTSGADDY MTKPFSLEELVARLRGLLRRSSHLERPADEALRVGDLTLDGASREVTRDGTPISLSSTEFELLRFLM RNPRRALSRTEILDRVWNYDFAGRTSIVDLYISYLRKKIDSDREPMIHTVRGIGYMLRPPE
C	*Mycobacterium tuberculosis* H37Rv	*tcrX*	MRRADGQPVTVLVVDDEPVLAEMVSMALRYEGWNITTAGDGSSAIAAARRQRPDVVVLDVML PDMSGLDVLHKLRSENPGLPVLLLTAKDAVEDRIAGLTAGGDDYVTKPFSIEEVVLRLRALLRRT GVTTVDSGAQLVVGDLVLDEDSHEVMRAGEPVSLTSTEFELLRFMMHNSKRVLSKAQILDRVWS YDFGGRSNIVELYISYLRKKIDNGREPMIHTLRGAGYVLKPAR
C	*Mycobacterium tuberculosis* H37Rv	*mrpA*	MRILVVDDDRAVRESLRRSLSFNGYSVELAHDGVEALDMIASDRPDALVLDVMMPRLDGLEVC RQLRGTGDDLPILVLTARDSVSERVAGLDAGADDYLPKPFALEELLARMRALLRRTKPEDAAES MAMRFSDLTLDPVTREVNRGQRRISLTRTEFALLEMLIANPRRVLTRSRILEEVWGFDFPTSGNAL EVYVGYLRRKTEADGEPRLIHTVRGVGYVLRETPP
C	*Pseudomonas aeruginosa* PAO1	*PA0756*	MRILLVEDHPQLAESVVQALKGAGWTVDLLQDGVAADLALASEEYALAILDVGLPRMDGFEVL ARLRGRGKTLPVLMLTARGEVKDRVHGLNLGADDYLAKPFELSELEARVKALLRRSVLGGEQLQ RCGALVYDLGTRRFSLDEQPLTLTSREQAVLEAMIARPGRVMSKEQLAAQVFGLDEEASADAIEI YVHRLRKKLEGGAVRIVTFRGLGYLLEAQGD
C	*Pseudomonas aeruginosa* PAO1	*PA1437*	MRVLIVEDEAKTADYLNRGLSEQGFTVDLADNGIDGRHLALHGEYDVIVLDVMLPGVDGYGVL RALRERRQTPVIMLTARERVEDRVRGLREGADDYLIKPFSFLELVARLQALTRRGGNHESHSQMR IADLSIDLLSRKVFRGNTRLELTAKEYALLCVLAQRSGEILSKTAIAELVWDINFDTDTNVVEVAIK RLRAKLDGPFENKLLHTIRGMGYVLENRALAESG
C	*Pseudomonas aeruginosa* PAO1	*pfeR*	MIVQPSAVAKGWPIATTLLPASCGPADPKPEPKPKQRRLCRKVFPLRARCGALAHCPIPGKNEIF TNVNHSHISIPSPRLLLVEDDPRLREDLDAHFRRRGFRVTVCGDGSHGLEAAGREAFDLVLLDIML PGLDGLALLESLRREQATPVMLMSALGAEQDRISGFTRGADDYLPKPFSLAELDARTDALLRRVR LDRLPLAQRRDTRLVFDDQAQDVLHQGLPAGLTPSEYRLLATLREHAGEALSKPFLYRSVLHRS YTRLDRGLDVHVCNLRRKLAVVAVRHLQIQAVRGQGYLLVETEHP
C	*Pseudomonas aeruginosa* PAO1	*PA4032*	MRVAILDDESAELDRVEQTLQQIPAQGEQAWTVHRFARGEDLLKQLKRETFDLLILDWQLPDLS GLQLLRWSREHLDAPPPAIMLTSRDAEQDIVQALNSGADDYVSKPFRPNELKARVAAVLRRHGG TRPAQHEVQTFNDLSFDDAELTVTRAGAPISLTEREYRLARCLFANLGRPLSREYLYERFWPHEE VLSSRPLDTHIYRLRNKLGLTAERGWQLLTIYGYGYRLESVATVD
C	*Pseudomonas aeruginosa* PAO1	*irlR*	MRILVIEDDTKTGEYLKKGLGESGYAVDWSQHGADGLYLALENRYDLVVLDVMLPGLDGWQIM EVLRKKHDVPVLFLTARDQLQDRIRGLELGADDYLVKPFSFTELLLRIRTLLRRGVVREAEQVQL ADLQLDVLRRKVSRQGQVIALTNKEFALLHLLMRREGEVLSRTLIASEVWDMNFDSDTNVVDVA IKRLRAKVDNPFPNKLIHTVRGIGYVCEERPCPPAAP
C	*Pseudomonas aeruginosa* PAO1	*PA0929*	MFPSLTPDPRLLAIEDDPTLGAHLFQHLNGSGFEVTWCRDGEEGLAAARSGGYDLILMDIMLPGR DGLEILRQLRQEQALPVILMSALGAEQDRIAGFSQGADDYLPKPFSLAELRVRIDAILRRIALERGG APGRCAEPLARPSLQFSADVCDVSLGERFAGLTPTEYRLLETFLAAEGETLTKAFLYQHVLHRGH TQHDRSLDMHVSHLRRKLQRLGYAGHQLHTVWGKGYVLTPAP
C	*Pseudomonas aeruginosa* PAO1	*PA2479*	MHVLLTEDDDLIASGIVAGLNAQGLTVDRVASAADTQALLQVARFDVLVLDLGLPDEDGLRLLQ RLRQQGVDLPVLVLTARDAVTDRVAGLQAGADDYLLKPFDLRELGARLHTLQRRSAGRCVNVI EHGRLSYDPSTRETWLDGRPVELSRREQALLQALLNNRGRILSGEQLKDSVYGFGDEVESNALNV HIHHLRRKLGNAIVQTVRGLGYRLGPARGDGDDA
C	*Pseudomonas aeruginosa* PAO1	*PA3204*	MSELLLIDDDRELCELLGTWLVQEGFSVRASHDGAQARRALAEQTPDAVVLDVMLPDGSGLELL KQLRGDHPDLPVLMLSARGEPLDRILGLELGADDYLAKPCDPRELTARLRAVLRRTHPAQPSAQ MQLGDLSLNLTRGVAQIDGQEISLTLSESRILEALLRQPGEPLDKQALAQLALGRKLTLYDRSLDM HVSNLRKKLGSHPDGSPRILALRGRGYYYSH
C	*Pseudomonas aeruginosa* PAO1	*PA2523*	MRILIIEDEVKTADYLHQGLTESGYIVDRANDGIDGLHMALQHPYELVILDVNLPGIDGWDLLRR LRERSSARVMMLTGHGRLTDKVRGLDLGADDFMVKPFQFPELLARVRSLLRRHDQAPMQDVLR VADLELDASRHRAFRGRVRINLTTKEFALLHLLMRRNGDVITRTQIISLIWDMNFDNDSNVVEVAI CRLRAKIDDGFDLKLIHTIRGVGYVLEARR
C	*Pseudomonas aeruginosa* PAO1	*copR*	MKLLIVEDEPRIGQYLRQGLAEAGFAVDLSDDGNEGEQLALGGDYDLLILDVMLPGRDGWQILRS VRDAGMTVPVLFLTARDAVEDRVRGLEQGADDYLVKPFAFVELLARVRTLLRRGSQQLQETTL QLADLELDLLRRRVQRQGKRIDLTAKEFALLELLRRSGEVLPKSLIASQVWDMNFDSDTNVIEV AIRRLRAKVDDDYPQRLIHTVRGMGYVLEERDE
C	*Pseudomonas aeruginosa* PAO1	*PA4381*	MRILVVEDNRDILANLADYLSLKGYTVDCAQDGLSGLHLAATEHYDLIVLDVMLPGIDGYALCR RLREDARRDTPVIMLTARDQLDDRLQGFRSGADDYLVKPFALSELSARIEAVLRRAQGGGRRELS VADLSYDLDTLEVKRAGKSLKLNPIGLKLLAVLMQKSPHVVRRDALEEAVWGDDCPDSDSLRS HVHQLRQVIDKPFSVALLHTVHGVGYRLAEEPNGV

Appendix Table 9. The amino acid sequence of OmpR family RRs. (Continued.)

Sub-family	Bacteral strain	Gene name	Amino acid sequence
C	*Pseudomonas aeruginosa* PAO1	*phoP*	MKLLVVEDEALLRHHLYTRLGEQGHVVDAVPDAEEALYRVSEYHHDLAVIDLGLPGMSGLDLIR ELRSQGKSFPILILTARGNWQDKVEGLAAGADDYVVKPFQFEELEARLNALLRRSSGFVQSTIEAG PLVLDLNRKQALVEEQPVALTAYEYRILEYLMRHHQQVVAKERLMEQLYPDDEERDANVIEVL VGRLRRKLEACGGFKPIDTVRGQGYLFTERCR
C	*Pseudomonas aeruginosa* PAO1	*kdpE*	MTQLQNSILLIDDEPQIRKFLRISLNAQGYRVLEAGTGEEGLAQAALNRPDLVVLDLGLPDRDGQ DILRDLREWSQVPVLVLSVRASEGEKVLALDGGANDYVTKPFGIQEFLARVRVLLRQAAQGESPE ASVAVGPLQVDFAYRRVTLEGAEVALTRKEYAVLAALARHLGRVVTQQQLLKDIWGPTHVEDT HYLRVVVGHLRQKLGDDPASPRFLVTEAGVGYRLRDS
C	*Pseudomonas aeruginosa* PAO1	*PA2657*	MRLLLVEDHVPLADELMASLTRQGYAVDWLADGRDAAVQGASEPYDLIILDLGLPGRPGLEILQ EWRGLGLATPVLILTARGSWAERIDGLKAGADDYLTKPFHPEELALRIQALLRRAHGLANQSQLE AAGLRLDEQRQCVCLNGADVDLTAAEFRLLRYFMLHPGQVLSKGHLAEHLYDGETERDSNVIEV HVNHLRRKLGREVIETRRGQGYRYAGVAAG
C	*Pseudomonas aeruginosa* PAO1	*PA3077*	MHIHVLVVEDNFDLAGTVIDYLEAAGVVCDHARDGQAGLNLARANRYDVILLDIMLPRINGRQ VCRQLREAGLQTPVLMLTALDTLQDKLDGFDAGADDYLLKPFELPELLVRLQALSRRRSGQAQR LQVDDLVMDLDSRQASRGGTPLALSPTAWKILECLMRASPALVTREQLGRSVWGDEPPESNTLN VHMHHLRRSTVDKGFATPLIHTLHSVGFQLERK
C	*Pseudomonas aeruginosa* PAO1	*pmrA*	MRILLAEDDLLLGDGIRAGLRLEGDTVEWVTDGVAAENALVTDEFDLLVLDIGLPRRSGLDILRN LRHQGLLTPVLLLTARDKVADRVAGLDSGADDYLTKPFDLDELQARVRALTRRTTGRALPQLV HGELRLDPATHQVTLSGQAVELAPREYALLRLLLENSGKVLSRNQLEQSLYGWSGDVESNAIEVH VHHLRRKLGNQLIRTVRGIGYGIDQPAP
C	*Corynebacterium glutamicum* ATCC 13032	*cgtR1*	MSKILLAEDDAGIADFIVRGLIREGFECEVTESGAEAFARAHSGDFDLMVLDLGLPHMDGTDVLE QLRNLQVTLPIIVLTARTNIEDRLRTLEGGADDYMPKPFQFAELLARIKLRLAKHTPQETPTDARV LRNGDLELDLRTQRVLIDGSWHDLSRREVDLLETLMRHPGQILSRVQLLRLVWDMDWDPGSNV VDVYIRALRKKIGAHRVETIRGSGYRLR
C	*Corynebacterium glutamicum* ATCC 13032	*cgtR2*	MFQRVDVLIGRKSVTDWKTKRVSMKILVVDDEQAVRDSLRRSLSFNGYNVVLAEDGIQALEMID KEQPALVILDVMMPGMDGLEVCRHLRSEGDDRPILILTARDNVSDRVGGLDAGADDYLAKPFAL EELLARVRSLVRRSAVESNQSSSIEQALLSCGDLTLDPESRDVYRNGRAISLTRTEFALLQLLLKNQ RKVLTRAQILEEVWGCDFPTSGNALEVYIGYLRRKTELEGEDRLIHTVRGVGYVLRETAP
C	*Corynebacterium glutamicum* ATCC 13032	*cgtR3*	MDNQSDGQIRVLVVDDEPNIVELLTVSLKFQGFAVMTANDGNEALKIARERFRPDAYILDVMMPG MDGFELLTKLRGEGLDSPVLYLTAKDAVEHRIHGLTIGADDYVTKPFSLEEVITRLRVILRRGGAV EEDTSTSLQYADLTLNDETHEVTKAGELIDLSPTEFNLLRYLMLNAEVVLSKAKILDNVWHYDFG GDGNVVESYISYLRRKVDTQDPQLIQTVRGVGYVLRTPRS
C	*Haemophilus influenzae* Rd KW20	*cpxR*	MSKLLLVDDDIELTELLSTLLELEGFDVETANNGLEALQKLNESYKLVLLDVMMPKLNGIETLKEI RKVSNVPVMMLTARGEDIDRVLGLELGADDCLPKPFNDRELIARIKAILRRSASPSNNISNVEILSF DGITLHFSHGIATYNEENLNLTDYEFKILCLLLKSKGNVVSREELSLEVMEKPLTPFDRSLDMHISN LRRKLPKRKNKPSWFKTLRGKGYALVT
C	*Haemophilus influenzae* Rd KW20	*ygiX*	MRILLIEDDNLIGNGLQIGLTKLGFAVDWFTDGKTGMAALTSAPYDAVVLDLTLPKLDGLEVLQQ WRSNHQDVPVLILTARDTLDERVKGLQSGADDYLCKPFALAEVAARLQALIRRRYGYHHSVIEQ AGVKLDQNQRSVWLNNQPISLTSREYKLLELFMLNKDRVLSRSSIEEKLSSWDEEISSGALDVHIY NLRQKLGKQFIRTVHGVGYALGQVEK
C	*Salmonella enterica* subsp. Enterica serovar Typhimurium str. LT2	*copR*	MTIMSSCWRFTDSLTSLWHTALMKILLIEDNQKTIEWVRQGLTEAGYVVDYACDGRDGLHLALQ EHYSLIILDIMLPGLDGWQVLRALRTAHQSPVICLTARDSVEDRVKGLEAGANDYLVKPFSFAEL LARVRAQLRQHVPAFTRLTINGLDMDATKQSVSRNGKPISLTRKEFLLLWLLASRAGEIVPRTAIA SEVWGINFDSETNTVDVAIRRLRAKVDDPFEKKLIMTVRGMGYRLQAETSQNG
C	*Salmonella enterica* subsp. Enterica serovar Typhimurium str. LT2	*kdpE*	MTNVLIVEDEQAIRRFLRAALEGDGLRVYEAETLQRGLLEAATRKPDLIILDLGLPDGDGIDFIRDL RQWSAIPVIVLSARSEESDKIAALDAGADDYLSKPFGIGELQARLRVALRRHAASPCADPIVRFSG VTVDLAARLIHRGDEEIHLTPIEFRLLAVLLNNTGKVLTQRQLLNQVWGPNAVEHSHYLRIYMGH LRQKLEQDPTRPRHFITETGIGYRFMP
C	*Salmonella enterica* subsp. Enterica serovar Typhimurium str. LT2	*phoP*	MMRVLVVEDNALLRHHLKVQLQDSGHQVDAAEDAREADYYLNEHLPDIAIVDLGLPDEDGLSL IRRWRSSDVSLPVLVLTAREGWQDKVEVLSSGADDYVTKPFHIEEVMARMQALMRRNSGLASQ VINIPPFQVDLSRRELSVNEEVIKLTAFEYTIMETLIRNNGKVVSKDSLMLQLYPDAELRESHTIDV LMGRLRKKIQAQYPHDVITTVRGQGYLFELR
C	*Salmonella enterica* subsp. Enterica serovar Typhimurium str. LT2	*qseB*	MRILLVEDDTLIGDGIKAGLSKMGFSVDWFTEGRPGKEALYSAPYDAVILDLTLPGMDGRDILRE WREKGKQEPVLILTARDALAERVEGLRLGADDYLCKPFALIEVAARLEALVRRASGQASSELRH GQVTLNPGNLVATLAGEPLALKPKEFALLELLLRNKGRVLPRKLIEEKLYNWDDDVSSNAVEVH VHHLRRKLGSEFIRTVHGIGYTLGDA
C	*Salmonella enterica* subsp. Enterica serovar Typhimurium str. LT2	*cpxR*	MNKILLVDDDRELTSLLKELLEMEGFNVLVAHDGEQALELLDDSIDLLLLDVMMPKKNGIDTLK ALRQTHQTPVIMLTARGSELDRVLGLELGADDYLPKPFNDRELVARIRAILRRSHWSEQQQSSDN GSPTLEVDALSLNPGRQEASFDGQTLELTGTEFTLLYLLAQHLGQVVSREHLSQEVLGKRLTPFDR AIDMHISNLRRKLPERKDGHPWFKTLRGRGYLMVSAS
C	*Salmonella enterica* subsp. Enterica serovar Typhimurium str. LT2	*basR*	MKILIVEDDTLLLQGLILAAQTEGYACDGVSTARAAEHSLESGHYSLMVLDLGLPDEDGLHFLTRI RQKKYTLPVLILTARDTLNDRITGLDVGADDYLVKPFALEELHARIRALLRRHNNQGESELTVGN LTLNIGRHQAWRDGQELTLTPKEYALLSRLMLKAGSPVHREILYNDIYNWDNEPSTNTLEVHIHN LRDKVGKSRIRTVRGFGYMLVATEES
C	*Shigella dysenteriae* 1617	*cpxR*	MNKILLVDDDRELTSLLKELLEMEGFNVIVAHDGEQALDLLDDSIDLLLLDVMMPKKNGIDTLK ALRQTHQTPVIMLTARGSELDRVLGLELGADDYLPKPFNDRELVARIRAILRRSHWSEQQQNND NGSPTLEVDALVLNPGRQEASFDGQTLELTGTEFTLLYLLAQHLGQVVSREHLSQEVLGKRLTPF DRAIDMHISNLRRKLPDRKDGHPWFKTLRGRGYLMVSAS
C	*Shigella dysenteriae* 1617	*kdpE*	MTNVLIVEDEQAIRRFLRTALEGDGMRVFEAETLQRGLLEAATRKPDLIILDLGLPDGDGIEFIRDL RQWSAVPVIVLSARSEESDKIAALDAGADDYLSKPFGIGELQARMRVALRRHSATAAPDPLVKFS DVTVDLAARVIHRGEEEVHLTPIEFRLLAVLLNNAEKVLTQRQLLNQVWGPNAVEHSHYLRIYM GHLRQKLEQDPARPSHFITETGIGYRFML
C	*Shigella dysenteriae* 1617	*qseB*	MRILLIEDDMLIGDGIKTGLSKMGFSVDWFTQGRQGKEALYSAPYDAVILDLTLPGMDGRDILRE WREKGQREPVLILTARDALEERVEGLRLGADDYLCKPFALIEVAARLEALMRRTNGQTSNELRH GNVMLDPGKRIATLAGEPLTLKPKEFALLELLMRNAGRVLPRKLIEEKLYTWDEEVTSNAVEVH VHHLRRKLGSDFIRTVHGIGYTLGEK
C	*Shigella dysenteriae* 1617	*yedW*	MSFEDSEKTSRVTLQQHYNFVMNQAVSITYDLWHIIFMKILLIEDNQRTQEWVTQGLSEAGYVID AVSDGRDGLYLALKDDYALIILDIMLPGMDGWQILQTLRTAKQTPVICLTARDSVDDRVRGLDSG ANDYLVKPFSFSELLARVRAQLRQHHALNSTLEISGLRMDSVSQSVSRDNISITLTRKEFQLLWLL ASRAGEIIPRTVIASEIWGINFDSDTNTVDVAIRRLRAKVDDPFPVMLPISRTCVFQ
C	*Shigella dysenteriae* 1617	*phoP*	MRVLVVEDNALLRHHLKVQIQDAGHQVDDAEDAKEADYYLNEHLPDIAIVDLGLPDEDGLSLIR RWRSNDVSLPILVLTARESWQDKVEVLSAGADDYVTKPFHIEEVMARMQALMRRNSGLASQVIS LPPFQVDLSRRELSINDEVIKLTAFEYTIMETLIRNNGKVVSKDSLMLQLYPDAELRESHTIDVLM GRLRKKIQAQYPQEVITTVRGQGYLFELR
D	*Bacillus subtilis* substr. subtilis str. 168	*ybdK*	MKGYRILIVEDDVMIGDLLQKILQREGYRVIWKTDGADVLSVIQKVDLVIMDVMLPGEDGYQMS AKIKKLGLGIPVIFLSARNDMDSKLQGLQIGEDYMVKPFDPRELLLRMRNMLEHHYGTFTQIKHL YIDAVTKKVFNESLHDEVLFTAIERKIFFYLYENRDSILTKEHFFEYLWQLEDRNPNIVNVHIKKIR AKINDQAGEMIENIYGEGYRLNTVVKK
D	*Bacillus subtilis* substr. subtilis str. 168	*spo0A*	MEKIKVCVADDNRELVSLLSEYIEGQEDMEVIGVAYNGQECLSLFKEKDPDVLVLDIIMPHLDGL AVLERLRESDLKKQPNVIMLTAFGQEDVTKKAVDLGASYFILKPFDMENLVGHIRQVSGNASSVT HRAPSSQSSIIRSSQPEPKKKNLDASITSIIHEIGVPAHIKGYLYLREAISMVYNDIELLGSITKVLYP DIAKKFNTTASRVERAIRHAIEVAWSRGNIDSISSLFGYTVSMTKAKPTNSEFIAMVADKLRLEHK AS

Appendix Table 9. The amino acid sequence of OmpR family RRs. (Continued.)

Sub-family	Bacteral strain	Gene name	Amino acid sequence
D	*Bacillus subtilis* substr. subtilis str. 168	*yrkQ*	MAYRILVVEDDEDIGDLLEESLTRAGYEVLRAKDGKRALQLVNDSLDLVILDIMMPGISGIETCQH IRKSSNVPILFLTARSSTLDKTEGLLAGGDDYMTKPFSEEELHARVIAQLRRYTIYQEKKEQEETFL IGGKLRVSEEFNEVWKEEKQIKLSDLEYRILKLLMNKRNKIFSAQNIYESVWGQPYFYCSNNTVM VHIRKLRSKIEDDPARPVYIKTEWGRGYRFGAS
D	*Bacillus subtilis* substr. subtilis str. 168	*ytsB*	MFKLLLIEDDESLFHEIKDRLTGWSYDVYGIQDFSQVLQEFAAVNPDCVIIDVQLPKFDGFHWCR LIRSRSNVPILFLSSRDHPADMVMSMQLGADDFIQKPFHFDVLIAKIQAMFRRVHHYNTEPSTIKT WCGAAVDAEQNLVSNDKGSVELTKNEMFILKQLIEQKNKIVSREELIRSLWNDERFVSDNTLTVN VNRLRKKLDALQLGAYIETKVGQGYIAKEEDKFYD
D	*Bacillus subtilis* substr. subtilis str. 168	*psdS*	MYRILLVEDDERIASLLGGHLQKYGYEVKIAEQLNDIKLEFAEMKPDLVLLDINLPFFDGFYWCR QIRTISNAPIIFISARTDELNQVMAIENGGDDYITKPFHLEVVMAKIKSVLRRTYGEYSPSLPQESRI VELGGLTIYPDQNEAEWNSVRILFSQKEFQLLSIFVREHKKIVSRDELLEALWDDVDFVDDNTLTV NVNRLRRKLENAGLTDCISTIRGQGYQFQVNRKDEAEC
D	*Bacillus subtilis* substr. subtilis str. 168	*ywpD*	MKIRERFSMVDLPVLIITAAIIGHDKYKAFHAGANDILQKPYHYSEFMARIQNLIMMKHTANQAT RMEMAFLQSQIKPHFLYNVLNTIISLTHLDIEKAREVTEEFTNYLRMSFDFQNTSAISSFRHELSIINS YLSIEKTRFSNRLEVLFDIDEDIDFILPPLMIQPLVENAVLHGVSKKRGGGWIKLTAKKQSKNEYHI KVEDNGPGITPEKQIDLLSTDFDRSVGLKNINQRLKHFCGSELMISSTPDAGTSVSMLIHLAETTGS PKELKDTERT
D	*Bacillus subtilis* substr. subtilis str. 168	*tpeK*	MNKIMIVEDSEDIRGLLQNYLEKYGYQTVVAADFTAVLDVFLREKPDVVLLDINLPAYDGYYW CRQIRQHSTSPIIFISARSGEMDQVMAIENGGDDYIEKPFSYDIVLAKIKSQIRRAYGEYAAKQGEK VVEYAGVQLFVERFELRFQDEKSELSKKESKLLEVLLERGEKVTSRDRLMEKTWDTDIFIDDNTL NVYITRLRKKLRELNAPVSIEAVRGEGYQLRAQS
D	*Bacillus subtilis* substr. subtilis str. 168	*ycbM*	MLVEDDHSISEMVDHYLTKEGFGIVHAFDGEEGIRLFQQGSYDLVLLDIMLPKLNGMDFLKIIREK SNIPVLMISAKDGDVDKALGLGFGADDYIAKPFSMIELTARVKAAIRRATQYSAEEPAVNKVIRIH QLAIDIDNVSVLKNGEPLQLTSTEWQLLCLFASNPKKVFTKEQIYRSVWNEEYFDDQNIINVHMR RLREKIEDDPSSPQYIKTLWGIGYKLGEF
D	*Bacillus subtilis* substr. subtilis str. 168	*yvrH*	MENASILIVDDEKAIVDMIKRVLEKEGYRNILDAASAEEAIPVVKANKVDLIVLDVMMGGMSGFE ACTLIREYSDAPIFFLTARSSDADKLSGFAVGADDYITKPFNPLELAARIRAHLKRTYQSKETSSNQ TYTYDYFTFSPQNAELIVGGEAVACSAQLLQLLQYFCEHPNVVLSKDQIYEKVWGYPSYGDNNT VMVHIRKLREKIERDPSNPEYIVTVRGLGYRFIPNPEGKRS
D	*Pseudomonas aeruginosa* PAO1	*PA5364*	MSKVSALVVDDAPFIRDLMKKGLRDNFPGLHIEEAVNGRKAQQLLSRQNVDLILCDWEMPEMS GLELLTWCRAQENLKTTPFIMVTSRGDKENVVQAIQAGVSDYIGKPFSNDQLVAKIKKALSRSGK LEALAAHAPRREIASGMANDSLAALTGGRAEVIKPAASPAKPAPAPKPASAPQASARPAGSGNP LGQAQLRLPQSSMPCVIKAVSLKEAQLVVKRADPLPQVLESAVLDLEENSDVARLNGYLHAIAA LEPKPDSDWLLLTLRFVDRDPQKLDYLSRLIARGSTQKHYVPGA
D	*Pseudomonas aeruginosa* PAO1	*PA2798*	MHKVSATLLIIDDDEVVRESLAAYLEDSNFKVLQALNGLQGLQIFESEQPDLVICDLRMPQIDGLE LIRRIRQTASETPIIVLSGAGVMSDAVEALRLGAADYLIKPLEDLAVLEHSVRRALDRAYLRVENQ RYRDKLEAANRELQASLNLLQEDQNAGRQVQMNMLPVTPWSIEGLEFSHRIIPSLYLSGDFVDYF RVDERRVAFYLADVSGHGASSAFVTVLLKFMTTRLLYESRRNGTLPEFKPSEVLAHINRGLINTKL GKHVTMLGGVIDLEKNSLTYSIGGHLPLPVLFVEGQAGYLEGRGLPVGLFDDATYDDRVMELPPS FSLSLFSDGILDVLPGATLKEKEASLPEQVAAAGGTLDGLRQVFGLANLAEMPDDIALLVLSRNLA
D	*Haemophilus influenzae* Rd KW20	*HI0219a*	MEDVDLNIMVAKTILEKLGHHVDVATNGKQAITLFEKNVYDILLLDIKLPDMSGFEIAQYLRENY ENGIYDFLPPMIAFTANVMQSEQEYLEMGMDGVLRKPISIKDLHHCLQQFFADESESIIEMNDDNE LSEQFDLALIETLGKSQILENLSLFKQTMPNYLAQLSKDNMKETEDTAHKIKGAAASVGLNHLRQ LADTLESAAKNSDVFNCGELIDKIGNLWLEDVEDLLKFCKF
D	*Salmonella enterica* subsp. Enterica serovar Typhimurium str. LT2	*rssB*	MTQPLVGKQILIVEDEPVFRSLLDSWFSSLGATTALAGDGVDALELMGRFTPDLMICDIAMPRMN GLKLVENLRNRGDQTPILVISATENMADIAKALRLGVEDVLLKPVKDLNRLRETVFACLYPNMF NSRVEEEERLFRDWDAMVSNPTAAAQLLQELQPPVQQVISHCRINYRQLVSADQPGLVLDIAPLS DNELAFYCLDVTRAGDNGVLAALLLRALFNGLLQDQLGQQKHRLPELGALLKQVNHLLRQANL PGQFPLFVGYYHSELKNLILVSAGLNATLNTGAHQVQISSGVPLGTLGNAYLNQLSQRCDSWQCQ IWGAGGRLRLMLSAE